The modification of organic materials by plasmas and ion beams as studied by ESCA

David Richard Hutton

THE MODIFICATION OF ORGANIC MATERIALS BY PLASMAS AND ION BEAMS AS STUDIED BY ESCA

by

DAVID RICHARD HUTTON (B.Sc.(Hons.))

(Dunelm)

A Candidate for the Degree of Doctor of Philosophy

Collingwood College,
University of Durham.

November 1983

To My Parents

and

Christine

ACKNOWLEDGEMENTS

I would like to express my thanks to the many individuals who have given their help and assistance so freely during my period of study in Durham. Firstly, I would like to thank my supervisor, Professor David T. Clark, for introducing me to the field of surface chemistry and ESCA, and for his help, guidance and encouragement during the course of this research.

Thanks are also due to my colleages, Bill Brennan, Rosemary Wilson, Dr. Hugh Munro, Andy Fowler, Steve Johnson, Jeff Eaves and Rob Allaker for their help, friendship and "useful discussions" over a wide range of topics, throughout. I am also indebted to the Science and Engineering Research Council (SERC) for the provision of a studentship and equipment.

Finally, I would like to thank Mrs. Marion Wilson for her great secretarial skill and patience in typing this manuscript.

ABSTRACT

X-ray photoelectron spectroscopy (XPS or ESCA) has been employed to investigate the changes in the surface chemistry of polymers produced by their exposure to plasmas and ion beams and the chemistry of thin polymeric films produced by the ion beam irradiation of films of condensed organic material.

Modification by hydrogen plasmas of fluoropolymers is shown to result in extensive defluorination and hydrogenation of the surface regions of the polymer to a depth of $\sim$20Å. In the initial stages of the reaction ESCA analysis reveals the presence of a smooth reaction gradient within the ESCA sampling depth. The modification is accompanied by extensive crosslinking of the polymer surface. A model is also proposed to account for these observations.

In order to try and gain an insight into the contributions of the various components of a plasma with polymer surfaces the interaction of low energy (1-5keV) argon ions with fluoropolymer and polymers containing carbon hydrogen and oxygen were studied. The reaction leads to the depletion of the surface region in the most electronegative components of the polymer. The modification, irrespective of the beam energy used, is homogeneous within the ESCA sampling depth using $Mg_{K\alpha_{1,2}}$ radiation. The polymers all lead to the formation of a highly crosslinked, unsaturated carbonaceous surface layer on bombardment. This defunctionalisation is marked in the ESCA spectra by modifications in the lineshape of the C_{1s} photoionisation peak, the asymmetry of which has been found to, in a qualitative sense at least, reflect the presence of unsaturation in the systems.

The exposure of condensed films of hexafluorobenzene to relatively low doses of argon ions has been shown to result in

the formation of a thin film of an involatile polymeric residue. The product bears a striking resemblance in its chemistry to that of plasma polymerised films of hexafluorobenzene. Apart from the potential ability of such films, *e.g.* as dielectric films in microelectronics fabrication, they also illustrate the link between the interactions of ion beams with organic materials and plasmolysis of such materials. The thermal stability of films produced by the ion beam induced polymerisation and plasma polymerisation of hexafluorobenzene is also investigated.

MEMORANDUM

The work described in this thesis was carried out at the University of Durham between October 1980 and September 1983. It has not been submitted for any other degree and is the original work of the author except where acknowledged by reference.

CONTENTS

CHAPTER ONE

ELECTRON SPECTROSCOPY FOR CHEMICAL APPLICATIONS (ESCA)

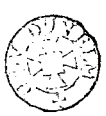

1.1 An Introduction

In essence the ESCA experiment involves the measurement of the binding energies of electrons emitted from a sample, be it a gas, liquid or a solid, when irradiated with a mono-energetic source of soft X-rays, *in vacuo*. In this fashion a spectrum is obtained which exhibits a series of discrete bands which reflect the electronic structure and composition of the sample.

It is only comparatively recently that ESCA has emerged as one of the most versatile and potent techniques for the investigation of the structure, bonding and reactivity of materials and in particular, of their surfaces.[1] Photo-electron spectroscopy was essentially developed during the nineteen fifties and sixties, the first commercial spectro-meters appearing in the late sixties. Earlier experiments in the decades following Einstein's[2] formulation of the photo-electric effect in terms of photons, were hampered by severe experimental difficulties of resolution and electron detection. These studies were carried out independently by Robinson[3] and de Broglie[4] and later by Van Akker and Watson,[5] attempting to obtain X-ray excited photoelectron spectra from a variety of materials ranging from thin metal foils to inorganic salts. It was not until the early nineteen fifties that the potential of the technique began to be realised with the development of a spectrometer capable of hitherto unheard of resolution and accuracy by Siegbahn and coworkers at the Institute of Physics, Uppsala University, Sweden.[6,7] This new found resolution enabled them to observe for the first time chemically induced shifts in the binding energies of core electrons.[7] From the

first observations that core photoelectron peak intensities could be used quantitatively by Steinhardt and coworkers[8] and the observation of chemical shifts in core electron binding energies, by Siegbahn and coworkers[8] many more distinct chemical and physical effects have been observed. Concomitant with this have been numerous developments in interpretive theory. Thus from analysing various aspects of an X-ray photoelectron spectrum a hierarchy of information levels becomes available. It is this spread of information levels that makes ESCA useful to such a broad range of disciplines, finding application in all areas of chemistry and materials science. This diversity of information will become apparent from the following discussion.

Accounts of the early work of the Uppsala group are contained in Siegbahn's two books "ESCA: Atomic, Molecular and Solid State Structure Studied by Means of Electron Spectroscopy"[8] and "ESCA Applied to Free Molecules".[10] K. Siegbahn also gave a thorough historical account of the development of the technique (with particular emphasis on the work of the Uppsala group) in his Nobel lecture address.[11] The early history of electron spectroscopy is also to be found reviewed by Jenkin, Leckey and Liesegang.[12] The assembly of a collection of "Benchmark Papers" by Carlson[13] serves to document some phases of the development of the technique.

The acronym, ESCA, (Electron Spectroscopy for Chemical Analysis) was originally coined by Siegbahn, he later amended it the more general Electron Spectroscopy for Chemical Applications. The technique is also commonly known as X-ray Photoelectron Spectroscopy (XPS) and less commonly as:

High Energy Photoelectron Spectroscopy (HEPS)

Induced Electron Emission Spectroscopy (IEES)

Photoelectron Spectroscopy of the Inner Shell (PESIS)

There exists a plethora of techniques by means of which electrons characteristic of a sample may be generated, involving electron ejection as a result of collison of particles or photons with a sample. The generic term "Electron Spectroscopy" embraces all of these. It is worthy of note however that ESCA is amongst these the most general and widespread of these techniques in its application. Detailed discussions of the range of techniques which may be applied are to be found in reviews by Rhodin and Gadzuk[14] and Baker and Brundle.[15] Of these probes, those involving the use of photons as a means of generating characteristic electrons are of greatest use in the non-destructive analysis of polymer surfaces, employing much milder radiation doses.

1.2 Fundamental Electronic Processes Involved in ESCA

1.2.1 Photoionisation

Irradiation of a molecule with a monoenergetic beam of photons causes the photoejection of electrons with binding energies less than the photon energy of the exciting radiation. The total kinetic energy (KE) of the ejected electron is given by equation 1.1.

$$KE = h\nu - BE - E_r \qquad (1.1)$$

where h is Planck's constant

ν is the frequency of the incident radiation

B.E. is the binding energy of the photoemitted electron,

defined as the positive energy required to remove the electron to infinity with zero kinetic energy,

E_r is the recoil energy of the atom or molecule.

This last quantity E_r has been shown by Siegbahn and coworkers[8] to be negligible for typical soft X-ray sources used in ESCA, *e.g.* $Mg_{K\alpha_{1,2}}$ (1253.6 eV) and $Al_{K\alpha_{1,2}}$ (1486.6 eV). However employing harder X-ray sources *e.g.* $Ag_{K\alpha}$ (22000 eV), the recoil energies of light atoms are no longer negligible, Cederbaum and Domcke[16] have shown that these effects can lead to perturbations of the vibrational band profiles of molecules containing light atoms where E_r is now significant. However in routine studies with X-ray sources of moderate photon energies, recoil energies may be neglected and equation 1.1 reduces to equation 1.2:

$$KE = h\nu - BE \qquad (1.2)$$

The lifetimes of the core-hole states formed in such photo-ionisation events are typically 10^{-13} - 10^{-15} seconds.[17]

It is important to understand the relationship that exists between the experimentally observed binding energies for solids and those obtained for free molecules as compared with values calculated theoretically in *ab initio* and semi-empirical LCAO-MO-SCF treatments.

In the case of a conducting sample the most convenient reference level is the Fermi level. In a metal this level is defined as the highest occupied level at absolute zero. (Sometimes also referred to as the "electron chemical potential")

The work function, ϕ_s, for a solid is defined as the energy difference between the free electron (vacuum) level and the Fermi energy of the solid. The vacuum levels of the solid

sample and the spectrometer may however differ and hence in analysis the electron may experience a retarding or accelerating potential equal to $\phi_s - \phi_{spec}$ where ϕ_{spec} is the work function of the spectrometer.[8] In the ESCA experiment, the kinetic energy of the electron as it enters the analyser that is measured, taking zero binding energy to be the Fermi level of the sample, the following equation results:

$$BE = h\nu - KE - \phi_{spec}. \qquad (1.3)$$

However for insulating samples such as polymers, the situation is complicated, the Fermi level is not so well defined analytically, lying somewhere between the filled valence levels and the empty conduction band.[8] An additional complication arises from the charging of insulating samples on irradiation, equation 1.3 assumes equilibrium conditions. If, however, the resistance of the sample is high compared with the currents required to neutralise the electron holes created by the photoionisation processes, then the sample surface will charge until an equilibrium potential is reached at which the production of holes is offset by the neutralisation by conduction from the sample backing and the capture of stray electrons from the vacuum system. This stray electron flux on the sample is made up from slow electrons photoemitted from the sample and from photoelectrons generated by X-ray impact on the window of the X-ray source and chamber walls. For a non-conducting sample it has been shown that this stray flux can contribute up to 99% of the total photoemitted flux.[18,19]

The problem of extracting absolute binding energies is, in practice, circumvented by the use of reference standards to calibrate the binding energy scale.

1.2.2 Processes Accompanying The Photoionisation Event

The initial photoionisation event may be accompanied by a variety of processes which may be divided into two categories depending upon the time scale relative to the photoionisation event. Slow processes such as X-ray fluorescence and Auger electron have negligible effect upon the kinetic energy of the photoejected electron. Electronic relaxation processes, shake-up, shake-off, and the interaction of conduction electrons with the core hole occur on a similar time scale and result in a modification of the kinetic energy of the emitted photoelectron. These primary, and secondary decay processes are illustrated schematically in Figure 1.1

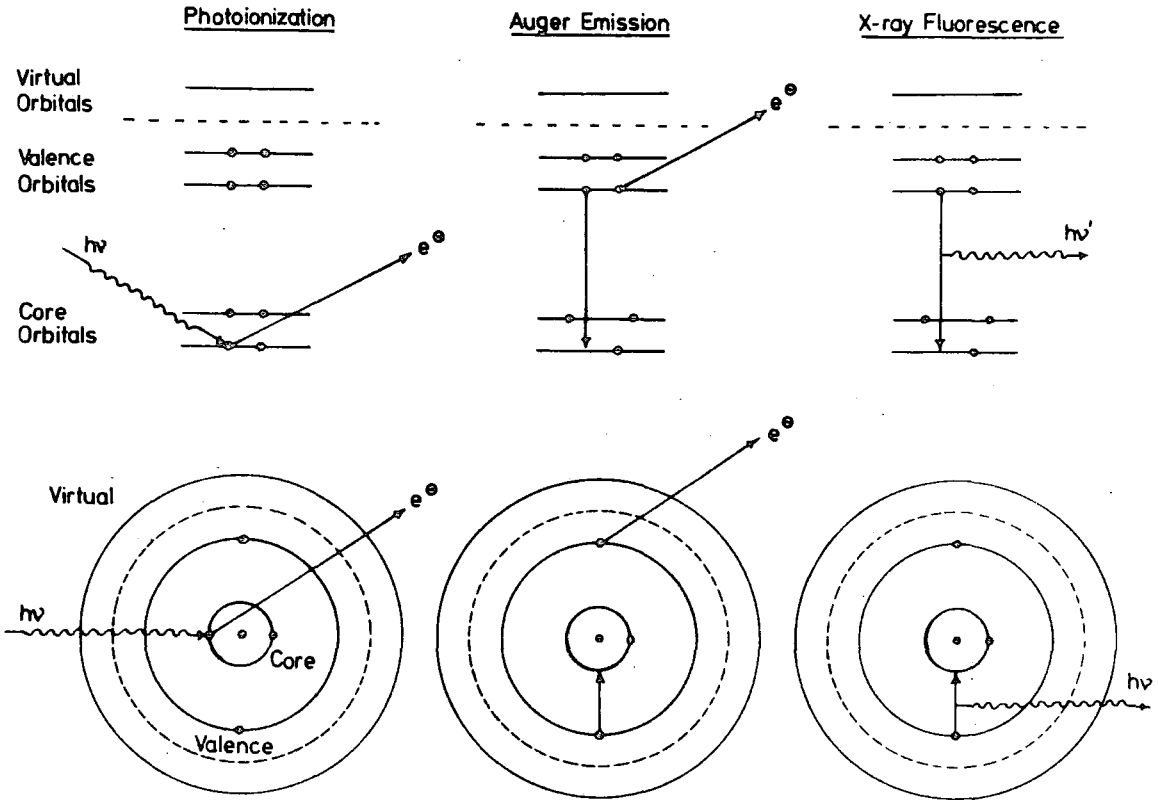

Figure 1.1 The Photoionisation Event

1.2.3 Electronic Relaxation

Accompanying the photoionisation process, which is complete within a time span of approximately 10^{-17} seconds, there is a widespread electronic relaxation of the valence electrons[20-22] as they relax to stabilise the incipient core-hole. Theoretical and experimental investigations[23-26] have shown that for a given core level this relaxation energy is a sensitive function of the electronic structure of a molecule. Salaneck[27] has also shown that in the solid state in addition to these intramolecular electronic relaxation effects, there also exista a smaller intermolecular relaxation effect due to the electronic polarisation of electrons in molecules surrounding the molecule which experiences the photoionisation event. The relaxation energy has been found to be relatively unimportant in describing shifts in binding energies, since differences in relaxation energy between closely related molecules are small and so cause only small changes in binding energies.

There have been many theoretical investigations of the chemical shift in core electron binding energies at a variety of levels. At the simplest level, Koopmans'[28] method for calculation of the absolute values of binding energies relies only upon the ground state properties of a wave function. The relaxation of the valence levels in response to the decreased shielding of the nuclear charge is not considered. Thus Koopmans' method tends to overestimate binding energies and as it is the relaxation energy which is most sensitive to the chemical environment of the atom on which the core-hole is produced, can lead to incorrect description of chemical shifts as Koopmans' approximation neglects relaxation. More sophisticated treatments[29,30] centre on non-empirical LCAO SCF calcul-

ations on both the ground state and core ionised state. Calculations on the former yielding the Koopmans' binding energy and, energy differences between the states, the relaxation energy, R.E., equation 1.4

$$R.E. = BE(Koopmans) - BE\ (\Delta SCF) \qquad (1.4)$$

1.2.4 Shake-up and Shake-off Phenomena

The removal of a core electron, which is almost completely shielding as far as concerns the valence electrons, is accompanied by substantial reorganisation of the valence electrons. This perturbation yields a finite probability for photoionisation to be accompanied by the simultaneous excitation of a valence electron from an occupied, to a higher bound state, (shake-up), ionisation of a valence electron (shake-off) or the transition of an electron from a higher orbital to an orbital of lower energy (shake-down).[57] Analogous to shake-up and shake-off processes, in conductors there exists a continuous density of states curve above the Fermi level which provides a continuous range of allowed one-electron excitation energies. Whereas in an isolated molecule a discrete series of excitations accompanying the photoionisation event may be allowed, in a conductor a continuous range is available. Thus for an isolated molecule or a polymer where the feature giving rise to the shake-up feature is essentially isolated (*e.g.* a pendant phenyl group in polystyrene) a sharp set of satellite lines below a roughly symmetric one electron transition peak is obtained.[34,101-103] However in a conductor, an asymmetric tailing of the main peak is obtained.[33]

These phenomena occur concomitant with and on a similar time scale to photoionisation resulting in a modification

of the primary photoionisation peak, producing satellite peaks or an asymmetric tailing to the lower kinetic energy side of the main peak.

These processes derive their energy from the single electron process, thus lowering the KE of the primary photoelectron. Thus equation 1.2 has to be revised to account for these processes:

$$KE = h\nu - BE - \bar{E} \qquad (1.5)$$

where $\bar{E}$ is the energy of the electron process.

These excitations follow monopole selection rules, $J = \Delta L = \Delta S = \Delta M_j = \Delta M_L = \Delta M_s = 0$, and may be in some ways viewed as an analogue of ultraviolet spectroscopy in ESCA, though the analogy should not be taken too far.

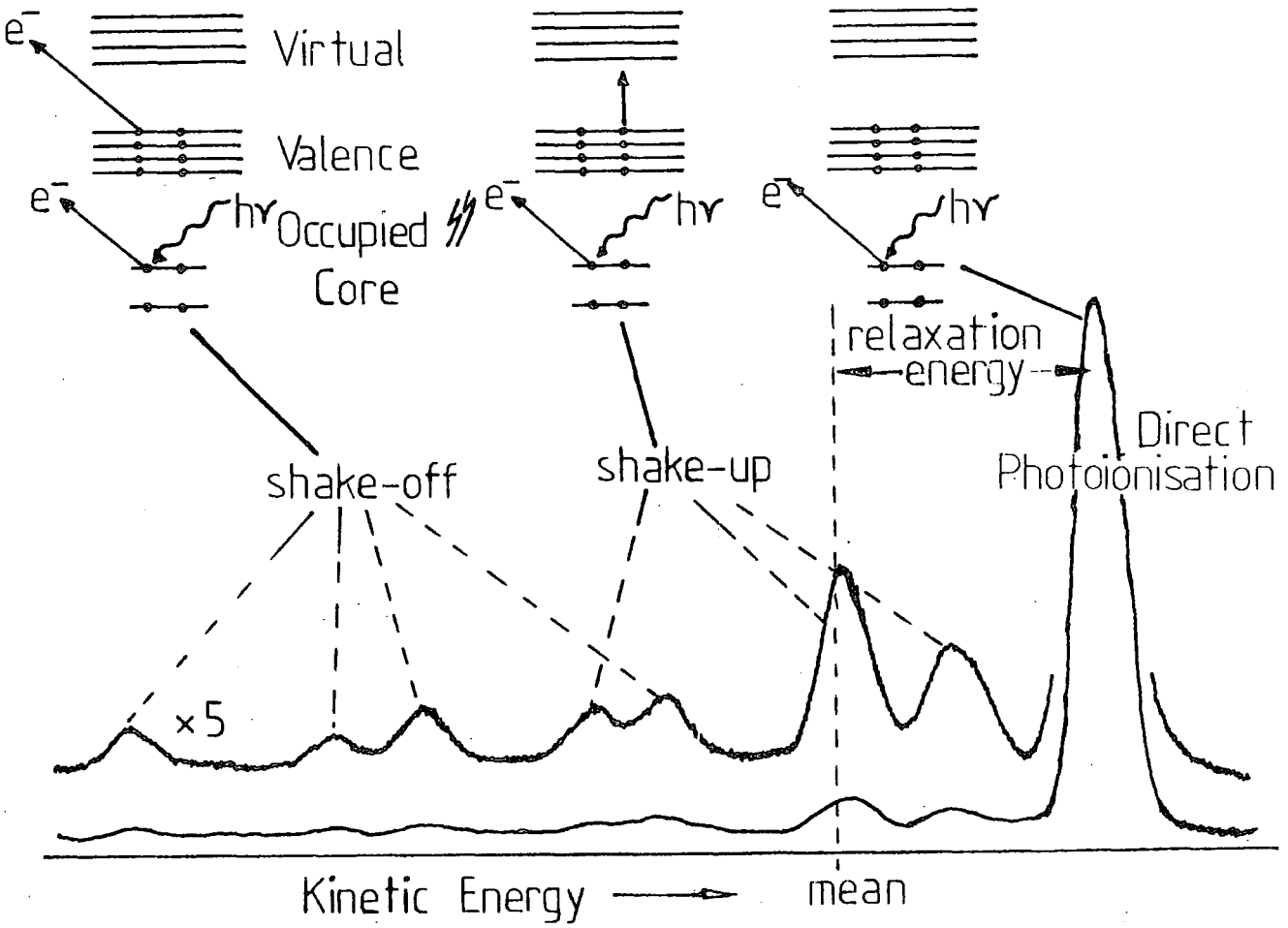

Figure 1.2 Relationship between relaxation energy, Koopmans' theorem, (mean) and the direct photoionisation shake-up and shake-off peaks

The theoretical relationship between the intensities of shake-up and shake-off intensities and relaxation energies has been discussed by Manne and Åberg.[31] They have shown that the weighted mean of the direct photoionisation, shake-off and shake-up peaks, corresponds to the binding energy of the unrelaxed system (see Figure 1.2). The transition probabilities are it is clear, low for high energy shake-off processes, higher probabilities existing for transitions falling reasonably close to the centroid of the system. In the solid state the interpretation of shake-up and shake-off features is hampered by the presence of a general inelastic tail, which peaks some 20eV to the lower kinetic energy side of the direct photoionisation peak, swamping all but the high intensity low energy shake-up peaks. A review of some aspects of shake-up effects has been given by Baker and Brisk.[32] In the case of polymers, a detailed study of the effects of substitution of the pendant phenyl groups of polystyrene on the position and form of shake-up satellites has been made by Clark and Dilks.[34] Further consideration of shake-up in large polycyclic aromatic systems and degraded polymeric systems will be given later.

In general as the size of the conjugated system giving rise to the low energy shake-up transitions grows and in doing so the range of transitions available also grows, the shake-up satellites become less distinct, sinking into an asymmetric tailing of the direct photoionisation peak. Conversely strong shake-up peaks may be erroneously interpreted in terms of chemical shift effects.

Shake-up and shake-off structure has been studied in a range of organic[99-100] and inorganic[97-98] materials (in particular the transition elements). Such structure has also been

studied to help elucidate details of structure and bonding in polymeric materials[101-103] not immediately attainable from the primary information levels in ESCA (*e.g.* chemical shifts).

1.2.5 Auger Emission and X-ray Fluorescence

De-excitation of the core hole produced by photoionisation occurs by two main routes, X-ray Fluorescence and Auger emission, both processes being slow compared to the initial photoionisation event. For lighter atoms Auger emission is the dominant mechanism, X-ray fluorescence dominating for heavier elements. The probability for each process varies with the atomic number of the atom as shown in Figure 1.3.

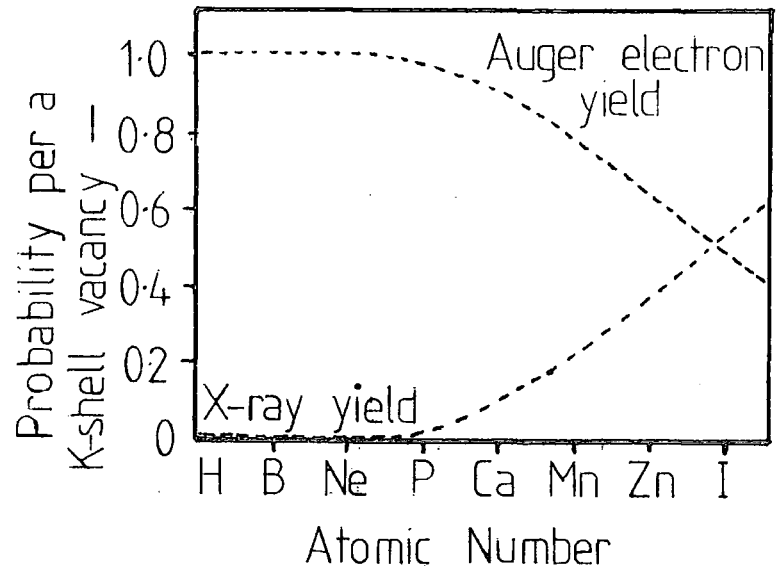

Figure 1.3 Efficiency of Auger and X-ray Fluorescence processes as a function of atomic number

Auger emission may be viewed as a two step process involving the initial ejection of an electron from an inner shell by a photon followed by the decay of an electron from an upper level

to the vacancy in the inner shell concomitant with the emission of a second electron.[35-40] This is indicated schematically in Figure 1.4.

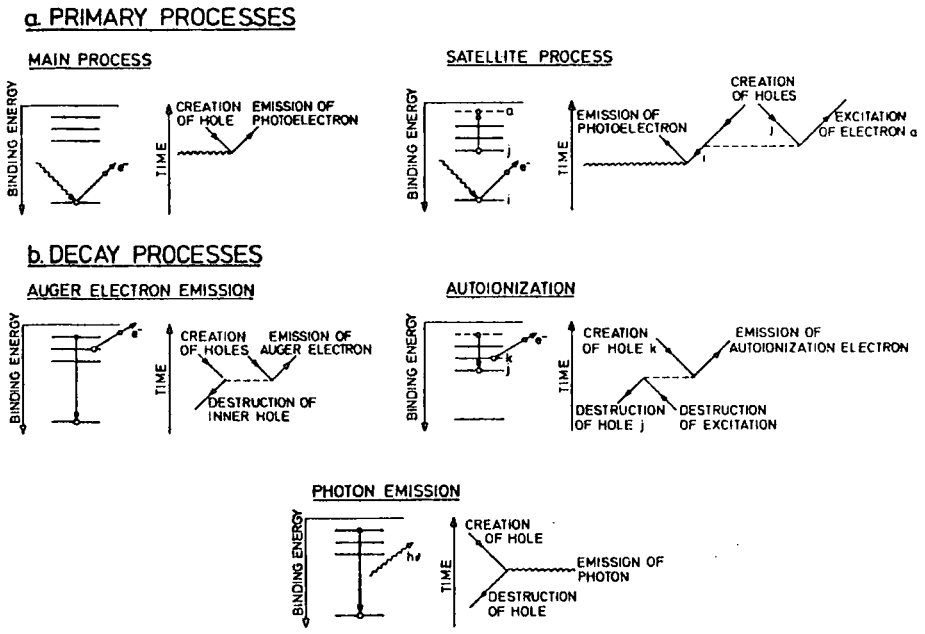

Figure 1.4 (a) Photoionisation, (b) Auger Emission and X-ray Fluorescence

In general for an Auger transition involving a set of levels KLM, a peak appears at:

$$E_{(2)} = E_K - E_L - E_M\,(Z+\Delta) - \phi_A \qquad (1.6)$$

where Z is the atomic number of the element

Δ = 1 (due to extra positive charge on the loss of an electron)

ϕ_A = Analyser work function

E_K is the energy of the K level transition

E_L is the energy of the L level transition

E_M is the energy of the M level transition.

This formulation represents an oversimplification as the final state of the doubly ionised ion must also be defined, the effects of coupling in the singly ionised and doubly ionised states must also be considered. In elements of atomic number less than 40 where the electronic vacancy in the inner shell is filled by an electron from another inner shell (Coster-Kronig transitions[39]) the Auger spectrum is of use in analysing inner shell transitions, these are very efficient processes leading to very short lifetimes with well resolved Auger spectra.

The X-ray excited carbon Auger spectra of various polymers have been studied by Houston *et al*,[41] however the spectra are tedious to acquire and their interpretation and assignment difficult.

The second process mentioned, X-ray fluorescence, leads to the emission of characteristic X-rays and is used as a sensitive means of quantitative analysis for heavier elements.

Auger Electron Spectroscopy, in which Auger electrons characteristic of the sample are, in general, generated by the bombardment of a sample with an electron beam of energy typically ∿2keV is a sensitive analysis technique in its own right. It is a highly surface sensitive technique, the sampling depth of the exciting electrons being only about five atomic layers.[44] The use of the technique in the interrogation of polymeric surfaces is limited due to the radiation damage[42,43] caused by the incident electron beam which delivers typically a dose three orders of magnitude larger than a normal ESCA experiment.

As an aid to the identification of chemical states in XPS, Wagner[43] has promoted the concept of the Auger parameter. About half the naturally occurring elements exhibit Auger lines in XPS spectra when excited with $Mg_{K\alpha_{1,2}}$ or $Al_{K\alpha_{1,2}}$ radiation, of these twenty-two elements exhibit narrow, intense core-type Auger transitions. Chemical shifts in these Auger lines are different from and normally greater than those in the photoelectron lines of the same element. When the energies of the most intense photoelectron lines are plotted against those of the most intense or sharp Auger lines for compounds containing a given element a two dimensional plot is obtained. Such plots are useful in identifying the chemical states of elements in compounds. Wagner has also developed the concept of the Auger parameter, that is the kinetic energy of the sharpest Auger line of an element minus that of the most intense photoelectron line. This quantity is particularly attractive practically, as it is independent of sample charging. (More recently the modified Auger parameter, *i.e.* the kinetic energy of the Auger line minus the binding energy of the photoelectron peak has been adopted as it is independent of the energy of the exciting radiation and always positive). A review of the Auger parameter and its use has recently been given by Wagner.[45] Experimentally in XPS, X-ray excited photoelectron peaks may be distinguished from Auger peaks by a change in energy of exciting radiation, the position of Auger peaks in the spectra will remain unchanged whereas the kinetic energy of photoelectron peaks will change.

1.3 Features of ESCA Spectra

1.3.1 Chemical Shifts

The binding energies of core level electrons in an atom are essentially characteristic of that particular element.[1] They are localised and tightly bound and as such do not take part in bonding. They are however sensitive to the local environment of an atom, small changes in the chemical environment of an atom giving rise to measurable changes or shifts in the binding energies of the photoemitted electrons,[47,48] these shifts often being characteristic of the presence of a particular structural feature in the sample. A particularly dramatic illustration is provided by the C_{1s} spectrum of ethyl trifluoroacetate,[10] here shown in Figure 1.5.

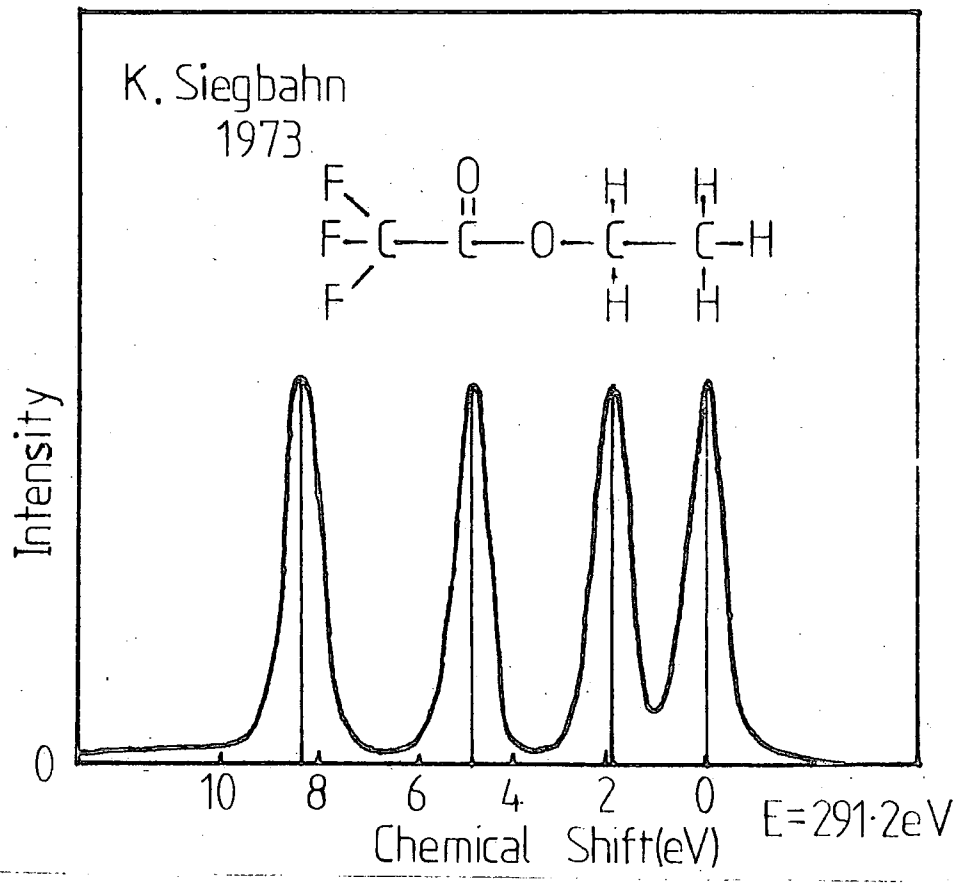

Figure 1.5 C_{1s} spectrum of ethyl trifluoroacetate

A study of the shifts in core levels as a function of substituent for a wide range of polymers was undertaken experimentally by Thomas,[49] and is displayed in Table 1.1. Compilations of similar information for other core levels exist[50] but as such assemblies of data are culled from a wide variety of sources, problems of energy-referencing may creep in.[51] Such assemblies of data should be treated as a guide rather than gospel.

Emphasising the close relationship between theory and experiment in ESCA, a variety of approaches exist for the calculation of chemical shifts, *inter alia*.

(1) Koopmans' Theorem[28]

(2) Core Hole Calculations (ΔSCF)[23]

(3) Equivalent Cores Model[52]

(4) Madelung Charge Potential Model[10]

(5) Quantum Mechanical Potential Model[53-55]

(6) Many body formalism.

The range of chemical shifts exhibited by core levels can in some cases be greater (up to ≈9eV in perfluorinated carbon species).

A complete discussion of the theoretical basis of the physical processes involved in photoemission has been given by Fadley.[56]

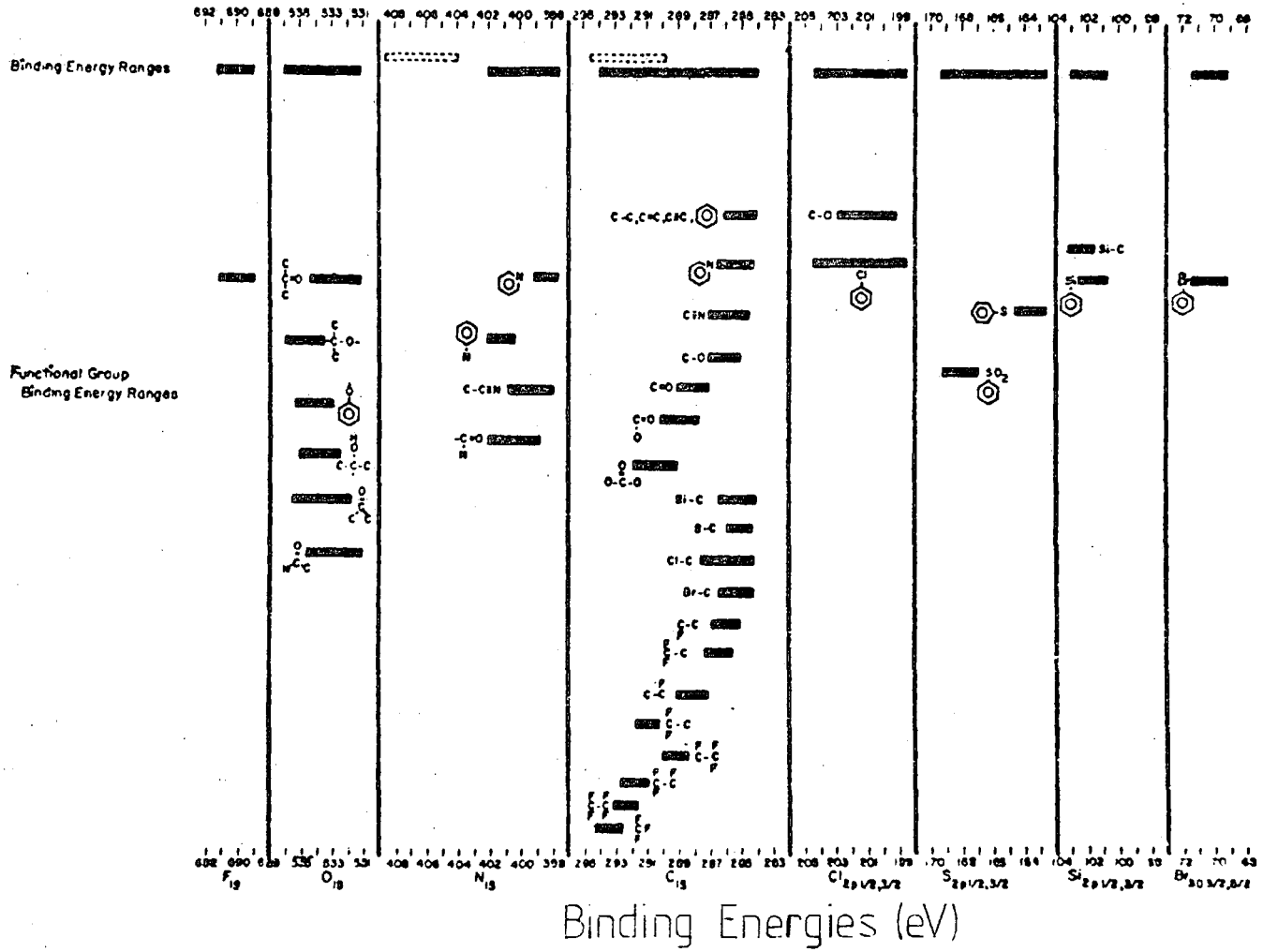

TABLE 1.1 Characteristic core level binding energies for various structural features in polymers

1.4 Fine Structure

1.4.1 Multiplet Splitting

The multiplet splitting of core levels results from the interaction of the spin of the unpaired electron resulting from the photoionisation process with the spins of other unpaired electrons present in the system. Many examples are to be found in the core level spectra of transition element compounds, their theoretical interpretation is only relatively straightforward for s-hole states based upon Van Vleck's vector coupling model.[58] The magnitude of the splitting provides information on the degree of localisation of the unpaired electrons on the atom where the core-hole is generated. Fadley has reviewed multiplet splittings in photoelectron spectroscopy.[59]

1.4.2 Spin-Orbit Splitting

In photoionisation from an orbital of orbital quantum number (l) greater than 0, (*i.e.* not from an s orbital) coupling occurs between the spin (S) and orbital angular momenta (L) to yield total momenta (J) resulting in the peak appearing as a doublet in the ESCA spectrum.[8] When spin-orbit coupling is weak compared with electrostatic interactions then the orbital angular momenta will couple to give a resultant L and the individual spin momenta will also couple to give a resultant S the resulting momenta then couple to give J, this is known as the Russell-Saunders coupling scheme (L+S=J). At the other extreme, where the spin-orbit coupling energy is large compared with the electrostatic energy then the individual spin and angular momenta of the electrons couple to give a resultant j. The coupling of these resultant j's yields final

total momenta J. In this case the orbital and spin momenta are individually coupled, the coupling scheme is known as the jj coupling scheme. The former Russell-Saunders coupling scheme is applicable to light elements, up to the lanthanides, but for heavier elements the jj coupling scheme is used.

The ratio of intensities of the components of the doublet obtained in the ESCA spectrum are proportional to the ratio of the degeneracies (2J+1) of the states. The relative intensities of the states arising from s, p, d and f levels are shown in Table 1.2 and examples of this type of splitting in ESCA spectra are displayed in Figure 1.6.

TABLE 1.2 J states for s, p, d and f orbitals

Orbital	Orbital Quantum No.	Total Quantum No.	Intensity Ratio
	l	J = (l ± s)	(2J+1) : (2J+1)
s	0	$^1/_2$	singlet
p	1	$^1/_2$, $^3/_2$	1 : 2
d	2	$^3/_2$, $^5/_2$	2 : 3
f	3	$^5/_2$, $^7/_2$	3 : 4

1.4.3 Electrostatic Splitting

A further type of splitting has also been observed in the ESCA spectra of some tin, gold, uranium and thorium compounds[63,64] attributed to the differential interaction between an internal electrostatic field and the spin states of the core level being investigated. However in organic polymers the inherently amorphous structure precludes the

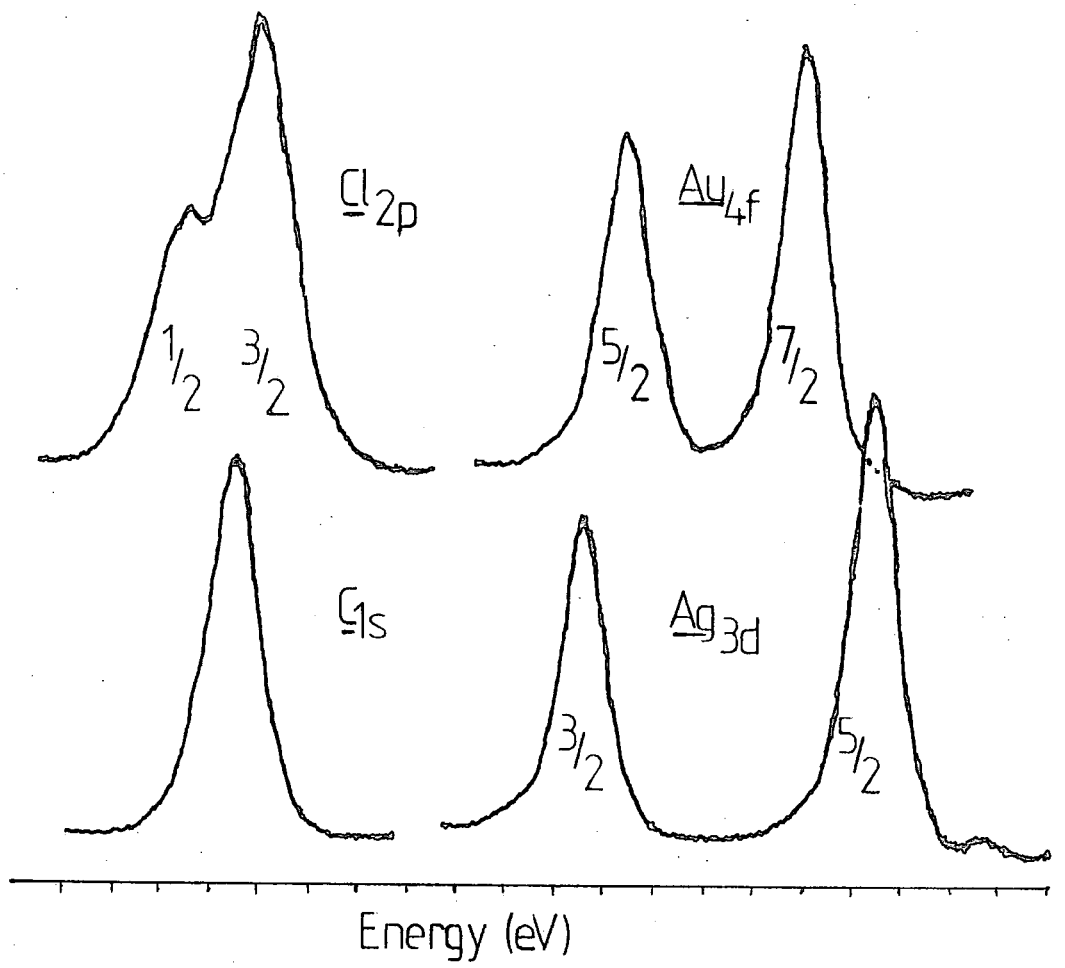

Figure 1.6 Spin-orbit splittings in C_{1s}, Cl_{2p}, Ag_{3d}, and Au_{4f} core levels

establishment of such fields and it is unlikely therefore that such splitting will be observed in polymers.

1.5 Valence Bands

Whereas much information concerning structure and bonding may be inferred from shifts in core level binding energies, the

valence bonds of polymers also contain much valuable information especially for systems which display no chemical shift effects, *e.g.* polyethylene and polypropylene (see Figure 1.7).

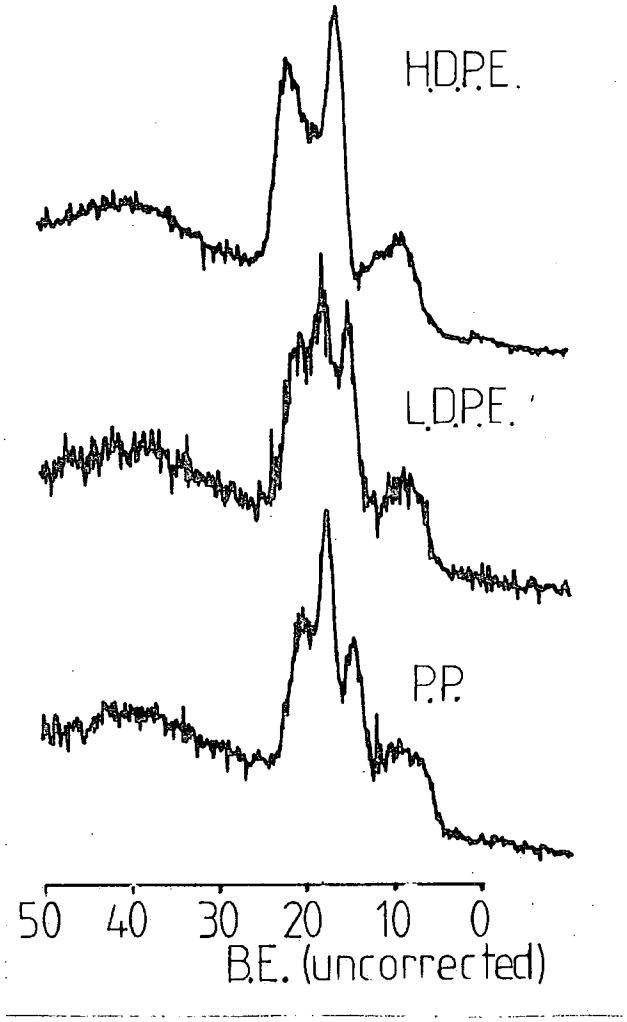

Figure 1.7 XPS valence bond spectra of high density polyethylene, low density polyethylene and polypropylene

Identical in the C_{1s} region they are clearly distinguishable from the valence regions of the XPS spectra. However to extract all this information requires the support of quantum mechanical calculations and comparison with other types of

experimental data for a full interpretation. They can however be readily used to "fingerprint" materials. Beyond the monitoring of substituent effects, valence band spectra can also be used to characterise purely hydrogen and carbon containing chains, isomerism (structural isomerism and stereoisomerism) and crystalline structure.[65] In the study of the valence region, although UPS (Ultra-violet Photoelectron Spectroscopy) and XPS provide complementary information, the XPS data has some advantages. Using a high energy photon source all the valence levels may be studied, the kinetic energy range of the photoemitted electrons is small compared with their energy, there is little variation in the mean free paths of the emitted electrons over the region. In gas phase work the resolution of a UV lamp (a few meV) offers substantial advantages over an X-ray excited spectrum in terms of resolution. However in a solid, molecular orbitals are grouped into bands, broadened by vibrational excitation, they become unresolved. It has been found that in polymers the use of UV lamp does not offer any substantial advantage over an XPS experiment.

The photoionisation cross-section for a given orbital varies with the energy of the excitation source. Using a UV source the photoionisation cross-section for C_{2p} orbitals is larger than that for C_{2s} orbitals. The reverse obtains for X-ray excitation. Thus comparison of the UPS and XPS spectra offers an aid to assignment, the XPS spectra emphasising the easier to interpret C_{2s} level.

The amount of information that can be gleaned from such spectra has to be balanced against the much longer acquisition times required to produce high quality spectra as compared with core level studies. The photoionisation cross-section for valence levels to $Mg_{K\alpha}$ and $Al_{K\alpha}$ radiation are much lower than for core levels. There is a requirement also to use mono-

chromated X-ray sources to obliviate the need for complex background subtraction and satellite removal treatments for all but qualitative "fingerprint" work. In contrast to core levels, which essentially sense short range effects, the valence region reflects the longer range electronic effects and order present in polymers.

1.6 Sample Charging and Energy Referencing

For conducting samples in electrical contact with the spectrometer the Fermi level provides a convenient level for energy referencing. However for insulating samples or samples not in electrical contact with the spectrometer energy referencing is not so straightforward (Figure 1.8). For insulating samples the Fermi level is not well-defined in the XPS spectrum.

"Sample charging" arises from the inability of an insulating sample to replace electrons lost by photoemission. An equilibrium situation is established when the photoemission current is balanced by the sample attracting electrons from the sample backing or by the capture of stray electrons from the vacuum[18,19] system. As a result the sample surface rises to a net positive potential, photoemitted electrons from the sample experience a net retardation and hence appear at higher apparent binding energies.

For a sample which charges uniformly all photoelectrons leaving the sample are affected by the same retardation and shifted by the same amount. The energy equation is thus modified,

$$KE = h\nu - BE - \phi_s - \Delta \qquad (1.7)$$

where Δ is the energy shift due to the positive charging of the sample. A non-uniform distribution of surface charging can arise in some samples (*e.g.* fluorographites[66]) leading to a broadening of the photoelectron peaks as Δ varies over the sample surface. Such cases may be revealed by applying a bias voltage of the order of 10-20V to the sample, the broadening is increased until the domains become resolvable.

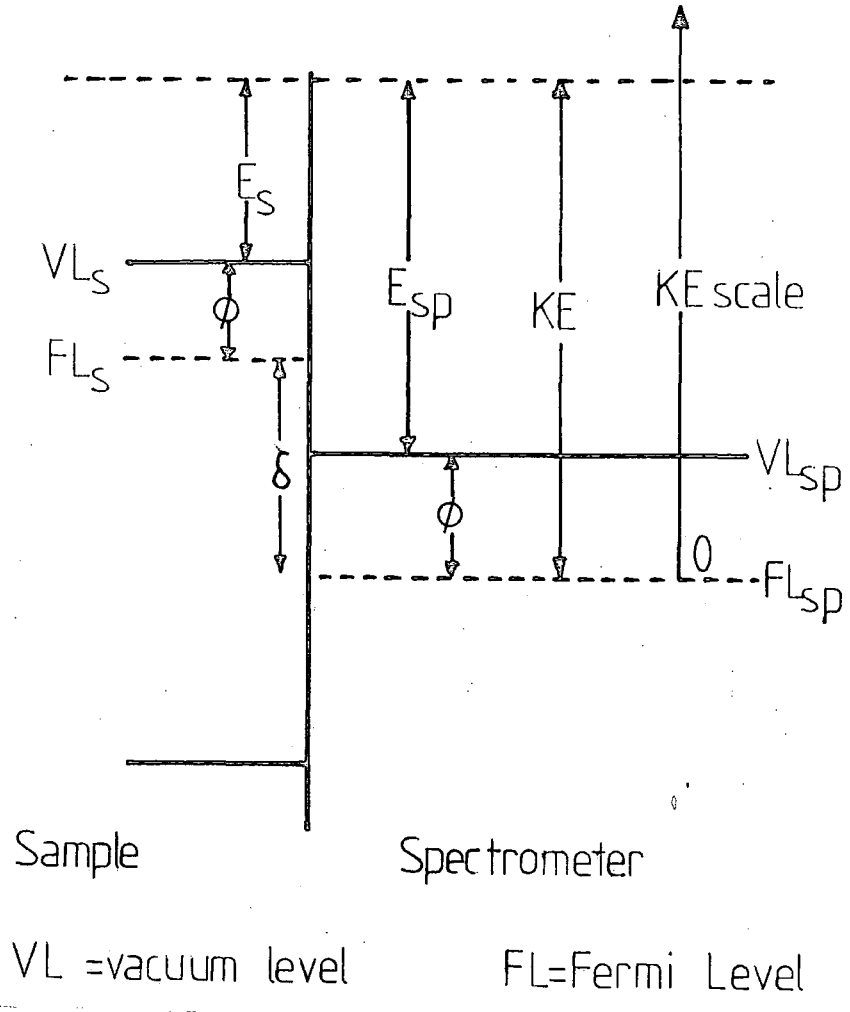

Figure 1.8 Relationship between the vacuum level and Fermi level for a sample isolated from the spectrometer

Charging may be detected by varying the incident electron flux on the sample using a low energy electron flood gun.[67] If charging is present, this extra flux will cause the photoelectron peaks to move to lower apparent binding energy. The use of flood guns is especially useful in work involving monochromatised X-ray sources, here the secondary electron flux from the adjacent window of an X-ray gun is not present, in its absence insulating samples may charge dramatically.[69,70] However samples can become negatively charged due to overcompensation. (In optimising the electron flux, one criterion of it used, is the line width of the photoemission peaks, some workers having minimised this quantity do not seem perturbed by the negative charging exhibited by the sample).

An alternative approach to the problem has been to illuminate the sample chamber with U.V. radiation from a low pressure, low power mercury lamp through a quartz viewpoint.[68] Sufficient secondary electrons are generated from the sample chamber walls to reduce charging to a low level.

In the case of polymeric samples and indeed many samples the most facile method of circumventing the problems of energy referencing caused by sample charging is by the use of a suitable reference peak. The observed shift in this reference peak is then used to correct the kinetic energies of other peaks observed in the spectra and thus find their true binding energies. The most commonly used calibrants used in polymer investigations are the C_{1s} peak due to (CH_2) environments either inherent in the sample or in adventitious hydrocarbon deposited as a contaminant layer in high vacuum at 285eV.[8,96], or the use of the $Au_{4f_{7/2}}$ level at 83.8eV, if the sample has been deposited on a gold substrate.

Other methods employed have included the gold decoration of the sample surface which is fraught with difficulties involved with islanding and chemical reaction[71-73] with the substrate. The implantation of argon ions and the use of the Ar_{2p} lines of the implanted argon as a reference has also been suggested.[74]

A detailed study of sample charging phenomena and the ESCA analysis of polymer samples was made by Clark, Dilks and Thomas.[69,70] Sample charging was found to be a sensitive probe of the outermost few tens of Angstroms of a sample in its own right. Over a wide range of operating conditions equilibrium sample charging shifts were found to be characteristic of, and show a strong dependence upon, the total photoionisation cross-section of the sample. The changes in charging with increasing hydrocarbon contamination were also observed. A strong correlation between the fluorine content of a surface and the equilibrium charging attained was noted for an ethylene-tetrafluoroethylene copolymer defluorinated by exposure to an argon plasma.[75-78] A similar correlation has been observed for the defluorination of PTFE by a hydrogen plasma (see Chapter Three).

1.7 Linewidths and Lineshape Analysis

The large inherent linewidths of core level signals in ESCA spectra,[8] comparable in magnitude to the magnitude of chemical shifts to a system has necessitated the use of curve-fitting procedures for accurate lineshape analysis to delineate the core environments within a given envelope. The dominating contribution to broad linewidths comes from the inherent line-

width of the polychromatic X-ray photon source normally used, this can be improved by the use of monochromatized X-ray sources. Even using monochromatized sources the requirement for lineshape analysis remains to fully quantify the available information.

The measured linewidth for a core level may be expressed as a convolution of several effects.

$$(\Delta E_m)^2 = (\Delta E_x)^2 + (\Delta E_s)^2 + (\Delta E_{cl})^2 \qquad (1.8)$$

where ΔE_m is the observed FWHM of the photoelectron peak,

ΔE_x is the FWHM of the exciting X-ray source, *ca* 0.7eV for $Mg_{K\alpha_{1,2}}$ source, 0.9eV for $Al_{K\alpha_{1,2}}$,

ΔE_s is the contribution to the FWHM due to the spectrometer (*i.e.* analayser aberrations, slit widths),

ΔE_{cl} is the natural width of the core level examined. This also includes the solid state broadening effects not directly associated with the life-time of the core-hole state for solid samples, including variations in chemical shift due to differences in lattice environments.

The contributions to the overall line shape of the X-ray source and the core-level are essentially Lorentzian in character. The spectrometer resolution function represents a Gaussian contribution to the overall lineshape. The convolution of these various factors leads to a hybrid shape, essentially Gaussian but with Lorentzian character in the tails. For insulators it has been shown that the assumption of a pure Gaussian lineshape for observed peaks introduces only a small error in the lineshape analysis.[10] However in the case of

metals the use of symmetric lineshapes may be inappropriate,[80] even in the examination of polymer surfaces the validity of using symmetric lineshapes in determining the overlapping peaks in complex XPS spectra has been questioned.[81] A variety of lineshapes have been proposed such as Lorentzian functions,[82] linear and product combinations of Gaussian and Lorentzian functions[79,83] and composite functions with an asymmetric tailing to lower kinetic energies.

The resolution of complex lineshapes may be aided by the mathematical enhancement of resolution to deconvolute instrumental and source broadening factors from the observed spectra by iterative or Fourier transform techniques. Such methods have been reviewed by Carley and Joyner,[84] Ebel and Gurker[85] and Wertheim.[86]

Such deconvolutions aid curve-fitting techniques by improving resolution and thus aiding component identification in complex lineshapes, however component analysis is still required.

In the analysis of peak profiles both digital and analogue aids (such as the Dupont 310 Curve Resolver) are available for the synthesis of peak shapes from a variety of peak shapes and their comparison with the experimentally acquired data. Such systems allow close control to be exercised over the position, width and height of the component variables. However such curve-fitting procedures require a sound theoretical background to obtain meaningful results, the solutions produced are rarely unique and must be examined in the chemical context, *i.e.* is it chemically sound and consistent with data given by other core levels examined or other spectral features? The essential philosophy behind lineshape analysis is outlined in Figure 1.9. An

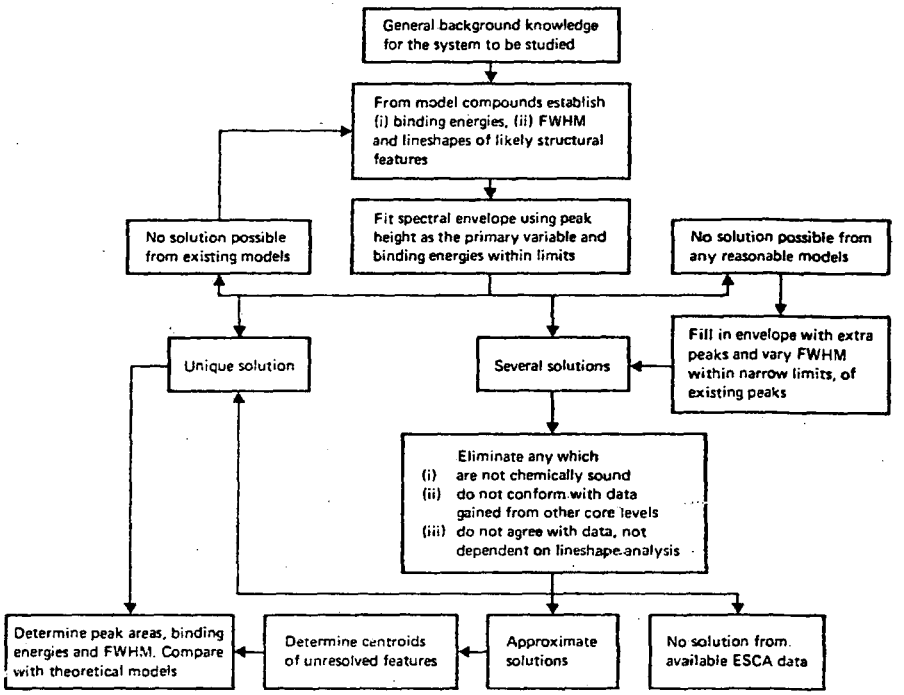

Figure 1.9 Lineshape analysis by curve-fitting; flowchart of procedure

example of curve-fitting of a C_{1s} level of a polymer, polyethylene terephthalate, is given in Figure 1.10. In the work in this thesis curve-fitting has been performed both by analogue simulation using Dupont 310 curve resolver for data acquired in analogue form and digitally, using the data analysis package of the DS300 data system attached to the larger, ES300 spectrometer.

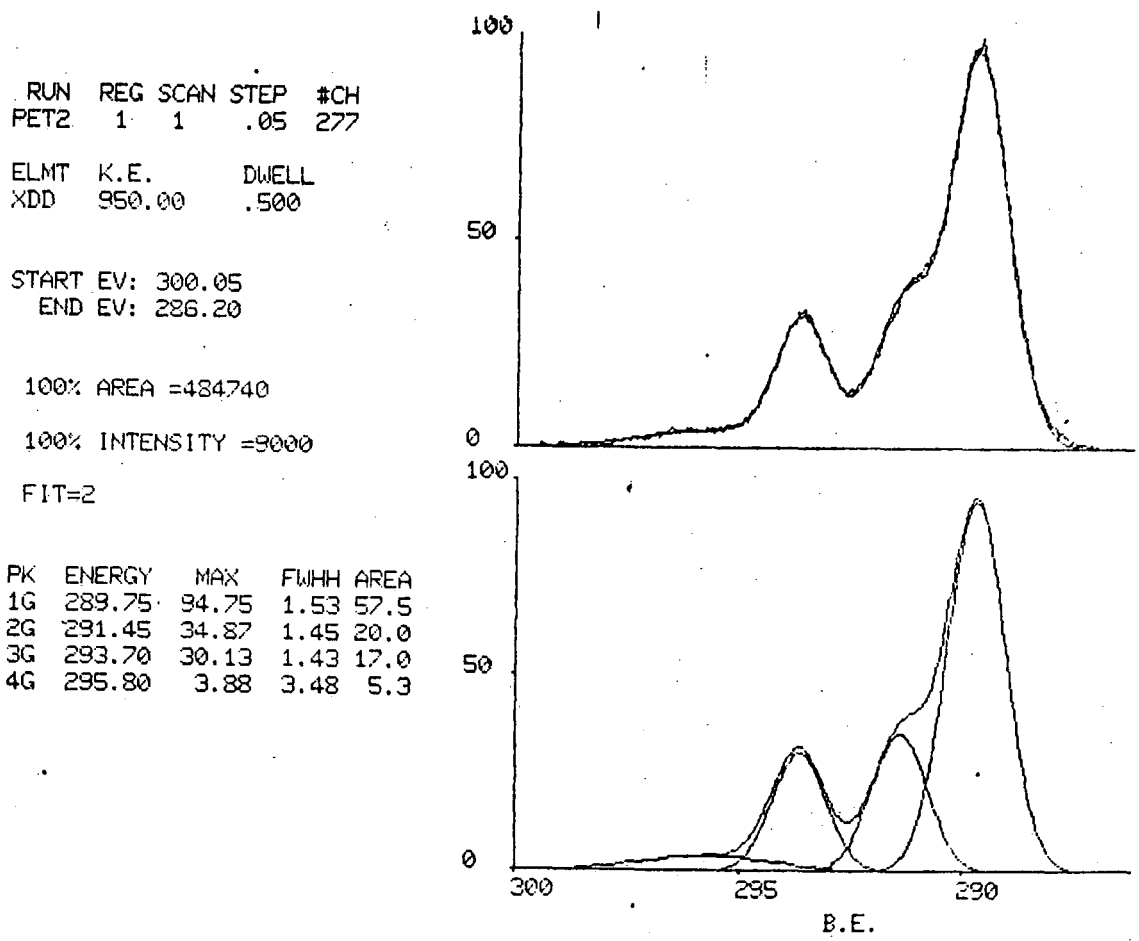

Figure 1.10 Polyethylene terephthalate (PET)

1.8 Signal Intensities

The general geometry of the ESCA experiment employing a fixed arrangement of analyser and X-ray source is in Figure 1.11; $h\nu$ represents the incident X-ray flux and e^- the fraction of the electrons which enter the analyser. ϕ is the angle between the incident X-rays and the analyser entrance slit. θ describes the angle of the escaping electrons with respect to a direction normal to the sample's surface. Electrons emitted from a point a depth d below the sample's surface thus travel a distance $d/\cos\theta$ in the sample to escape from the sample's surface. Due to the short mean free paths of

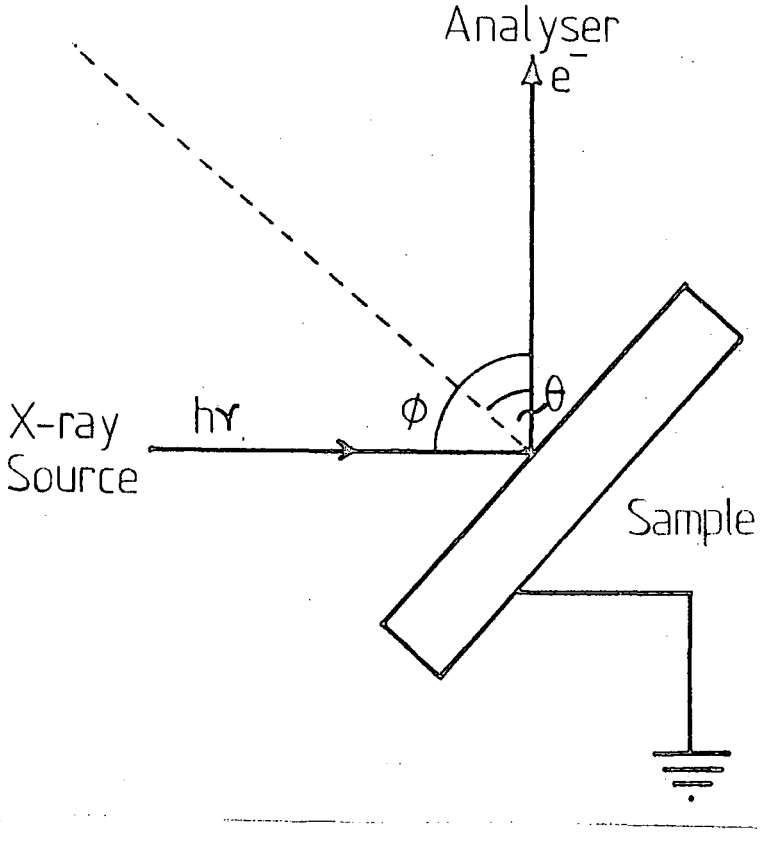

Figure 1.11 Schematic of sample geometry relative to the X-ray source and analyser

electrons in solids (see Section 1.9), by varying the "take-off" angle θ it is possible to analyse electrons originating from surface and subsurface regions of the polymer. At high values of θ electrons must travel longer distances in the sample to escape the sample's surface, only those electrons originating from the surfacemost regions will escape without experiencing inelastic collision and thus losing their characteristic energy and hence the information they convey. Thus variable take-off angle studies offer the possibility of the analytical depth profiling of a surface. (Returning to Figure 1.11 - in the spectrometers used in this investigation: ES200AA/B $\phi = 90^{o}$, in the case of the ES300 equipped with the Ti/Mg dual anode source ϕ is fixed but less well defined $\sim 70^{o}$).

Considering an infinitely thick homogeneous sample, the inelastic photoionisation peak intensity for photoelectrons originating from a core level is given by:

$$dI_i = F\alpha_i N_i k_i e^{-x/\lambda_i} dx. \qquad (1.9)$$

where I_i is the intensity arising from a core level i

F_i is the exciting photon flux (not considered to be attenuated over the ESCA sampling depth).

α_i is the photoionisation cross-section for core level i

k_i is a spectrometer factor

N_i is the number of atoms per unit volume on which the core level is is localised

λ_i is the inelastic mean free path of electrons emitted from core level i.

Integration of this equation gives:

$$I_i = \int_0^\infty F\alpha_i N_i k_i e^{-x/\lambda_i} dx \qquad (1.10)$$

and $$I_i = F\alpha_i N_i k_i \lambda_i \qquad (1.11)$$

Examining these parameters in more detail:

F, the X-ray flux depends primarily upon the operating power and efficiency of the X-ray gun,

α_i the cross-section for photoionisation for a given core level,

i describes the probability that a core level will be ionised when irradiated by a photon of a given energy,[87] being a function both of the core level and the energy of the incident photon. The α_i is also dependent upon the angle of detection with respect to the angle of incidence of the photons ϕ hence is also weighted to include only those electrons emitted within the acceptance angle of the analyser lens system. The total photoionisation cross section, α_i, is given by[88-89]

$$\alpha_i = \frac{\alpha_i^{TOT}}{4\pi} \left[1 - {}^1/_4 \beta_i (3\cos^2\phi - 1) \right] \qquad (1.12)$$

α_i^{TOT} is the total cross-section of the core level i, and β_i the asymmetry parameter for that level. For a given spectrometer ϕ and hence α_i is normally constant. The cross sections α_i may be calculated from fundamental atomic properties[87] or determined experimentally.[10] The cross-sections for photoionisation of most elements to $Mg_{K\alpha_{1,2}}$ and $Al_{K\alpha_{1,2}}$ radiation are within two orders of magnitude of that of the C_{1s} levels,[87] and hence has a convenient sensitivity range to many elements.

k_i the spectrometer factor is an instrument dependent parameter reflecting the efficiency of the detection system and the transmission of analyser to electrons of various kinetic energies

and the solid angle of acceptance of the analyser. It also depends on the mode in which the analyser is operated, present retard energy (FAT) or present retard to pass energy ratio (FRR).

The inelastic mean free path of the photoemitted electrons in the medium from which they are emitted, is defined as the distance in the solid that electrons of a given energy can travel before $^1/_e$ of them have not suffered energy loss through inelastic collision. This quantity may be calculated theoretically[90] or determined experimentally.[91-93] λ_i is a function of electron energy ranging from about 4Å for electrons of energy 80eV to about 40Å for electrons of ∿4000eV kinetic energy. Another useful quantity, the sampling depth (often confused with λ_i) is the depth from which 95% of the signal from a given core level is derived,

$$\text{Sampling depth} = -\lambda \ln 0.05 \approx 3\lambda \qquad (1.13)$$

and is a useful quantity in discussing the surface sensitivity of ESCA data.

The final quantity n_i, the number of atoms per unit volume on which the core level is is localised. Thus it can be seen from equation 1.12 that the relative intensities of core levels will be related to the overall stoichiometry of the atoms in the sample. Thus for two core levels i e j

$$\frac{I_i}{I_j} = \frac{F\alpha_i N_i k_i \lambda_i}{F\alpha_j N_j k_j \lambda_j} \qquad (1.14)$$

If i and j correspond to differing chemical environments of the same core level

$$\frac{I_i}{I_j} = \frac{N_i}{N_j} \quad F\alpha_i N_i k_i \lambda_i = F\alpha_j N_j k_j \lambda_j$$

If however i ≠ j, then rearranging (1.14)

$$\frac{N_i}{N_j} = \frac{I_i}{I_j}\left(\frac{k_j \alpha_j \lambda_j}{k_i \alpha_i \lambda_i}\right)$$

the bracketed quantity, the sensitivity factor may be determined experimentally from samples of known stoichiometry. These quantities are spectrometer dependent.

1.9 Analytical Depth Profiling

Often in the analysis of polymer surfaces by ESCA the situation is encountered where the composition of the surface layers differs from that of the bulk or subsurface, there may be a smooth gradient from a surface composition to the bulk composition with depth or more commonly, a contamination layer may be present on the surface. Examining the latter case from which a treatment of the former may be developed:-

Consider a sample to be divided into an overlayer of material of depth d, of differing composition to the substrate on which it lies as shown in Figure 1.12. The signal arising from the overlayer alone may be expressed from equation 1.9 integrating between x=0 and x=d as:

$$I_i^{over} = F\alpha_i N_i k_i \lambda_i \left(1-e^{-d/\lambda_i}\right) \qquad (1.15)$$

Similarly integrating between x=d and x=∞ the signal derived from the substrate is:

$$I_j^{sub} = F\alpha_j N_j k_j \lambda_j e^{-d/\lambda_j} \qquad (1.16)$$

These expressions are derived for the case where photoelectrons escape normal to the sample surface but are readily adaptable

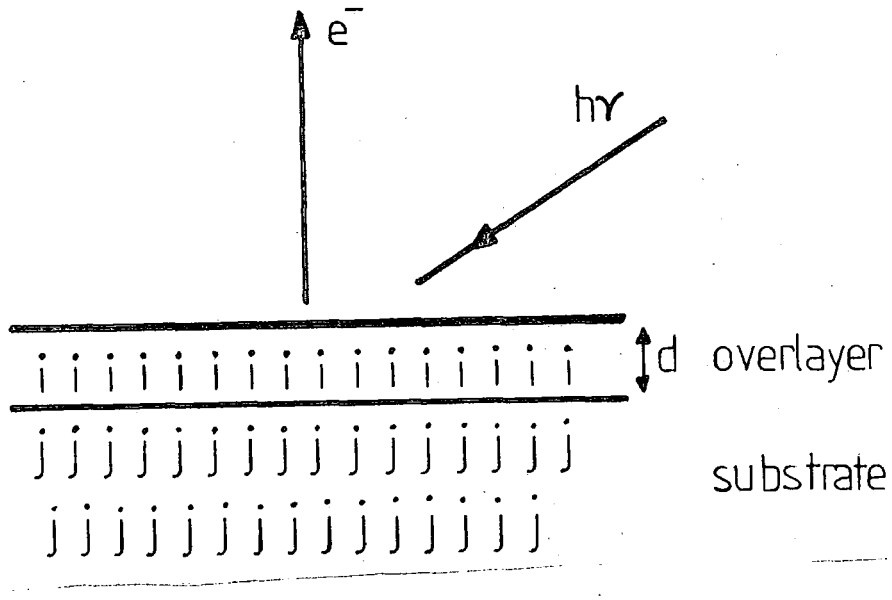

Figure 1.12 Substrate-Overlayer Model

to the case of angular dependent measurements. For a take-off angle of

$$I_i^{over} = F\alpha_i N_i k_i \lambda_i \left(1-e^{-d/\lambda_i \cos\theta}\right) \qquad (1.17)$$

and

$$I_j^{sub} = F\alpha_i N_i k_i \lambda_i \, e^{-d/\lambda_i \cos\theta} \qquad (1.18)$$

Thus it can be seen as $\theta \to \pi/2$ that the signals derived from the overlayer come to dominate the spectra. Beyond the simple substrate-overlayer model by the appropriate subtractions and additions of equations 1.16 and 1.17 the contribution to the observed spectrum at a given take-off angle of any layer within the sample may be determined. Thus it can be seen how the sampling depth varies with take-off angle.

Consideration of the general correlation between the electron mean free paths and electron kinetic energy as illustrated by Figure 1.13 shows that in the energy range of interest to ESCA (>300eV), the mean free path increases with kinetic energ

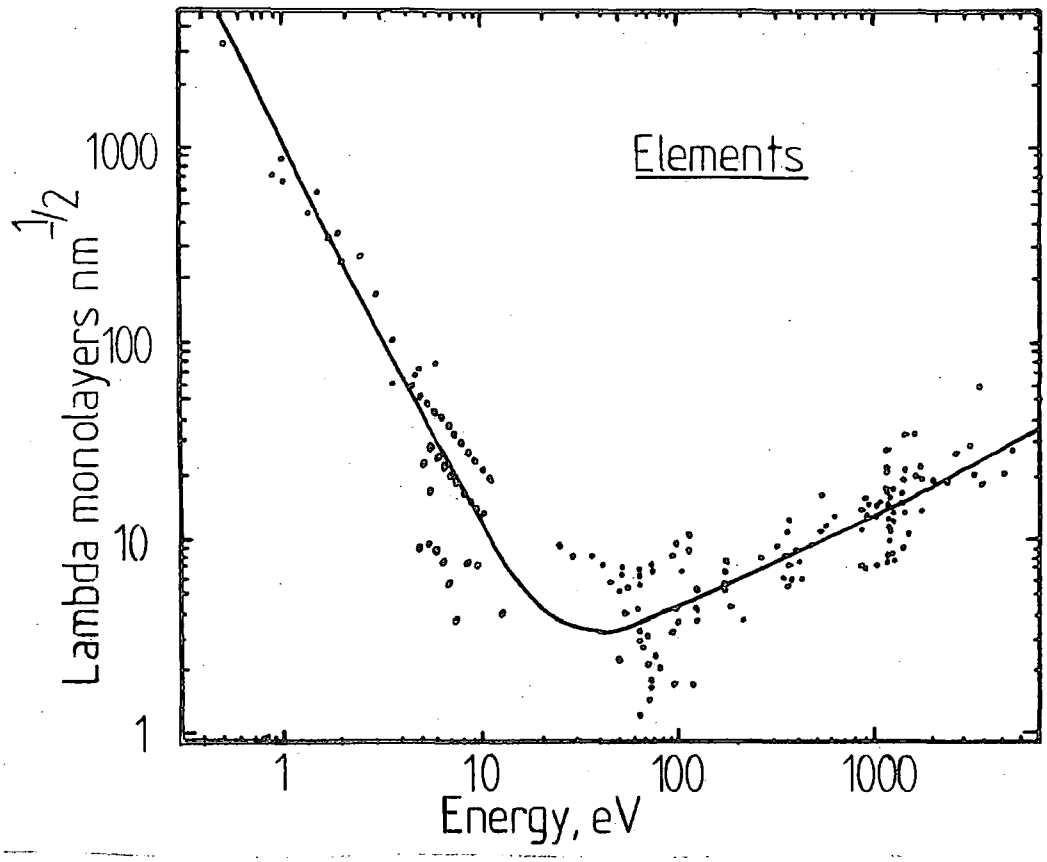

Figure 1.13 Inelastic mean free paths of photoemitted electrons

Thus the attenuation of a signal derived from the substrate by an overlayer will depend strongly on the kinetic energy of the photoemitted electron. This may be exploited in a number of ways. With a given exciting photon energy, the ratioing of two core levels from a given atom, *e.g.* the F_{1s} and essentially core like F_{2s} in a fluoro polymer surface. The F_{1s}/F_{2s} ratio will serve as a measure of the vertical homogeneity of the surface. If a surface is defluorinated in the very surface or covered by a hydrocarbon overlayer the attenuation of the F_{1s} signal by the overlayer will be more marked than for the F_{2s} signal, hence the F_{1s}/F_{2s} intensity ratio will decrease.

If exciting radiation of higher photon energy, *e.g.* a $Ti_{K\alpha_{1,2}}$ (4510eV) source is used, the kinetic energies of electrons emitted from the same levels as studied with the softer

$Mg_{K\alpha_{1,2}}$ source will be correspondingly higher and hence possess longer inelastic mean free paths.[93] Hence a harder source is seen to possess a greater sampling depth (equation 1.13).

Thus from a combination of variable take-off angle measurements over a series of levels and by the use of a variety of X-ray sources a depth profile of the distribution of various components in a surface may be built up.

1.10 The ESCA Instrumentation

The work presented in this thesis was carried out on two spectrometers, an AEI ES200 AA/B and a customised KRATOS ES300 spectrometer. Though they differ in detail of design; the basic principle of operation is the same in each case. A schematic of the essential components of an ESCA spectrometer is given below in Figure 1.14 showing:

(1) X-ray source
(2) Sample chamber
(3) Electron energy analyser
(4) Electron detection and data handling.

1.10.1 X-ray Sources

In each spectrometer, the primary excitation source is an X-ray gun of the Henke or hidden filament type,[94] which protrudes into the source region but is isolated from it by a thin aluminium foil window. The function of the window is to protect the X-ray source from contamination from the sample analysis chamber and to prevent excessive background interference from stray electrons from the X-ray source. To reduce

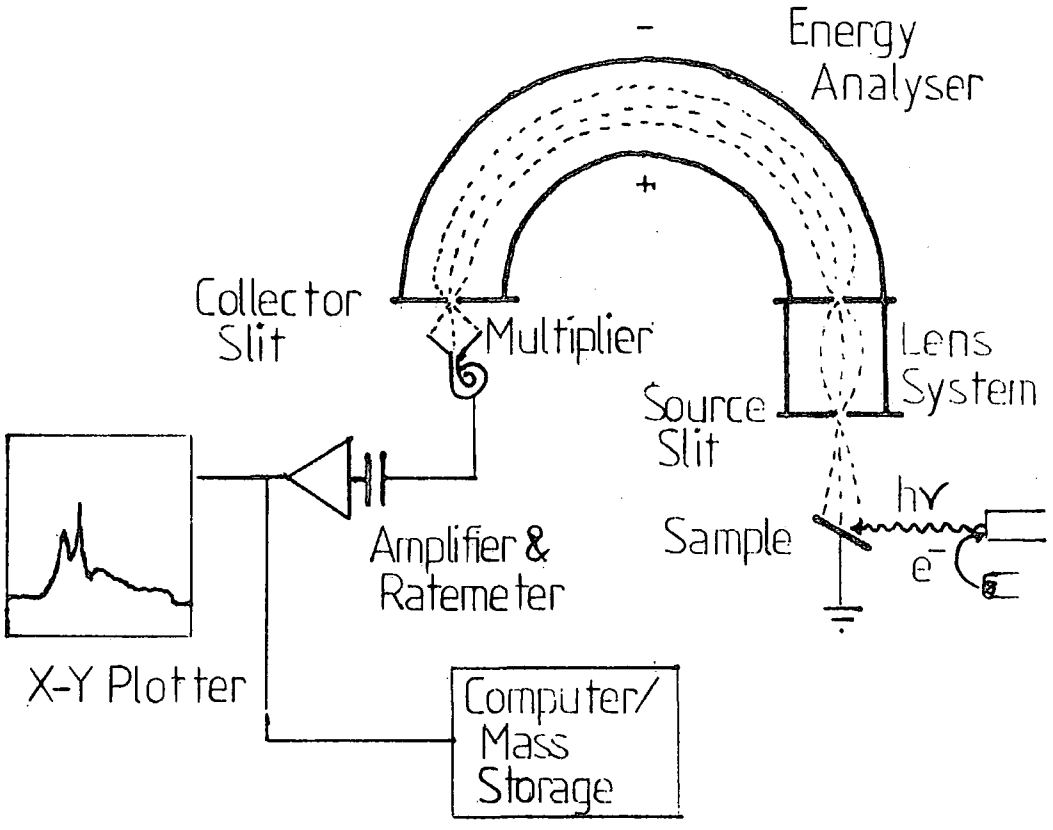

Figure 1.14 Schematic of ESCA Instrumentation

the risk of X-rays being generated from collision of electrons with the window the emission filament is operated at near ground potential, whilst the target operates at high positive potential *ca* +10-+15kV. A target is characterised by the photon energy of its characteristic line and the width of that line. For monochromatized Mg and Al X-ray sources the component line widths are ∿0.6eV and ∿0.9eV respectively.[8] The photon energy determines the highest binding energy of electrons that can be excited and hence their kinetic energies and mean free paths.

A typical non-monochromatic X-ray spectrum for a tungsten anode is shown in Figure 1.15, the spectrum consists of the characteristic line spectrum of the anode superimposed on a

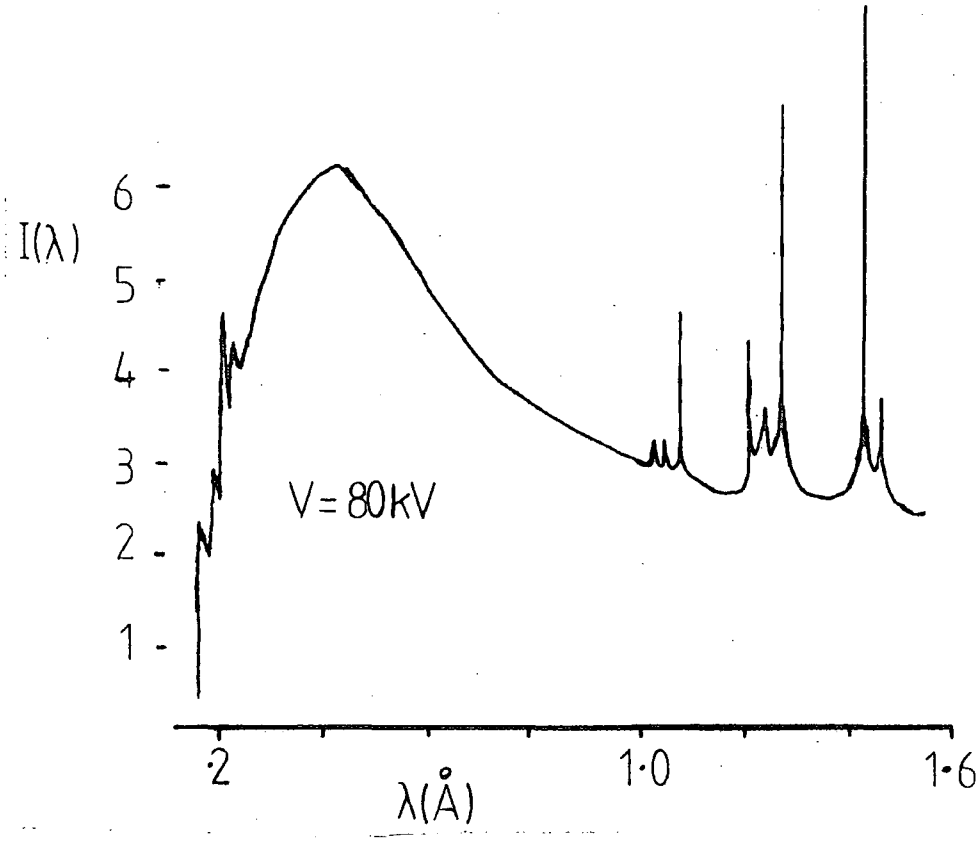

Figure 1.15 X-Ray emission spectrum from a tungsten anode

continuum (bremsstrahlung),[111] the intensity of the characteristic lines relative to the continuum of the bremsstrahlung depending upon the operating conditions in particular the accelerating voltage used.

Soft X-ray sources are most commonly employed in ESCA *e.g.* $Mg_{K\alpha}$ ($h\nu$ = 1253.6eV) and $Al_{K\alpha}$ ($h\nu$ = 1486.6eV). Harder X-ray sources such as $Cu_{K\alpha}$, ($h\nu$ = 8048eV) and $Cr_{K\alpha}$, ($h\nu$ = 5415eV) finding only occasional use. The $Ti_{k\alpha}$ source of intermediate energy, 4510eV has also been used. The use of these harder X-ray sources is likely in future Auger work.

The ES200 AA/B spectrometer is equipped with a single $Mg_{K\alpha}$ source of Henke design driven by a Marconi Elliott GX5 high voltage supply with integrally variable voltage in the region of 0-60kV and 0.80mA emission current. Under normal operating conditions the flux of X-rays is of the order of 0.1 rads s^{-1}.[95]

The ES300 spectrometer is equipped with a dual-anode X-ray gun.[108] with magnesium and titanium targets and a monochromatised $Al_{K\alpha_{1,2}}$ X-ray source.[10] The monochromatised source employs a microfocus X-ray gun and diffraction from quartz crystals cut parallel to the $10\bar{1}0$ plane and the appropriate Bragg angle of 78.5° to achieve X-ray line widths of ∿0.2eV. A range of other monochromatic X-ray sources have also been used.

Under normal operating conditions the X-ray fluxes employed cause little or no radiation damage to the majority of systems, that is to say, the spectra obtained show no time dependence under X-ray irradiation. Certain systems (in particular chloro-polymers), do display evidence of degradation (*e.g.* dehydrochlorination) under X-ray irradiation. One of the most notable exceptions is poly(thiocarbonyl fluoride) which rapidly depolymerises under X-ray irradiation. The polymers studied in this thesis did not, in the main, show any such evidence of degradation at least during the timescale of the measurement. It has been shown that under irradiation from the harder $Ti_{K\alpha}$ source cellulose nitrates[104] decompose and the well-known X-ray induced degradation of polyvinylchloride also proceeds rapidly.[105] Whilst not showing any evidence of degradation under irradiation by the $Ti_{K\alpha}$ source in terms of a time dependence of the spectra obtained, prolonged irradiation of PTFE was marked by embrittlement of the sample. Working at higher X-ray fluxes, Wheeler and Pepper[106] have studied the X-ray degradation of PTFE on prolonged exposure.

An extensive survey of the photon sources commonly employed in photoelectron spectroscopy has been compiled by H. Siegbahn.[107] Synchrotron radiation has also, with monochromatisation, been

used in photoelectron spectroscopy; providing continuously variable photon energies from 20eV up to 1000eV with a variety of monochromators. Such sources provide polarised radiation.

The characteristic emissions of Mg and Al anodes used in ESCA are derived from K series transitions. In addition to the $K\alpha_{1,2}$ line a series of satellites to this main exciting line are also present, giving rise to satellite peaks in the photoemission spectra. These satellites may be removed from the exciting radiation by monochromation or their artefacts, satellites present in the photoelectron spectra may be removed by appropriate numerical manipulation. The position and intensity of these satellites relative to the major peak is given below in Table 1.3.

TABLE 1.3 X-Ray Satellite Energies and Intensities[50]

Kα		$\alpha_{1,2}$	α_3	α_4	α_5	α_6	β
Mg	displacement (eV)	0	8.4	10.2	17.5	20.0	48.5
	Relative Intensity	100	8.0	4.1	0.55	0.45	0.5
Al	displacement (eV)	0	9.8	11.8	20.1	23.4	69.7
	Relative Intensity	100	6.4	3.2	0.4	0.3	0.55

1.10.2 Sample Analysis Chamber

Figures 1.16 and 1.17 display schematic drawings of the ES200 AA/B and ES300 spectrometer sample analysis chambers, indicating the relative positions of the sample, X-ray sources and analyser. The sample chambers are in each case equipped with a variety of access ports and viewports.

Figure 1.16 Schematic of ES200 Sample Analysis Chamber (SAC)

A. Analyser. B. $Mg_{K\alpha}$ X-ray Source. C. $Al_{K\alpha}$ X-ray Source.
M. Monochromator. S. Sample Analysis Position.
V. Viewport.

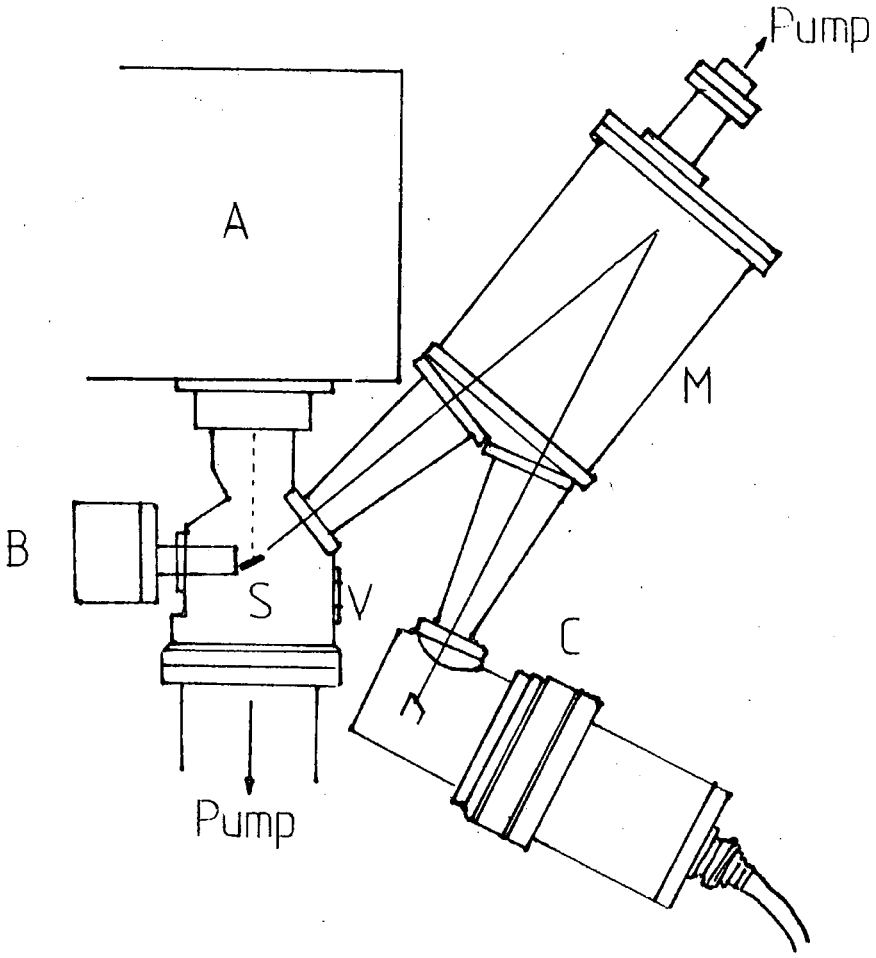

Figure 1.17 Schematic of ES300 Sample Analysis Chamber (SAC)

A. Analyser. B. To Pumping. C. Catcher Tray. D. Penning Gauge. F. AG5 Ion Gun and Wien Filter. H. Viewport. I. Sample Insertion Lock. J. Insertion Lock for Reservoir Shaft. K. Unused. L. Viewport. M. To Monochromated $Al_{K\alpha 1,2}$ Source. P. Insertion Probe. S. Sample in Analysis position in front of X-ray source.

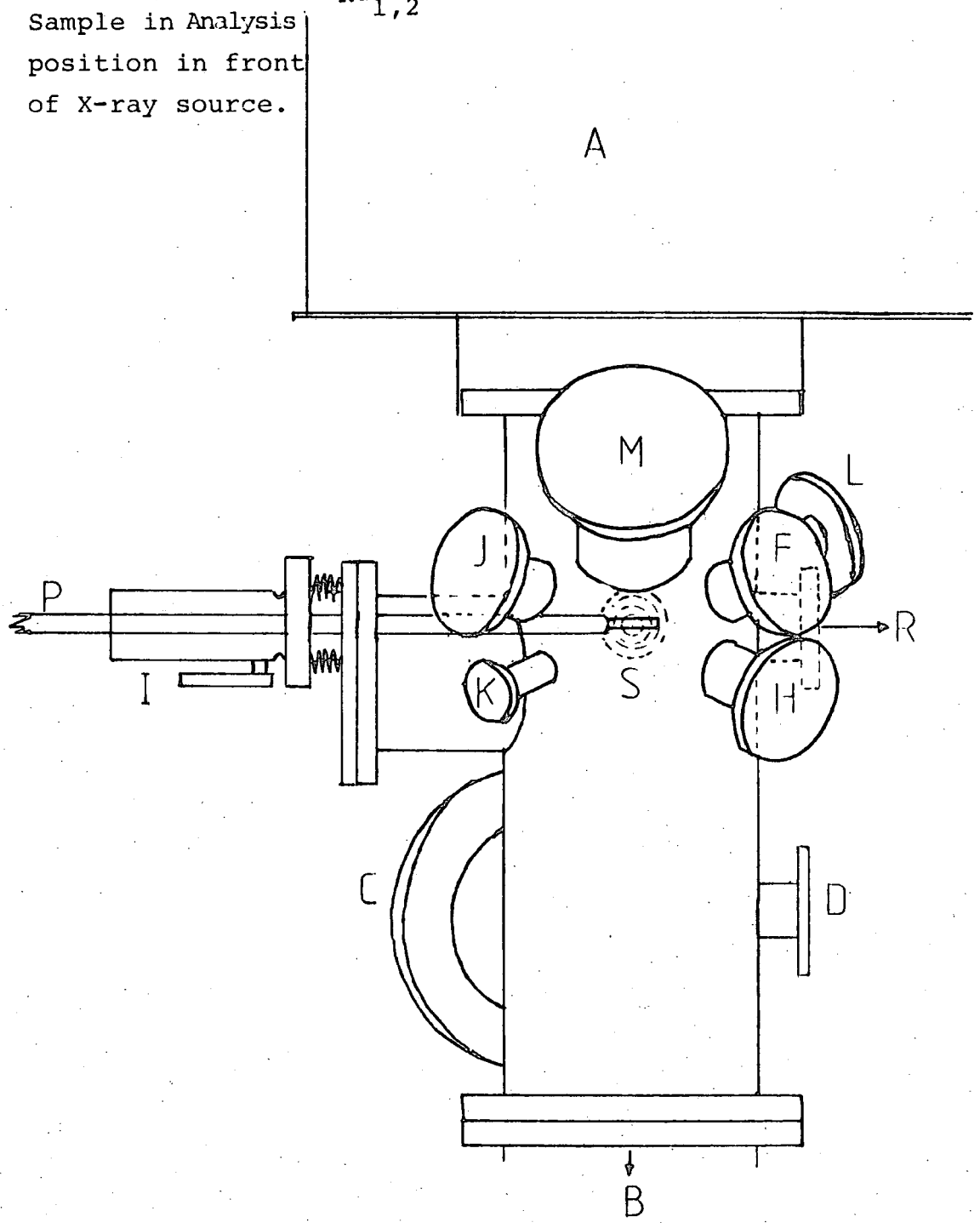

In each case fast entry insertion locks permit rapid sample introduction. Reaction chambers for '*in situ*' sample treatments may be attached to these insertion locks. The larger ES300 spectrometer also possesses a sample preparation chamber independently pumped by an Edwards E04 diffusion pump with a long-life cold trap backed by an Edwards EDM6 rotary pump. This chamber may be used at pressures between atmospheric and ultra high vacuum ($<10^{-10}$torr) without adversely affecting the pressure in the sample analysis chamber. This sample preparation chamber is also equipped with an electron gun (VG LEG31) a variety of view posts, and three insertion locks so as to provide for the simultaneous deposition of material from 2 reservoir shafts.

The ES200 sample chamber and analyser are independently pumped by liquid nitrogen cold trapped diffusion pumps, as is the X-ray source. The ES200 spectrometer operates typically at a base pressure of 2×10^{-8} torr. The ES300 spectrometer employs electrically driven turbomolecular pumps for pumping of the sample chamber and analyser regions, using Alcatel 370 ls^{-1} and 120 ls^{-1} pumps respectively. The dual anode X-ray gun and monochromator are pumped by small ion pumps. The base pressure in this system is typically 2×10^{-9} torr.

1.10.3 Electron Energy Analyser

Both spectrometers employ hemispherical double focusing analysers based upon the principle described by Purcell.[109] The analyser is screened from external magnetic fields by Mu-metal shields. A survey of the various types of the various types of analysers that have been employed in

electron spectroscopy and the principles behind their action is given in reference. For ESCA an analyser must be capable of resolution of at least 1 in 10^4. The analyser resolution is related to R, the mean radius of the hemispheres and the combined width of the source and collector slits, W, by

$$\frac{\Delta E}{E} = \frac{W}{R} \qquad (1.19)$$

Resolution may be improved by:

(1) Reducing the slit widths, which also reduces the intensity
(2) Increasing the radius of the hemispheres
(3) By pre-retarding the electrons prior to their entry into the analyser.

In practice a compromise is made on slit widths and the radii of the hemispheres so as to obtain reasonable count rates. A focusing and retarding lens arrangement is also used to slow the electrons prior to entry into the analyser thus reducing the resolution requirements of the analyser. The lens system[112] allows the analyser to be located a convenient distance physically from the sample. Lens systems have been developed which allow the area sampled by the analyser to be varied, the analyser may be zoomed in and out. The next logical step is to develop an imaging system around such a lens system perhaps as an alternative to the magnetic lens system developed by Turner[110] *et al.*

The analyser may be operated in two modes:

(1) The retarding potential applied to the lens is scanned and the pass energy as dictated by the potential applied across the hemispheres, is kept constant,

or (2) Scanning the retarding potential and the potential between the analyser hemispheres in unison, keeping a constant ratio between the two potentials.

The first method of fixed analyser transmission, (FAT), has greater sensitivity at lower kinetic energies ($S\alpha^{1}/E$), resolution being fixed throughout the scan range. The second, fixed retardation ratio, (FRR), has greater sensitivity at higher kinetic energies ($S\alpha E$), resolution is not here constant throughout the scan range. In this work the FRR mode has been exclusively employed. A discussion of the sampling area and sensitivity of the analysers on the ES200 and ES800 machines together with those of other commercial spectrometers has recently been given by Seah.[115]

1.10.4 Electron Detection and Data Acquisition

Electrons emerging from the exit slit of the analyser pass into the inlet aperture of a channeltron electron multiplier. The output pulses from the multiplier are amplified by a head preamplifier and fed to a data handling system to generate ESCA spectra by one of two methods -

(1) The continuous scan, the pass energy of the analyser is ramped in a linear fashion with time from a start KE, a ratemeter monitoring the signals from the multiplier, thus a plot of counts per second versus kinetic energy of the electrons may be plotted on an X-Y recorder.

(2) The step scan. The pass energy of the analyser is increased in preset increments. At each step the counts are (a) measured for a fixed time, or (b) a fixed number of counts are timed. The data from such step scans is

then stored in a multichannel analyser or transferred directly *via* a suitable interface to a mini or microcomputer based data system to be recorded on hard or floppy discs. In this fashion many scans can be accumulated to average out random fluctuations in background, and thus the signal to noise ratio of the final spectra improved.

Over prolonged periods of data acquisition, care must be taken to avoid artefacts such as sample decomposition, time dependent charging or hydrocarbon contamination which will produce erroneous spectra. By the same token computerised system is an ideal method to study such phenomena.

The advent of multidetector arrays not only opens up the possibility of vastly increased rates of data acquisition (through the simultaneous acquisition of data over many spectral elements) but also of another method of photoelectron spectroscopic imaging.

The spectrometers used in this study can both produce spectra in analogue form on an x-y plotter, additionally the ES200 can record spectra digitally using a multichannel analyser. In its normal mode of operation the ES300 spectrometer is controlled by the KRATOS DS300 data system.

The DS300 data system is based on an LSI-11 minicomputer running under RT-11. Data acquired is stored on floppy disc. In addition to controlling the acquisition of data by the spectrometer permitting the repeated scanning of up to 10 regions, the data system also provides for the simultaneous analysis of data. The data analysis package provides for, *inter alia*, the addition, comparison, subtraction, differentiation and integration of spectra, the subtraction of satellites from spectra and a peak fitting/synthesis package.

1.11 Sample Handling

1.11.1 Solid Samples

Solid samples in the form of films or powders may conveniently be studied mounted on to the spectrometer probe tip using double sided "Scotch" adhesive insulating tape, such sample mounting immediately results in sample changing effects. This can be avoided by the deposition of the sample as a thin film onto a gold substrate by evaporation of a solution or by sublimation, for example. Powdered samples may also be pressed into a gauze or a soft foil such as indium. More awkward samples such as strips or wires may be mounted in a sample chuck.

A typical sample insertion probe has facilities for the heating and cooling of the sample between liquid nitrogen temperatures and +600^{o}C, by electrical heating. The cooling of the sample enables volatile solids to be studied. Volatile solids are often studied by the sublimation of a sample from a capillary tube to a cooled probe tip.

1.11.2 Liquids

The study of liquids by ESCA is less well developed. The vapour pressures of many liquids and solvents at room temperature are greater than 0.1 torr, thus heavy differential pumping is required to reduce the pressure over a short distance. The sample must also be renewed rapidly and it should be possible to distinguish the gas and liquid phase spectra. These criteria have led to the development of a number of specialised sub-millimeter[113] liquid beam arrangements and methods based upon wetted metal surfaces.[114]

More routinely liquids may be introduced *via* injection into a heatable (25^{o}-150^{o}C) evacuated reservoir shaft. Effusion of this material through a Metrosil leak into high vacuum, and its condensation on to a pre-cooled gold plate attached to the tip of a sample probe produces a sample surface which is being continuously renewed, in this way contamination and radiation effects are reduced.

1.11.3 Gases

Gases may be studied either in the condensed phase using a cooled probe or using purpose built gas cells and differential pumping, in the gas phase.[23]

Such studies in the gas phase have the advantage of the elimination of solid state broadening and sample charging effects, (energy referencing is easily achieved by the admixing of a reference gas, *e.g.* Neon, with the sample of interest). Radiation damage is of no importance unless the sample is recirculated. Inelastic losses (extrinsic processes) and shake-up and shake-off (intrinsic processes) may be distinguished by varying the sample pressure. The absence of so many complicating factors makes the direct comparison of experimentally derived and theoretical parameters simpler.

1.12 ESCA: An Appraisal

ESCA as should be apparent from the aforegoing discussion, is a technique wide ranging in its scope and capabilities;

(1) The technique gives absolute binding energies, relative peak areas and shifts in binding energies: thus permitting

elemental analysis and mapping in solids, identification of structural features, short range effects directly, and longer range indirectly.

(2) Shake-up and shake-off satellites may be observed, their energy separation with respect to the direct photoionisation peaks and relative intensities of components of singlet and triplet origin yield more long and short range information.

(3) Multiplet effects enable the spin states of systems to be interrogated.

(4) Valence levels provide a probe for longer range effects.

(5) Angular dependence studies enable depth dependent data to be obtained for solids. For gases the angular dependence of photoionisation cross-sections and the asymmetry parameter may be probed.

With the exception of hydrogen and helium for which the core levels are also the valence levels ESCA is in principle applicable to any element in the periodic table. The sample requirements are small, *e.g.* 10^{-3}g of a solid, 0.1µl of a liquid or 0.5cc of a gas at STP. The technique is essentially non-destructive. The information obtained from the ESCA experiment spans many levels and is often complementary to that obtained by other techniques and is directly relatable to the molecular structure and bonding of a system, thus also dovetailing with theoretical investigations.

The disadvantages of ESCA are few. The costs are quite high, both in initial outlay and running costs. The technique has superior depth resolution, $\sim$100Å but the spatial resolution poor. If the surface layer is comparatively thick, $\sim$100 Å,

then it is not possible to determine the bulk composition by ESCA without the removal of the sample surface either by sectioning or scraping or (less desirable) by ion milling.

CHAPTER TWO

PHYSICOCHEMICAL ASPECTS OF PLASMAS AND ION BEAM BOMBARDMENT

2.1 Plasmas

2.1.1 Fundamental Aspects of Plasmas

By subjecting a gas at the appropriate pressure to an electric or electromagnetic field, a discharge may be obtained. The term plasma refers to a partially ionised gaseous state consisting of molecules, atoms and ions in both ground and excited states (including metastable states) and electrons such that the concentration of positively and negatively charged species result in dose to overall electrical neutrality. The term plasma was coined by Langmuir[116] to denote the main part of the gas discharge (as opposed to the region in the immediate vicinity of a reactor wall or electrode, which was denoted as a sheath). De-excitation of excited states (electronic, vibrational and rotational) produces a wide range of electromagnetic radiation. Plasmas are characterised by their electron density and the average electron energy. The ubiquitous nature of plasmas is emphasised by Figure 2.1, in which the various plasmas found in nature and produced in the laboratory are summarised. The regime of most interest to chemists is that of the glow discharge or non-equilibrium, "cool" plasma, characterised by electron densities in the range 10^{9}-10^{12} cm^{-3} and average electron energies in the range 1-10eV. Cool or non-equilibrium plasmas are characterised by electron temperatures some two orders of magnitude greater than the Boltzmann temperatures of the ions and molecules, which are roughly ambient. This contrasts with the "hot" or equilibrium plasmas, *eg* arcs and plasma torches, which are characterised by a high gas temperature and an approximate equality between gas and electron temperatures.

Figure 2.1 Plasmas characterised by their charge density and electron energy

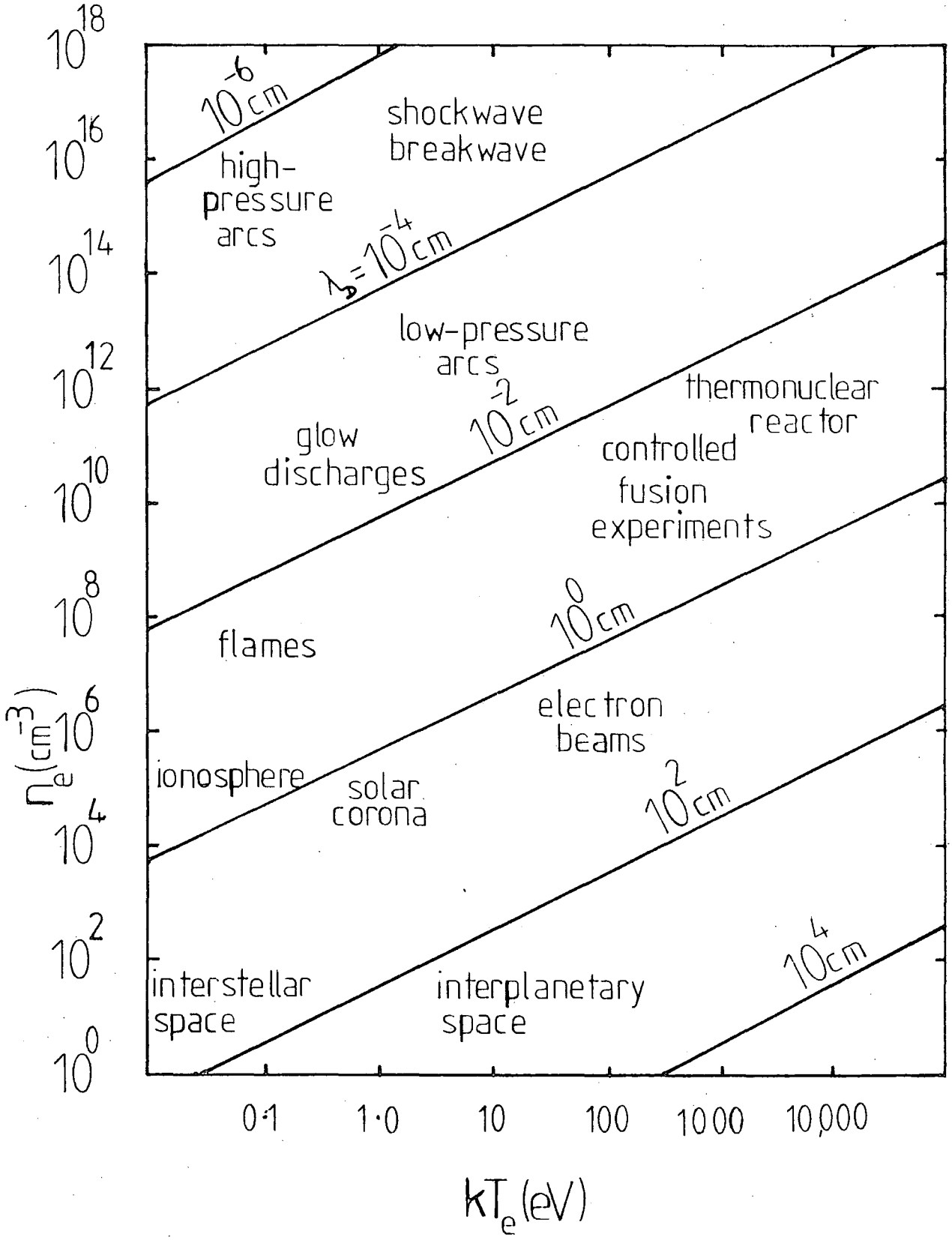

The plasma criterion of overall electrical neutrality is satisfied when the dimensions of the discharged volume are significantly greater than the Debye length,[117] λ_D given by equation 2.1. λ_D defines the distance over which a charge

$$\lambda_D = \left(\frac{E_o kT_e}{ne^2}\right)^{\frac{1}{2}}$$

imbalance may exist. E_o is the permitivity of free space, k is the Boltzmann constant, Te is the electron temperature, n the electron density and e the charge on the electron.

In the gas phase, the dominant mechanism of energy transfer is by electron impact (Figure 2.2), electrons, accelerated by the applied field, collide with the gas molecules to yield radicals, metastables, ions and more electrons. Elastic collisions lead to only a very small energy transfer. Few attempts have been made to characterise plasmas in terms of the energy distributions of ions, electrons and metastables. For simple systems expressions describing electron energy distributions as a function of energy imput, discharge dimensions, gas pressure and properties of the discharge gas lead to a Maxwellian distribution of electron energies, Figure 2.3 depicts the situation for hydrogen. Experimentally the average electron energies may be analysed by electrical probe measurements[118-119] and direct electron sampling.[75] Though such measurements are hampered by the disturbance of the electron energy distribution by the presence of the probe or charging of materials introduced into the plasma environment. Plasmas also provide a copious source of electromagnetic radiation from the vacuum ultraviolet through the visible to the infra-red.

Figure 2.2 Collision processes in plasmas

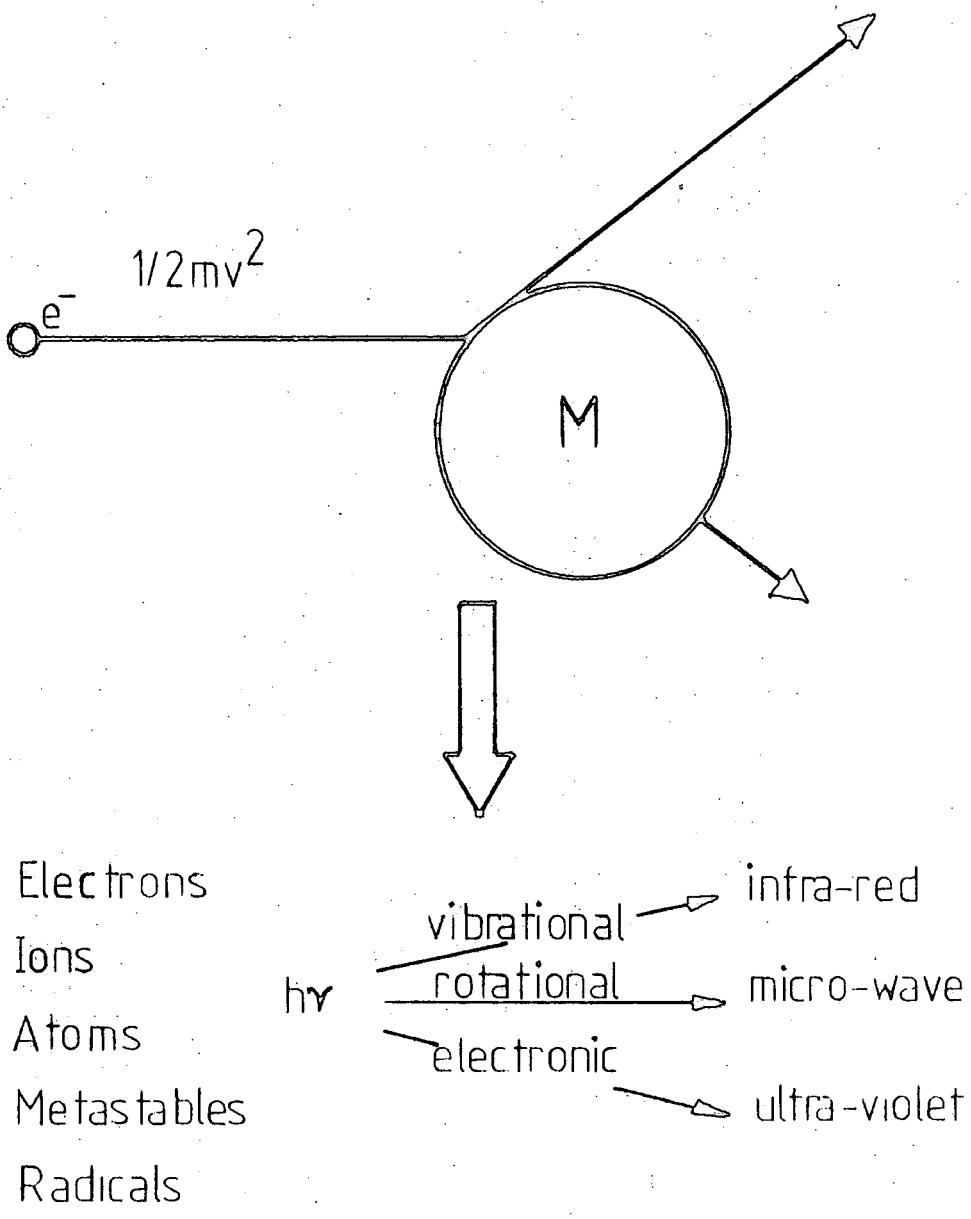

Figure 2.3 Maxwellian distribution of electron energies

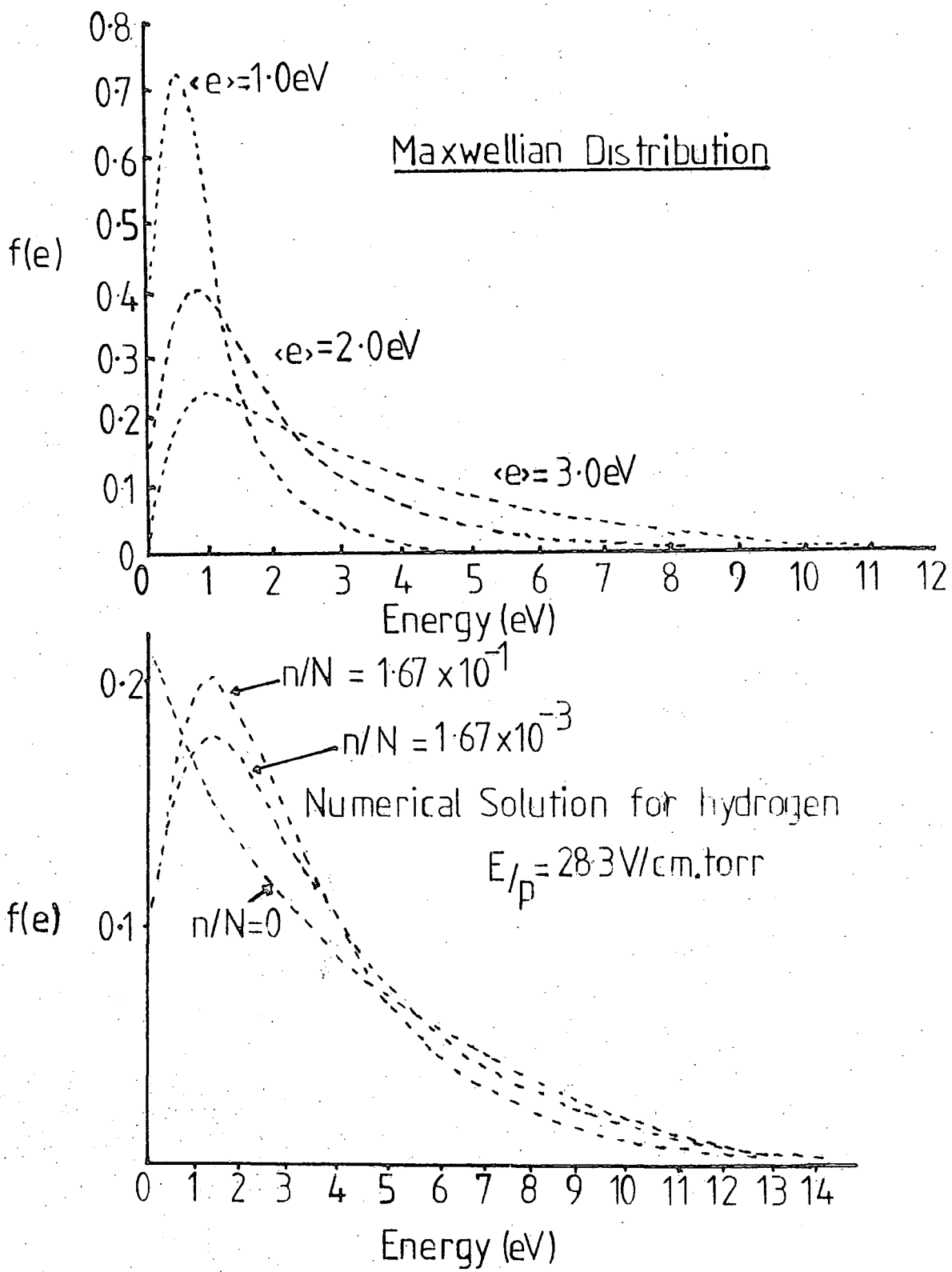

2.1.2 Techniques

Three distinct areas are of interest: the source of electrical power to sustain the plasma; the coupling mechanism; and what is loosely termed "the plasma environment". This is illustrated schematically in Figure 2.4. Early work mostly involved the use of electroded AC and DC discharge[120-123] sources, however the greater flexibility and closer control over operating parameters has shifted the emphasis towards the use of electrodeless inductively coupled radio frequency and microwave plasmas.

Electroded discharges, in which electrodes are placed within the discharging medium may involve D.C. or A.C. and R.F. power. These systems suffer from electrode contamination during use, material being spattered from and deposited on the electrodes during the experiment. More flexible arrangements involve the use of electrodeless R.F. discharges, for instance inductively or capacitively coupled system or systems involving a microwave cavity which may be of a demountable form conveniently attached externally to a cylindrical reactor.[124]

The operating parameters of a glow discharge experiment are those of power input and operating pressure. Powers ranging from 0.1W to several kilowatts may be used. Low frequency and DC discharges are usually characterised in terms of the voltage and current supplied to the electrodes (typically in the range 10-100V and $\sim$1A at $\sim$1 torr pressure). R.F. and microwave discharges require somewhat more expensive and complex instrumentation to characterise: operating pressures ranging from $\sim$0.01 torr with R.F. and microwave discharges to atmospheric pressure for D.C. discharges. Lower power levels ($<$1.0W) are

Figure 2.4 Elements of a Glow Discharge Experiment

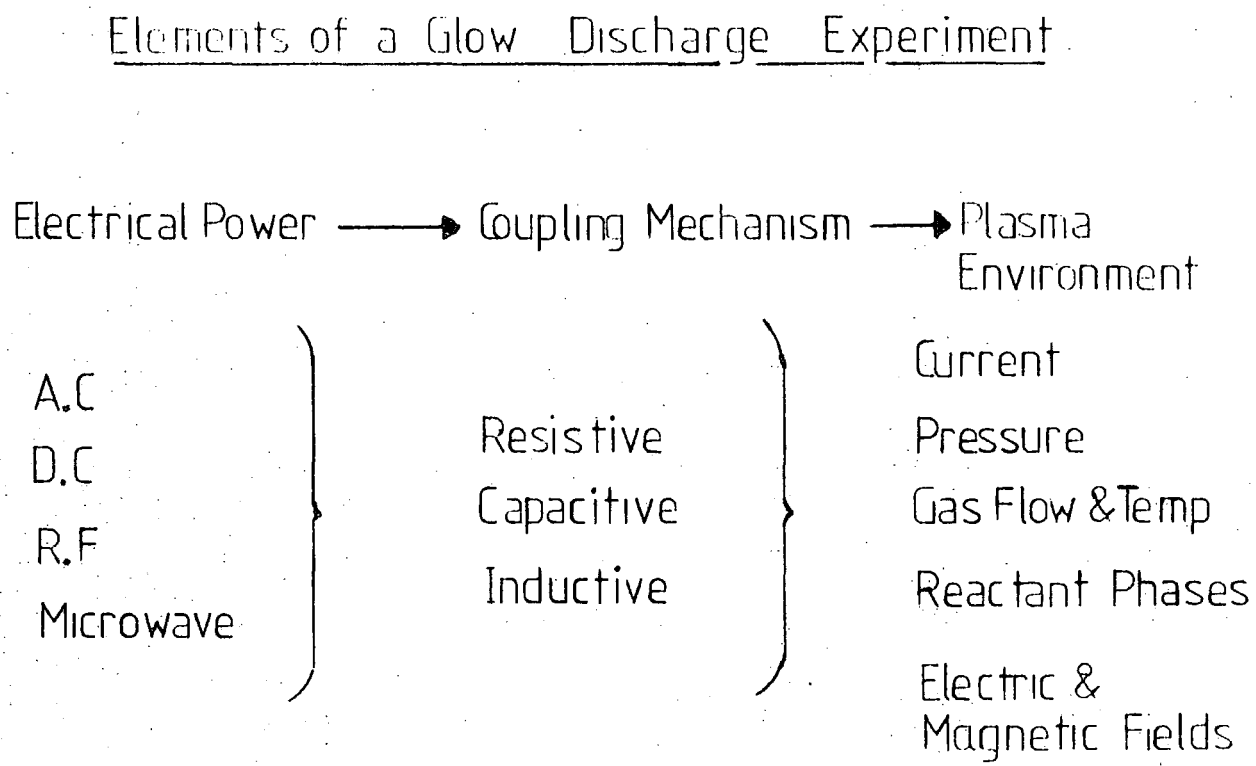

generally difficult to sustain but when using R.F. power stable discharges may be maintained by pulsing the power input on the millisecond timescale.

2.1.3 Reactive Species in Plasmas

Plasmas contain a wide variety of species formed by the collision of electrons accelerated by the electric field with the gas. Many of these species are sufficiently energetic to cause chemical reactions, the energies typically associated with such species and some bond energies for organic molecules are compared in Figure 2.5. A plasma typically contains electrons ions (positive and negative, metstables, neutral molecules and free radicals in ground and excited states and emits photons of a variety of energies. Thus a plasma is seen to be a complex entity overall, only for the simplest systems has any attempt been made to characterise a given system under standard operating conditions.[125] Discussions of more complex systems[126] notably perfluoroaromatic and perfluoroheterocyclic polymer forming systems have centred upon the prediction of what states and pathways to rearrangement might be possible given some idea of the electron energy distribution of such plasmas. On the basis of detailed semiempirical L.C.A.O. molecular orbital calculations the relative importance of a variety of postulated intermediates in the polymerisation process has been discussed. The work in this thesis has concentrated upon treatments excited in hydrogen (Chapter Three). Detailed coverage of the chemical aspects of electrical discharges is to be found in the books by McTaggart[127] and Hollahan and Bell.[128]

Figure 2.5 Energetics of Typical Plasma Species

Energies associated with a glow discharge.

	eV
Electrons	0 – 20
Ions	0 – 2
Metastables	0 – 20
U.V/visible	3 – 40

bond energies:-

C—H	4·3	C=O	8·0
C—N	2·9	C—C	3·4
C—Cl	3·4	C=C	6·1
C—F	4·4	C≡C	8·0

Whilst electrons play a dominant role in the plasma itself, in the interaction of plasmas with polymer surfaces their role is thought to be secondary. Extrapolating from mean free paths obtained for electrons in polymers at higher kinetic energies using the generalised form of the mean free path as a function of energy suggests mean free paths in the range of hundreds of Ångstroms for low energy electrons in polymers. This being the case, direct energy transfer in the surface region is expected to be relatively small.[129] Such arguments are based upon an inversion of the situation encountered in the determination sampling depths in photoelectron spectroscopy. However the electron flux from a plasma impinging upon a surface may not be incident normal to the surface and the energy distribution may be perturbed by the formation of a sheath layer round an insulating sample immersed in a plasma. Secondary electrons can also be generated by ions colliding with the substrate.

The role of direct energy transfer by ions and metastables to the polymer matrix in the surface modification of polymers by inert gas discharges has been stressed in the work of Clark and Dilks.[130] Ions approaching metal surfaces are neutralised with high efficiency in an Auger type process,[131] such interactions forming the basis for a sensitive spectroscopic technique developed by Hagstrum[132] (Ion Neutralisation Spectroscopy). The mean free paths of argon ions and metstables are expected to be of the order of a few monolayers. The mean free paths of chemically reactive radicals, *eg* hydrogen atoms in surfaces are less well investigated. Sticking coefficients and recombination coefficients for radicals on well characterised surfaces are virtually unknown.[131] The interaction of

of hydrogen atoms with polymer surfaces has been estimated to take place over a wide range of depth scales (see Chapter Three)

The interaction of surfaces with low pressure plasmas has been the subject of an extensive and lucid review by Winters,[131] in which the separate roles of ions, electrons and neutrals in surface modification are detailed, though the review centres on electroded systems.

The production of ions and radicals within the polymer matrix by exposure to a plasma provide a variety of mechanisms by which the surfaces of polymers may be functionalised and crosslinked.

2.1.4 Applications of Plasma Chemistry

Plasma chemistry has found application to a wide range of topics of academic and technological interest, in many cases the driving force being the development of a process to avoid the use of "wet" solution techniques, gas discharges offering a cleaner, dry technique with a high degree of control. Some areas in which plasma chemistry has found application are detailed below. Prominent amongst these applications are the deposition and removal of thin films, inorganic and organic by plasma techniques often involved in the electronics industry.

TABLE 2.1 Scope of Application of Plasma Techniques

(i)	Chemistry:	synthesis rearrangement degradation polymerisation
(ii)	Surface modification of polymers:	
		cross-linking oxidation grafting

(Table 2.1 contd.....)

(iii) Ashing, Etching and Sputtering:

Sample preparation for trace element analysis
Sample thinning
Thin film (resist) removal.

The possibilities for the use of cool plasma technique in preparative organic chemistry have been investigated by a number of workers, notably by Suhr[133] and co-workers. Cool plasmas offering a variety of means, *eg* electrons, photons, by means of which energy may be transferred to molecules. Reactions typically occurring in glow discharges are:

(1) Generation of atoms or radicals

(2) Isomerisation

(3) Elimination of atoms or small molecules

(4) Dimerisation, polymerisation

(5) Complete scrambling or destruction of molecules.

Parallels have been drawn between the products of reactions in plasma discharges and those of photolysis[133] and pyrolysis[134] reactions. Often the relationship between the products and reactants is complex and the mechanisms of reaction difficult to study. The operating parameters of pressure, flowrate and power must be optimised for every reaction.

Of the possible reactions outlined above, polymerisation is an ever present problem in plasma organic synthesis, but has spawned a particularly active area of research in the glow discharge synthesis of polymers.[1,136,145] Plasma polymer-

isation offers the capability of producing thin, uniform, pinhole free films having desirable chemical, electrical and mechanical properties. The process suffers however from the disadvantage that films cannot be produced to a predetermined stoichiometry, the films are highly crosslinked and thick films are brittle and discoloured.

The basis experimental arrangement involves the introduction of a monomer into an appropriate reactor in which the discharge is excited, the polymer being deposited over the internal surfaces of the reactor. The monomer vapour may be diluted with a variety of carrier gases (usually noble gases) or reactive gases added. Due to the intractable nature of these films, the solution based techniques of polymer characterisation cannot be applied. A number of techniques have been applied to the characterisation of such films, amongst these ESCA has proved particularly valuable.

Plasmas have also been used to graft material to polymer surfaces,[137-139] either by the deposition of a plasma polymerised film upon the surface or its activation for the initiation of a conventional free-radical polymerisation process at the surface.

Plasmas may also be used in the initiation of more normal types of polymerisation. The formation of a polymer film at the interface of a monomer and its vapour by a glow discharge created by a leak tester (Tesla coil) has been reported by Otazai *et al*[135] and Kikuchi and Tsuda.[143] Osada, Bell and Shen[144] have used this principle to polymerise liquid vinyl monomers by inserting a sealed ampoule between a pair of parallel-plate electrodes connected to a 13.5MHz RF generator.

The polymers formed are very high molecular weight products, containing no traces of catalyst or initiator residues.

Plasmas excited in a variety of gases have also been employed to modify the surface properties of polymeric materials. Further consideration of this aspect of plasma chemistry will be given in Chapter Three.

2.2 Ion Beams

2.2.1 The Interactions of Ion Beams with Polymer Surfaces

In order to understand the complex processes involved in plasma-surface interactions attention has been focussed upon the use of controlled beams and well-defined surfaces to model these interactions in an attempt to abstract one element of a plasma from those available.[140-141] Such studies are also worthwhile pursuing in their own right, providing a controlled method for the treatment of specific areas of a surface, naively bearing the same relationship to plasma modification as ion beam lithography to plasma ashing. Suggestions that the synergistic effects between ions electrons, ions, photons and radicals impinging on surfaces immersed in a plasma should be studied, should ideally wait until the effects of each in isolation is understood.[140]

Broad classification of the effects of ions impinging on surfaces into physical and chemical have been attempted.[142] Physical interactions including such processes as ion implantation, spattering scattering, surface reconstruction, surface heating and the dissociation by collision of impinging molecular

ions. Chemical interactions include the chemical reactions of the impinging ions with the substrate, *eg* chemisorption and adsorption, and the formation of new chemical bonds within the substrate. As a result of these interactions atomic and molecular species, electrons and photons are emitted; the study of the range of positively and negatively charged ions emitted on bombardment forming the basis of the secondary ion mass spectroscopy of surfaces.

2.2.2 The Depth of Ion Beam Modification

Attempts to understand the interaction of ions with surfaces have centred upon classical treatments of the nuclear-nuclear interactions[146] between the nucleii in the surface and the incoming ion, these being the dominant mechanism governing the depth of penetration of ions into surfaces, *ie* billiard ball type collisions.

Such a treatment forms the basis of the treatment developed by Linhard, Schaff and Schiøtt[147,148] (LSS theory). Whilst adequate in predicting ion ranges and implantation depths and hence approximately the thickness of the damaged layer for higher ion energies (≥10 keV) LSS theory is poorer in predicting ranges at lower incident ion energies. Whilst at lower ion energies, ∿1 keV the depth of damage has been found to depend on the $^{2}/_{3}$ power of the ion energy as predicted by the low energy nuclear limit of LSS theory, the predicted ranges are lower than the experimental ranges by a factor of 3-4.[149,150] Extrapolation to lower Z target materials is also considered risky, though LSS theory has been invoked by authors to predict ion ranges in polymers at low ion beam energies (1 keV).[151,146] Figure 2.6 shows

Figure 2.6 Argon Ion Ranges as Predicted by LSS Theory

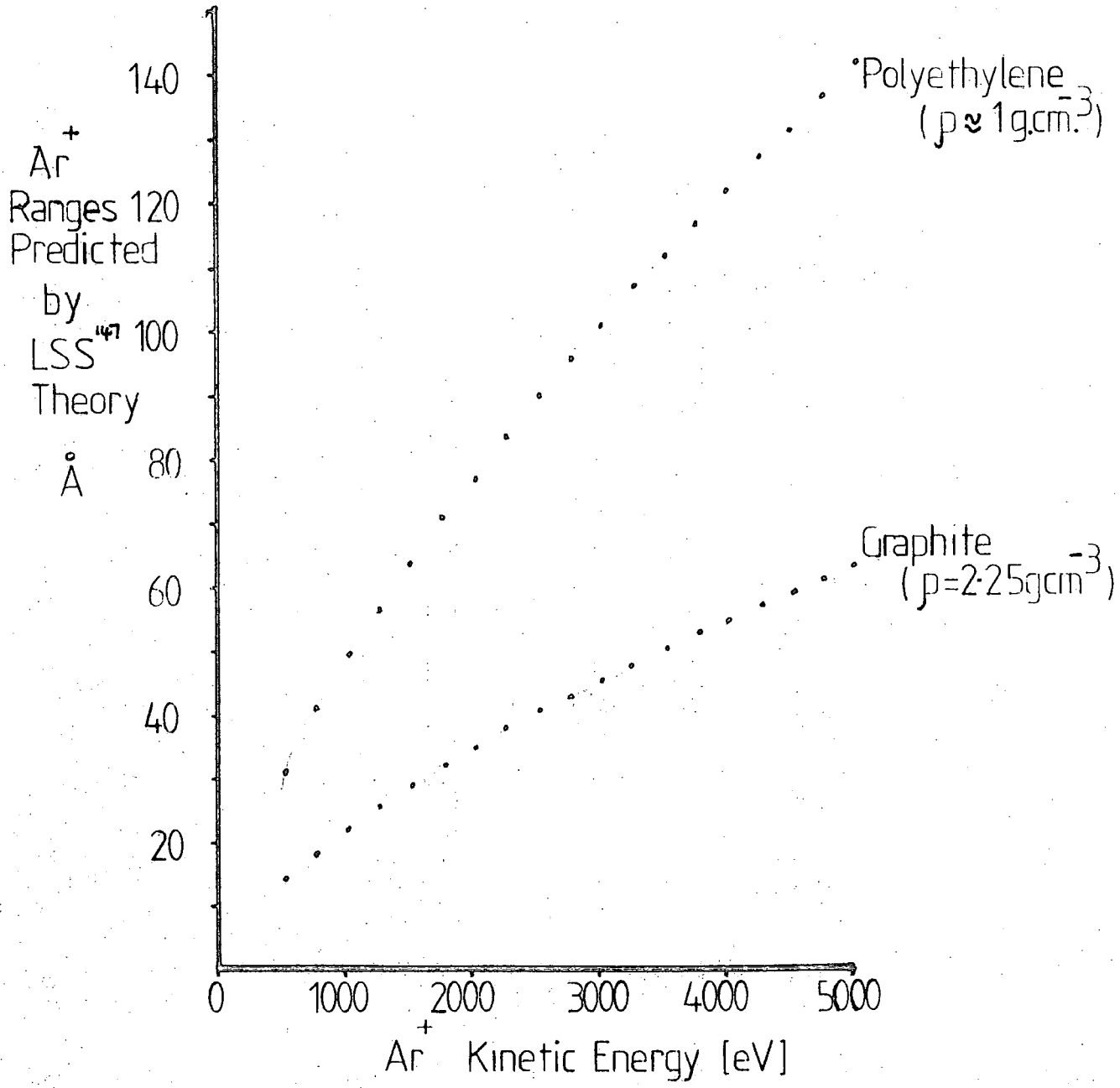

the variation of ion ranges with energy predicted for argon ions in graphite (ρ = 2.25g/cm^3) and a polymer ($\rho \sim$1g/cm^3). At lower energies estimates of ion ranges and damage depths in inorganic solids have been made using ESCA measurements. At lower ion energies, as the ion is slowed by collision within the medium, electronic stopping mechanisms become more important.

2.2.3 Modifications Introduced by Ion Beam Bombardment

When ions impinge upon a surface a variety of changes are to be expected:[152] (Figure 2.7).

(a) Loss of surface atoms from the very surface due to emission of atomic and molecular particles and recoil implantation.

(b) Implantation of primary ions and recoil surface atoms.

(c) Lattice reconstruction.

(d) Chemical effects, *eg* bond breaking and formation.

In secondary Ion Mass Spectrometry, SIMS, mass analysis of the emitted secondary ions is used to infer the chemical composition and structure of the surface region. These changes in the surface are also accompanied by secondary electron and photon emission.

Ions approaching metal surfaces stand a high probability of being neutralised, the probability that this neutralisation process is accompanied by photon emission being very small.[132] The neutralisation is accompanied by the secondary emission of electrons in an Auger type process. Such processes form the basis of Ion Neutralisation Spectroscopy developed by Hagstrum.[132] At low ion energies, $<$1kV most secondary electrons are emitted as a consequence of the potential energy of the in-

Figure 2.7 Ion Bombardment Induced Charges in a Solid

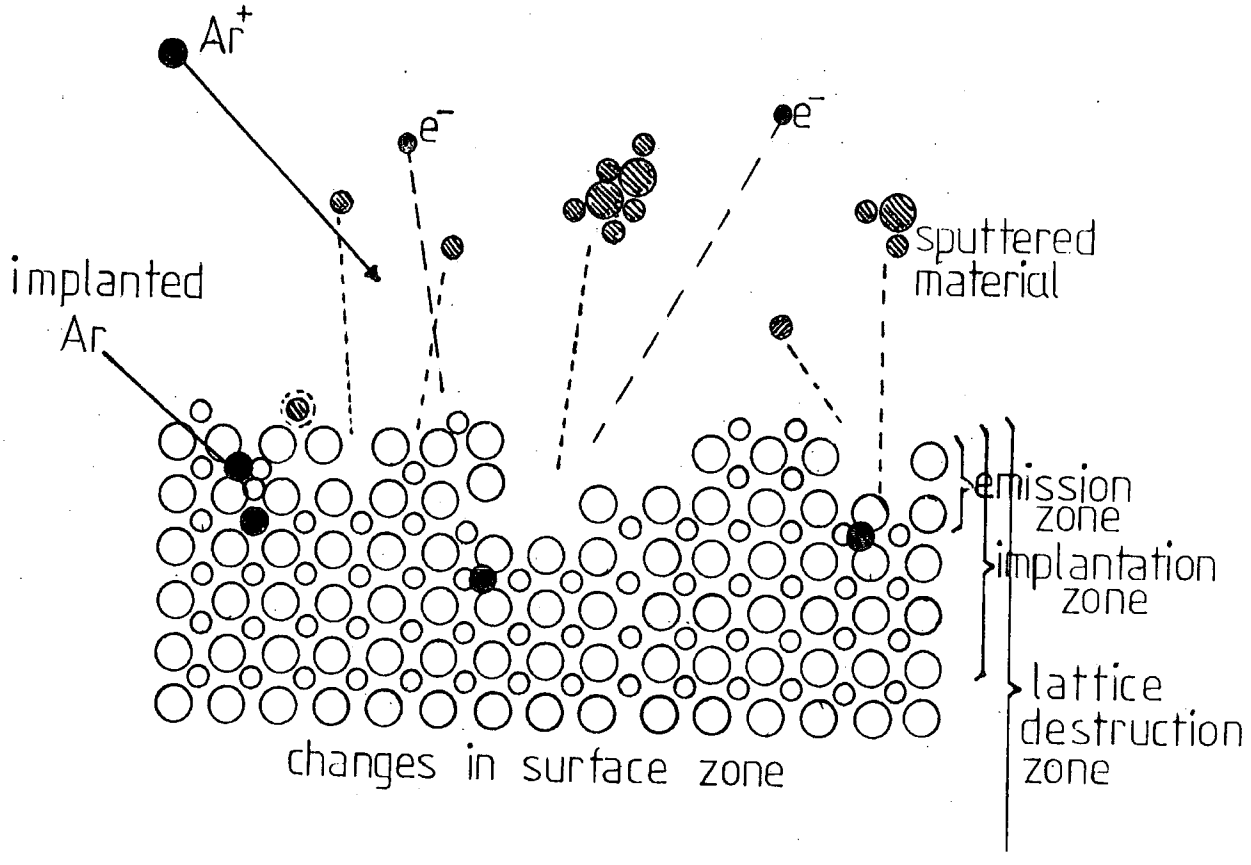

coming ion, at higher energies kinetic ejection of electrons becomes important, increasingly so as the kinetic energy of the impinging ion is raised. Thus as the ion is stopped in the solid, a flux of low energy (<20eV) secondary electrons is generated, the yield of secondary electrons having been correlated with the electronic stopping power, the energy loss per unit pathlength due to electronic excitations within the substrate.

When an ion approaches a surface, it is neutralised and then begins to lose energy to the lattice *via* electronic and nuclear collisional processes, at lower ion energies, <5keV, nuclear collisional losses dominate. The energy deposited in these so-called "nuclear loss" processes leads to motion of the lattice atoms. Most theories to describe the interaction of the incident ions rely on being able to treat the path of the ion in the solid as a series of binary collisions. During penetration into the lattice as the energy of the particle is dissipated only a small fraction of the energy is imparted to particles with momentum directions pointing out of the surface. The average energy of these sputtered partices is ∿5-15 eV for incident ion energies of a few keV.[153] Only a small proportion of the spattered particles are charged.

The ejection of material from a surface under bombardment by energetic ions or neutrals is known as sputtering. The sputtering yield is defined as the number of target atoms ejected per incident ion. In the application of secondary ion emission as an analytical tool it is necessary to establish a relationship between the atomic and molecular structure of the surface and of the emitted species. Where the sputtering yield of one component of a surface is higher than another, the surface will be depleted more rapidly of that component. Sputtering

coefficients have been determined for the pure elements,[154,156] however, in multicomponent systems the situation is complicated, a range of ions, over and above the range of simple clusters emitted by pare elements, can be emitted, each with its own sputtering probability.[152] At a more qualitative level the ion bombardment of organic surfaces results in the formation of series of molecular ions, the spectra of which are readily interpretable given the familiar basis of the electron impact ionisation mass spectroscopy of organic compounds.[153] In this case the structure of the surface may be inferred from the fragments produced.

When species are removed from a surface or displaced, a vacancy is created and the surface will then reconstruct or rearrange. New bonds are formed. This is especially evident in organic systems where molecules undergo extensive crosslinking upon bombardment.

The process of secondary ion emission has been treated theoretically by a number of workers,[157-159] notable amongst these being Andersen.[159] Andersen postulates the formation of a dense plasma in the bombarded area and the existence of an equilibrium between neutral and charged species and electrons.

In secondary ion mass spectroscopy a somewhat artificial partition is made between the so-called, low damage, low dose or static SIMS and the higher doses of dynamic SIMS. In static SIMS low currents ($<1 nA/cm^2$) are used so as to guarantee a low probability of the areas perturbed by ions sampling the surface overlapping each other during an experiment.[152] Interpretations of this criterion in the literature appear to vary. In a dynamic SIMS experiment, high primary ion current densities are used resulting in the removal of many monolayers of material

whereas at the current densities used in static SIMS a monolayer of material might have a lifetime of many hours.

In this thesis ESCA has been employed to investigate some facets of the interaction of ion beams with polymer surfaces. The current densities and doses employed are intermediate between the two regimes of static and dynamic SIMS.

2.2.4 Ion Induced Modification of Polymer Systems

Studies of the low energy ion bombardment of polymer surfaces spanning a wide range of operating conditions have been reported in the literature.[160-170] A wide range of ions, from noble gas ions to ions derived from molecular species such as CF_4 and N_2 are employed. Ion fluxes varying over six orders of magnitude, from the regime of static SIMS to the fluxes generated by devices designed for ion implantation and spacecraft propulsion, have been used. The ion beam modification of polymer surfaces produces both physical and chemical changes in the surface. At higher fluxes sputtering results in the rapid removal of the surface layers of the polymer, crystalline polymers yield high aspect core structures on bombardment, amorphous polymers undergoing rapid etching at surface defects. Dwight[141] found these etching and sputtering processes to have little relationship to the chemical functionality present in the original polymer. The ESCA analysis of this bombarded layer found a carbonaceous layer, denuded of the most electronegative elements in the polymer. The fluxes employed in these studies were of the order of 0.1 mA/cm^2, exposure times ranging from minutes to hours. Using quartz-microbalance techniques to monitor the sputtering rates, ESCA being employed to monitor the chemistry of the selvidge layer after bombardment Ullewig

and Evans[164] investigated the sputtering of siloxane films, polymethylmethacrylate and polystyrene films. Whilst the sp ttering of the polymers was found to differ, it was concluded that on sputtering the polymers approached a common structure after extended periods of bombardment.

Sovey[166] has employed higher argon ion fluxes in investigating the sp ctering behaviour of fluoropolymer films at low ion energies (250-1000eV), the etch rates were found to increase by about a factor of ten as the ion energy was varied from 250 to 1000 eV. At the current densities employed the sample had to be cooled. The ESCA spectra of the exposed samples, whilst still displaying a high degree of fluorocarbon functionality, the C_{1s} spectra reveal the formation of carbonaceous, lower binding energy materials, similar to that observed by Gossedge[168] upon argon ion bombardment of P.T.F.E. Rabalais[151] has also investigated the bombardment of teflon surfaces by argon and xenon ion beams, the ESCA spectra reveal modification which is qualitatively the same as that found in previous studies. The emphasis in this work is on the implantation and trapping of the inert gas atoms on bombardment and the saturation dose required, not the minimum dose required to produce a modified surface. In a preliminary experiment Clark[167] investigated the interaction of a 2kV, 5μA argon ion beam with a tetrafluoroethylene-ethylene copolymer surface for exposures of up to 30s. (The current density used is not stated and the experiment is complicated by the presence of the UV-visible discharge from the cold cathode ion source employed). The effects of the ion beam irradiation of this polymer is comparable to those produced by the exposure of the same polymer to an argon glow discharge as investigated by Clark and Dilks.[130]

Working at much lower ion current densities, Holm and Storp[162-164] showed that after only a relatively by low energy argon ions, changes were readily observed in the surface regions of polystyrene. A treatment time of 20 sec. at 800mA/cm^2 by 5keV argon ions ($\equiv 1.10^{14}$ ions per cm^2) is sufficient to destroy the shake-up satellite to the C_{1s} signal in the ESCA spectrum. From this it was concluded that destruction of the phenyl group had taken place, *ie* "one of the most stable basic units of organic chemistry" had been destroyed. On prolonged bombardment, the C_{1s} spectrum broadens and develops an asymmetric tailing to higher binding energies. An organic salt, zinc phenyl sulphinate, was found to be similarly sensitive.

The modification of polymer surfaces by inert gas ion beams has also been investigated in the context of SIMS and ISS investigations of polymer surfaces. Gardella and Hercules have investigated the surface sensitivity of ISS as demonstrated by the fact that whilst the initial spectra of PTFE show only a peak due to F due to shielding of the carbon skeleton by F atoms, ion beam induced damage, *ie* C and O detectable, became apparent after only 4.5 x 10^{16} ions cm^{-2} (Ne^+ at 2kV). This represents a dose at least 3 orders of magnitude greater than that required to detect modification of the sample surface in the C_{1s} spectra of PTFE. Briggs[178] has shown that the ion dose required to cause extensive damage to a polymer is much less than that inferred by Gardella and Hercules.[170] The same authors have used SIMS and ESCA to investigate polyalkylmethacrylates and the hydrolysis of polymethyl and t-butyl methacrylate surfaces. From their investigations they concluded that reaction was best followed by SIMS, ESCA was not sensitive enough to detect the small degree of hydrolysis that had occurred. However their experimental conditions were poorly characterised.

Campana *et al*[165] used SIMS to study a similar series of alkyl methacrylate polymers under somewhat better characterised conditions. In a series of papers, mindful of the extreme sensitivity of polymeric materials to damage by ion and electron beams, Briggs[153,160,161,172] has obtained very good signal to noise ratio spectra for a series of polymers using very low damage conditions (ion current densities $\sim$1nA cm^{-2}). Only on extended bombardment at this current density was ion beam induced damage noted in the ESCA spectra.

Using relatively high energy beams of F^+, Weber *et al*[175] have implanted films of polyacetylene. The treated film showed improved electrical properties and resistance to atmospheric oxidation. Using ESCA the implanted fluorine is deduced to be covalently bound to the polymer chain, though the C_{1s} core level spectra for the implanted films are not presented, the extent of crosslinking of, and damage to the polymer due to such treatment was not considered.

Rabalais *et al*[146] have used fluorine-containing ion beams derived from tetrafluoromethane to fluorinate polybutadiene, polystyrene and polyacetylene films, ESCA being used to characterise the functionalised surfaces. Bombardment with F^+ ions (4.5×10^{14} ions cm^{-2}) and CF_3^+($F^+ \equiv 6.2 \times 10^{14}$ ions cm^{-2}) introduces -CHF- and $-CF_2-$ functionalities, equivalent to the fluorination of a 2-8Å thick surface layer.

Using high fluxes of ions derived from oxygen and nitrogen, Mayoux *et al*[177] have produced extensive functionalisation of polyethylene surfaces detectable in the MATR. IR spectra of the irradiated surface.

Investigations of the ion beam modification of polymer surfaces have followed essentially two paths: the use of high doses to modify polymer surfaces, often using ion doses many times that required to form an equilibrium selvidge layer; ion beam methods of surface analysis, in which modification of the surface is implicit, however the modification should not be so great as to falsify the results of the analysis. Relatively little attention has been paid to the chemistry of the boundary layer formed by treatment of polymer surfaces with low doses of ions.

CHAPTER THREE

THE INTERACTIONS OF A HYDROGEN PLASMA WITH FLUOROPOLYMER SURFACES

3.1 Introduction

Polytetrafluoroethene, PTFE, displays many highly desirable bulk and surface properties, *eg*. its high thermal stability, chemical inertness,[179,180] low surface energy[181] and extremely low coefficient of friction.[182,183] These properties, which often dictate the polymer's choice for a given application, paradoxically present considerable problems, (*eg*. of adhesion or wettability) in creating an interface to another material: forming an adhesive bond to or coating PTFE being virtually impossible without some form of pretreatment of the polymer surface.

In this context, a variety of treatments have been employed to activate PTFE surfaces to promote adhesion. A review of some of these treatments has recently been given by Dahm.[178] A cross-section of methods employed is given below.

(a) Sodium-liquid ammonia[185] and sodium naphthalide treatments[184].

(b) Reduction with an electrochemically generated tetra-alkyl ammonium radical anion salt solution.[186]

(c) Treatment at elevated temperatures with alkali metal vapours derived from a variety of sources.[189]

(d) Treatment with alkali metal amalgams.[187,188]

(e) Electrochemical reduction of a surface when placed in contact with a metal cathode in a non-aqueous electrolyte.[187]

(f) Treatment with a Corona discharge.[190]

(g) Electron[191] and Ion beam irradiation[192,168] (see Chapter Four).

(h) Vacuum deposition of metals, with or without[193,194] subsequent removal.

(i) Plasma modification[195] and grafting techniques.[199]

To date the "wet" techniques have been most fully exploited commercially however the difficulty of controlling the depth profile of the modification and problems of impurities introduced by solution techniques has focussed interest on the use of gas-solid discharge techniques to effect controlled changes in surface chemistry.

In elucidating the mechanisms of action of the various treatments, the tools of surface science (*eg*. ESCA, SIMS, ISS) have been used extensively to monitor the introduction of functional groups and changes in surface chemistry produced by these treatments. In investigating the surface treatments produced by solution techniques ESCA has been used by several groups to investigate the nature of the carbonaceous layer produced. Brecht *et al*[196] and Dwight and Riggs[197] independently investigated the defluorinated surface and showed the surface to consist mainly of carbon though a large amount of oxygen was also detected even when the surfaces were prepared in an inert atmosphere glove box. In the course of their studies of PTFE-metal interactions Cadman and Gossedge[168] made extensive use of ESCA, touching also upon the defluorination of PTFE produced by Argon ion bombardment of the surface. Several groups of workers have employed ESCA in the study of modifications of fluoropolymer surfaces produced by the vacuum deposition of metal films[198,192] and their subsequent removal.[198]

The use of glow discharge and corona treatments to produce surface modifications in fluoropolymers[195,201-204] has also been

extensively studied. Such studies have shown that in contrast to the drastic changes in properties such as colour and texture of the polymer surface induced by wet chemical techniques, discharge treatments can effect controlled changes in surface chemistry whilst limiting the depth of the altered layer so as not to seriously affect the appearance of the surface. In some early work Schonhorn and Hansen[195,199] found that the exposure of polyolefins and perfluoropolymers to low power RF electrodeless discharges in inert gases produced large improvements in the bondability of the surfaces, comparable to those improvements obtainable *via* wet chemical methods: this improvement in adhesion being attributed to the formation of a highly crosslinked surface layer. Schonhorn dubbed this treatment CASING,[199] (Crosslinking by Activated Species of Inert Gases).

Subsequent ESCA studies on prototype fluoropolymer systems have allowed a detailed interrogation of surface chemistry as a function of reaction parameters. Such studies have allowed the relative importance of direct energy transfer and radiative processes to be estimated. Whilst extended reaction times may be required for a sufficiently highly crosslinked surface to be formed as in the previously mentioned experiments of Schonhorn *et al*,[200] using ESCA, quite drastic changes in surface chemistry become apparent after very modest treatments. Early studies by Hollahan[206] aimed to render polymer surfaces biocompatible included the interaction of PTFE with plasmas excited in NH_3 and N_2/H_2 mixtures: the goal being the introduction of amino groups into the polymer surface, the concentration of these groups being determined by the surface's uptake of radioactively labelled heparin molecules. Qualitative

observation of wettability were also made. The long exposure times and the high powers employed in the work (RF plasma capacitively coupled >200W, >3 hrs) must also have produced great changes not only in the surface chemistry but also well into the bulk, the morphology of the surface also being severely effected. An early ESCA study[204] of this system, under more controlled conditions revealed that both nitrogen and oxygen functionalities were introduced by ammonia and nitrogen/hydrogen discharge treatments. The interpretation of the ESCA data however was hampered by the lack of sufficient background data at that time with which to make peak component assignments. The time dependence of the treatment was investigated to a limited extent, no attempt was however made to investigate the power dependence. Complementary studies of the IR spectra and contact angles were also reported. The treatment however produced a darkening of the polymer surface and scanning electron microscopy revealed extensive physical modification of the surfaces.

In another ESCA study, Yasuda and co-workers[201] investigated, qualitatively, the effects of discharges in argon and nitrogen on the surface chemistry of a range of polymers. PTFE was found to be particularly susceptible to defluorination and the introduction of oxygen and nitrogen moieties into its surface.

Mass spectroscopic analysis of the reaction products from the interaction of a variety of noble gases and reactive gases such as oxygen and hydrogen has been used to investigate the interactions of discharges with PTFE surfaces.[207] In these studies the major species detected contained only one carbon

atom. Fragments containing more than one carbon atom were rare. In a hydrogen discharge little etching was observed. This study was however conducted on plasma polymerised tetrafluoroethene, whose structure may not be directly comparable with PTFE obtained by more conventional routes.

In studying the interaction of plasmas with polymer surfaces a variety of probes are commonly used ranging from measurements of contact angles and adhesive bond strengths from the results of which the polarity of the surface may be inferred and its chemistry speculated upon, through multiple total internal reflection infra-red studies which probe the topmost micron of a surface but often fail to reveal the chemical modifications of surfaces brought about by very light discharge treatments. There have also been a limited number of studies by ESR of hydrogen discharge[208,209,215] treated PTFE but these provide no direct indication of modifications in surface chemistry, merely confirming the role of radicals in the process.

Previous work in these laboratories by Clark and Dilks[72,78,130] has shown the utility of ESCA for monitoring, in considerable detail, the changes in surface chemistry produced by mild plasma treatments. More recently attention has turned to the interaction of reactive gas plasmas to effect the functionalisation of polymer surfaces.

In this study the interaction of PTFE surfaces with low powered inductively coupled RF plasmas excited in hydrogen has been investigated. Under the operating conditions employed, the predominant reactive species present was atomic hydrogen.

At higher discharge pressures (30-300 Torr) hydrogen atoms combine in three-body collisions to give persistent, unstable molecules which retain much of the energy of recombination. The plasma condition of overall electrical neutrality is fulfilled by the presence of H_3^+, H_2^+ and H^+ species up to an ion density of 10^9-10^{11} ions per cm^3. [127] In summary then the reactions in the discharge could be due to the following species: hydrogen atoms ($H^\cdot$), excited hydrogen atoms ($H^{\cdot *}$), excited hydrogen molecules H_2^*), the ions mentioned above and low energy electrons.

3.2 Experimental

3.2.1 Plasma Instrumentation and Reactors

Two reactor configurations were employed in the study. In a preliminary series of experiments, plasma modifications were effected using an inverted "T" shaped reactor as indicated schematically in Figure 3.1(a): samples being introduced *via* a detachable end cap sealed with a viton "O" ring. The sample rested on a glass slide lying in the lower tube of the reactor, at the bridge of the "T". The apparatus was constructed of glass ∿6cm internal diameter with a 10 turn, 7μH copper coil electrode wound externally as indicated. In this arrangement the sample lay some 12cm below the centre of the discharge zone.

More detailed investigations were conducted in a second reactor of differing construction as illustrated in Figure 3.1(b). This reactor consisted of a flanged Pyrex tube, 16cm in length, 5cm in diameter, mounted sandwiched between two

Figure 3.1 Reactor Configurations Employed

(a)

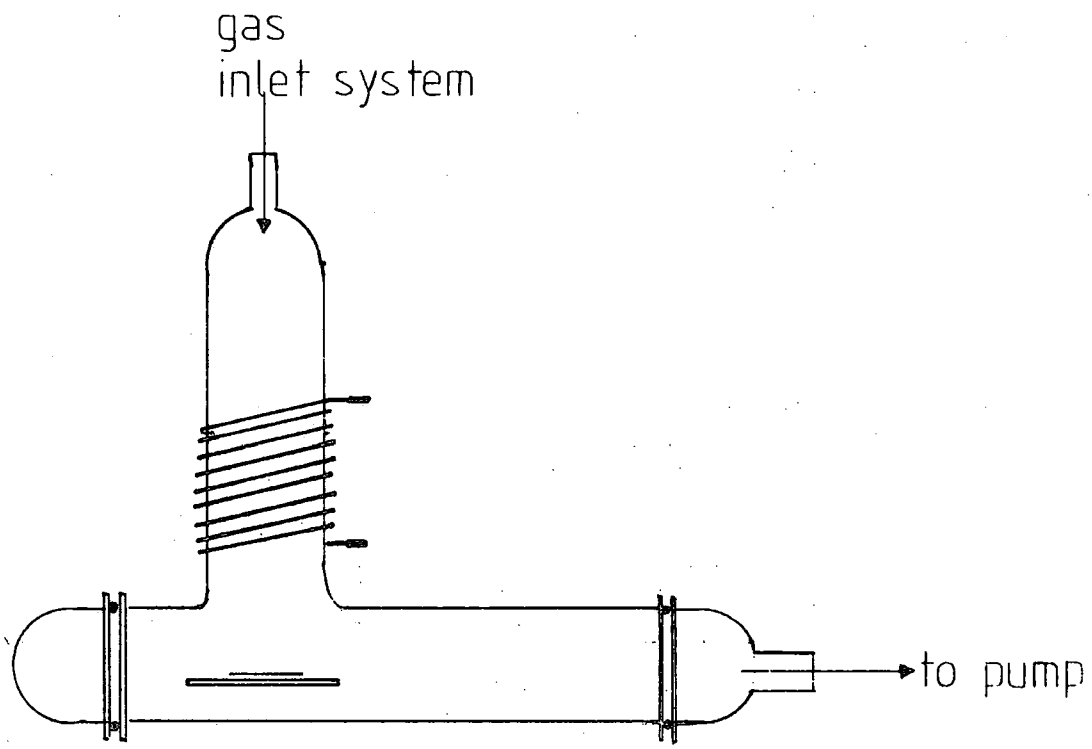

(b)

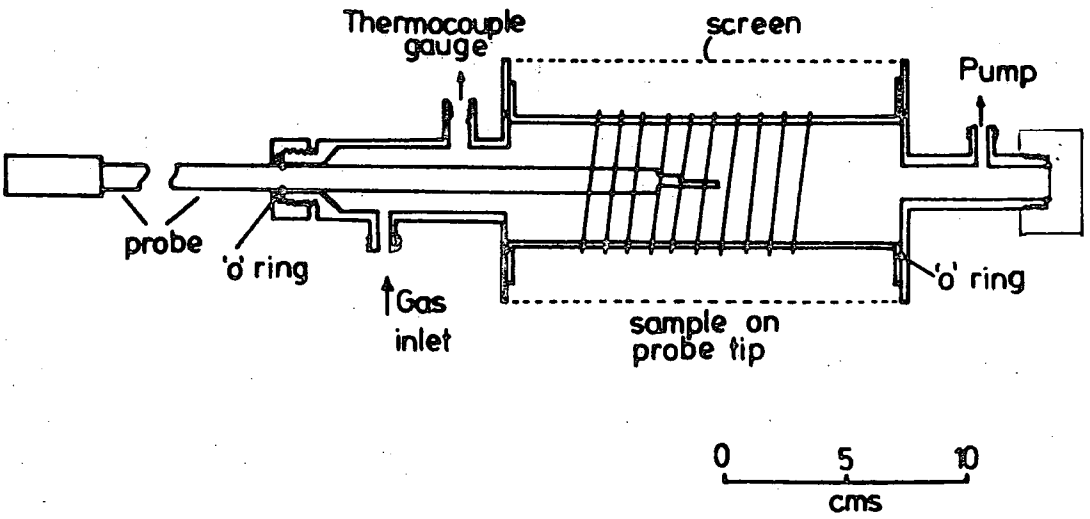

stainless steel flanges sealing on recessed "O" rings. The system was pumped *via* a $^{3}/_{8}$" flexible tube connected to a vacuum line. Samples were mounted on a double sided stainless steel probe-tip attached to a ½" diameter stainless steel probe sealing on "O" rings, which allowed the rapid removal of the sample for analysis. Discharges were excited *via* an externally wound 9 turn, 6μH copper coil electrode. In this reactor the sample was positioned at the very centre of the glow region, the sample probe axis being concentric with that of the exciting coil. This contrasts with the sample position in the previously described reactor.

Prior to use each reactor was cleaned by exciting a hydrogen plasma at a power loading of ∿30W for ½ hr. In this way the transfer of hydrocarbon contamination from the reactor walls to the polymer surface during treatment was minimised. A hydrogen plasma has also been found to be very effective in removing hydrocarbon contamination from gold substrates employed in many studies in these laboratories.

In each case the reactors were connected to a vacuum line of grease-free construction pumped by a 200 l min^{-1} two stage rotary pump, (Edwards ED200): pressure measurement being achieved in the former case by a Pirani gauge and in the latter by a thermocouple vacuum gauge calibrated using a McLeod gauge. Taking into account the respective sensitivies of the gauge heads to hydrogen, the preliminary work was conducted at .08 torr and the more detailed investigations at .12 torr, in each case using a 0.2 torr graduation as a convenient set point in setting the correct pressure; gas being introduced *via* a leak valve.

Plasmas were excited by a Tegal Corporation 13.56MHz radio-frequency generator capable of delivering a power output from 0.05-100 watts, continuously variable. At low powers the generator was operated in a pulsed mode to give greater stability to the plasma when low average power loadings were required. The generator was matched to the external inductive load *via* an L -C matching network, power transferred and standing wave ratios being monitored by a Heathkit HM102 RF power meter. This network serves to match the external load to the output impedance of the generator thus ensuring maximum power transfer to the external circuit and protect the generator.

3.2.2 Polymer Samples and Sample Preparation

The investigation concerned itself with two homopolymers studied in film form:

(1) Polytetrafluoroethene, PTFE obtained as a skived film from James Walker Ltd.

(2) Polyvinylidene fluoride PVF_2 obtained as a drawn film from Cellomer Associates, Webster, N.Y.

The films were used in their "as received" forms without any pretreatment. In preliminary work samples were placed on a glass slide in the reactor and exposed to a plasma prior to mounting on a double sided probe tip for ESCA analysis. In the case of the second reactor, samples were mounted on a double sided spectrometer probe tip by means of double sided "Scotch" adhesive tape prior to plasma modification. ESCA analysis of samples was initiated within 5 minutes of their exposure and took approximately 50 minutes to complete.

3.2.3 Experimental Procedure

In each case the samples were introduced into the reactor and the system evacuated to 5 x 10^{-3} torr. The system was then flushed with hydrogen gas, re-evacuated and then let up to the required pressure (0.2 torr, nominal) *via* a leak valve. Hydrogen gas from a standard laboratory cylinder, obtained from the British Oxygen Co. was used without further purification. Hydrogen flow rates were measured by valving-off the reactor and monitoring the initial rate of pressure rise in the reactor. The vacuum line and reactor were then allowed to purge for twenty minutes before a discharge was initiated. The adjustment of the power output and matching of the RF generator was done before the introduction of the sample to the system. Powers ranging from 0.1W to 10W were employed, for treatment times of up to 256 seconds. To achieve a stable discharge at the lower end of this range of powers the pulsing facility of the generator was used: the characteristic electromagnetic emission of a hydrogen discharge being a purple glow. In the "T" shaped reactor the sample sat immediately downstream of the coil region where the most intense glow was to be found. The glow extending into the horizontal limb of the reactor extended either side of the sample. In the flanged reactor the sample was, attached to the probe, immersed in the glow region of the coil.

3.2.4 Contact Angle Measurements

The contact angles to water of treated surfaces were measured using a simple sessile drop measurement in which a drop of water (1µl) was placed on the surface and its dimensions measured using a microscope fitted with a goniometer eye-piece.

3.2.5 ESCA Instrumentation and Data Analysis

Spectra of the untreated and plasma modified samples were in the main recorded on the AEI ES200 AA/B spectrometer using $Mg_{K\alpha_{1,2}}$ radiation as previously described. To exploit the greater sampling depth offered by the harder $Ti_{K\alpha}$ X-ray source, the Kratos ES300 spectrometer was also used. Binding energies are quoted to an accuracy of ±0.2eV and area ratios, determined from curve-fitting procedures using a Dupont 310 Analogue Curve Resolver, to an accuracy of ±5%. Assignment of the peaks of the curve-fitted C_{1s} spectra is made on the basis of the extensive studies of fluoropolymers of Clark and Thomas[76] and is set out at length in ref. 205. Figure 3.2 shows an example of such a curve-fitting procedure. Peaks from 292.2eV to 290.6eV are assigned to CF_2 groups having a variety of encironments ranging from two $\underline{C}F_2$ groups (as in untreated PTFE, to a $\underline{C}F_2$ in an essentially hydrocarbon environment. Peaks from 286.7 to 285.0eV are assigned to carbon in essentially hydrocarbon-like environments with a variety of β substituents. Peaks in the intermediate region are assignable to groups such as -$\underline{C}$FH- which can span a range of binding energies from *ca.* 288.9-287.9eV.[76,210] However analysis of this region is complicated by the oxygen uptake of the polymer films on plasma treatment, carbonyl features will also contribute to this region.

3.3 Results and Discussion

3.3.1 Preliminary Experiments

Preliminary experiments to assess the changes in

Figure 3.2 Component Analysis of the C_{1s} Level of a Hydrogen Plasma treated sample of PTFE

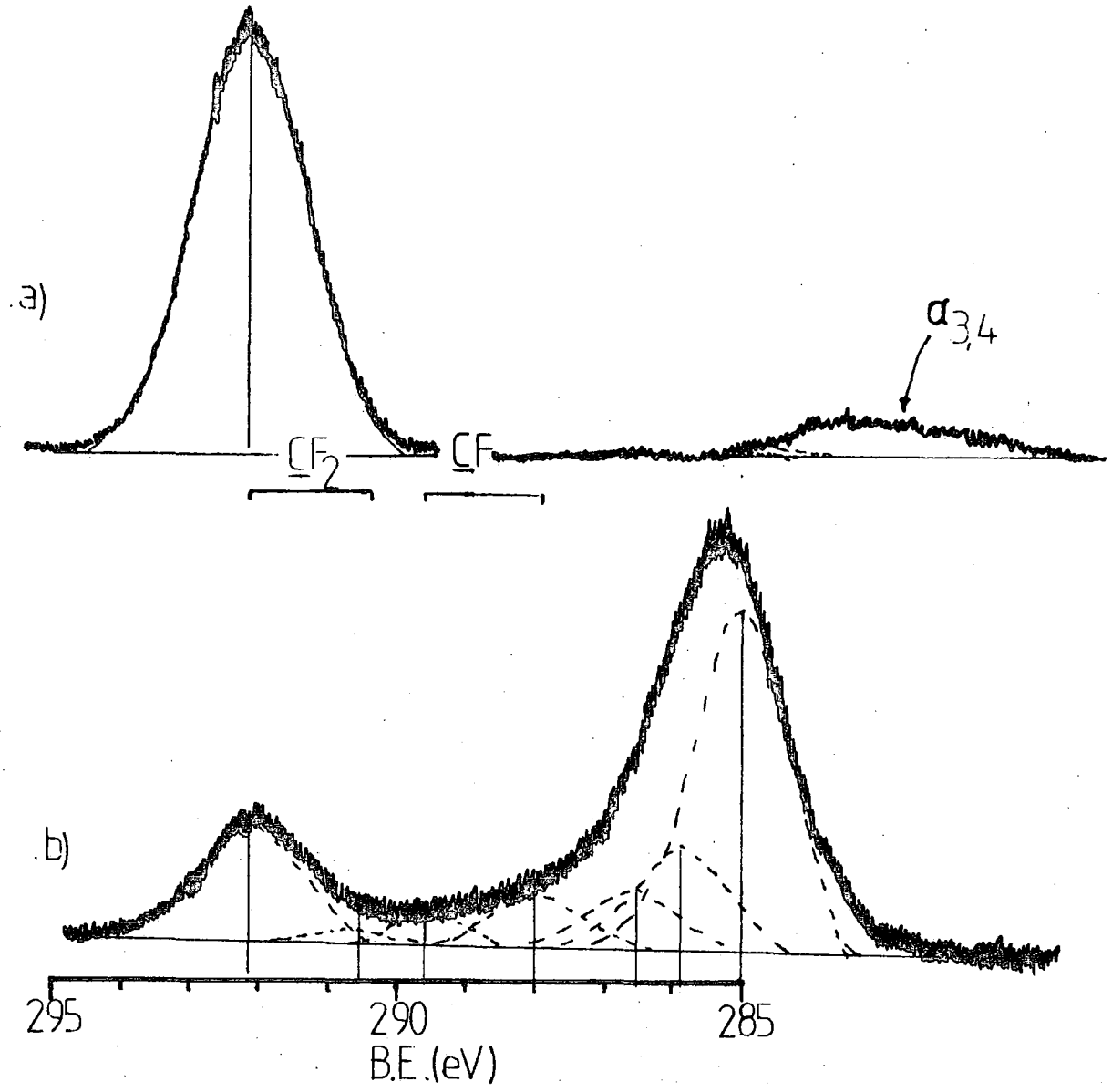

surface chemistry effected by a hydrogen plasma were carried out in the inverted 'T' shape reactor. Initially experiments involved a power input of 5 watts at a pressure of .08 torr of hydrogen, for reaction times in the range 0-128 seconds. The great reactivity of the PTFE towards the hydrogen plasma is evident from the C_{1s} spectra shown in Figure 3.3. At 70° take-off angle (Figure 3.3) the spectra reveal a very rapid loss of $\underline{C}F_2$ components at high binding energies, such that after a treatment time of 64 sec. the C_{1s} spectrum is dominated by the component at 285eV corresponding to carbon atoms in an environment devoid of fluorine substituents in either an α or β position. This extensive defluorination in the surface is also evidenced by the decline of the F_{1s} signal relative to the C_{1s}. The dominant reaction being $CF_2 \longrightarrow -\underset{|}{\overset{|}{C}}-$, with little evidence for the generation of intermediate structures based on CF components. (This contrasts with results recorded on the inert gas plasma treatment of copolymers of ethylene and tetrafluoroethylene).

Comparison of the spectra taken at take-off angles of 30° and 70° (Figures 3.3(a) and 3.3.(b)) reveal the surface nature of the reaction, the spectra taken at the higher take-off angle show an equilibrium surface structure is established after an exposure period of ≈64 secs. Even after prolonged treatment the extent of defluorination revealed by the spectra taken at the higher take-off angle is not matched by that reflected by the deeper sampling spectra recorded at 30° take-off angle. The treatment is thus seen to be vertically inhomogeneous within the ESCA sampling depth.

Figure 3.3 C_{1s} Core Level Spectra of PTFE Samples treated in a Hydrogen Plasma in Reactor shown in Figure 3.1(a) for take-off angles of 30° and 70°

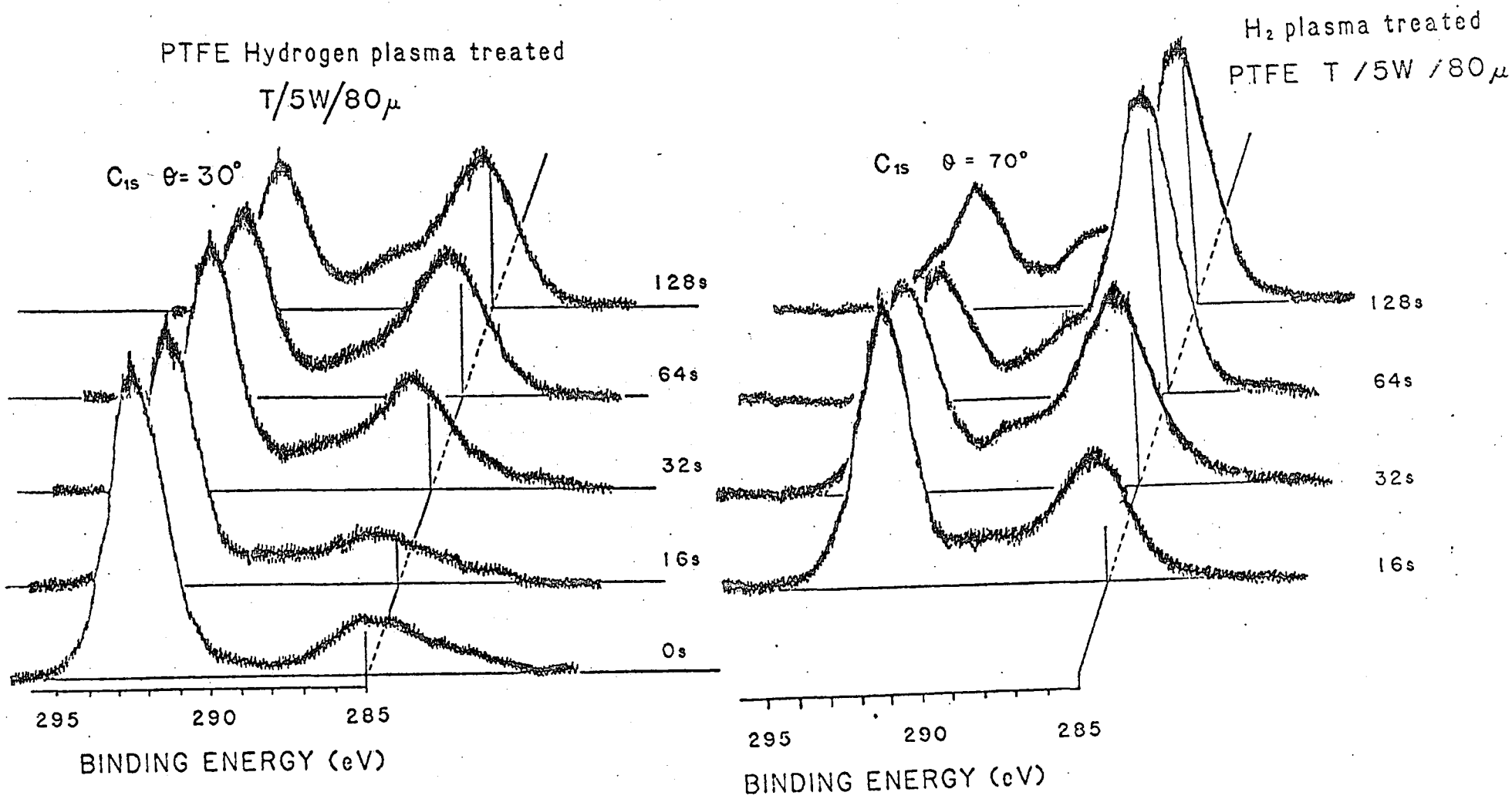

The dramatic change in surface chemistry is also reflected in the contact angle (sessile drop) with water; this is shown in Figure 3.4. Such are the adhesion properties of the treated surface, that after 64 sec. good adhesion is obtained with nitrocellulose based paints in the standard scotchtape test, in marked contrast to untreated PTFE.

3.3.2 Kinetic Studies of the Surface Modification

These preliminary studies indicated a facile surface transformation of PTFE by means of a hydrogen plasma and indicated that a detailed semiquantitative kinetic study should be undertaken. In this study reactor configuration (b) in Figure 3.1(b) was employed. The lower flow rates in this reactor allowed a much lower power input to be employed to maintain a comparable $^{W}/_{FM}$ parameter to that of the preliminary studies.

The experiments involved, *inter alia*:

(a) time dependence of the reaction at fixed power; and

(b) the power dependence at fixed exposure times.

The experiments were carried out with total inputs of 0.1 watt and at 1 watt and 5 watts; for the 2 lowest power settings pulsed plasmas were employed.

3.3.3 Time Dependence at 0.1 watt

The C_{1s} and F_{1s} spectra for a range of treatment times at 0.1 watt power input are shown in Figures 3.5(a),3.5(b). These spectra reveal the great reactivity of PTFE to low power plasma treatments. Even for a 2 sec. exposure there is a significant change in the surface chemistry, the decrease in

Figure 3.4 Variation in the Contact Angle to water of a PTFE Surface treated in Reactor (a) (5W, 0.2 torr H_2) with treatment time

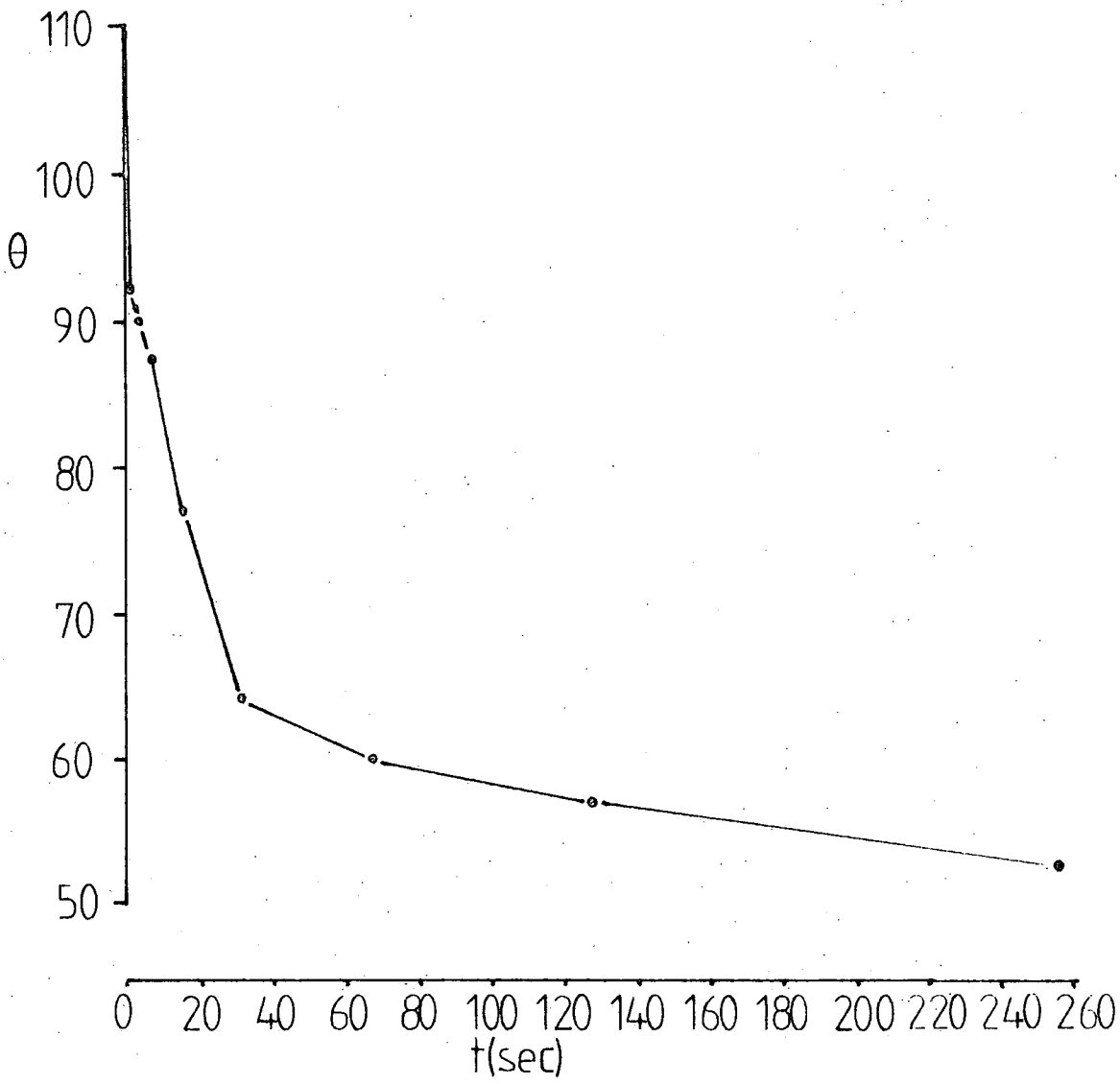

(a)

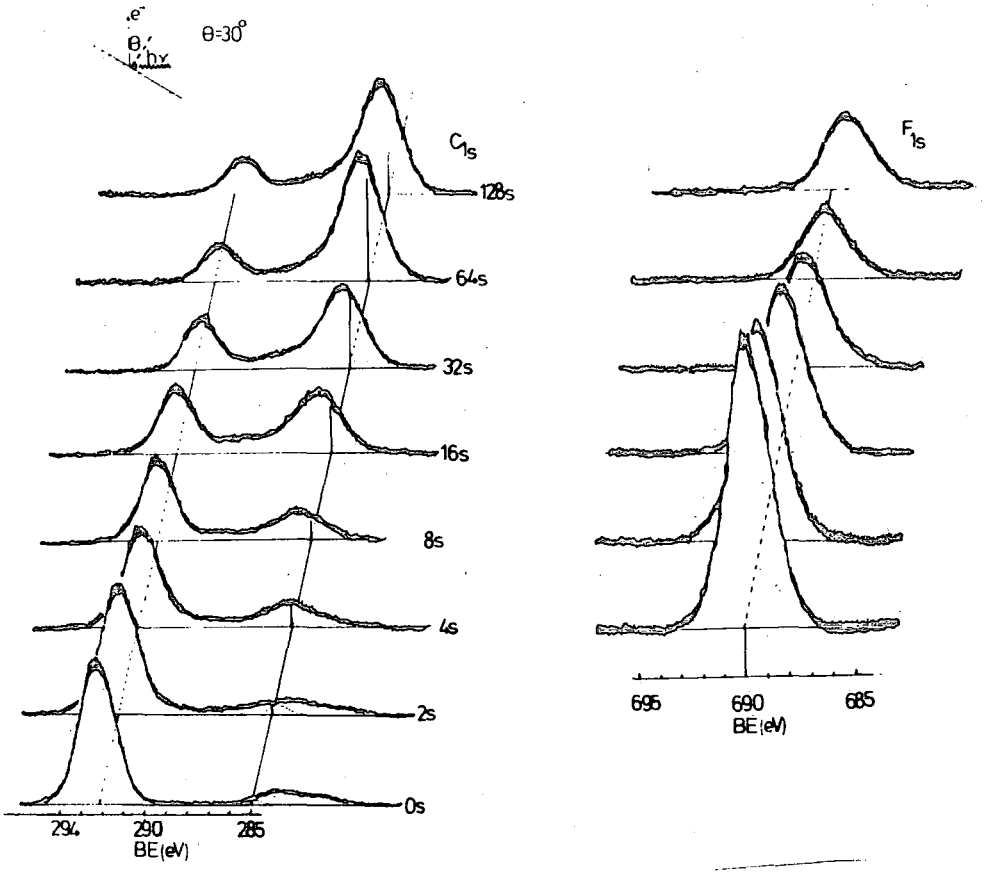

(b)

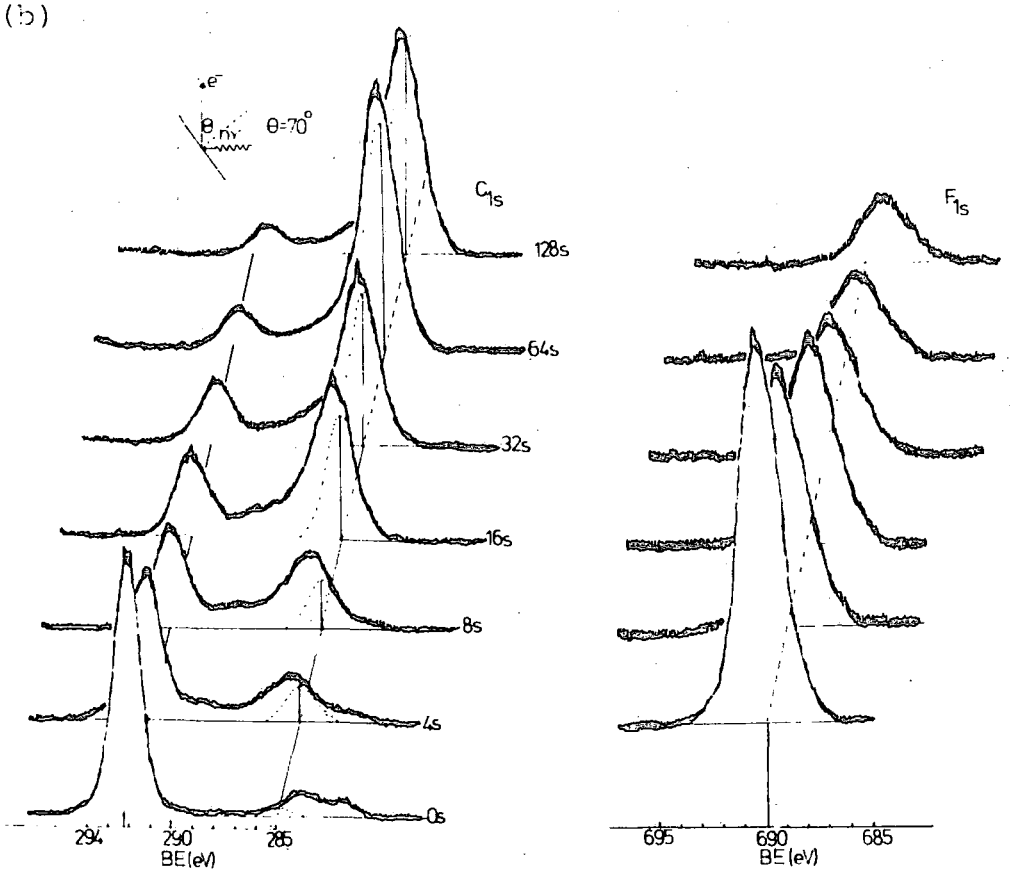

Figure 3.5 Core Level Spectra at 30° and 70° take-off angles for PTFE treated in a Hydrogen Plasma (0.1W, 0.2 torr H_2) for increasing reaction times

the fluorine content of the surface regions being revealed by the decrease in intensity of the component arising from $\underline{C}F_2$ structural features and concomitant rise of the lower binding energy component associated with $\underline{C}H$ environments. The spectra also illustrate the vertical inhomogeneity of the reaction, *e.g.* after 16s treatment the integrated intensities of the component signals expressed as a percentage of the C_{1s} signal intensity are $\underline{C}F_2$: $\underline{C}F$, $\underline{C}$=O, *etc*: $\underline{C}$ 44.0 : 13.0 : 43.0 at $\theta = 30^{o}$ and 25.5 : 11.5 : 62.0 at $\theta = 70^{o}$, emphasising the surface nature of the defluorination reaction. However the integrated C_{1s} intensity ratio for spectra recorded at 30^{o} and 70^{o} take-off angles remains essentially constant, indicating little difference in the number density of carbon atoms over the 2 depth scales appropriate to the 2 take-off angles. The absolute integrated intensities however do show variations at each take-off angle (Figure 3.6) indicating changes in interchain spacing as a function of reaction time. Thus the integrated C_{1s} signal intensity initially drops and then rises to a value some 20% higher than for PTFE, suggesting a degree of cross-linking in the final structure. Thus, the core level spectra reveal the substantial loss of fluorine accompanying hydrogen plasma treatment, the main process being the conversion of $-\underline{C}F_2-$ functionalities into $-\underset{|}{\underline{C}}-H$ groups with the notable absence of β $\underset{|}{\underline{C}}-F$ functionalities, the main component after extended treatment being located at 285eV binding energy.

A further manifestation of the change in surface chemistry is the dynamic equilibrium charging shift for the sample as a function of reaction time. It has been previously noted that charging shifts provide an important monitor on

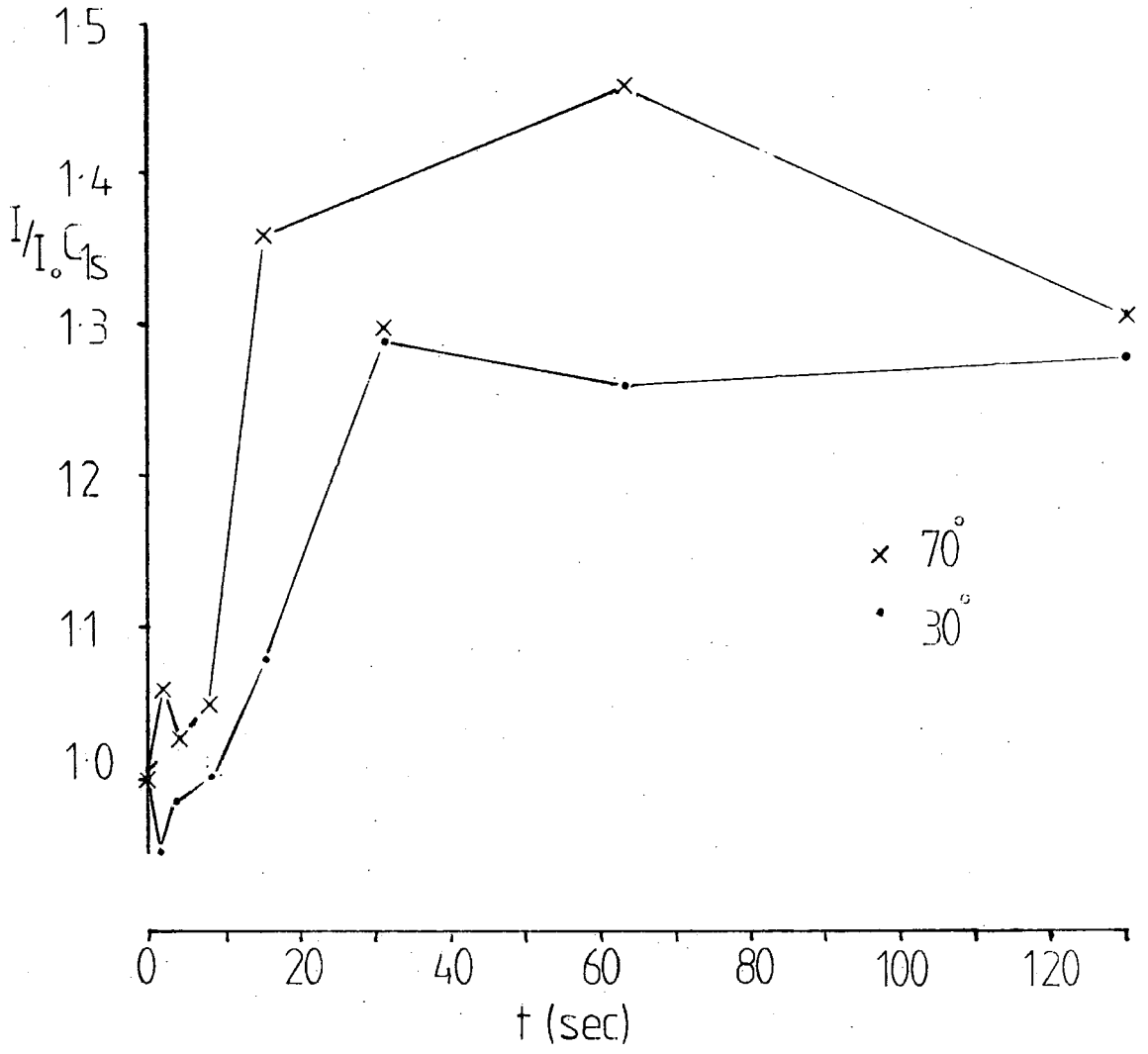

Figure 3.6 Variation in the Absolute Integrated Intensity of the C_{1s} Level relative to that of untreated PTFE with treatment time

structure in the surface regions and Figure 3.7(a,b) shows the charging shift as a function of reaction. Using the equilibrium charging shifts obtained from polyethylene and PTFE under the conditions that these spectra were run it can be shown that the shift follows the fraction of $\underline{C}F_2$ groups in the surface region. The equilibrium surface charging shift attained by a system has been shown to depend upon the sum of the total photoionisation cross-sections of the elements present in the sample surface. Fluorine has a high total photoionisation cross-section whereas that of hydrogen is very small as the surface is depleted of fluorine the equilibrium sample charging is seen to decrease, This emphasises the great surface dependence of sample charging phenomena.

The C_{1s} spectra in Figure 3.5 reveal that the centroid of the $\underline{C}F_2$ component shifts to lower binding energies as the reaction proceeds, indicating that as the reaction proceeds the $\underline{C}F_2$ groups remaining are located in environments predominantly without β CF_2 groups.

At longer reaction times, a small high binding energy shoulder develops the peak due to $-\underline{C}F_2-$ functionalities, indicative of the development of a small percentage (1-2%) of CF_3 groups; perhaps produced by the interaction of HF produced by the defluorination reaction with radical species produced by chain scission, or by the abstraction by such a radical of a fluorine atom from an adjacent chain. Their development is restricted to the extreme surface regions of the polymer. The possibility of this shoulder being due to the development of shake-up structures from unsaturation is discounted, the unsaturation in polyisoprene has been found to disappear rapidly on exposure to a hydrogen plasma.

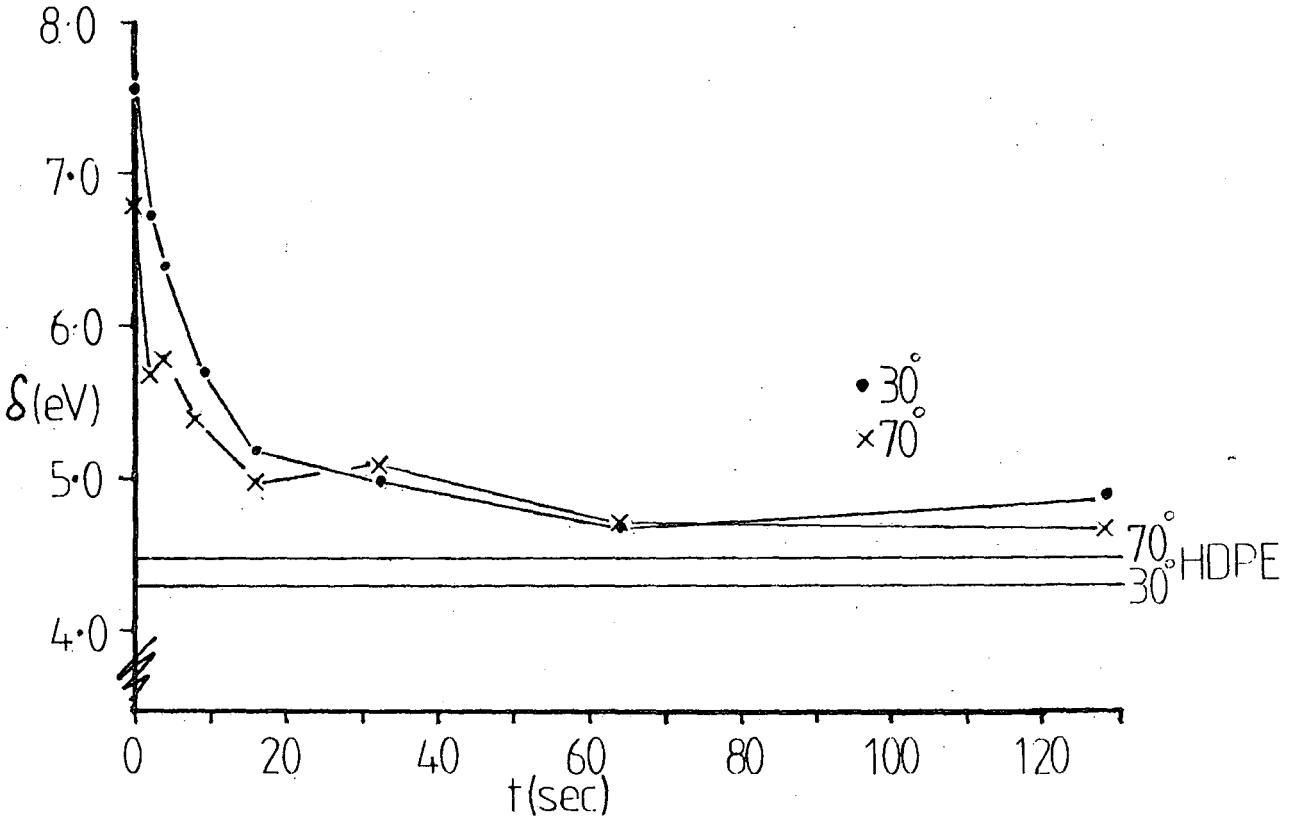

Figure 3.7 (a) Variation in the Equilibrium charging Shift attained by a treated PTFE Sample during ESCA analysis as a function of treatment time

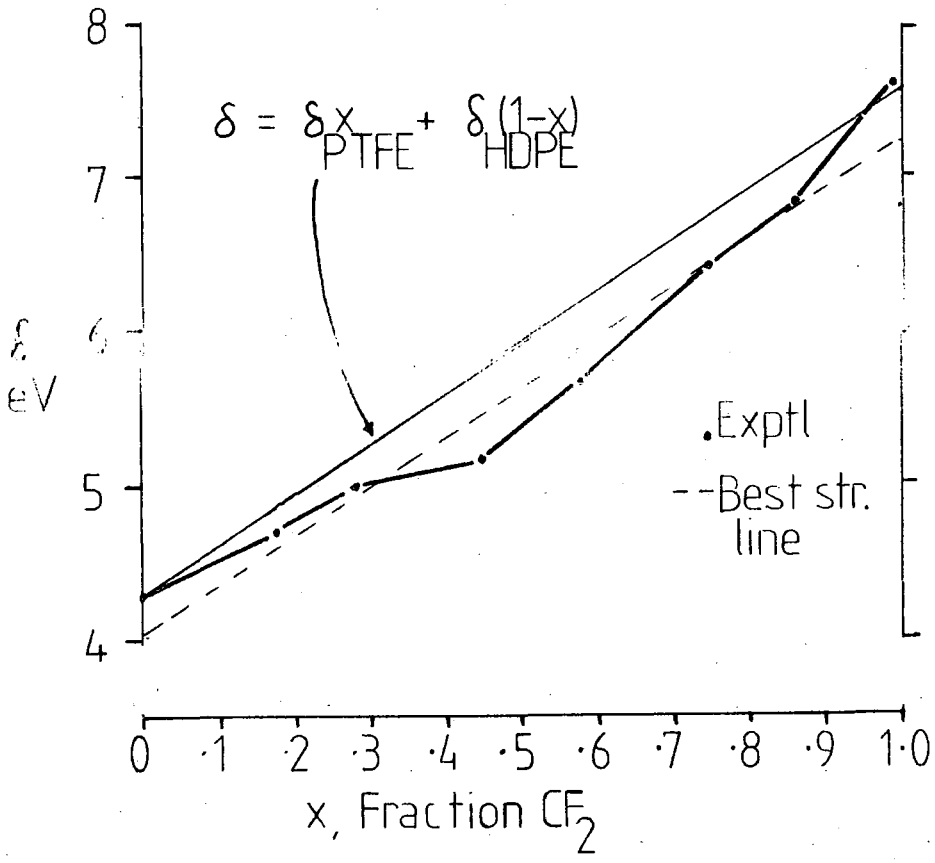

Figure 3.7 (b) Variation in Equilibrium charging attained with Surface Composition

Analysis of the untreated PTFE revealed a very low degree of oxygen incorporation in the polymer surface. As the reaction proceeds oxygen is incorporated into the surface, the overall O_{1s} signal intensity rising to 12-13% of the intensity of the C_{1s} peak. This situation obtains after 32sec. treatment time and is invariant with increasing treatment time. The comparison of C_{1s}:O_{1s} signal intensity ratios at the two take-off angles employed in this study with reaction time shows the oxygen incorporation to be uniform within the ESCA sampling depth. This contrasts with studies of the oxygen plasma treatment of polyethylene where a gradient was detected in the introduction of oxygen functionalities into the surface. The extreme surface sensitivity of the oxygen plasma treatment being attributed to the diffusion limited nature of the reaction the reactive species (*e.g.* O, $.O_2^+$ *etc.*) reacting with low activation energy. In this study the homogeneous nature of the oxygen uptake would suggest the scavenging of radical sites produced by exposure to the plasma treatment by low levels of oxygen dissolved in the polymer or desorbed from the walls of the reactor. This oxygen uptake is also found even when elaborate precautions are taken to exclude and remove oxygen from the system. Similar problems were encountered by Clark and Dilks[130] in their studies of the argon plasma treatment of fluoropolymer surfaces.

The broadness of the O_{1s} signal is due to the presence of oxygen containing structural features in a variety of fluoro- and hydrocarbon-like environments. These oxygen containing functionalities contribute a variety of components to the C_{1s} envelope, between the decaying $-\underline{C}F_2-$ feature and the emergent $-\underline{C}H$ environments.

Figure 3.8 Relative Intensities of the Components of the C_{1s} Spectrum as a function of reaction time.
(a) at a 30° take-off angle, (b) at a 70° take-off angle

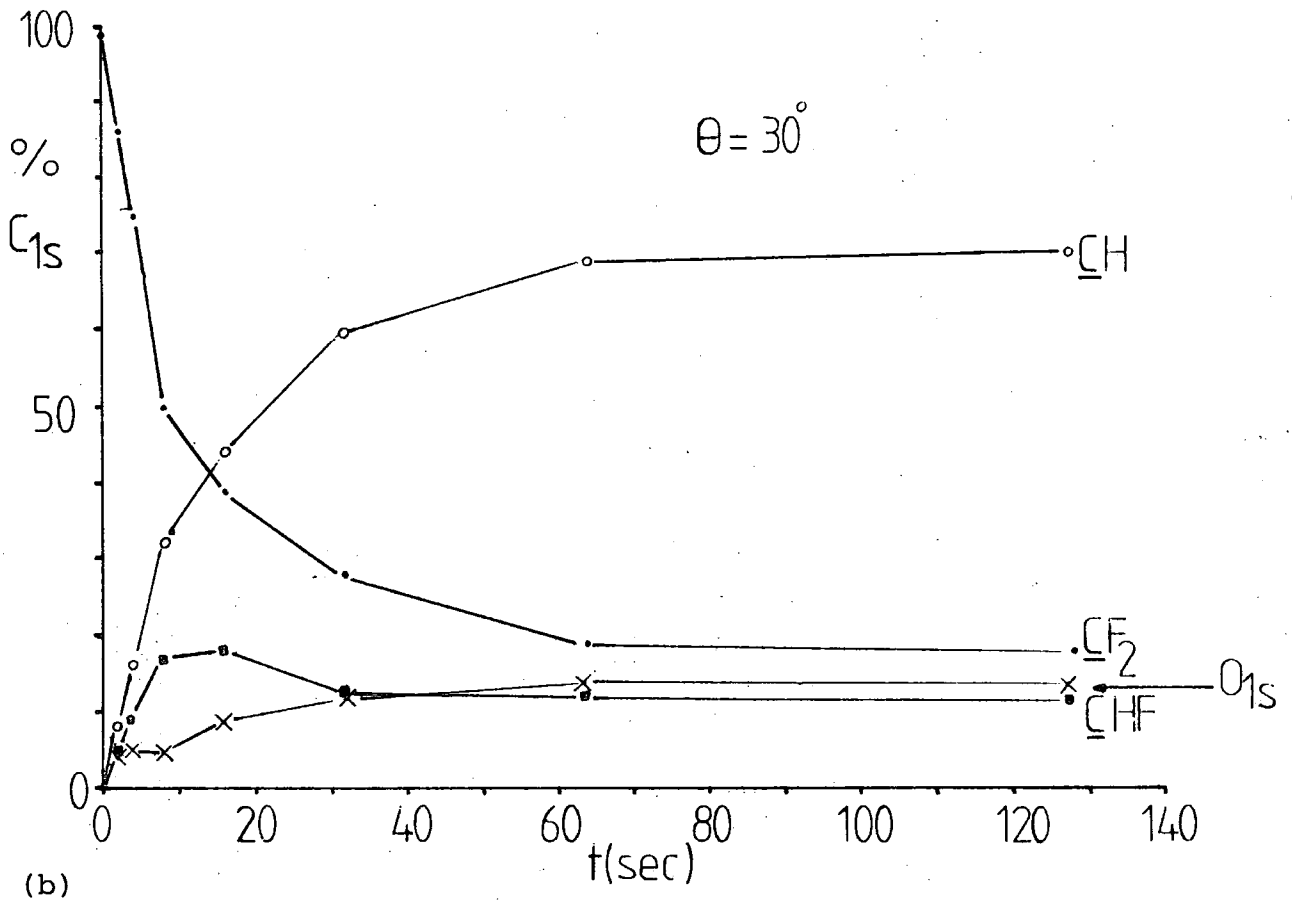

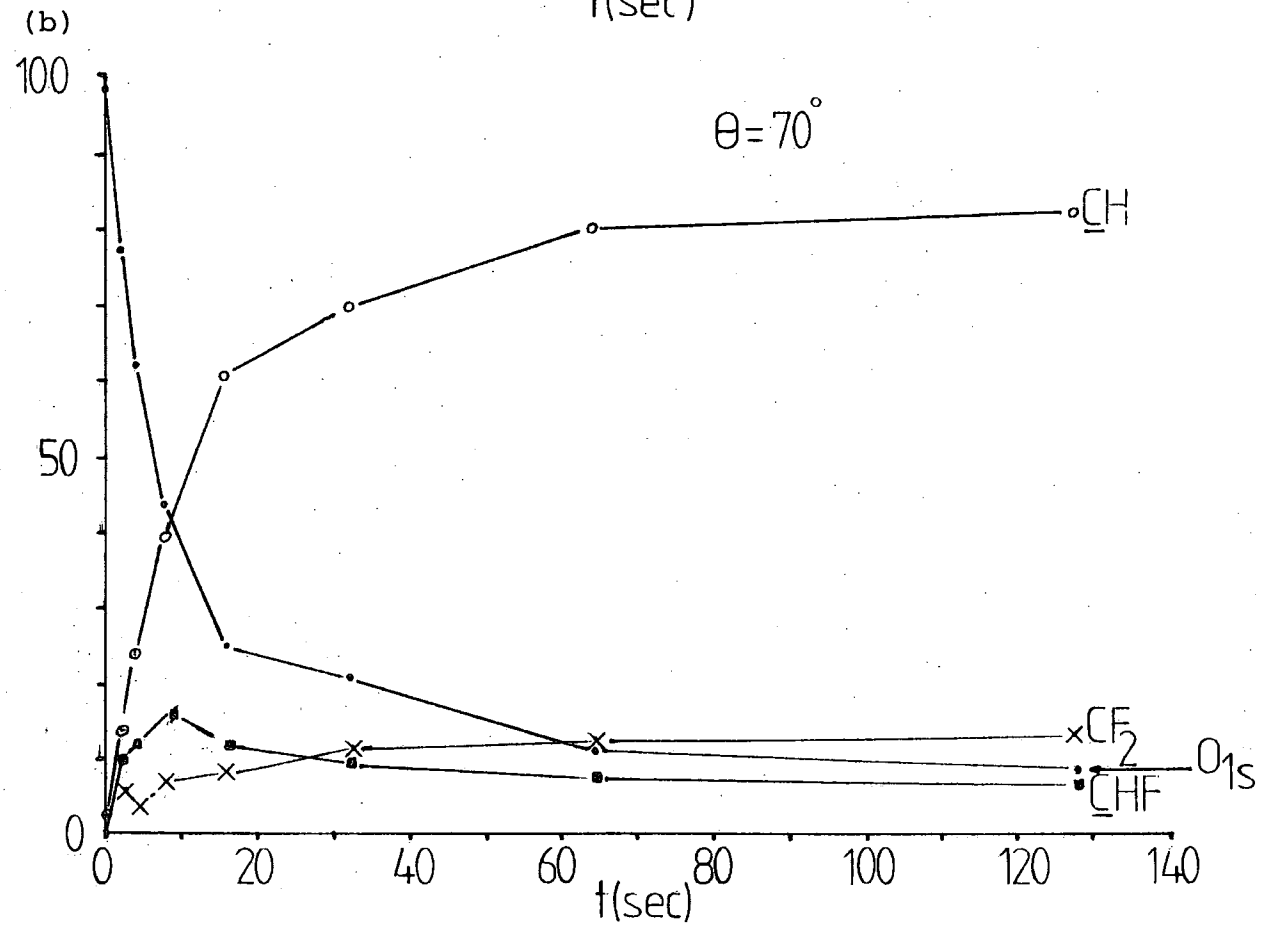

To monitor the rate processes occurring during the reaction, the spectra provide several convenient components, namely: the F_{1s} levels and the $\underline{C}F_2$ and $\underline{C}H$ components of the C_{1s} spectra. The progress of the reaction with depth into the surface is facilitated by the recording of the essentially core-like F_{2s} spectra. From studying the relative intensities of the F_{1s} and $\underline{C}F_2$ component of the C_{1s} envelope and the F_{2s} levels which span a range of kinetic energies and hence sampling depths, the depth profile of the defluorination may be examined.

The variation with time of the contributions of the $\underline{C}F_2$ and $\underline{C}H$ components to the C_{1s} envelope at the two take-off angles, 30^{o} and 70^{o} employed in this study are shown in Figures 3.8(a) and (b). The F_{1s}/C_{1s} intensity ratios variation with increasing reaction time is illustrated in Figure 3.9.

As a first attempt to gain an insight into the mechanism of the reaction plots of the natural logarithm of the fractional contributions of the CF_2 and CH features to the C_{1s} envelope and of the integrated intensity of the F_{1s} levels (with respect to the C_{1s} level as an internal standard), as a function of treatment time were made for the data acquired at each take-off angle. Such plots are illustrated in Figure 3.10.

These plots display curvature which could be naively attributed to a reaction involving more than one rate process. Comparison of the initial rates of reaction obtained for each plot are given below (Table 3.1). From this data it can be seen that whichever facet of the spectra is chosen to monitor the reaction the data at the higher take-off angle, *i.e.* the more surface sensitive measurement, leads to a higher initial

Figure 3.9 Variation in the F_{1s} signal as a function of reaction time for 30° and 70° take-off angles

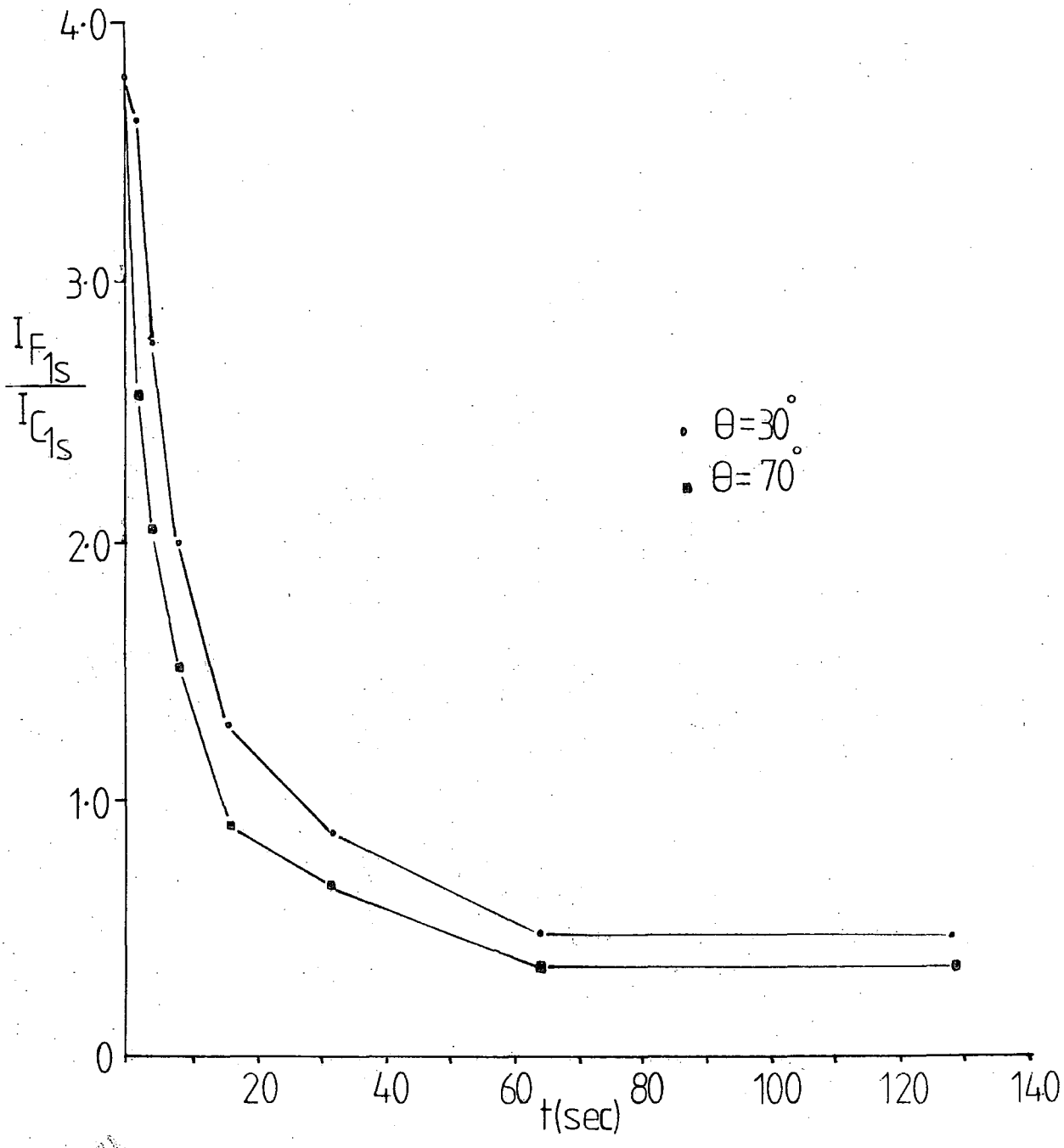

Figure 3.10 $\ln {}^{I}/_{I_{C_{1s}}}$ *versus* reaction time for the F_{1s} level and of the C_{1s} level at (a) 30° and (b) 70° take-off angles.

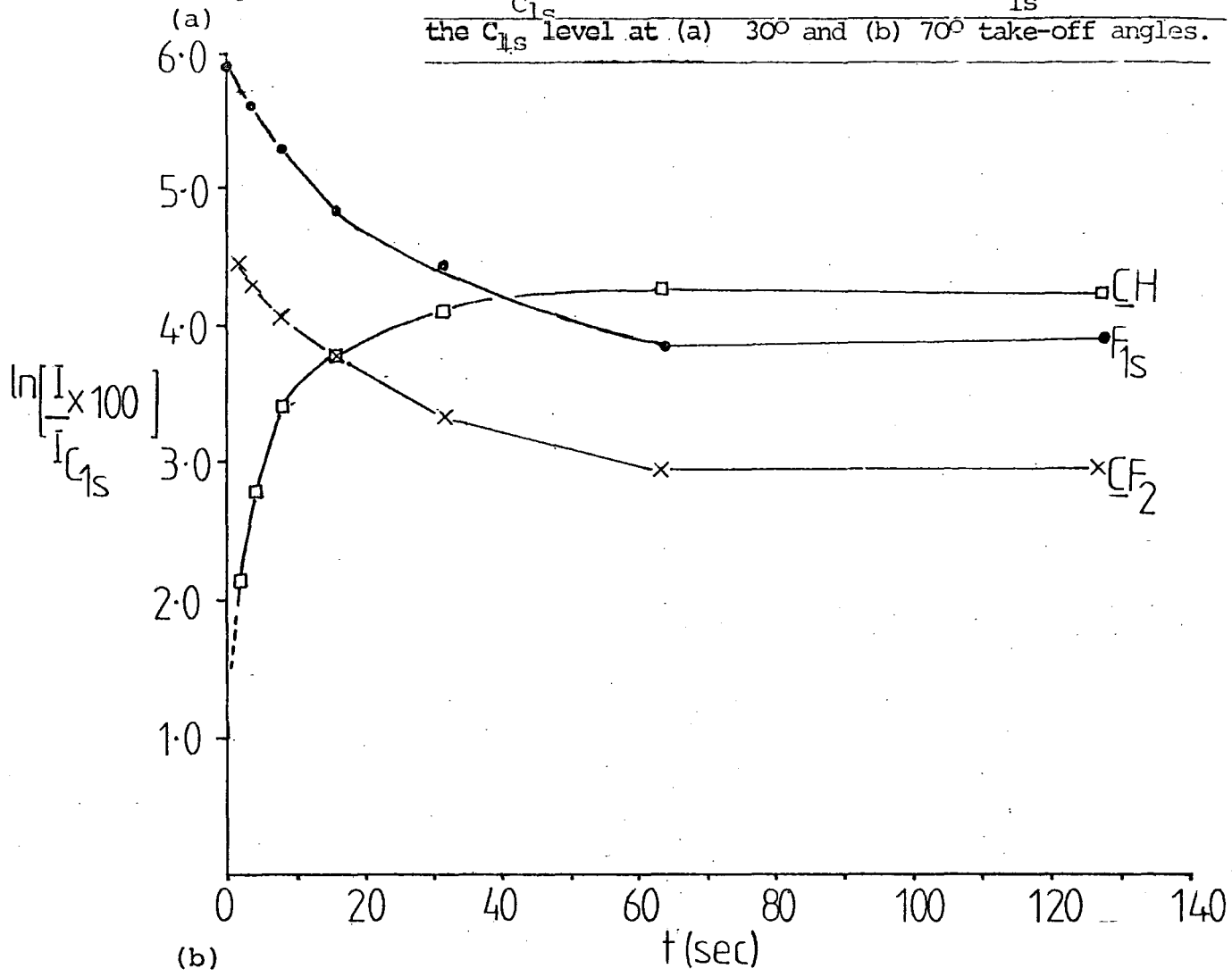

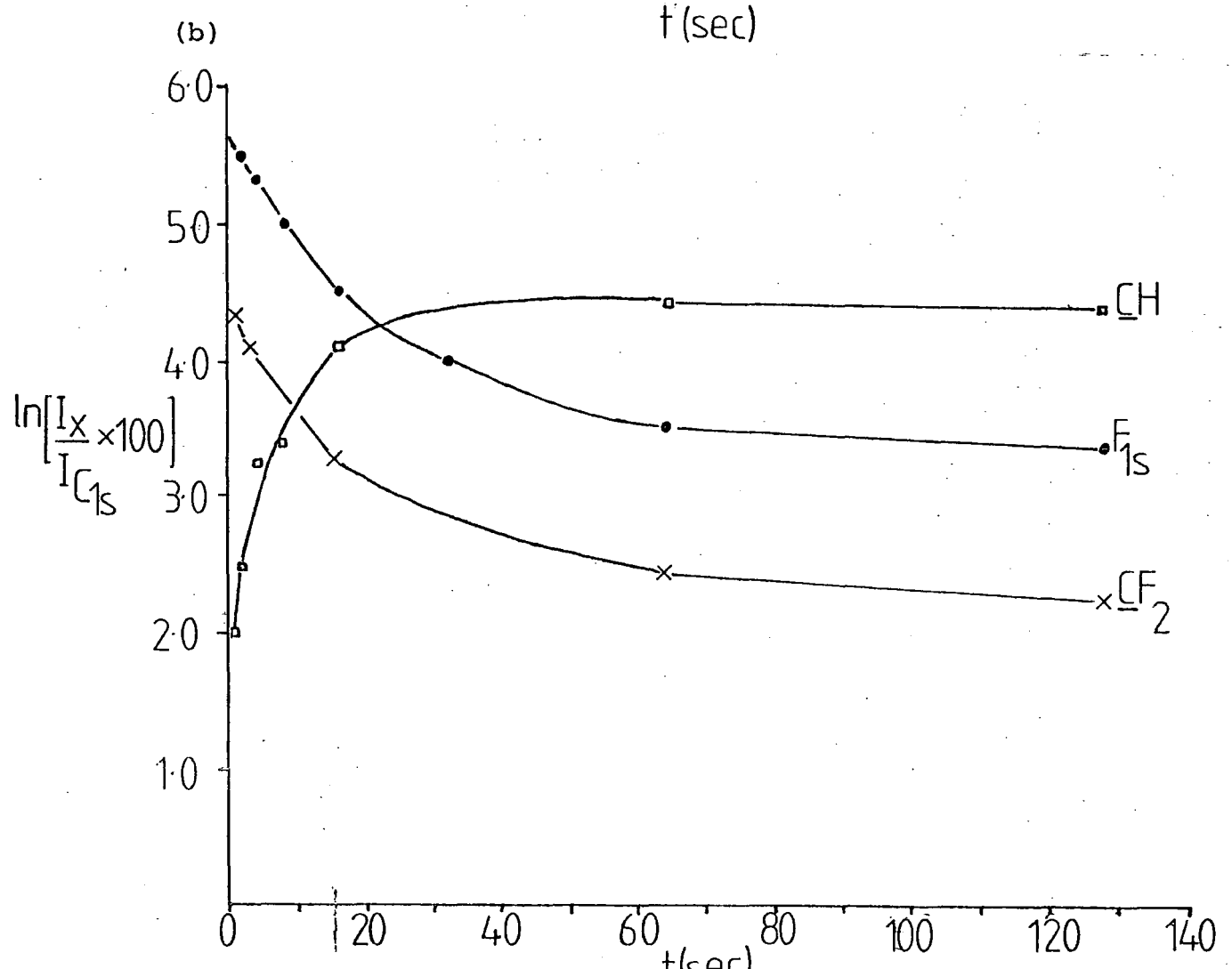

TABLE 3.1

s^{-1}	30^{o}	70^{o}
$R_{F_{1s}}$	.07	.08
R_{CH}	.21	.20
R_{CF}	.06	.09

rate constant than the data accumulated at the lower, more sub-surface sensitive angle. There is a gradient in the rate and extent of reaction between the very surface and sub-surface of the polymer This effect would be accentuated by the exponential weighting of the sensitivity of the ESCA technique to the surface most regions of a sample. As the overlayer *etc.* develops it does so in the region of the sample where ESCA is most sensitive, the signal from the fluorine containing moieties which recede into the subsurface as the reaction progresses are also attenuated by this layer. Using the large difference in the sampling depths of the F_{1s} and F_{2s} levels further insight as to the progress of reaction can be gained from a plot of the ratio of the intensities of these two levels as a function of time and take-off angle (Figure 3.11). The ratio decreases with time indicating the more rapid defluorination of the surface regions as postulated earlier in this discussion, more interestingly the F_{1s}/F_{2s} ratios for the two take-off angles at a given reaction time are approximately the same, only showing divergence at extended reaction times, indicative of a smooth reaction gradient with depth as opposed to the reaction proceeding in a surface boundary layer or uniform reaction within the ESCA sampling depth.

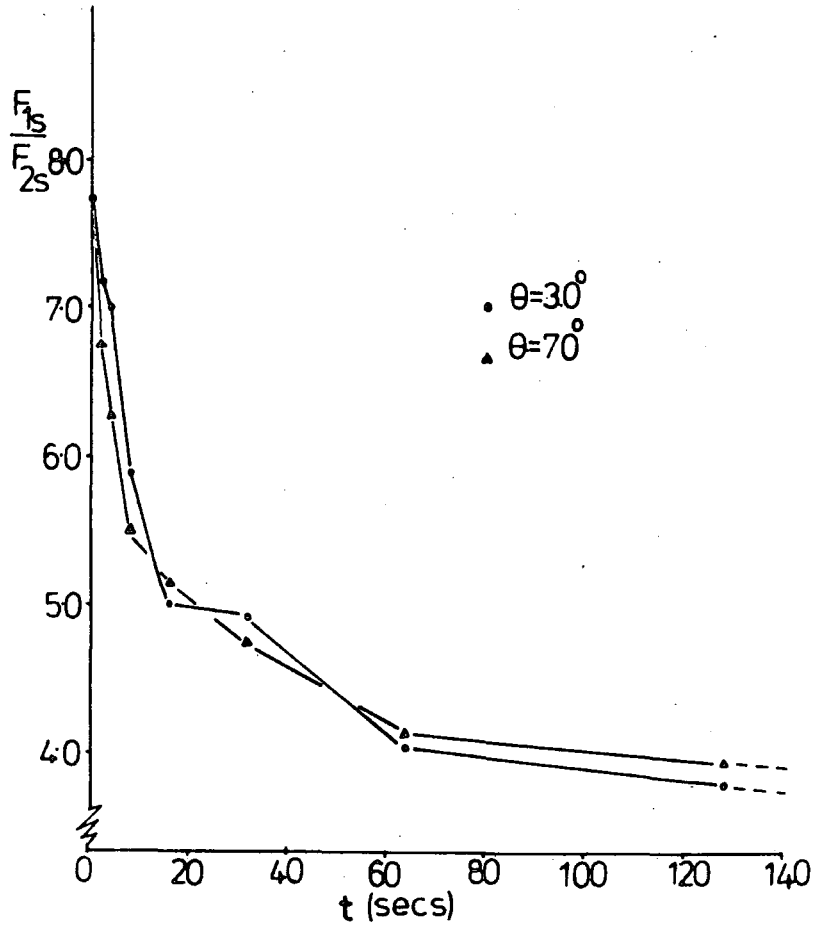

Figure 3.11 F_{1s}/F_{2s} intensity ratio as a function of reaction time

The extreme surface nature of the reaction is emphasised by the comparison of C_{1s} spectra obtained for a treated sample of PTFE using $Mg_{K\alpha}$ and $Ti_{K\alpha}$ X-ray sources. Whereas in the more surface sensitive $Mg_{K\alpha}$ spectra the $\underline{C}$, hydrocarbon like component dominates the spectrum, in the corresponding $Ti_{K\alpha}$ spectrum (Figure 3.12) the reverse holds, the original $\underline{C}F_2$ environments still dominate the spectrum. This is equivalent, from the $Ti_{K\alpha}$ spectrum, to an overlayer of $\simeq 16\text{Å}$ of hydrocarbon like material on the sample but this is not borne out by the $Mg_{K\alpha}$ spectrum. Again a depth gradient in the reaction is indicated.

3.3.4 Modelling of the Kinetics and Depth Profile of Reaction and Comparison with Experiment

From the foregoing discussion it is apparent that in the initial stages of the reaction of a hydrogen plasma with a PTFE, there exists a depth profile encompassing different extents of defluorination. The method of varying the photoelectron take-off angle for depth profiling in XPS has received much attention. However in a kinetic study, the prospect of having to perform a full angle resolved study for each kinetic point is daunting. As a compromise the spectra were taken for two take-off angles (30° and 70°) and for core-levels spanning a range of sampling depths (F_{1s}, C_{1s}, F_{2s}). This provides a more dynamic method of obtaining depth profile information than by monitoring a single pair of core-levels with varying take-off angle. Algorithms for modelling the angular behaviour of XPS signals corresponding to postulated depth profiles containing concentration gradients and for predicting the form of concentration gradients from such data have

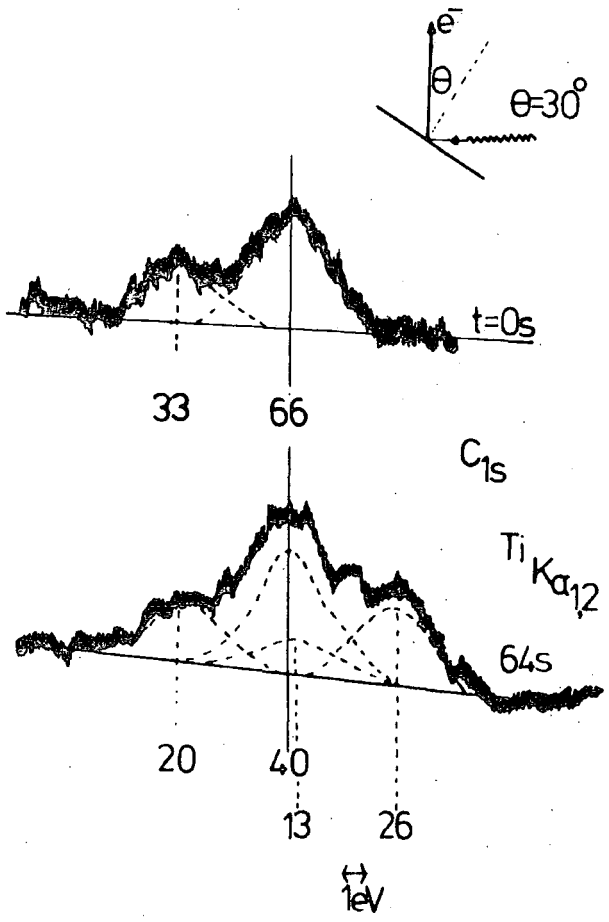

Figure 3.12 Comparison of $Ti_{K\alpha}$ excited C_{1s} spectra of a Sample of PTFE treated for 64S in a Plasma at 0.1W (0.2 torr H_2) with that of an untreated sample

appeared in the literature.[211,212] (Though it is worth noting that due to the number of variables in these treatments it is not possible to work backwards from a set of experimental data to a unique depth profile).

In order to quantify the data and understand how such a reaction profile could arise the effect of various depth concentration profiles of a reactant diffusing into the polymer surface and reacting with the polymer matrix, in a reaction which is first order with respect to the reacting species (*e.g.* $H^{\bullet}$) and the polymer CF_2 groups was proposed as a model. The profile is assumed to be constant, as might obtain were the diffusing reactant to be consumed by recombination of reactive species (*e.g.* $H^{\bullet} + H^{\bullet} + M \longrightarrow H_2 + M$), where the chaperone, M, is the polymer matrix) or deactivation of a metastable reactive species M^{*} by collision with the matrix, the rate of consumption of the species by the reaction with the polymer being slow compared with the recombination or deactivation reaction. Alternatively the reaction to remove the reactive species may never terminate, *i.e.* the defluorinated product is also reacting with the reactive species.

Due to this gradient in concentration of the reacting species with depth, H(x), the extent of reaction at a given time will also vary with depth. Dividing the surface into a series of n monolayers of thickness d. The extent of reaction at a time t is given by Y_n (as measured by the fraction of the original $\underline{C}F_2$ groups present in the polymer layer remaining being $1-Y_n$). The situation is illustrated in Figure 3.13.

Recalling the contribution to the overall intensity of a core level, dI, from an infinitesimally small depth element

Figure 3.13 Model adopted for data computer algorithm

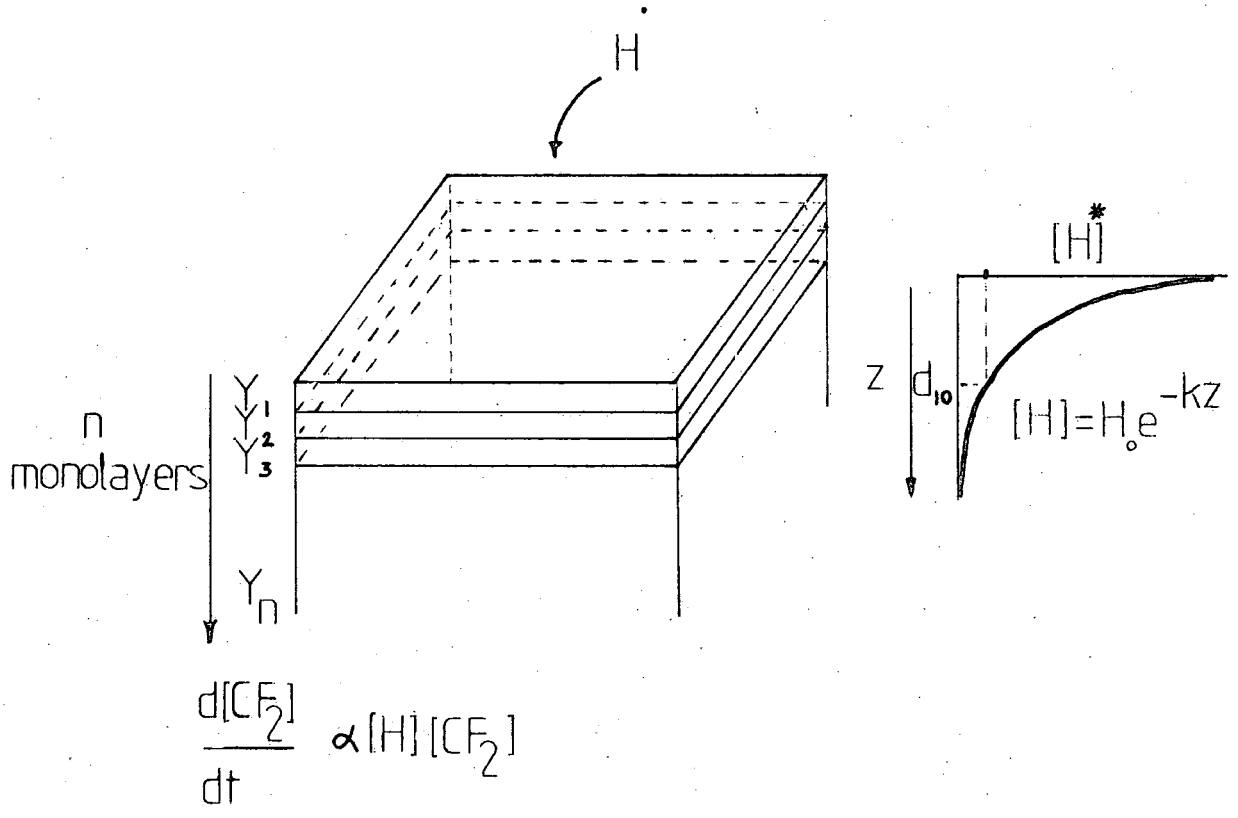

dz to be given by:

$$dI = Fn_i \alpha_i k_i e^{-z/\lambda \cos\theta} dz \qquad (3.1)$$

where all symbols have their usual meanings as given in Chapter One.

Consider the integrated form of this equation for the $\underline{C}F_2$ component of the C_{1s} signal at time t. Replacing the integral over all the levels by a summation.

$$I^t_{CF_2} = K \sum_{i=1}^{n} (1-Y_i)_t \int_{Z_i}^{Z_i+d} d^{-Z/\lambda_{C_{1s}} \cos\theta} dz. \qquad (3.2)$$

Similarly for the $\underline{C}H$ component:

$$I^t_{CH_2} = K \sum_{i=1}^{n} (1-Y_i)_t \int_{Z_i}^{Z_i+d} e^{-Z/\lambda_{C_{1s}} \cos\theta} dz. \qquad (3.3)$$

The intensities of the F_{1s} level and F_{2s} level may be similarly expressed as:

$$I^t_{F_{1s}} = K_1 \sum_{i=1}^{n} 2\,(1-Y)_t \int_{Z_i}^{Z_i+d} e^{-Z/\lambda_{F_{1s}} \cos\theta} dz. \qquad (3.4)$$

$$I^t_{F_{2s}} = K_2 \sum_{i=1}^{n} 2\,(1-Y)_t \int_{Z_i}^{Z_i+d} e^{-Z/\lambda_{F_{2s}} \cos\theta} dz. \qquad (3.5)$$

For convenience the intensities are all ratioed to the total integrated intensity of the C_{1s} level.

$$I_{C_{1s}} = K \sum_{i=1}^{n} \int_{Z_i}^{Z_i+d} e^{-Z/\lambda_{C_{1s}} \cos\theta} dz. \qquad (3.6)$$

The variation of the extent of reaction, Y, with time is taken to follow a pseudo first-order reaction, weighted by the relative hydrogen concentration in that layer, $Y_i = H_i e.^{-kt}$, The overall reaction being second order.

The model takes as its input data: the inelastic mean free paths, λ_i, of electrons emitted from the F_{1s}, C_{1s} and F_{2s} levels by irradiation of a polymeric sample with $Mg_{K\alpha_{1,2}}$ radiation (here taken as 9Å, 15Å and 22Å respectively); the relative sensitivity factors between the levels; the number and depth of the monolayers to be considered; the form of the distribution of the reactive species derived from the plasma with depth (initially an exponential decrease in concentration with depth was used) relative to a surface value of unity; the "time" in units of kt over which the progress of the reaction was to be monitored.

The model was implemented in a computer program (see Appendix 1) written in the Applesoft derivative of BASIC for an Apple II Europlus computer with 48K of available memory. (The code also being adapted to run on a smaller Epson HX20 computer, a listing is to be found in appendices). The program provides as output: the relative weighting given to each monolayer for each core level for each take-off angle; the relative concentration of reactive species with monolayer; the variation of $\underline{C}F_2$, $\underline{C}H$ components of the C_{1s} level, F_{1s} and F_{2s} levels relative to the intensity of the C_{1s} level with time; the variation of the F_{1s}/F_s ratio with time; predicted "initial rates" based on the observation of the C_{1s} and F_{1s} levels in the spectra that would be obtained from reaction in such a

system; the program also produces some graphical output of the extent of reaction in each monolayer with time and of first order plots for the loss of $\underline{C}F_2$ features and production of $\underline{C}H$ carbonaceous features, examples are shown in Figure 3.14.

At the lowest level, confirmation was sought from this model that, at least in a qualitative sense, such data is described previously: in particular the range of first-order rate constants and the $^{F_{1s}}/_{F_{2s}}$ ratios' behaviour.

More quantitatively, estimates of the rate constants and reactant and product distribution with depth were sought. The sensitivity of the model to the form of the depth distribution of reactive species was also explored.

From the model it was confirmed that range of psuedo first order rate constants would be produced by monitoring the fate of the various core levels in the polymer and that the $^{F_{1s}}/_{F_{2s}}$ ratios at 30^{o} and 70^{o} take-off angles decreased in unison, at least in the initial stages of reaction. Reproducing, at least in a qualitative sense the behaviour of the experimentally obtained ESCA data. This situation obtained for a range of assumed exponentially decreasing reactive species concentrations with depth (characterised by a depth d_{10} by which the concentration had dropped to 10% of its initial surface value of unity).

Quantitative comparisons drawn between the computed data for a range of d_{10}'s and the experimentally derived data allowed the reaction to be ascribed to a single rate process with a psuedo first-order rate constant of $0.12s^{-1}(\pm.03)$ occurring due to a constant exponential concentration gradient of reactive species which falls to 10% of its surface value

Figure 3.14 Predicted extents of reaction in each monolayer *versus* time and first-order plots generated by computer model

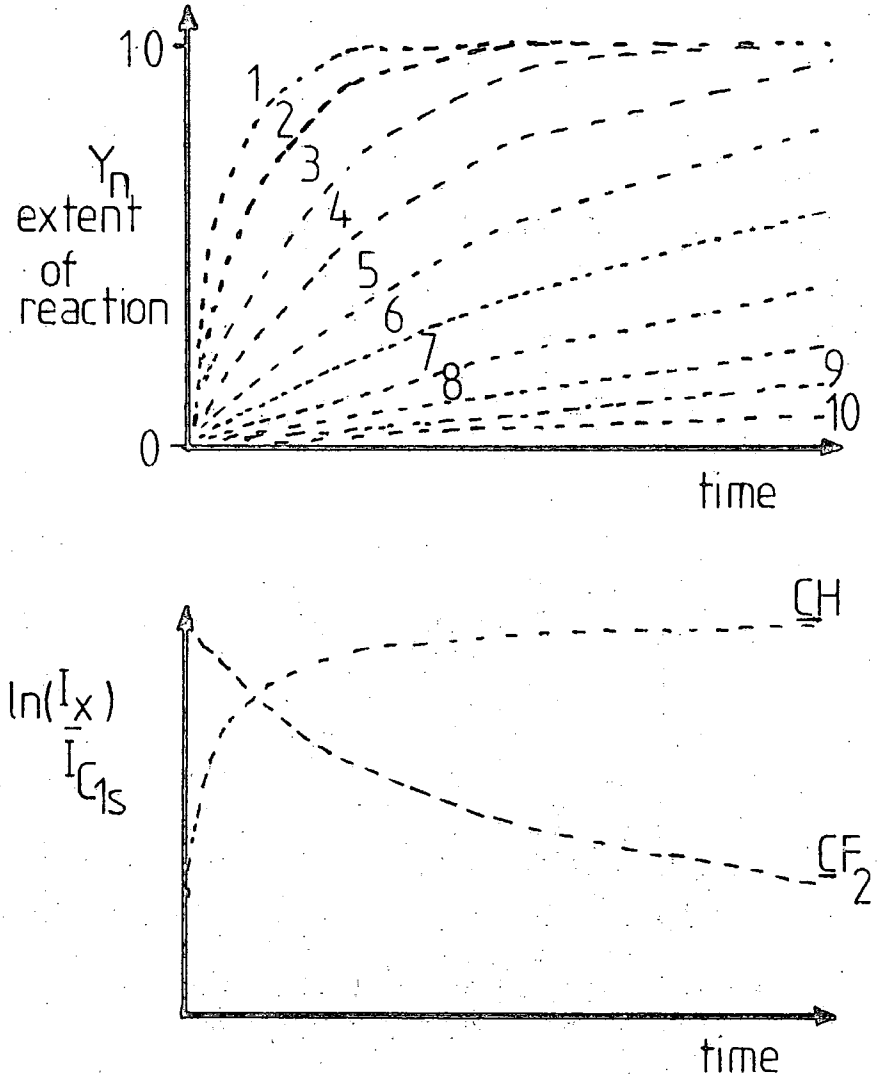

after ∿20Å. This is in accord with the work of Heller *et al*[213] who found that in organic single crystals at room temperature all the hydrogen atoms diffusing into the crystals reacted within a few molecular diameters of the surface. (Though other authors investigating the reaction of H· atoms in n-alkanes at -196°C [214] and solid aromatic hydrocarbons at room temperature[216] have arrived at estimates of H· atoms ranging several orders of magnitude higher than this work).

The model was found to be insensitive to the form of the distribution of reactive species with depth, comparison of linear, exponential and Gaussian (Fickian) profiles dropping to 10% of their surface value after 20Å showed little variation in the behaviour of the predicted reaction profiles, rate constants, etc.

In view of the vast spread of ranges predicted by various authors for thermal hydrogen atoms in frozen organic liquids and crystals ranging from 10^{-4} cm[214] and 10^{-5} cm[216] to a few molecular diameters *ca* 20Å as found in this study it is interesting to speculate whether this would lead to a differential reactivity between the crystalline and amorphous regions of a polymer: the range being lower and the reaction therefore more concentrated in the surface in highly crystalline of the polymer. Using Electron Spin Resonance Spectroscopy (ESR), Dubinskaya has studied the reaction of hydrogen atoms generated by a microwave discharge with thin films of polymers deposited on an Aerosil support, at low temperatures.[217-219] Whilst the reaction with polyisobutylene[217] films is uniform throughout the film, it is restricted to the top <200Å of the surface in polymethylmethacrylate and polyvinylalcohol films.[218-21]

Differential rates of reaction for the crystalline and amorphous regions of polymeric materials exposed to plasma discharges have been proposed by other authors.

Attempts to understand the existence of concentration gradient of hydrogen atoms in the polymer surface as a balance between the diffusion of the species into the polymer and reactions to remove the species, *e.g.* reaction with the polymer matrix, ($H^{\cdot} + CH_2$ or $CF_2 \longrightarrow -\dot{C}H-$ or $-\dot{C}F- + H_2$) or recombination of the species ($H^{\cdot} + H^{\cdot} + M \longrightarrow H_2 + M$, M being the polymer matrix), as outlined in treatments by Jost,[220] Crank[221] or Frank-Kamenetskii[222,223] lead to either excessively small estimates of the diffusion coefficient for hydrogen atoms (*cf.* values for *e.g.* N_2 in PTFE) given the depth of reaction or conversely using an assumed value of diffusion coefficient for $H^{\cdot}$ in PTFE, a depth of reaction of the order of 10^{-4}cm (10000Å). The non-continuous nature of the surface phase may not make it amenable to such treatments. Instead a distribution depending upon a Beer Lambert type attenuation with depth is envisaged. Even when the surface layer is completely defluorinated, *i.e.* hydrogenated, this layer will continue to consume $H^{\cdot}$ in exchanging hydrogen atoms in the polymer backbone. Thus the concentration gradient of reactive species will remain essentially static.

The model takes no account of any side reactions, *e.g.* oxidation from water produced by the interaction of the plasma with the glass walls of the reactor, crosslinking (which will in turn alter the number density of carbon atoms and also reduce the ability of reactive species to permeate the matrix) or the changing rate of reaction as the basic reaction changes from defluorination and hydrogenation of a fluoropolymer matrix

to an exchange reaction between hydrogen atoms and an essentially hydrocarbon matrix.

3.3.5 Time Dependence at Higher Discharge Power Loadings

A limited study of the reaction was also made for two higher power loadings (1.0W and 5.0W) the pressure and flow rate being maintained as before. Due to the extreme rapidity of the reaction which is essentially complete after 60s. at·1W, at discharges powers in escess of 1.0W the reaction is too fast to monitor by the technique used here. At 1W the reaction is essentially complete after 20s.(see Figure 3.15). Even at higher powers the final extent of reaction remains constant, it appears to only be possible to remove up to *ca.* 80% of the fluorine present in the polymer surface. Throughout the reaction at each power the surface, as monitored by spectra taken at 70^{o} take-off angle, is seen to be more highly defluorinated than the subsurface. As remarked upon before in consideration of the data obtained at .1W, the $^{F_{1s}}/_{F_{2s}}$ ratio is seen to drop with increasing reaction time to a limiting value of *ca.* 3. As before the $^{F_{1s}}/_{F_{2s}}$ ratio from spectra run at 70^{o} is seen to drop in unison with the data obtained at 30^{o} again revealing the presence of a reaction gradient within the surface, although a less marked reaction gradient than exists in the early stages of reaction at .1W discharge power. At extended reaction times at higher power loadings somewhat erratic results are obtained. Whereas at lower powers .1W at extended reaction times an equilibrium degree of defluorination is obtained, at higher powers this equilibrium extent of reaction is not reproducible. A plausible explanation may lie in the increasing contribution of ablative processes at higher discharge powers.

Figure 3.15 Variation of (a) the F_{1s}/C_{1s} and (b) F_{1s}/F_{2s} intensity ratios as a function of reaction time at the higher power of 1W.

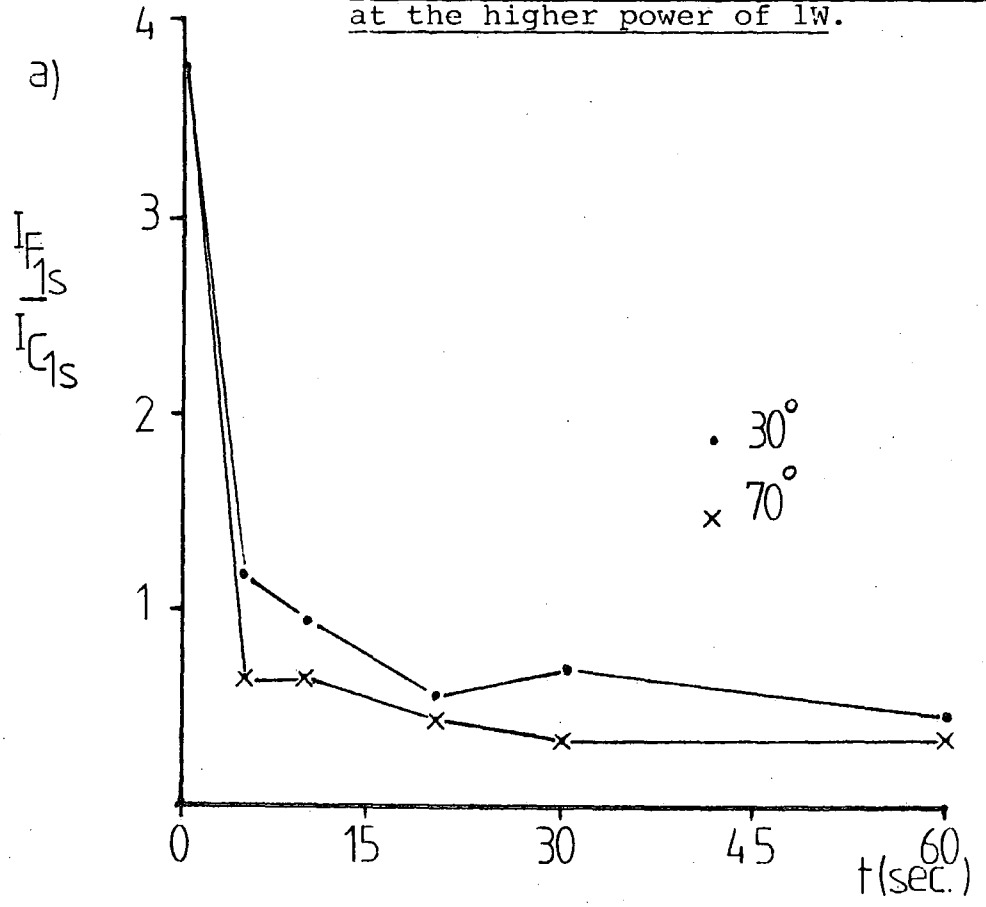

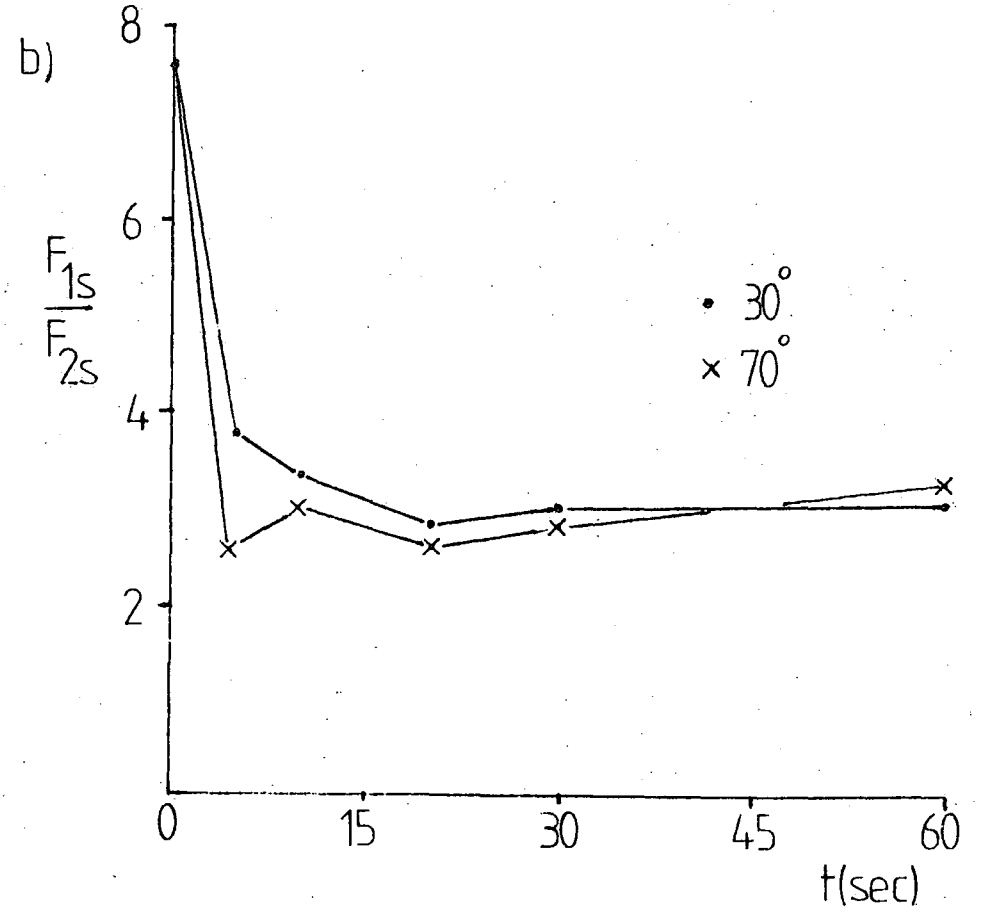

3.3.6 Comparison of the Reaction of Hydrogen Plasma at 0.1W Polyvinylidene Fluoride with that of Polytetrafluoroethylene

For comparison purposes a brief study of the interaction of a hydrogen plasma with polyvinylidene fluoride was made. Again extensive and rapid defluorination of the surface regions of the polymer results. As can be seen from Figures 3.16 the reaction proceeds most rapidly in the surface regions of the polymer. No build up of intermediate $\underline{C}F$ moieties is observed. Again the existence of a reaction gradient is evidenced by comparison of C:F stoichiometries derived from $^{F_{1s}}/_{C_{1s}}$ ratios $^{\underline{C}F_2}/_{C_{1s_{TOT}}}$ at 30^o and 70^o take-off angles, which decrease in the order $S_{F_{1s}}^{70^o} > S_{F_{1s}}^{30^o} > S_{C_{1s}}^{70^o} > S_{C_{1s}}^{30^o}$. This is supported as before by the $^{F_{1s}}/_{F_{2s}}$ ratios for the two take-off angles which again decrease in parallel with each other, Figure 3.17. Estimations of the rate of reaction derived from first order plots for the various levels F_{1s}, C_{1s} ($\underline{C}F_2$, $\underline{C}H$) at each take-off angle do however show a greater measure of agreement than for PTFE. However the rapidity of the reaction plasma with PVF_2 makes the reaction difficult to follow in its initial stages. Notably, treatment of PVF_2 with a hydrogen plasma for extended periods results in a slightly higher degree of defluorination than in PTFE, (*ca.* 10% of 15-20%).

Polyvinylidene fluoride was chosen as representative of an intermediate state in the defluorination of PTFE (*i.e.* $\sim$ 50% reaction). Crude estimation of the initial rates of reaction shows the initial rates of reaction for PTFE and PVF_2 to be comparable in magnitude. The defluorination of PVF_2 has a half-life of $\sim$6sec., compared with *ca.* 16secs. for PTFE indicating that the reaction of PVF_2 with the hydrogen

Figure 3.16 Variation of F_{1s}/C_{1s} intensity ratio as a function of reaction time for Polyvinylidene Fluoride

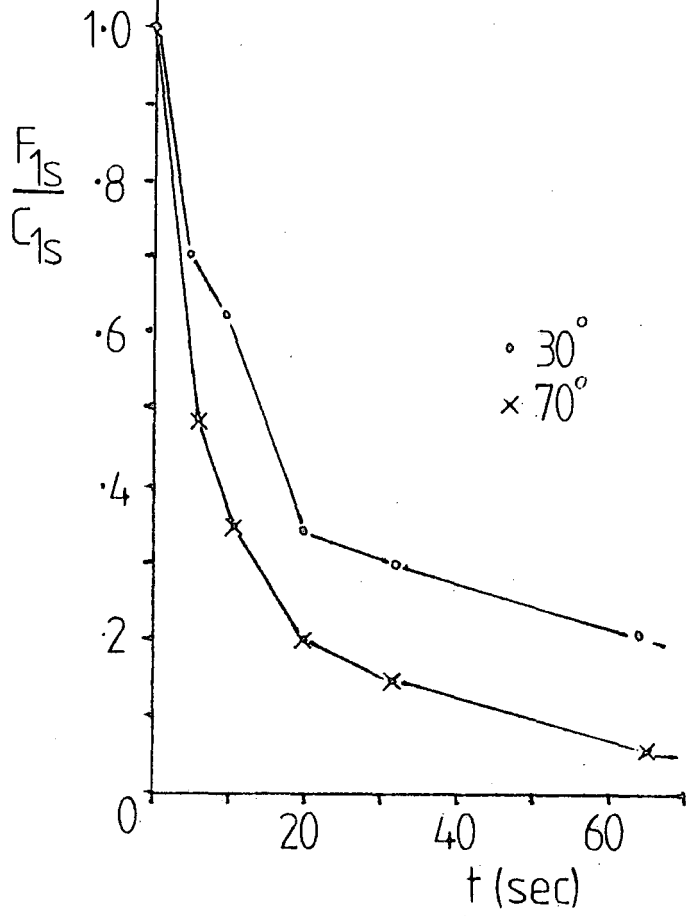

Figure 3.17 F_{1s}/F_{2s} intensity ratio as a function of reaction time for Polyvinylidene Fluoride

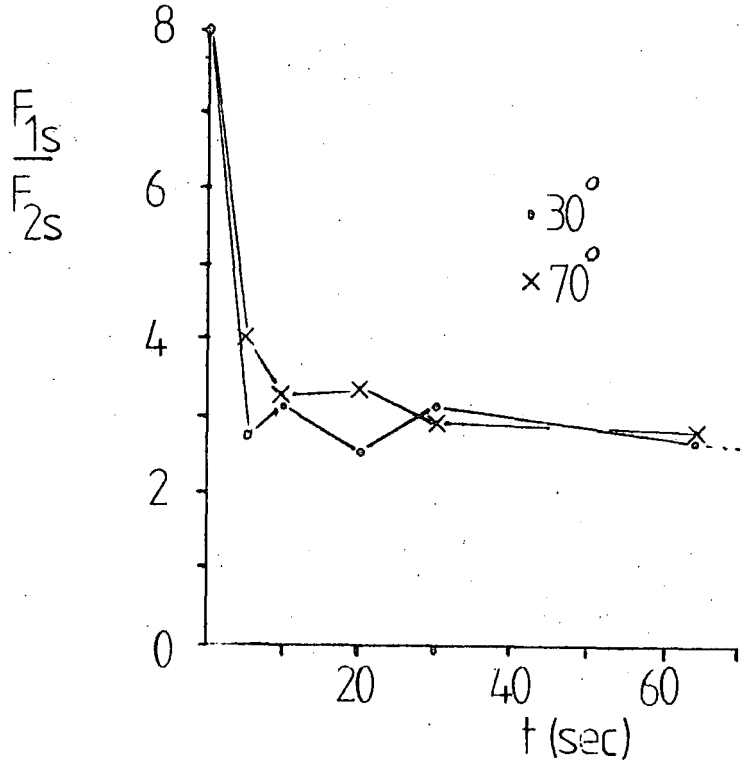

plasma proceeds appreciably faster than with PTFE. This would suggest the initial attack of H$^{\bullet}$ on the polymer chain and fluorine abstraction as being the rate determining step in the reaction with PTFE.

3.4 Conclusion

In conclusion possible mechanisms for the reaction are considered. In previous kinetic studies of the surface defunctionalisation of fluoropolymers by inert gas discharges Clark and Dilks[75,130] stressed the relative importance of direct and radiative energy transfer processes by means of which energy was transferred to the polymer lattice (the former being the shorter ranged and most dominant process in the cross-linking of the polymer surface). In these treatments damage was restricted to the outermost atomic layers of the polymer, being readily explicable in terms of a substrate and overlayer type model, and a rapid reaction due to direct energy transfer to the lattice by metastable species and a slower longer range, radiative component due to the copious output of the plasmas in the UV and vacuum UV regions.

A hydrogen plasma represents a departure from this scheme, in that the species in the plasma may react chemically and combine with the polymer surface to form stable products. Gallaher *et al*,[224] have observed the formation of hydrogen fluoride from the interaction of PTFE with a hydrogen plasma by monitoring the infrared emission spectrum. A mechanism was also formulated on the basis of attack by hydrogen atoms on the polymer. In the following discussion it is assumed that hydrogen atoms play the major role in the reaction, the ranges of ions in the solid being low

There is surprisingly little in the literature concerning the interaction of hydrogen atoms ($H^{\cdot}$) with perfluorinated systems.[226] In such studies that have appeared no reaction was found between $H^{\cdot}$ and CF_4 at room temperature. The reaction of fluoromethane, CH_3F with $H^{\cdot}$ has been studied by flame techniques over the temperature range 858-933K, by Parsamyan *et al*[225], the activation energy for the process was found to be low $\sim$4kcal mol^{-1}. In studying the reactions of fluoroethanes, Scott and Jennings[227] found the initial reaction to be the abstraction of a hydrogen atom and subsequent addition of a hydrogen atom to the resultant radical to yield a vibrationally excited molecule which decomposes by the elimination of HF in preference to destabilisation by collision. $H^{\cdot}$ addition to the resultant olefin would again result in radical formation. In the case of fluoroethylenes, Scott and Jennings[227] found hydrogen atoms to add preferentially to the less fluorinated carbon of fluorethylenes, the major reaction products being formed by combination and disproportionation of the resultant radicals. Less important products of the reaction arising from the addition of $H^{\cdot}$ to the original olefin to form a vibrationally excited molecule which is stabilised by collision or decomposes with the elimination of HF. In a polymer matrix, the possibility of quenching of such excited states by the matrix has to be considered.

Published rate constants for the reaction of hydrogen atoms with methane fall into two distinct groups:[226] (a) those having high activation energies (11-16 kcal mol^{-1}) and correspondingly high pre-exponential factor and, (b) low activation energies, (4-8 kcal mol^{-1}) and a low pre-exponential factor

in the range 10^{10}-10^{13} cc mol^{-1} $sec.^{-1}$. For higher alkanes the activation energies fall into the range 6-8 kcal mol^{-1} and pre-exponential factors *ca.* 10^{14}cc mol^{-1} $sec.^{-1}$.

In the light of these data and the observation of the production of vibrationally excited hydrogen fluoride from the interaction of plasmas excited in hydrogen and deuterium and mixtures thereof with PTFE by Gallaher *et al*[224] an outline reaction scheme is proposed. As to the efficiency of the reaction, the sticking coefficient of hydrogen atoms on PTFE is very small, indeed PTFE coatings have been used to poison the walls of reactors to hydrogen atom recombination.[228] (Though in the light of the data presented here, perhaps polyethylene would be a better choice). The heats of adsorption of H$^{\cdot}$ on polymer surfaces have been determined by Dubinskaya[218] to be in the range 400-800 cal per mol, *i.e.* very small.

The reaction is envisaged to involve the initial abstraction of a fluorine atom from the polymer chain by a hydrogen atom.

$$\text{-}CF_2\text{-}CF_2\text{-}CF_2\text{-}CF_2\text{-} + H^{\cdot} \longrightarrow HF + \text{-}\dot{C}F\text{-}CF_2\text{-}CF_2\text{-}CF_2\text{-}_n$$

The driving force behind the reaction being the highly exothermic nature of the reaction due to the high heat of formation of HF (-65.1 kcal mol^{-1}). Recombinations of the radical with a hydrogen atom leading to the formation of a vibrationally excited chain segment which may be quenched by the lattice or decompose with the elimination of HF.

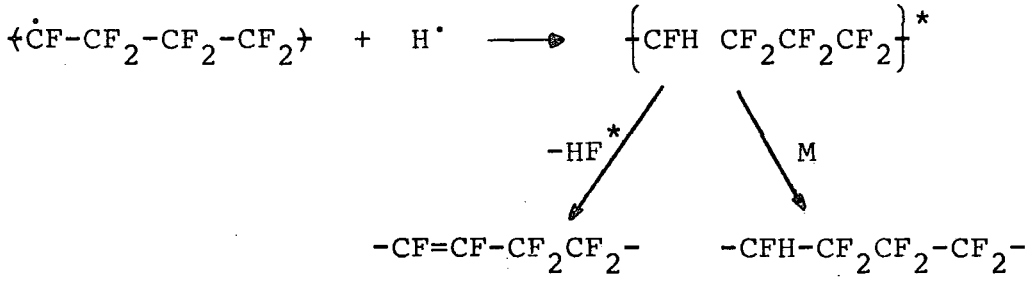

As discussed previously any unsaturation produced could be rapidly saturated by H· or from radical sites able to disproportionate (chain scission) or abstract atoms from adjacent chains (radical transfer) or recombine to yield a crosslink.

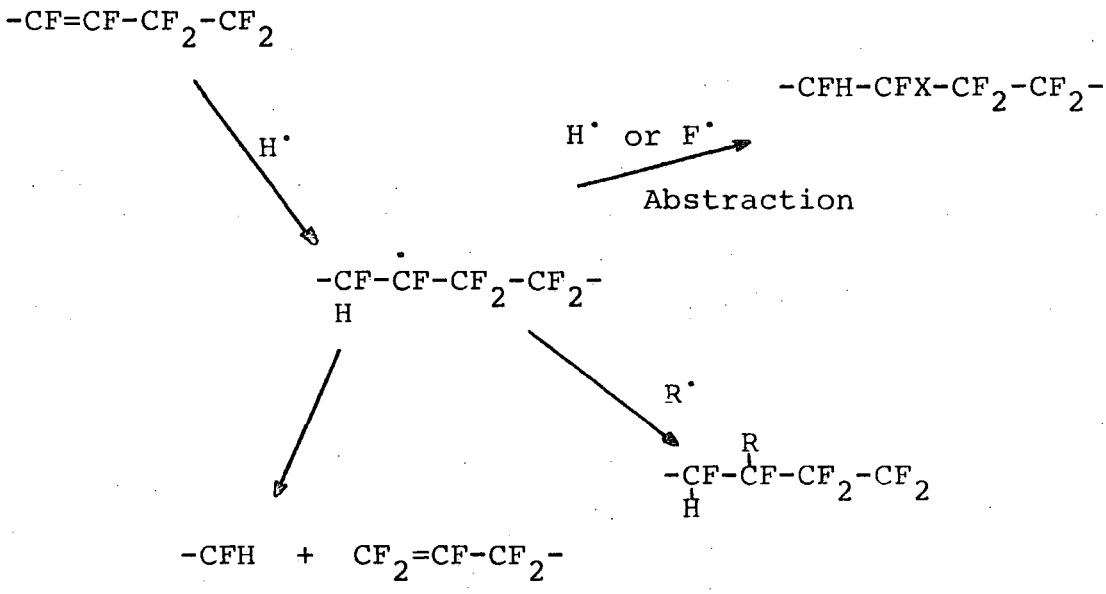

Once hydrogen has been incorporated into the polymer chain abstraction of hydrogen from the polymer chain, readdition of H· and elimination of HF from the vibrationally excited chain segment may provide a preferred reaction pathway: side reactions such as oxygen uptake and crosslinking being due to the interaction of residual oxygen containing species with radicals and the recombination of radicals respectively. Even when the matrix is defluorinated in the surface regions the abstraction of hydrogen atoms and crosslinking reactions will continue, thus maintaining an approximately static hydrogen atom concentration profile into the polymer. The rate of

reaction dominating over diffusional processes. No consideration has been given to thermal effects due to the heat of reaction dissipated in a shallow surface layer.

After prolonged treatment of a PTFE film for Multiple Attenuated Total Internal Reflection Infra-red measurements (MATR), though the spectra revealed no evidence of reaction on the depth scale sampled by MATR with a KSR-5 element, the adhesion of the sample to the infra-red element was markedly improved, on removal cohesive failure occurred in the polymer, indicative of a crosslinked surface layer displaying improved adhesion characterisation. The crosslinking in depth of the sample being attributed to the slower, longer range radiative processes occurring.

The reaction of a hydrogen plasma with a fluoropolymer surface has been shown to produce a useful modification of the surface properties of these polymers: the modification being restricted to a very thin (*ca.* 20Å) barrier layer in PTFE.

CHAPTER FOUR

THE ARGON ION BOMBARDMENT OF FLUOROPOLYMER SURFACES

4.1 The Argon Ion Bombardment of Fluoropolymer Surfaces

Plasma-surface interactions have come to form the basis of many processes for the modification of the surface properties of industrial materials, being involved in plasma-etching,[229-232] plasma assisted chemical[233-235] vapour deposition, plasma polymerisation[126,205,236,237] and plasma ashing,[238] processes. In particular the modification of polymer surfaces, to improve properties such as the wettability, printability, chemical composition and electrical conductivity, has been an area of sustained interest.[204,206, 236] As outlined in introducing Chapter Three, whilst displaying considerable inertness to chemical and thermal treatments fluoropolymers are particularly susceptible to radiation damage.[239,240] Fluorocarbon polymers are affected by radiation in one of two distinct ways depending upon their composition.[240] In general those that are completely fluorocarbon, suffer rapid molecular-weight degradation and crosslinking to a lesser degree. Those containing hydrogen are rapidly crosslinked to form networks. Thus in the modification of fluoropolymers, plasma, ion and electron beam processes provide particularly attractive routes. By the same token, polymers which are particularly liable to modification by such treatments provide an interesting insight into the mechanisms of interaction of such species with surfaces. The effects of the interaction of plasmas, both non-equilibrium and thermal, with surfaces, has been ascribed variously to the action of one or more of the components (metastables, ions, electrons) upon the surface.[131]

At first sight, the use of a controlled beam of ions upon a well defined surface, offers a method of examining the effect of one of these components in isolation. Whilst wide in their

application, the mechanisms of plasma processes are poorly understood. Such studies are also pertinent to the application of surface probes such as Secondary Ion Mass Spectroscopy (SIMS) and Ion Scattering Spectroscopy (ISS) to sensitive organic materials. On ion bombardment of a surface four distinct types of surface modification may be delineated:[152]

(a) the loss of surface atoms from the emission zone due to the emission of atomic and molecular particles and the recoil complantation and cascade mixing of atoms in a surface;

(b) the implantation of the primary ions or recoil surface atoms;

(c) changes in lattice structure, *e.g.* the amorphisation or creation of defects and imperfections within a surface;

(d) chemical effects, the breaking and formation of bonds, especially pertinent to the analysis of organic materials where, whilst being amorphous, the connectivity is particularly well defined.

In discussing the effects of ion bombardment upon surfaces, Benninghoven[152] has distinguished between "first order" and "second order" effects. First order effects concentrate upon the rearrangements in terms of structure and composition occurring in the region of impact of a primary ion before the emission of a secondary ion which SIMS uses to characterise second order effects centre upon the surface cumulative effects of ion bombardment upon the matrix.

Argon ion bombardment forms the basis of the CASING[199] process for the improvement of the adhesive bonding properties of polymer surfaces. In ESCA and Auger investigations of metal/metal oxide interfaces and semiconductor surfaces, argon ion

bombardment to ablate away the surface, is a widely used technique for effecting analytical depth profiles. Under the normal operating conditions (high accelerating voltages and relatively high beam currents) the argon ion sputtering of polymeric surfaces is extremely rapid. At lower ion doses and dose rates polymer surfaces may be readily crosslinked, whilst ablation of the surface is kept to a minimum. Figure 4.1 shows the C_{1s} and F_{1s} core level spectra of a largely alternating tetrafluoroethylene-ethylene copolymer exposed to a 2keV beam of argon ions for successive 5 second periods at a beam current of 4μA.[167] The ion source used in this experiment was a cold-cathode discharge type and hence also produced a colliminated beam of vacuum U.V. light incident upon the sample. The results are nevertheless quite striking, argon ion bombardment is seen to cause extensive degradation of the polymer surface. This polymer has also been the subject of an extensive ESCA study of the modification of polymer surfaces by plasmas excited in inert gases by Clark and Dilks.[21-22] On this basis the tetrafluoroethylene-ethylene copolymer was chosen to be the subject of a more detailed investigation of the effects of argon ion bombardment upon polymer surfaces. This polymer having featured in extensive ESCA investigations previously conducted in these laboratories. Its structure is known to be largely alternating and it exhibits a large chemical shift range, the contribution of the tetrafluoroethylene components being ∿4.7eV removed from that arising from the ethylene components. The C_{1s} core level is thus well resolved: any changes in structure are thus readily apparent.

Figure 4.1

Ethylene - Tetrafluoroethylene copolymer
2KV Ar ion 5 sec. 5μA
rapid scan

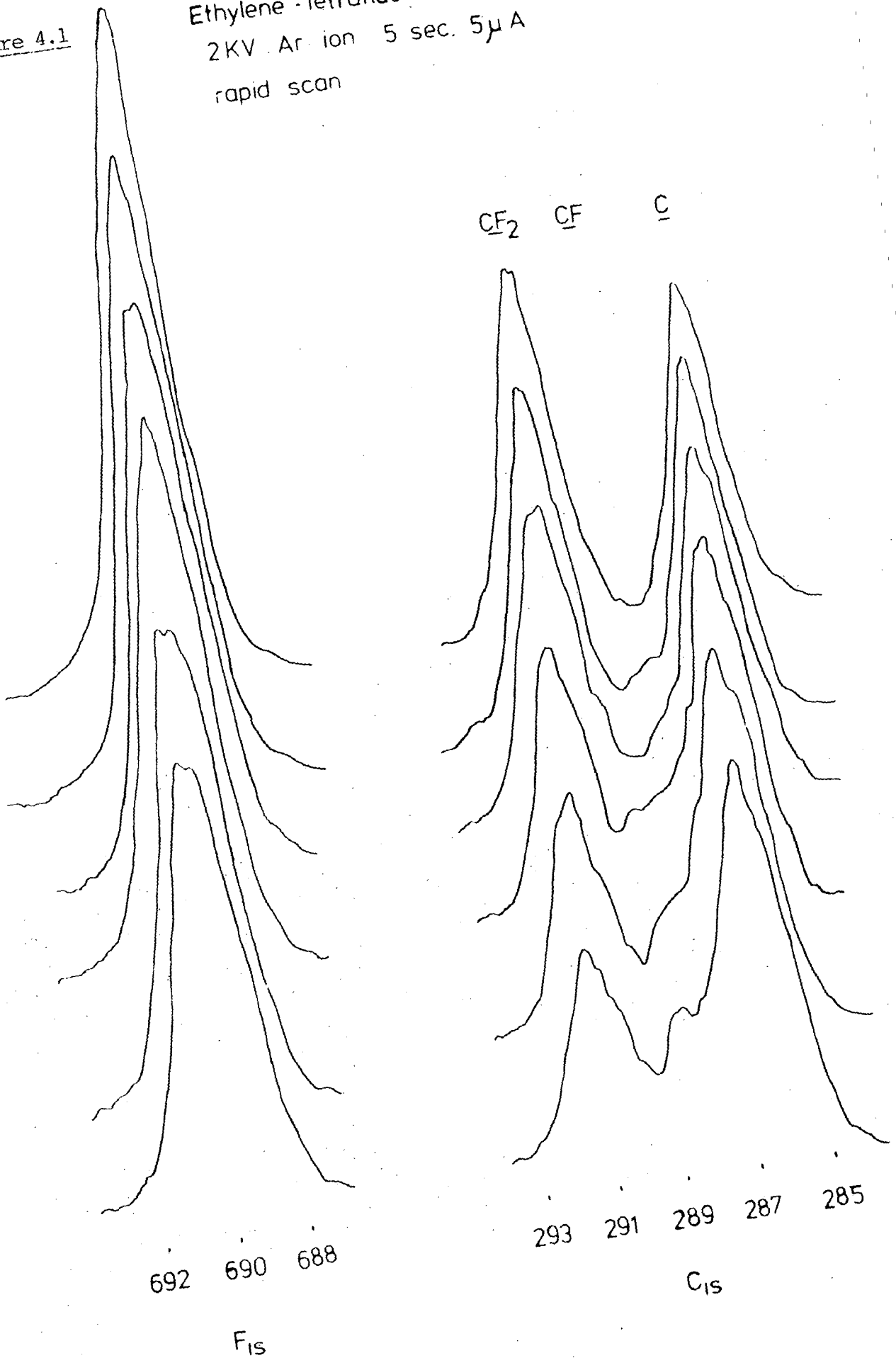

4.2 Experimental

4.2.1 Samples

Samples of ethylene-tetrafluoroethylene copolymer (52% TFE) as a 30μ extruded film polytetrafluoroethylene as a 100μ skived film were studied attached to a standard three-sided spectrometer probe tip with double sided "Scotch" tape. Research grade argon (B.O.C. Ltd.) was used in conjunction with a Dow Gas Purifier to remove trace oxygen and water. To investigate the possibility of sample contamination by the ion beam polymerisation of residual hydrocarbons present in the vacuum system[23] the interaction of ion beams with gold foil samples was also studied.

4.2.2 Instrumentation

Spectra of the treated samples were recorded using the KRATOS ES300 spectrometer using $Mg_{K\alpha_{1,2}}$ and $Ti_{K\alpha_{1,2}}$ radiation. Binding energies and area ratios were determined by curvefitting procedures using the DS300 data system to a precision of ±0.2eV and ±5% respectively. Gaussian components being used to fit the envelopes and an 'S'-shaped, Shirley type background[241] subtraction procedure being used throughout prior to curve-fitting.

In situ argon ion bombardment was carried out at ambient temperature with an ion beam angle of incidence of $\approx 60^{o}$ (relative to the sample normal) using a differentially pumped VG Scientific AG5 electron impact ionisation ion gun, operated at an argon pressure in the source region of $\sim 5 \times 10^{-5}$ torr (maximum), fitted with a Wien mass filter. (The configuration of the ion gun and SAC is shown in Figure 4.2). The ion beam

(A)

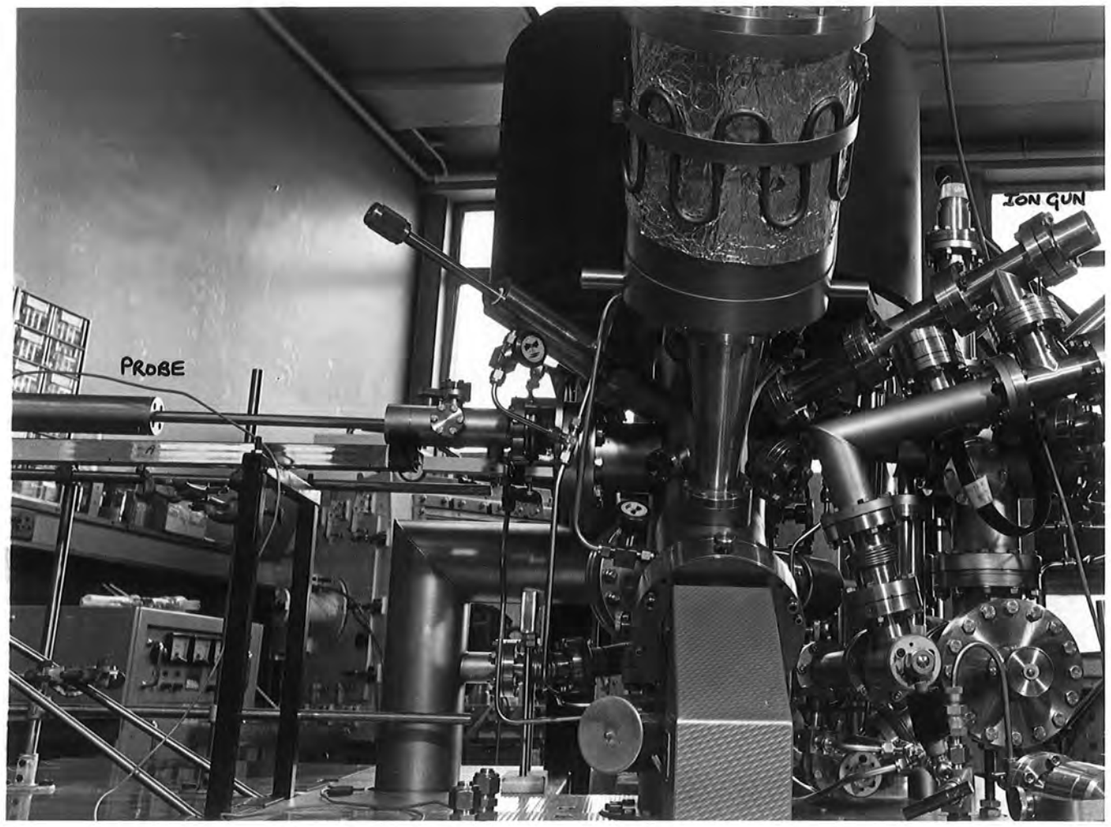

Figure 4.2 General view of ES300 Spectrometer showing the configuration of the argon ion gun with respect to the various insertion locks and the sample analysis chamber.

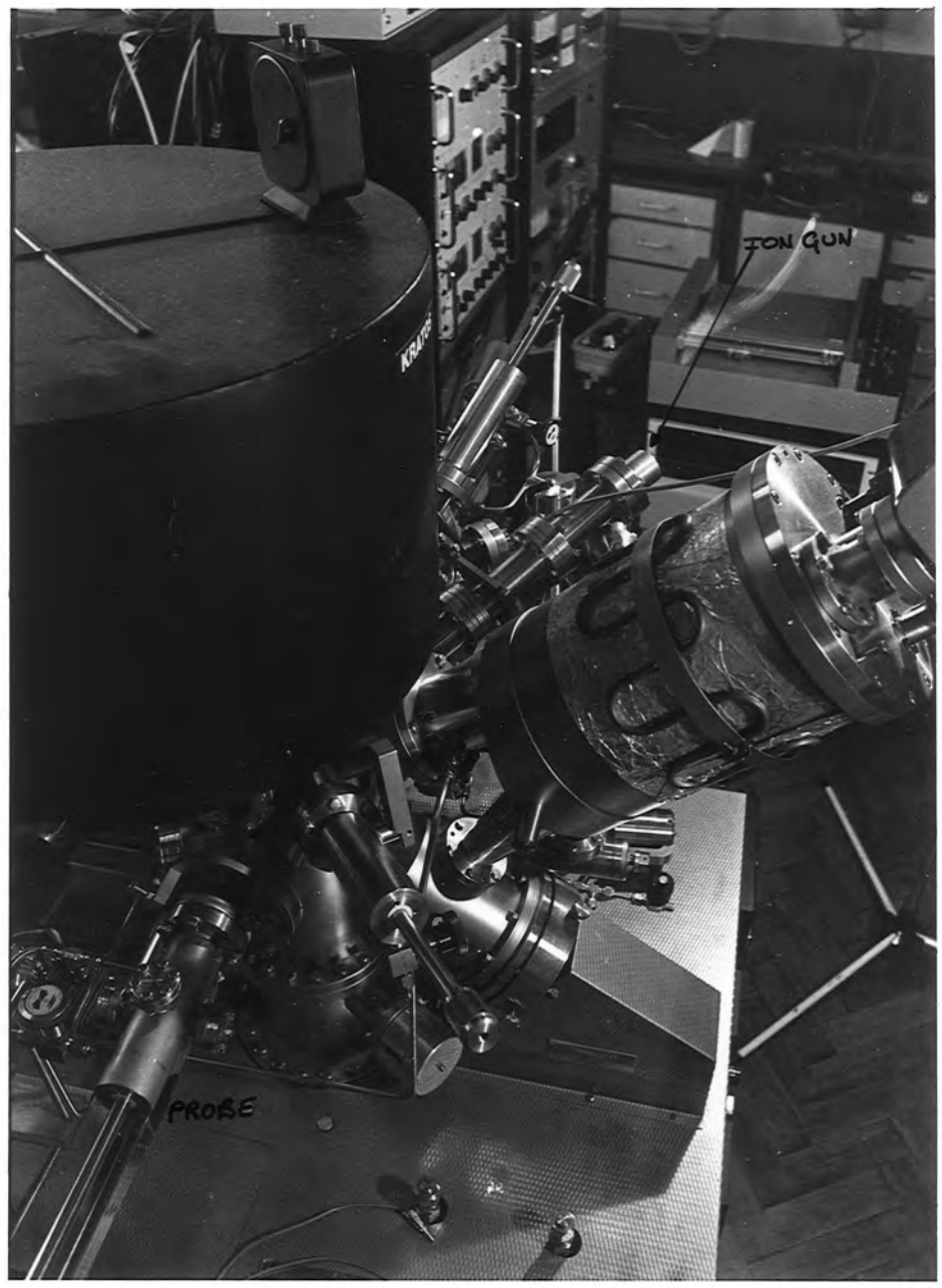

(B)

(c)

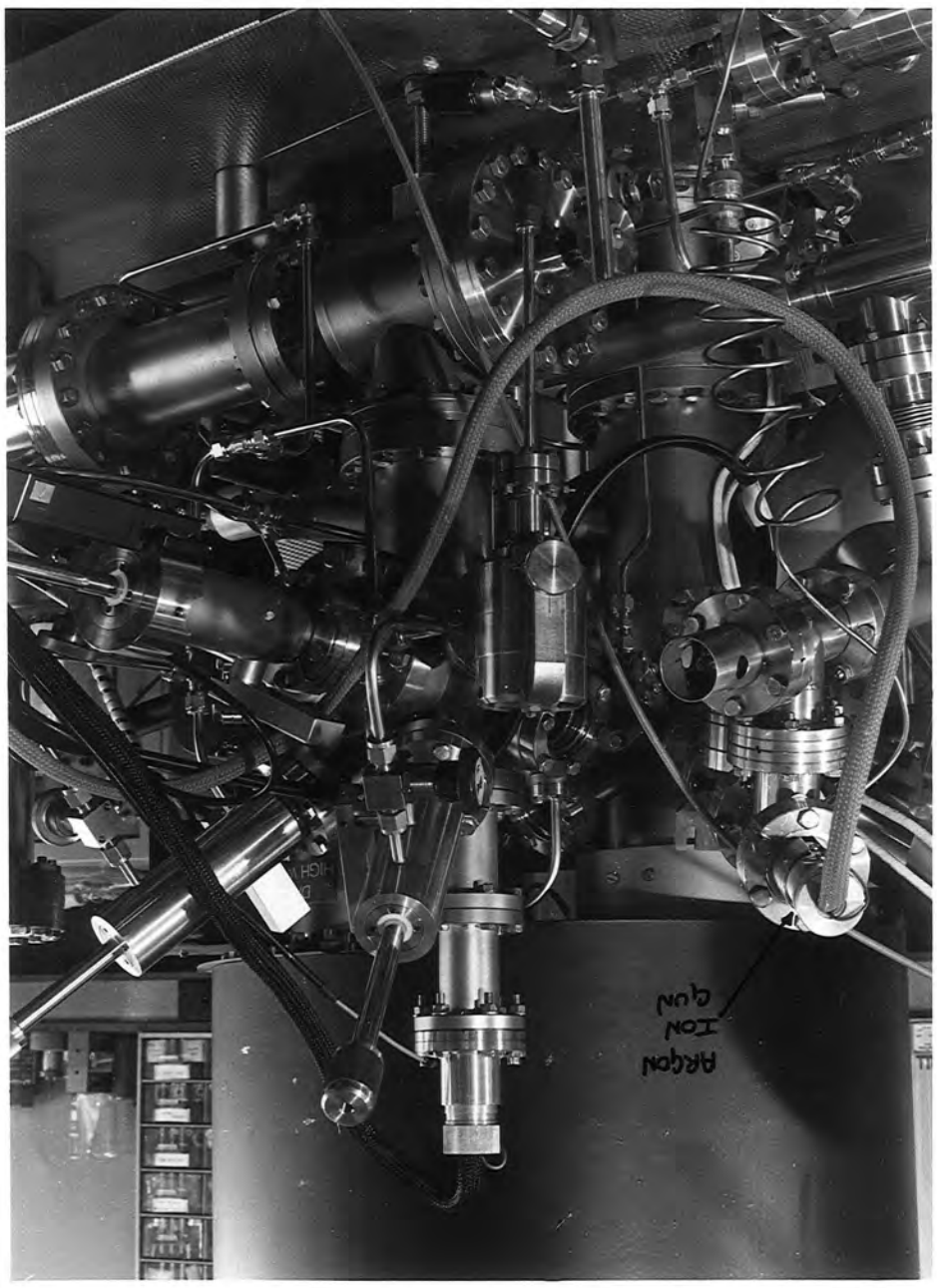

was rastered over the sample surface, the maximum area of irradiation was in general several times greater than that of the sample area of the probe tip. The ion gun delivers a poorly focussed beam and hence was always rastered over the sample surface to average out any inhomogeneities in the beam. Ion beam currents (unsuppressed) were measured by means of a Faraday plate earthed through a Keithley 621 electrometer. The Ar^+ ions used in these experiments spanned an energy range from 1 to 5 keV. No charge neutralisation was employed. The area bombarded and beam alignment were determined in a variety of ways: (1) movement of the sampling plate in the area bonbarded; (a) etching through thin gold films evaporated onto glass substrates; (3) at higher beam currents, observing the fluorescence of a KBr disc in the beam.

4.3 Results and Discussion

4.3.1 Preliminary Observations on the Argon Ion Modification of Fluoropolymers

Preliminary experiments have established that the argon ion induced modification of tetrafluoroethylene-ethylene copolymer and polytetrafluoroethylene surfaces may be observed in the core-level spectra of the polymers after significantly lower ion doses than employed in previous ESCA studies of the ion beam modification of polymers.

Initially a current density of 200nA cm^{-2} was employed (this being equivalent to an ion flux of $\sim 1.25 \times 10^{12}$ ions cm^{-2} sec^{-1}), the sample being exposed to the ion beam so that the total exposure times amounted to 10, 20, 40, 90, 160, 250 and 360 seconds. Figure 4.3 displays the C_{1s} and F_{1s} core

Figure 4.3 C_{1s} and F_{1s} Core Level Spectra for a sample of TE copolymer bombarded with argon ions (2.5keV, 200 nA cm^{-2}) as a function of reaction time

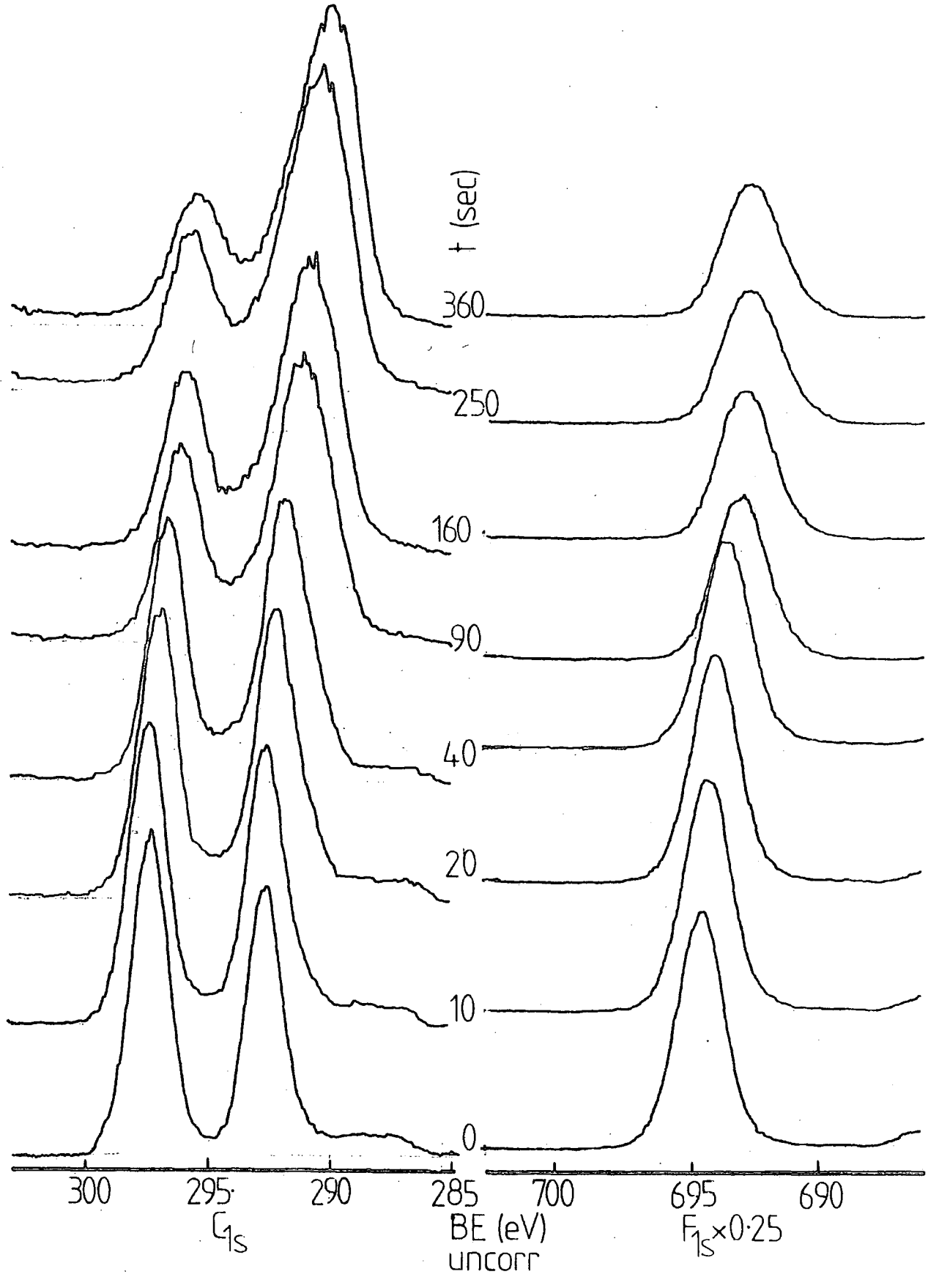

level spectra for a sample of the tetrafluoroethylene-ethylene (∿52% TFE) copolymer treated with 2.5 keV argon ions for periods up to 360 seconds. By way of comparison the corresponding spectra for a sample of PTFE, similarly treated, are displayed in Figure 4.4.

The ESCA spectra of the copolymer reveal extensive loss of fluorine from the polymer surface on argon ion bombardment. The integrated intensity of the F_{1s} signal decreases relative to that of C_{1s} level and within the C_{1s} envelope, the high binding energy $\underline{C}F_2$ component (281.4 eV) decreases in intensity relative to features due to $\underline{C}H_2$ groups adjacent to $\underline{C}F_2$ groups (286.7 eV) and lower binding energy $\underline{C}H_2$, $\underline{C}H$ (285 eV) functionalities, with the concomitant emergence of components of binding energy intermediate between those of the $\underline{C}F_2$ and $\underline{C}H_2$ components of the spectra of the untreated polymer due to $\underline{C}F$ features (∿288.5 eV). The modification is also accompanied by substantial increases in the FWHMs of the C_{1s} and F_{1s} levels, reflecting the range of chemical environments present in the treated polymer surface.

The treatment of PTFE is marked by the appearance of a broad range of features to the lower binding energy side of the $\underline{C}F_2$ component of the $\underline{C}_{1s}$ envelope. The $\underline{C}F_2$ component remains the most prominent feature of the C_{1s} envelope throughout. The modification of the polymer is characterised by the development of a tailing of the C_{1s} spectrum to lower binding energies, representing $\underline{C}F_2$, $\underline{C}F$ and $\underline{C}$ environments with a variety of β substituents. (In an α position fluorine exerts a substituent effect, an additive shift to higher binding energies of ≃2.7 eV and as a β substituent a shift of ~0.7 eV per

Figure 4.4 Core Level Spectra for PTFE treated with argon ions (2.5 keV, 200 nA cm^{-2}) as a function of reaction time

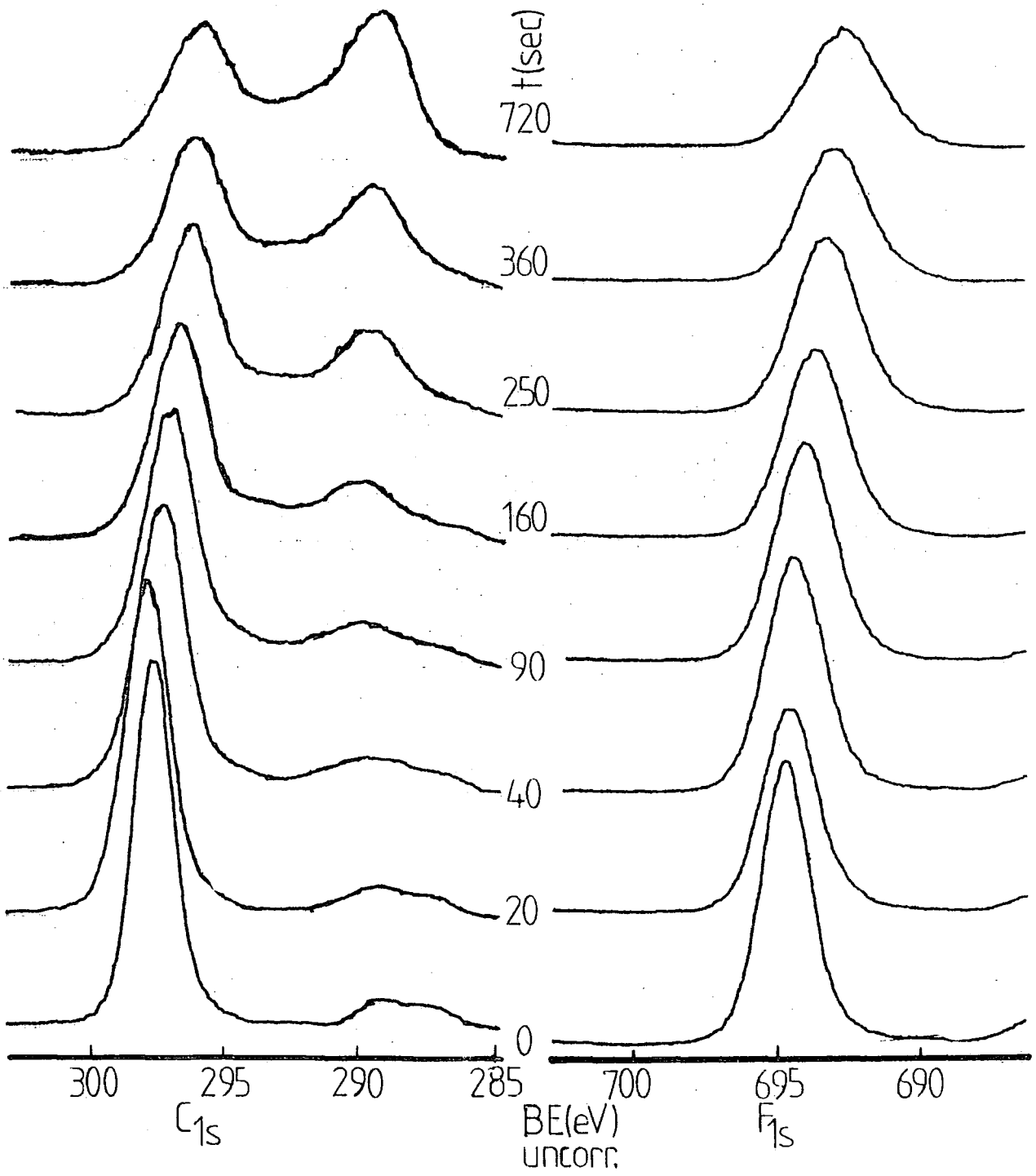

fluorine: the two effects being approximately additive). Thus this tailing is essentially featureless representing a wide range of chemical environments.

The spectra displayed in Figures 4.3 and 4.4 were obtained at a take-off angle of 30^{o}, the corresponding data obtained at the more surface sensitive, 70^{o} take-off angle mirror the situation almost exactly. Subtraction of the spectra obtained at 30^{o} and 70^{o} after normalisation, revealing only small differences attributable to slight hydrocarbon contamination accumulated over an experimental run. In each case the treatment appears to be uniform throughout the sampling depth of the C_{1s} level with $Mg_{K\alpha}$ excitation (*i.e.* $3\lambda \sim 36\mathring{A}$).

The ion beam polymerisation of extraneous hydrocarbon contamination in untrapped diffusion pumped systems has been reported. To exclude this possibility, a cleaned gold sample was bombarded under similar conditions to those employed in the treatment of the polymer surfaces. The hydrocarbon contamination was slightly decreased by the treatment.

Only on prolonged bombardment, $>2.10^{15}$ ions cm^{-2}, is any discolouration of the polymers observed, a slight yellowing of the previously white or colourless film being noted. Difference UV spectra of the exposed and unexposed films did not yield any useful information, the absorption being broad and essentially featureless.

4.3.2 The Ion Energy and Dose Dependence of the Modification of Tetrafluoroethylene/Ethylene Copolymer

Samples of the copolymer were exposed to incremental doses of argon ions up to 4.5×10^{14} ions cm^{-2} for

ion energies from 1.5 to 3.5 keV. Only the initial stages of reaction were investigated: almost complete defluorination of the surface regions being possible upon extended bombardment.

The untreated copolymer exhibited a low level of surface oxidation, giving rise to a small O_{1s} signal (∿1.5% of the intensity of the C_{1s} level ≡ <1 atom % in the surface). Argon ion bombardment resulted in the further decrease of this low level of surface oxidation.

Figure 4.3 represents the changes in the C_{1s} and F_{1s} spectra of the copolymer bombarded by 2.5 keV argon ions at a dose rate of 200nA cm^{-2}, 1.25 x 10^{12} ions sec^{-1} of the changes and modifications produced by argon ion bombardment by ions in the energy range 1.5 - 3.5 keV; Figure 4.3 is typical. The variation in ion energy only essentially influencing the rate of reaction, and in general the 2.5 keV data will be presented in discussing the data.

The data contained in Figure 4.3 is more conveniently represented graphically as in Figure 4.5 which traces the variation of the contributions of the various components of the C_{1s} level with increasing ion dose. The C_{1s} spectra broaden considerably on exposure to the ion beam, indicative of the range of chemical environments introduced. The defluorination of the surface is accompanied by and may to an extent be monitored by the approximately linear decrease in the equilibrium charging attained by the modified polymer surface on ESCA analysis. The C_{1s} profiles being analysed in terms of 4 major components, $\underline{C}F_2$ (B.E. ∿291.6 eV), $\underline{C}F$ (B.E. ∿288.6 eV), $\underline{C}H_2$ adjacent to CF_2 and $\underline{C}F$ groups in the range 286.6-285.9 eV and

Figure 4.5 Relative intensities of the components of the C_{1s} spectrum of tetrafluoroethylene/ethylene copolymer as a function of reaction time and accumulated ion dose

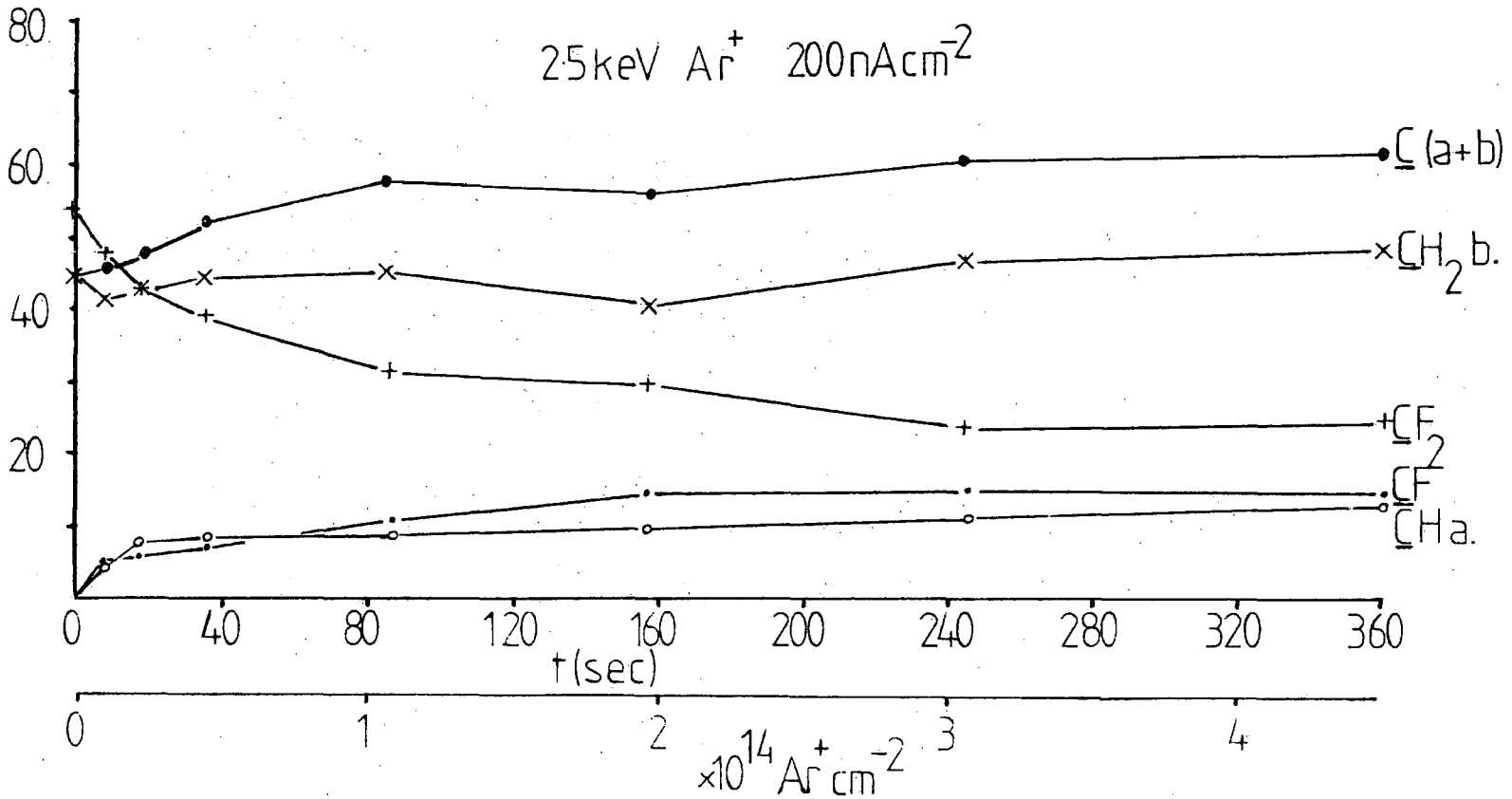

hydrocarbon/defluorinated carbon matrix at 285 eV. The attempt to distinguish between the last of these two environments is fraught with error and this region of the C_{1s} profile is best considered as a whole, embracing all carbon atoms not directly attached to fluorine.

The loss of $\underline{C}F_2$ groups from the surface is accompanied by the rise of the components due to carbonaceous material, the concentration of $\underline{C}F$ environments rises rapidly initially to a limiting value of ∿15% of the carbon envelope, though ultimately this is lost, only the single component due to carbonaceous material remaining. As the reaction tends to the almost complete defluorination of the surface layers of the polymer, further problems arise in curve-fitting the C_{1s} envelopes of the material.

The analysis is complicated by the emergence of carbonaceous features having apparent binding energies less than 285 eV. The charge referencing of the material is difficult. As the polymer is depleted of fluorine the formation of isolated CF_2 groups might be expected with the concomitant move to lower binding energy of the CF_2 groups remaining. When allowance is made for this the results appear to indicate the true binding energy of the carbonaceous material formed to be less than 285 eV. (Normally used as an energy reference in the ESCA analysis of polymeric materials). Prior to analysis the complicating $K\alpha_{3,4}$ satellites to the $\underline{C}F_2$ feature of the C_{1s} envelope were removed mathematically.

Figure 4.6 $\ln(^{F1s}/_{C1s})$, $\ln(^{\underline{CH}}/_{C1s})$, $\ln(^{\underline{CF_2}}/_{C1s})$ and $\ln(^{F2s}/_{C1s})$ *versus* reaction time for a sample of TE copolymer exposed to an argon ion beam (2.5 keV, 200 nA cm^{-2})

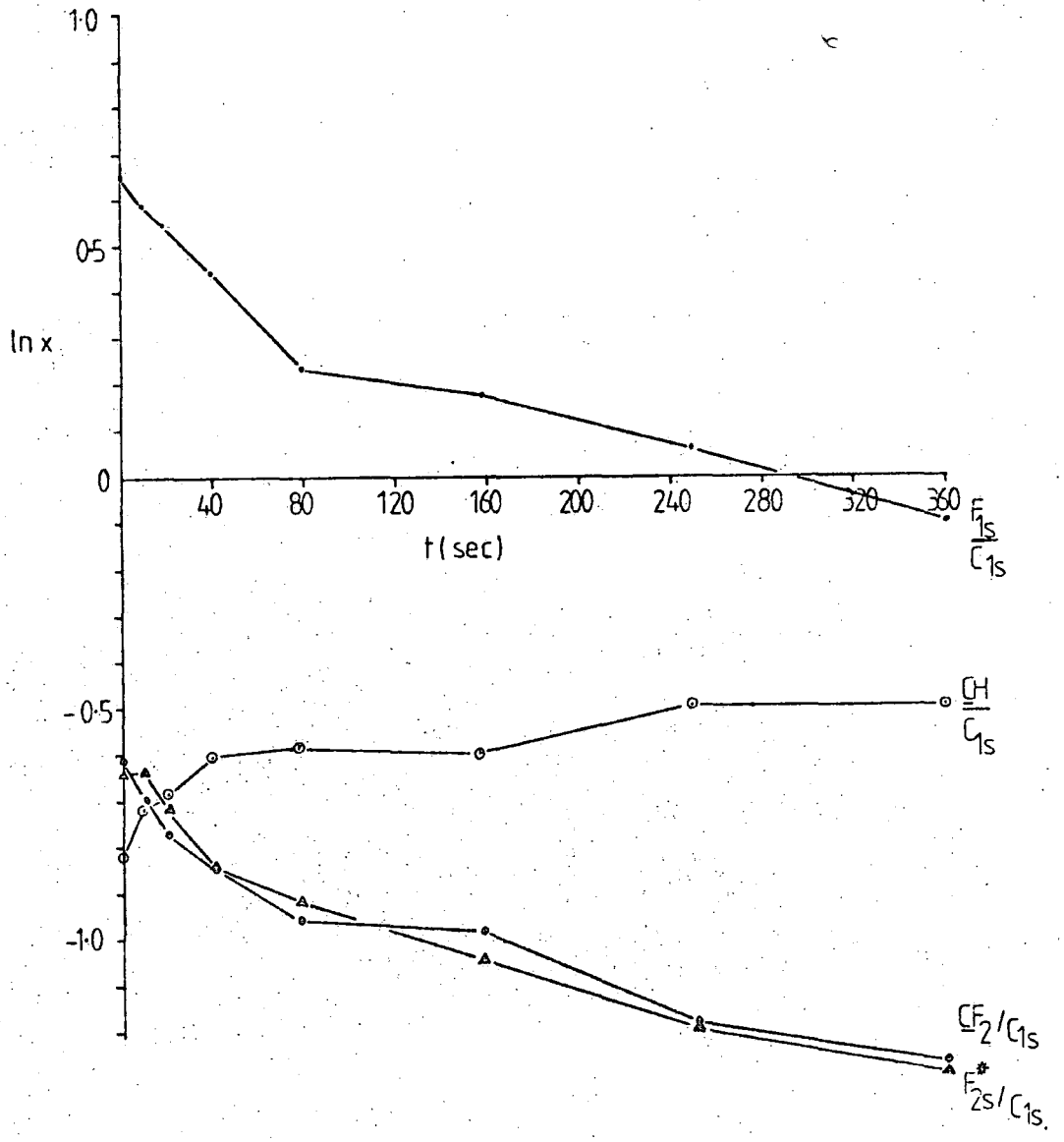

4.3.3 The Depth of Modification

The C_{1s} and F_{1s} core levels and the essentially core-like F_{2s} level, provide a range of probes with which the reaction's course over the depth scale appropriate to electrons derived from each may be monitored. As a starting point to attempt to gain some insight into the progress of the reaction, the reaction was considered to be first-order with respect to the surface concentration of the fluorine containing groups in the polymer. A plot of the natural logarithm of the ratio of the integrated intensity of the F_{1s} levels to that of the C_{1s} level *versus* the bombardment time or ions dose is shown in Figure 4.6 for the polymer bombarded with 2.5 keV ions. The corresponding plots for the $\underline{C}F_2/C_{1s}$ and F_{2s}/C_{1s} ratios is also included. The rates of reaction derived from the slopes of each plot ($\sim 1.2 \times 10^{-3}$ sec^{-1}, 9.6×10^{-16} ion^{-1}) are in close agreement, again reflecting the apparent vertical homogeneity of the reaction within the depth scale probed by the photoelectrons derived from the F_{1s} and C_{1s} levels using $Mg_{K\alpha}$ radiation ($\lambda_{F_{1s}}$ ~ 9Å, $\lambda_{C_{1s}}$ ~ 14Å, $\lambda_{F_{2s}}$ ~ 22Å - sampling depths, at 30^{o} take-off angle, of ~ 23Å, ~ 36Å and 57Å respectively). The apparent homogeneity of the reaction in the surface region is expressed in the close similarity of the C_{1s} spectra of the treated samples obtained at 30^{o} and the more surface sensitive, 70^{o} take-off angle is restated in a more dynamic fashion by the close agreement between the stoichiometries derived for altered layer calculated on the basis of the F_{1s}:C_{1s} intensity ratios and the $\underline{C}F_2$ and $\underline{C}F$ components of the C_{1s} level as shown in Figure 4.7. Attempts to use the F_{2s} level to derive stoichiometries for the altered layer from F_{1s}:C_{1s} intensity ratios were

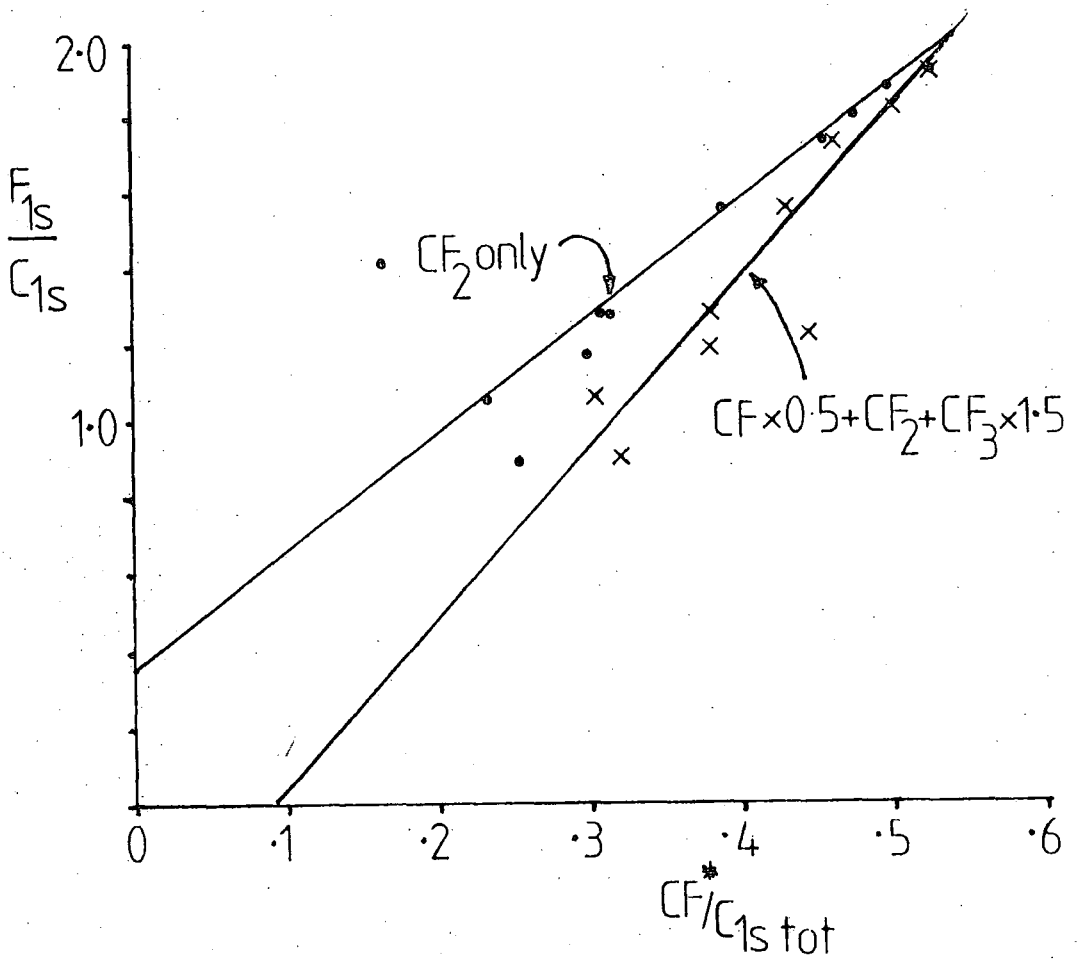

Figure 4.7 Correlation between stoichiometries derived from C_{1s} envelope component analysis and $C_{1s}:F_{1s}$ ratio

in poorer agreement with those determined from the more surface sensitive F_{1s} and C_{1s} levels, predicting slightly higher overall F:C stoichiometries. This is consistent with the formation of an overlayer of altered material upon a substrate of unaltered polymer. The F_{1s}/F_{2s} ratio varies in a somewhat erratic fashion (Figure 4.8) with increasing treatment time. (This being due in part to the somewhat poorer signal to noise ratios obtained for the F_{2s} spectra). However the F_{1s}/F_{2s} ratio shows a downward trend, decreasing by ∿10% during the course of the experiment.

Considering the C_{1s} and F_{1s} levels to reflect the stoichiometry of the altered overlayer of the polymer, model calculations show that the stoichiometries derived from these levels would be little affected by the presence of an altered layer 25-30Å deep, upon a substrate of unaltered copolymer. In the initial stages of reaction the fluorine content of the altered layer only differs slightly from that of the bulk, the F_{1s}/F_{2s} ratio is an insensitive probe in detecting this inhomogeneity. The defluorination of a surface layer 25-35 Å deep has been calculated to produce only *ca.* a 10% decrease in the F_{1s}/F_{2s} ratio for a surface layer having lost 50% of the fluorine compared to that present in the bulk polymer.

From the density of the polymer and assuming initially the reaction is confined to a 30Å thick surface layer, each incident argon ion is estimated to remove ∿15 F atoms. The results of this estimation are presented in Table 4.1 below. The estimate makes the somewhat unrealistic assumption that the number of C atoms in the surface does not change, these figures being deduced on the basis of the change in stoichiometry of the surface layer in the first 40 sec. of bombardment.

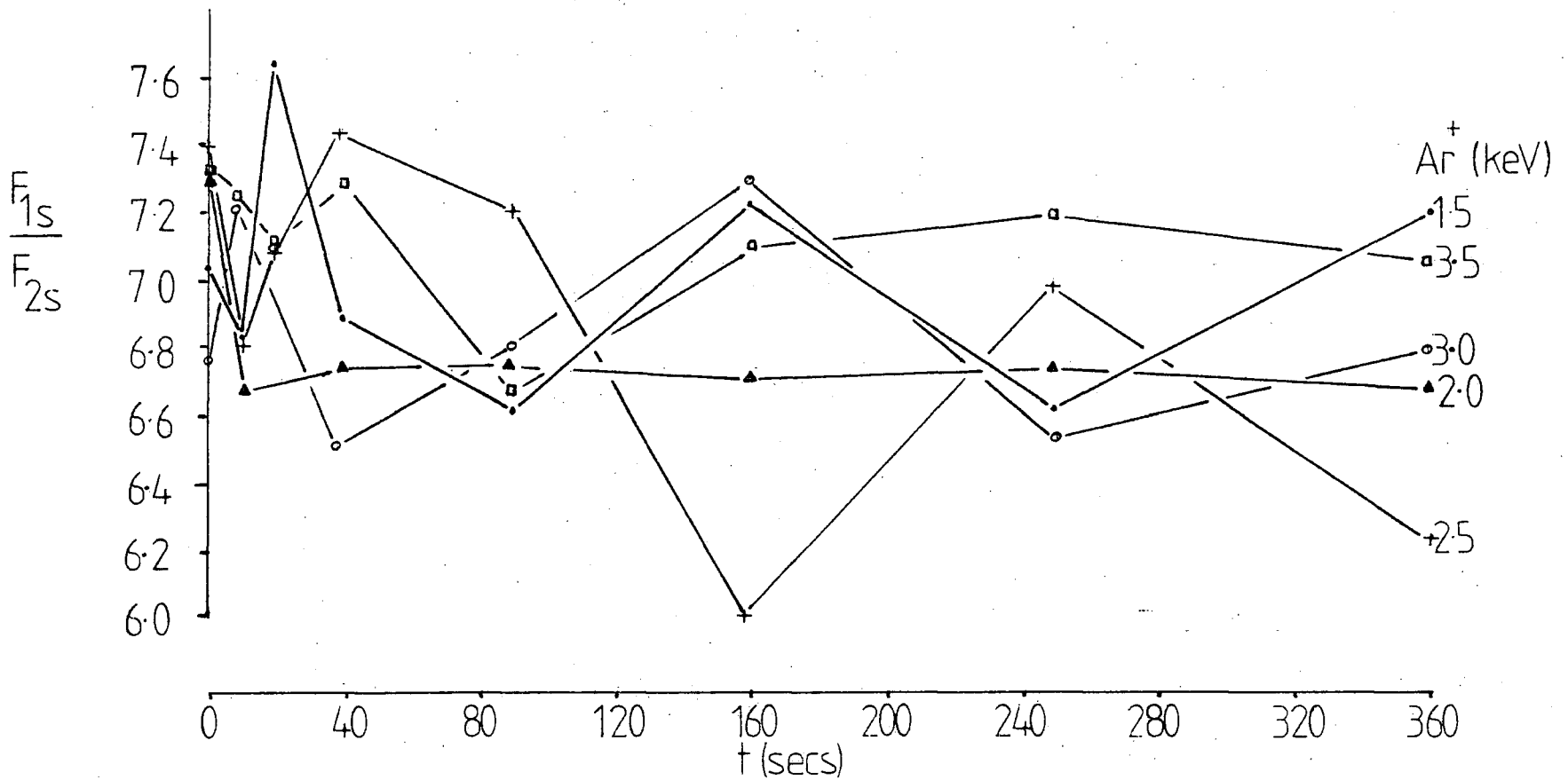

Figure 4.8 F_{1s}/F_{2s} ratios for samples of TE copolymer bombarded with argon ions (1.5 - 3.5 keV, 200 nA cm^{-2}).

TABLE 4.1 Crude Estimate of Sputtering Yield of Argon Ions

Incident Argon Ion Energy	F atoms per ion
1.5	25
2.0	19.2
2.5	16.0
3.0	14.0
3.5	14.0

ESCA analysis of samples of copolymer subjected to a total ion dose of ≈1 x 10^{14} ions cm^{-2} for argon ion energies of 2,3 and 4 keV using both $Mg_{K\alpha}$ and $Ti_{K\alpha}$ sources (spectra being taken at 35° and 70° take-off angles, $Mg_{K\alpha}$ and 35° take-off angle $Ti_{K\alpha}$). The $Mg_{K\alpha}$ data show the presence of a homogeneously defunctionalised surface overlayer, the 70° spectra yielding F_{1s}/F_{2s} ratios close to that for the pure polymer, *i.e.* ~7.6 whereas the F_{1s}/F_{2s} ratios in the 35° spectra are slightly reduced from this value. More graphically, the C_{1s} spectra excited by $Mg_{K\alpha}$ and $Ti_{K\alpha}$ radiation obtained at a take-off angle of 35° for a sample of copolymer treated with 2 keV argon ions are shown in Figure 4.9 together with the corresponding spectra for the untreated polymer; whilst the $Mg_{K\alpha}$ C_{1s} levels of the excited treated polymer have been much altered by the bombardment, this modification is less marked in the $Ti_{K\alpha}$ spectra. The polymer surface region probed by harder $Ti_{K\alpha}$ source bears a much closer resemblance to the spectra of the untreated polymer.

The copolymer was found to degrade upon prolonged exposure to $Ti_{K\alpha}$ X-rays, therefore spectra were run as rapidly as possible.

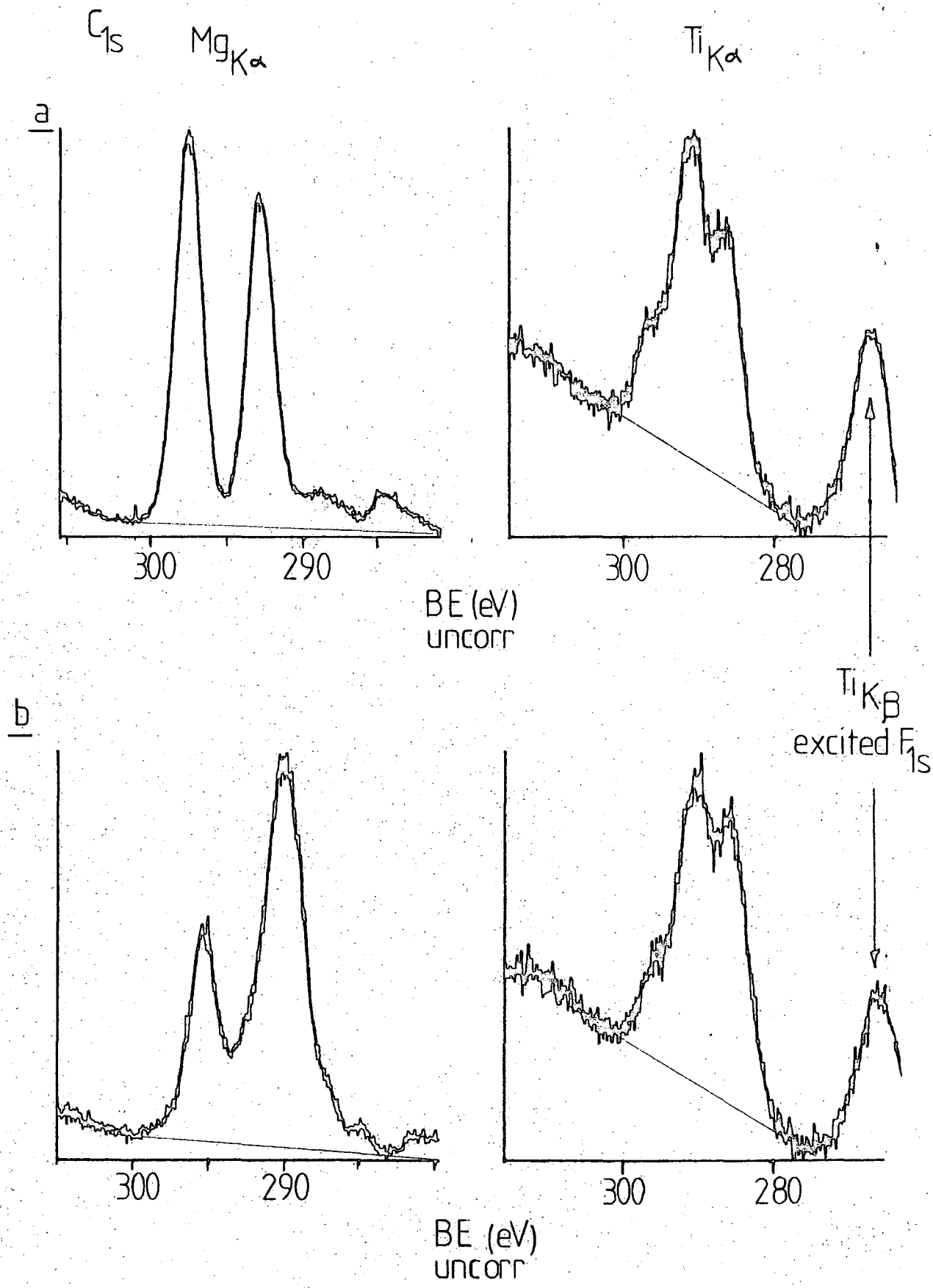

Figure 4.9 $Mg_{K\alpha}$ and $Ti_{K\alpha}$ excited C_{1s} spectra of an untreated copolymer surface and a surface treated with 2 keV argon ions (100 nA cm^{-2}, 900 sec.).

The apparent homogeneity of the surface layers of the bombarded polymer revealed by the comparison of stoichiometries derived from the C_{1s} and F_{1s} levels excited by $Mg_{K\alpha_{1,2}}$ radiation for 35° and 70° take-off angles suggests the formation of an overlayer of altered material. This stoichiometry is not reflected in the stoichiometries of the surface derived from the $Ti_{K\alpha_{1,2}}$ excited spectra, the deeper probing $Ti_{K\alpha_{1,2}}$ excited spectra taken at a take-off angle of 35° reflecting a higher fluorine content for the surface regions than the $Mg_{K\alpha_{1,2}}$ excited spectra. On this basis a sample model was adopted consisting of an overlayer of material of the stoichiometry predicted by the $Mg_{K\alpha_{1,2}}$ excited spectra upon a substrate of unaltered polymer. This substrate-overlayer type model has already been discussed in Chapter One. The $Ti_{K\alpha_{1,2}}$ data has then been used to attempt to estimate the depth of the modification. The stoichiometry reflected in the $Ti_{K\alpha_{1,2}}$ data representing the exponentially depth weighted average of the stoichiometry of the altered layer given by the $Mg_{K\alpha_{1,2}}$ excited spectra and the substrate of unaltered material.

The corresponding data for 3 and 4 keV argon ion bombardment show the same behaviour. In each case, on the basis of the mean free paths calculated for electrons photoemitted from the C_{1s} and F_{1s} levels by $Ti_{K\alpha}$ radiation[93] the depth of modification is estimated to be of the order of ∿30-35Å. If the damage is caused by ions alone this would correspond to a range of ≈60-70Å for ions in the polymer. In this analysis a simple overlayer of modified material on a substrate of untreated polymer is assumed. The substrate overlayer model has been already discussed in Chapter One. No conclusions however can be drawn as to the nature of chemistry of the polymer in

this interfacial region, which is undoubtedly graded and not abrupt as presented here. In angular dependent measurements conducted to determine the position of the interface in an SiO_2/Si structure, Hollinger *et al*[212] have estimated that the resolution of the ESCA technique is determining the position of the interface is limited to $\simeq \lambda/3$ (λ is the mean free path of the electrons emitted from the core-level under consideration).

4.3.4 Absolute Intensities

The defluorination reaction is accompanied by an increase in the absolute integrated intensity of the C_{1s} level, reflecting an increase in the number density of carbon atoms present in the polymer surface. This is illustrated in Figure 4.10 as a plot of the ratio of the total integrated intensity of the C_{1s} level at time t to the initial value of the quantity against treatment time (or total ion dose). The increase in this quantity being related to an increase in the number of carbon atoms per unit volume in the surface region sample as might be brought about by a reduction in the average interchain spacing by the elimination of bulky substituents or crosslinking of polymer chains. This quantity shows an initial rapid rise with bombardment which slows after ∿40 seconds treatment time (equivalent to an ion dose of 5×10^{13} ions cm^{-2}), by which stage the absolute integrated intensity of the C_{1s} level has risen by 10%, the stoichiometry of the film having dropped from $CF_{1.04}$ to $CF_{0.8}$. Beyond this stage, there is an apparent decrease in the number density of carbon atoms at the surface before once again increasing at a slower rate with increasing ion dose. This behaviour was noted over the range of ion energies used. The ratio rises to 1.25 after a total

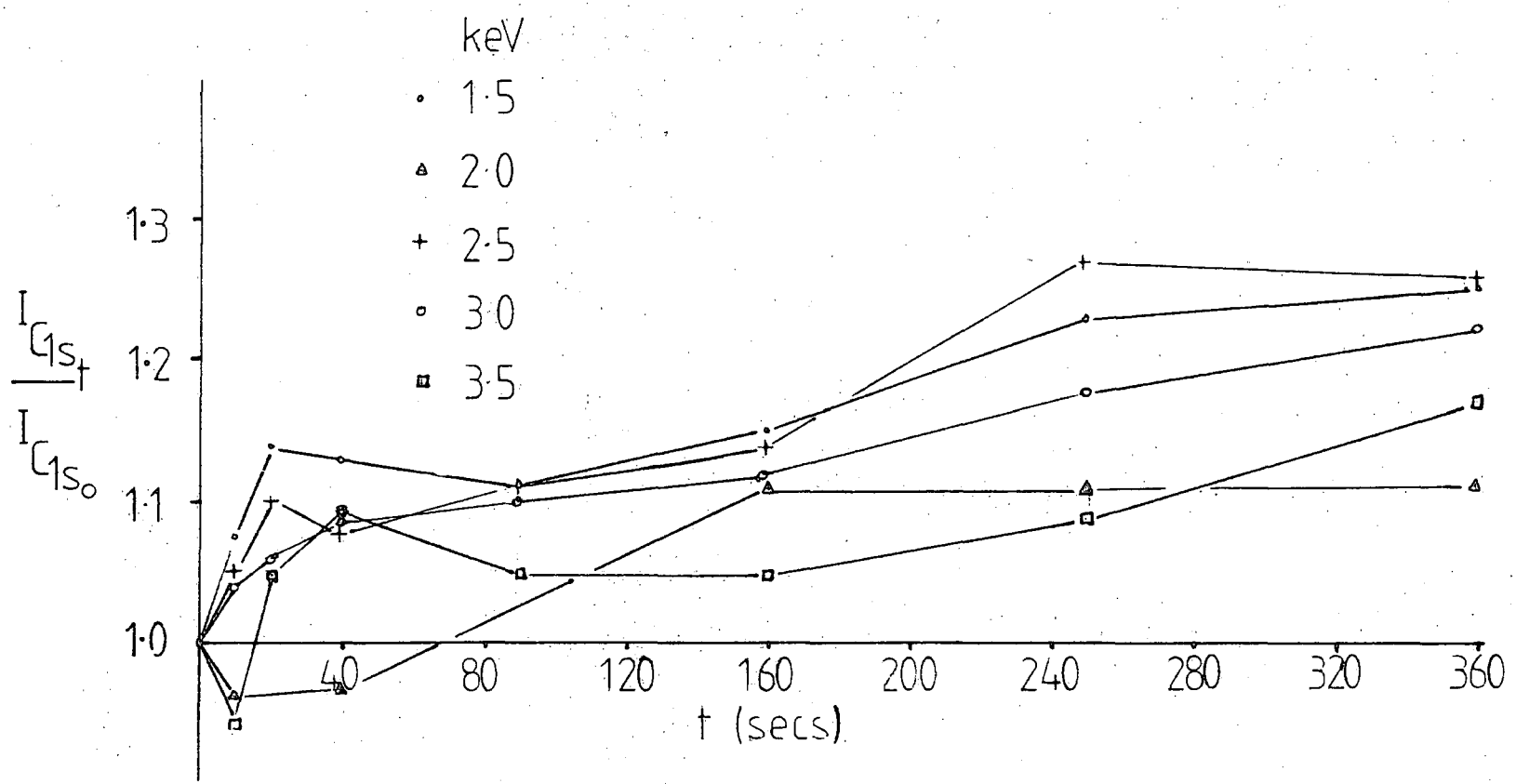

Figure 4.10 Variation in the integrated intensity of the C_{1s} level as a function of reaction time

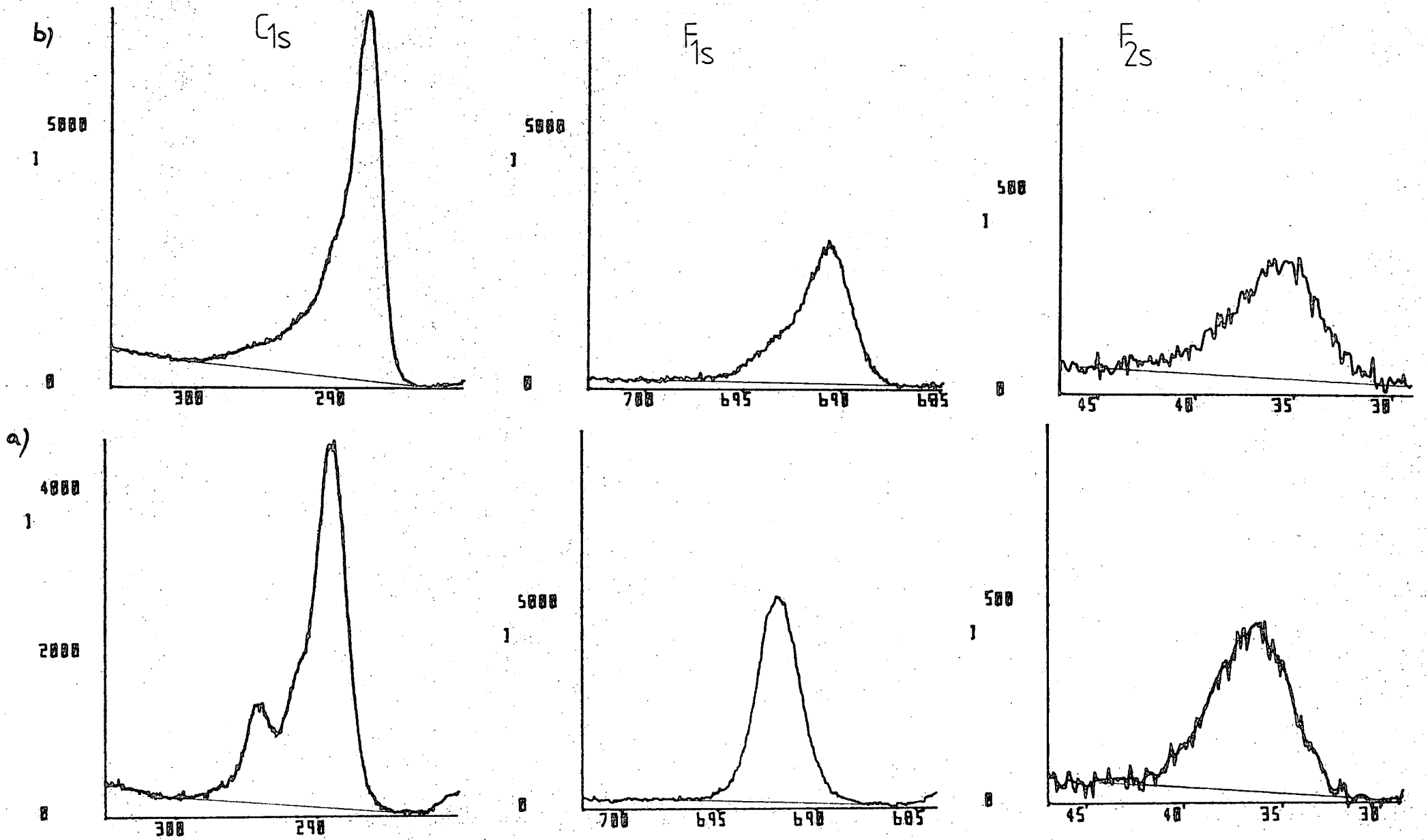

Figure 4.11 C_{1s}, F_{1s} and F_{2s} level spectra of samples of TE copolymer after ion doses of (a) 1.1×10^{14} ions cm^{-2} and (b) 10^{15} ions cm^{-2} showing the growing asymmetry of the levels.

ion dose of $\sim 5 \times 10^{14}$ ions cm^{-2}; (to be compared with there being $\sim 10^{15}$ carbon atoms cm^{-2} in a polymer surface).

Under bombardment by the low ion doses employed in these experiments no incorporation of argon into the polymer matrix was observed: no signal appropriate to the photoemission of electrons from the Ar_{2p} levels being observable. (This region is also complicated by the presence of the K_β satellite to the C_{1s} level).

Neglected in the aforegoing discussion, but implicit, is the unsaturation introduced into the polymer surface by argon ion bombardment. A slight yellowing of the films on prolonged bombardment has already been noted, indicating the formation of chromophores in the surface. Evidence for the formation of unsaturation in the surface from the ESCA data is scant. The formation of isolated double bonds would be accompanied by the development of a low intensity shake-up satellite to the C_{1s} spectrum some 7-10eV removed from the direct photoionisation peak. Thus such a weak feature would be masked by the components of the C_{1s} envelope or lost in the inelastic tail due to the low binding energy components of the C_{1s} level. After an ion dose of $\sim 1.1 \times 10^{14}$ ions cm^{-2} a slight asymmetry is seen to develop to the C_{1s} and F_{2s} envelopes. This is manifest as a slight raising of the background signal to the high binding energy side of the direct photoionisation peak (Figure 4.11(a)). After a dose of 10^{15} ions cm^{-2} the surface has been almost completely defluorinated, and the asymmetry in the C_{1s} level is now marked, as depicted in Figure 4.11(b These spectra represent the first stages in the defunctionalisation of the polymer matrix, often referred to as carbonisation

or graphitization of the surface (though these terms may be misleading). The formation of polyenes upon the radiolysis of polymers has been noted by a number of workers using a variety of probes. The thermolysis of the halogenated polymer, polyvinylchloride has been studied by a number of workers,[245,246] degradation by the elimination of hydrogen chloride resulting in the formation of polyene segments of the chain. The X-ray degradation of this polymer has also been studied by a variety of probes including ESCA, though in the interpretation of the ESCA data the formation of this unsaturation was neglected,[247] ESCA being used as a convenient method to monitor the stoichiometry of the polymer whilst subjecting it to X-ray degradation. The $Mg_{K\alpha}$ excited C_{1s} and Cl_{2p} spectra for a sample of polyvinylchloride exposed to a $Ti_{K\alpha}$ X-ray source (13.5 kV, 18mA) are presented in Figure 4.12. The loss of chlorine from the polymer is evidenced by the visible changes in the C_{1s} envelope and the C_{1s}/Cl_{2p} intensity ratio. Additionally the developing asymmetry of the C_{1s} peak is observable as a change in the apparent background on which the C_{1s} level sits. (The situation is complicated by the presence of the inelastic loss peak due to the nearby Cl_{2s} peak beneath the C_{1s} peak, but even when due allowance is made for this the C_{1s} level is seen to develop a tailing to higher binding energies). Similar results are obtained from the ion beam degradation of PVC under conditions similar to those employed in this current study of tetrafluoroethylene-ethylene copolymer.

The removal from the high vacuum environment of the spectrometer of the sample and its exposure to the atmosphere and bromine vapour for 30 minutes results in the incorporation of bromine and oxygen into the sample surface. The use

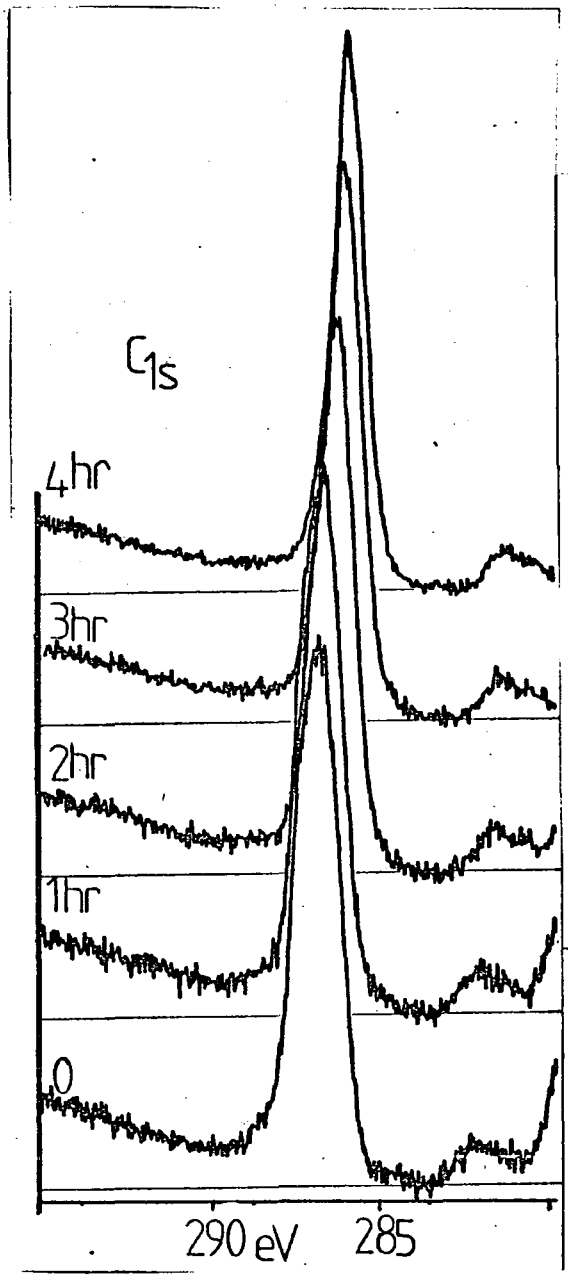

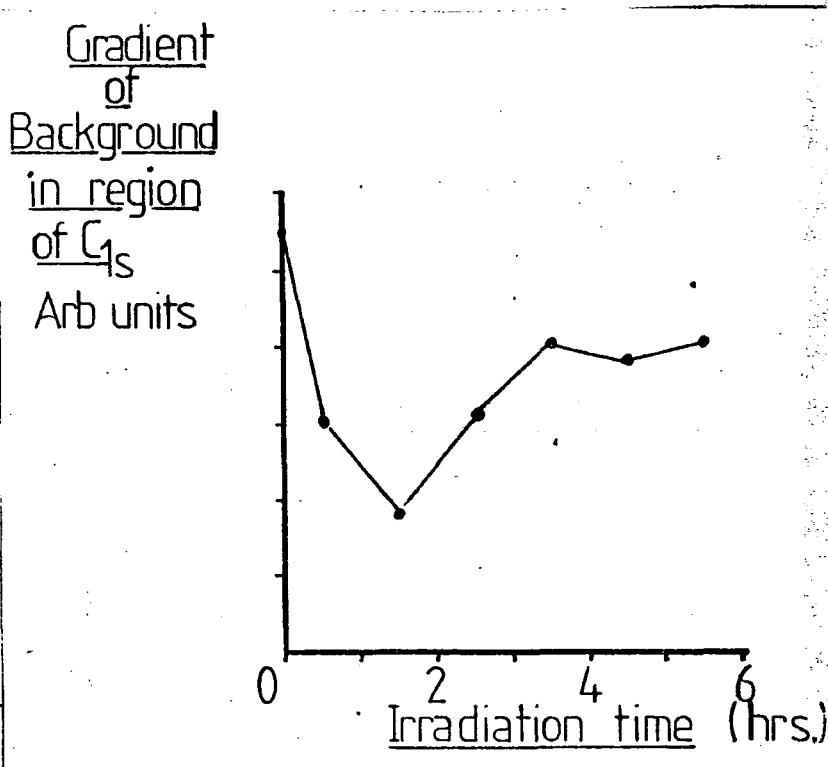

Figure 4.12 Effects of the X-ray induced dehydrochlorination of PVC upon the C_{1s} lineshape

of bromine to label unsaturation in polymeric materials for ESCA analysis has already been demonstrated by Briggs.[243] However bromine would also serve to label any radical sites introduced into the polymer surface by argon ion bombardment. Also were polyene type structures to be formed they too would be susceptible to atmospheric oxidation.[244]

4.3.5 Kinetic Studies of the Ion Beam Modification of Tetrafluoroethylene-Ethylene Copolymer

As an entry point into understanding the defluorination of the surface of a tetrafluoroethylene-ethylene copolymer by an argon ion beam consider the treatment of Benninghoven[152] of a single monolayer of material deposited upon a substrate, and the sputtering of that monolayer (though here, sputtering is taken to encompass material ejected by direct physical sputtering or as a result of chemical rearrangement of metastable species produced as a secondary result of argon ion bombardment). On sputtering, for a single monolayer of material, if it is chosen to monitor a given component of that surface whose relative surface coverage at time t=0 in $\theta(0)$, given an ion flux which is constant with time, this relative coverage will diminish as:

$$\theta(t) = \theta(0) \exp\left(^{-t}/_{\tau}\right) \qquad (4.1)$$

where τ is the average lifetime of a monolayer, being related to the incident ion flux, the sputtering yield of the monolayer to ions of a given energy and the number of particles per cm^{-2} in the monolayer.

The treatment has been found to produce uniform modification of the polymer throughout the depth scale probed by $Mg_{K\alpha}$ excited core-level spectra. Hence treating this layer

as a whole, by using the various core levels to probe the course of reaction, it was attempted to interpret the reaction in terms of a simple first-order type process. Plots of the natural logarithm of the ratios of the intensity of the F_{is}, F_{2s} and the CF_2 and CF features to that of the C_{is} core-level against time (or accumulated ion dose) show evidence of the involvement of at least 2 distinct processes in the reaction scheme (*viz* the plot shows very distinctive curvature), Figure 4.6 . Initially the defluorination of the polymer proceeds rapidly until ∿20% of the fluorine originally present in the polymer surface has been lost, thereafter the defluorination reaction proceeds at a much reduced rate. These features are illustrated in Figure 4.5 for the 2.5 keV argon ion bombardment of the copolymer. For a fixed ion flux of 200 nA cm^{-2} whereas the initial rates of reaction show a variation with the kinetic energy of the incident ion as shown in Figure 4.13. The rate of the slower defluorination process appears invariant to the incident ion energy. The transition between the initial rapid reaction and the slower, longer lived reaction is also echoed in the transition in the plot of the increase in absolute intensity of the C_{1s} level with increasing ion dose depicted in Figure 4.10. It is not clear however whether this transition is the cause or effect of the change in the rate of defluorination of the surface.

4.3.6 The Modification of Polytetrafluoroethylene (PTFE) Surfaces by Argon Ion Bombardment

In contrast to the ion beam modification of the TFE.E copolymer the argon ion bombardment of PTFE does not produce so extensive or so rapid defluorination of the polymer

Figure 4.13 Variation in reaction rate of tetrafluoroethylene/ethylene copolymer with incident argon ion energy

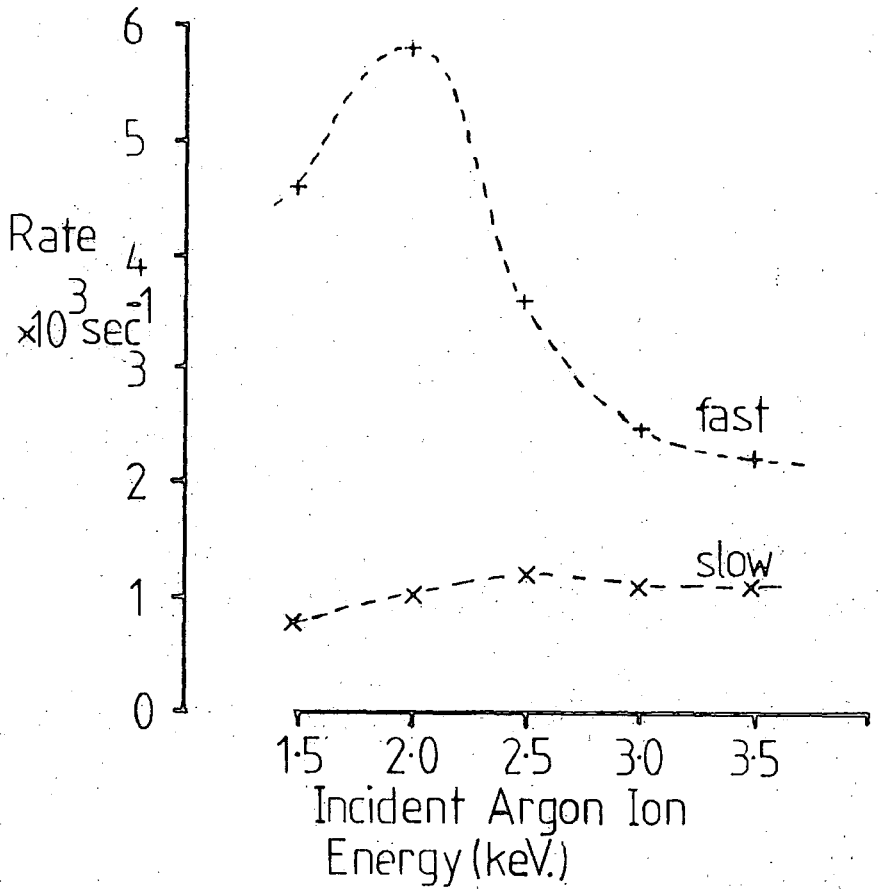

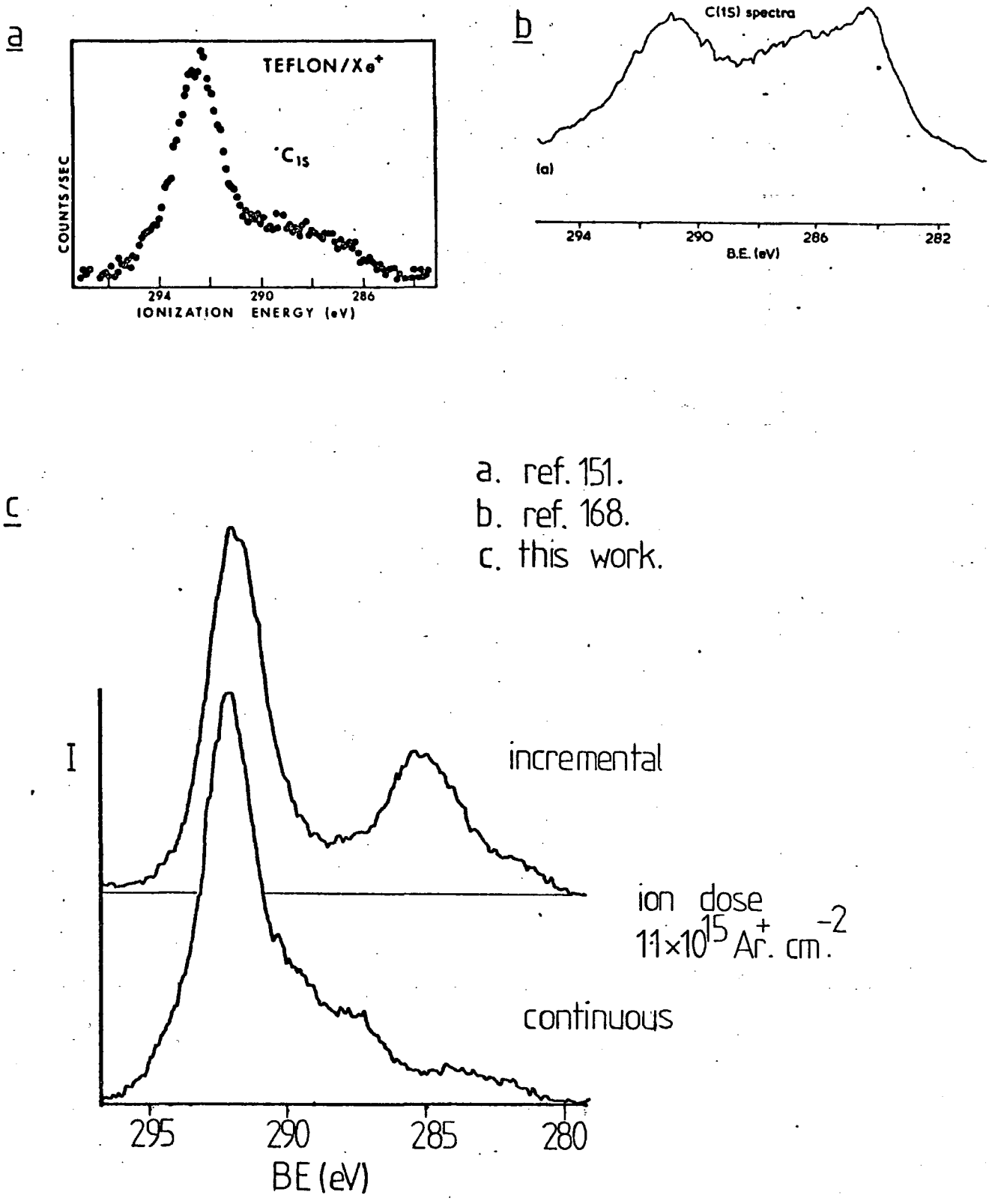

Figure 4.14 Effects of ion dose rate upon the C_{1s} lineshape of PTFE

surface under the same bombardment conditions. Samples of PTFE were exposed to incremental doses of argon ions up to 4.5×10^{14} ions cm^{-2} for ion energies from 1.5 to 3.5 keV. The spectra in Figure 4.4 typify the changes introduced into PTFE surfaces by argon ion bombardment, they relate to the treatment of PTFE by 2.5 keV argon ions at an ion beam current density of 200 nA cm^{-2}.

Whereas for the copolymer, the modification of the polymer surface from a single dose was found to produce an effect equivalent to that produced by a sequence of smaller doses (so as the total dose received by the polymer is the same in each case), this situation does not appear to obtain for PTFE; sequential doses leading to higher degrees of defluorination than a single bombardment. The possibility of hydrocarbon contamination from the vacuum system as a result of repeated ESCA analysis is discounted; the hydrocarbon levels in the sample analysis chamber being low (the argon ion gun can be used to bombard and clean the X-ray gun window and cap thus reducing the possibility of hydrocarbon contamination accumulating during analysis); C:F stoichiometries of the altered layer derived from the F_{1s}:C_{1s} integrated intensity ratios and from within the C_{1s} envelope are in close agreement. The "single shot" exposure of a sample produces a lower apparent degree of defluorination, and the lower binding energy carbonaceous material contributing less to the overall C_{1s} envelope. The C_{1s} envelope of PTFE after such a treatment is illustrated in Figure 4.14, it shows qualitatively the same profile as for PTFE bombarded with 500eV Xenon ions as presented in the work of Rabalais *et al.*[151] However differing markedly from the spectra presented by Cadman and Gossedge[168] in which much higher ion doses were employed

(500eV Ar^+ 1μA, 30 min), the C_{1s} envelope of the treated material showing a much more prominent feature due to carbonaceous material representing a surface much more depleted in fluorine (∿<50% of the fluorine content of the untreated polymer remaining) than found in the work presented here. Cadman and Gossedge[168] also noted that upon standing in UHV the surface of a treated sample became refluorinated, perhaps by the migration of low molecular weight polymer molecules to the surface on standing. In an attempt to reproduce this effect a sample of PTFE was exposed to an ion dose of 10^{15} ions cm^{-2} of 4 keV argon ions. No increase in the fluorine content of the surface was observed after periods of up to 8 hrs. standing in UHV at an ambient temperature of 25°C, subtraction of the initial spectra from those obtained on standing failed to reveal any significant differences, save for a slight accumulation of hydrocarbon. (The operating conditions of ion energy and beam current are not comparable with those employed by Cadman and Gossedge,[168] however the modification of the polymer surface has been found to vary little with ion energy. The higher fluxes employed by these workers may give rise to a much more disordered, open structure than the doses employed in this work: the dose rate employed in this work being estimated to be an order of magnitude lower than that employed in the work of Gossedge.[192] This may imply the presence of a more highly ordered, crosslinked surface layer preventing the migration of small polymer molecules to the surface. Indeed the low energy ion beam treatment of polymer surfaces forms the basis of an invention described in a patent for the production of a barrier layer on a PVC surface to prevent plasticizer migration).

The ion beam treatment of PTFE is accompanied by an increase in the total absolute integrated intensity of the C_{1s} peak at both take-off angles, 30^{o} and 70^{o}. The increase reflecting the decrease in the average interchain spacing as the polymer cross-links. In the sequentially treated surfaces, initially there is a decrease in the absolute intensity of the C_{1s} signal until ∿20% of the fluorine in the surface has been removed. This may be due to a requirement to remove a certain amount of fluorine from the polymer chains to permit movement and approach of two chains to form a crosslink, also to create sufficient active sites to promote cross-linking. Thereafter the absolute intensity increases as the polymer cross-links. (Such behaviour was also noted in the hydrogen plasma treatment of PTFE as described in Chapter Three).

A component analysis of the C_{1s} envelope with increasing accumulated ion dose of the spectra illustrated in Figure 4.4 is given in Figure 4.14. The component due to CF_2 features is seen to decay to ∿55% of the envelope, its demise is mirrored by the concomitant rise of features due to carbonaceous material $\underline{C}$. $\underline{C}F$ features rise rapidly to form ∿10% of the C_{1s} envelope. A small shoulder due to CF_3 functionalities forms on the high binding energy side of the $\underline{C}F_2$ component of the envelope at 293.5eV binding energy. The bombardment of the copolymer did not result in the appearance of any feature due to CF_3 groups. The formation of trifluoromethyl groups can be envisaged as arising from the recombination reaction between chain fragments and fluorine atoms formed by the kinetic dissociation of a polymer chain by an incident ion. The abstraction of a fluorine atom from another polymer chain by a radical is less likely, the reaction being at best thermoneutral

Figure 4.15 Variations in the relative intensities of the components of the C_{1s} spectrum of PTFE as a function of reaction time and accumulated ion dose when bombarded with 2.5 keV argon ions (200 nA cm^{-2})

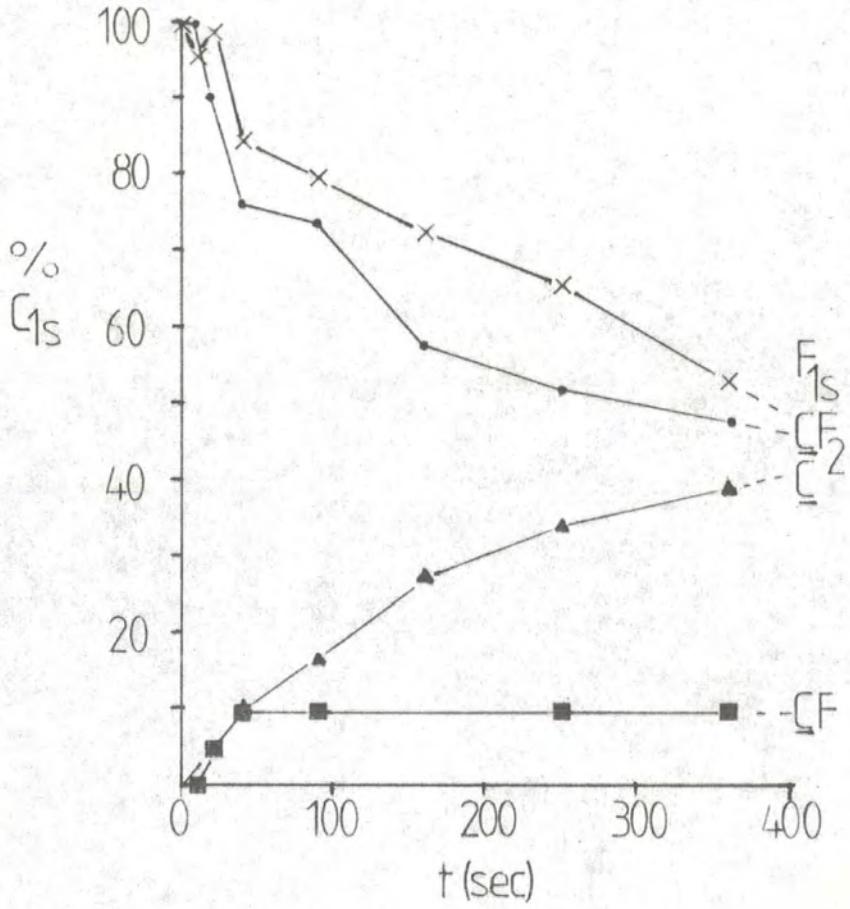

and possessing a high activation energy due to the strength of the C-F bond and the low polarisability of fluorine.

Throughout the reaction the position of the CF_2 component of the C_{1s} spectrum remains at 292.2eV. This is the binding energy appropriate to a CF_2 group in a perfluoro-environment, *i.e.* adjacent to other CF_2 groups. The implication being that the degradation of the chain is not random throughout its length but restricted to regions of the chain, portions of the chain remaining untouched. Whilst ESCA can be used to follow changes in the surface chemistry of the polymer on bombardment it yields no evidence for alternative mechanisms of degradation based on the loss of chain segments.

As noted before the copolymer the reaction appears to proceed rapidly initially, with psuedo first-order rate constants for the process of $\sim$6.2, 5.1 and 3.68 x 10^{-3} sec^{-1} for incident ion energies of 1.5, 2.5 and 3.5 keV respectively at an ion current density of 200nA cm^{-2}. The rates are comparable to those obtained for the copolymer, again the rate is seen to decrease with increasing ion energy. The second reaction appears to be considerably slower, no figure being put on this second rate constant. The first rate process representing the formation of an equilibrium surface layer, after this is established the defluorination slowing the reaction then consisting of the erosion of the surface whilst maintaining this barrier layer.

Upon prolonged treatment (30 min, 5 keV Ar^+ 100nA cm^{-2} the modification is found to be uniform throughout the sampling depths for C_{1s} electrons excited by $Mg_{K\alpha}$ and $Ti_{K\alpha}$ X-ray sources. The stoichiometry of the layer being the same (within the limits

of experimental error(derived $Mg_{K\alpha}$ and $Ti_{K\alpha}$ data. Thus the depth of the altered layer is at least the sampling depth of $Mg_{K\alpha}$ excited C_{1s} electrons, *i.e.* >36Å. The lack of sensitivity of the $Ti_{K\alpha}$ anode due to the poor signal to noise ratio of the spectra does not allow an upper limit to be placed on the depth of modification.

Treatment of an exposed sample to bromine vapour again results in the incorporation of bromine into the polymer surface, to a greater extent for PTFE than in the case of the copolymer.

4.3.7 Mechanistic Aspects of the Ion Beam Modification of a Tetrafluorethylene-Ethylene Copolymer and Polytetrafluoroethylene

The ion beam bombardment of these polymers is found to cause extensive defluorination of the polymer surfaces. It is important to note that ESCA only interrogates the chemistry of the altered layer produced by such treatment, the nature of the gaseous products of the reactions can only be inferred. During bombardment the pressure within the sample analysis chamber remains unchanged in the low 10^{-8} torr region. Whereas the bombardment of the copolymer is found to lead ultimately to the formation of an almost completely defluorinated surface, the extended treatment of a PTFE surface results only in an intermediate degree of defluorination (the exact extent depending upon the bombarding conditions). Previous ESCA studies of the surfaces of samples of PTFE bombarded by noble gas ions have shown two distinct types of modified layer: Cadman and Gossedge[168] bombarded PTFE with 500eV argon ions at an ion current of 1μA for 30 minutes, the resultant C_{1s} spectra had a doublet type

appearance, the intensity of the $\underline{C}F_2$ component being approximately matched by the intensity of that due to carbonaceous material at lower binding energies; Sovey[166] and Rabalais *et al*[151] obtained C_{1s} spectra which display a much lower carbonaceous component, the dose rates employed by Sovey[166] being two orders of magnitude greater than those of Cadman and Gossedge.[168] The former type of behaviour might be explicable in terms of hydrocarbon contamination of the sample surface, however angular dependent measurements reveal the modification to be uniform throughout the ESCA sampling depth. More plausible explanations would rest on differences in the relative proportions of the crystalline and amorphous regions of the polymer surface or a balance between the modification of the polymer surface and the sputtering of components of the surface.

Where for the copolymer the modification introduced by an ion dose accumulated in several stages is the same as that from a single dose, for PTFE this is not the case. In the case of PTFE higher degrees of defluorination are obtained from a dose accumulated in several stages, suggesting the involvement of a 'dark reaction'. At high dose rates the sputtering of fluorocarbon fragments being the dominating process. The main gaseous product of the plasma decomposition of PTFE has been found by Mathias and Miller[248] to be C_2F_4. If this were the main product of the argon ion modification of PTFE then little change would be observed in the C:F stoichiometry of the modified layer. Where for the copolymer, energy transferred to the lattice may be rapidly dissipated by the elimination of hydrogen fluoride, no such pathway exists for PTFE. The changes in the chemistry of the surface layer being due to the

attack of radicals on adjacent chains and radical recombination as the active species introduced by the bombardment decay. The somewhat higher incorporation of bromine into treated PTFE films would point to the introduction of somewhat higher concentrations of unsaturation or radicals into the surface of PTFE than for the copolymer.

The presence of unsaturation in the modified layers may only be inferred from the ESCA analysis from the stoichiometries of the altered layer and slight variations in the lineshape of the various core levels monitored. No distinct shake-up features being noted, though such features would be low in intensity and easily swamped. In each case the yellowing of the polymers upon prolonged bombardment would suggest the creation of conjugated polyene units. The introduction of unsaturation into PTFE has been observed by Ryan[249] who observed changes in the infra-red spectra of PTFE upon γ radiolysis. Other studies of the radiolysis of PTFE have identified CF_4 and F_2 as the main products of the radiolysis. The results of many such studies of the interaction of high energy radiation with PTFE have been reviewed by Charlesby.[250]

The energetics of the degradations of the copolymer and PTFE differ markedly. In PTFE the C-F bond is considerably stronger than the C-C bond, thus fission of the C-C bond is favoured, leading to the production of fluorocarbon fragments, the evolution of fluorine is less favourable, the F-F bond is weak, F obstruction by $F^{\cdot}$ would be a highly endothermic reaction with a high activation energy.

Contrastingly the degradation of the copolymer of tetrafluoroethylene and ethylene may occur by a variety of

routes, C-C and C-H bond fission may lead to a variety of radicals, the recombination of radicals producing a "hot" chain segment, de-excitation of which could result in the elimination of HF or H_2.

The rates of defluorination of the polymers are found to decrease with increasing incident ion energy. The decrease probably being due to the increased sputtering of segments of the polymer at higher ion energies.

As the particle enters the polymer, at high ion energies nuclear collisional processes are important, as the particles slows electronic excitation of the matrix becomes a more important stopping mechanism: the former resulting in the less specific fragmentation of the polymer matrix, and the latter process resulting in electronic excitation and the production of secondary electrons. The decomposition of valence ionised chain segments leading to the modification of the surface. The apparent lack of variation in the depth of modification introduced by bombardment with ions of various kinetic energies. This being explicable were the depth of modification to be dictated by the ranges of low energy electrons in the matrix rather than the range of the ions themselves.

4.4 Conclusions

The modification of the surfaces of PTFE and TFE.E co-polymer follows the trends observed for bulk polymers for the completely fluorocarbon polymer, PTFE, degradation dominates. For both polymers the rate of defluorination decreases with increasing treatment, reflecting the increased difficulty in

sputtering fragments from the cross-linked polymer. The ion beam treatment of polymer surfaces is seen to result in the formation of a modified layer several 10s of Angstroms deep on the polymer surface.

CHAPTER FIVE

THE ARGON ION BEAM MODIFICATION OF POLYMERS CONTAINING CARBON, HYDROGEN AND OXYGEN

5.1 Introduction

Interest has recently been shown in the use of ion beam techniques to modify the properties of polymers and organic compounds. Originally much of this type of work was directed toward the modification of the adhesion properties of materials for bonding and metallisation, with the widespread use of ion implantation equipment in the electronics industry, current interest has come to focus upon the use of ion beam techniques to modify the electrical properties of polymeric materials. The conductivities of films of polyacetylene[175] and polyphenylene sulphide[251] have been greatly enhanced by ion implantation into these films. In the case of polyphenylene sulphide (Ryton),[251] increases of 14 orders of magnitude in conductivity have been reported. The ion bombardment of polyacetylene has been shown to modify the conductivity, optical properties and the stability of such films to atmospheric oxidation. The ion bombardment of thin films of organic material (3, 4, 9, 10 perylenetetracarboxylic acid dianhydride, 1, 4, 5, 8 naphthalene tetracarboxylic acid dianhydride and nickel phthalocyanine) with 2MeV argon ions has been found to produce large conductivity changes in the films,[253] the films darkening and finally taking on a shiny black appearance on prolonged treatment. During the bombardment, up to 70% of the oxygen originally present in the films is lost. The same authors have also studied the modification of polyvinylchloride, polymethylmethacrylate and a proprietary resist material.[252] In each case the treatment of cast films of the materials is found to lead to the loss of the most electronegative elements present

in the polymers. At high electron and ion beam irradiation doses, polymer films commonly used as positive resists in electronic device fabrication behave like negative resists. At high ion beam doses the polymers darkened and became brittle. From detailed Raman measurements Kaplan *et al*[252] concluded that the altered film was essentially graphitic in character, consisting of graphite crystallites of dimensions of the order of 30Å. The conductivity of the films being ascribed to a hopping mechanism between crystallites, though the possibility of a one dimensional conduction mechanism was also considered. The darkening and defunctionalisation of polymers has also been observed using lower energy ion sources (in the keV range), though the modification is then restricted to the surface regions of the film, on contrast to the treatment by 2 MeV argon ions whose range in polymeric materials is of the order of a micron, and hence produced modification throughout a film. In the study of the effects of ion bombardment on polymer surfaces, ESCA has often been employed to interrogate the structure of the final surface produced.[162-164, 166-168, 175] In the current study the aim is to use ESCA in a more dynamic fashion to monitor the changes introduced by much lower ion doses in the very first stages of such reactions.

At first sight the ESCA analysis of purely hydrocarbon systems is very limited.[254,255] However the observation of low energy shake-up satellites in homopolymers has been shown to provide a useful extra level of information in reflecting the unsaturation or otherwise of a material.[34,256] The utility of shake-up structures as a probe to elucidate polymer

structure has been demonstrated by Clark and Dilks for a wide range of substituted polystyrenes and polymers containing pendant aromatic groups.[34,356] The origins of these features were briefly discussed in Chapter One.

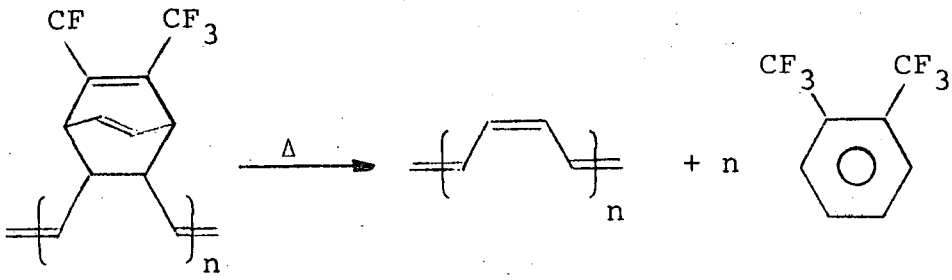

I. II.

Figure 5.1

5.2 Experimental

5.2.1 Samples

The investigations involved a total of nine different homopolymers studied in film form. The origins of the polymer samples are detailed below:

(1) High density polyethylene (HDPE) TFE 554 supplied by the Metal Box Company, containing the anti-oxidant Irganox 1076, [Octadecyl 3-(3,5-ditertbutyl-4-hydroxylphenyl)] at the 0.016% level.

(2) Low density polyethylene (LDPE) C37 TFE 628 also supplied by the Metal Box Company, containing low concentrations of the additives, Topanol OC [2,6-ditertbutyl-p-cresol] and Irganox 1010 [Pentaergthritol tetra-3-(3,5-ditertbutyl-4-hydroxylphenyl)propionate].

(3) Polyisoprene cast on to an aluminium foil substrate from a 2% wt/vol solution in chloroform.

(4) Polystyrene film was supplied by Prof. A. Curtis of Glasgow University.

(5) Polyacetylene was produced *in situ* under high vacuum conditions of a pre-polymer I shown in Figure 5.1. The pre-polymer was kindly supplied by Dr. J.H. Edwards of Durham University. The pre-polymer was dip coated from acetone solution on to a standard ES300 probe tip and introduced under an H_2 atmosphere into the sample analysis chamber of the spectrometer in the normal fashion. The pre-polymer I was then decomposed by raising the temperature of the sample to 60^{o}C by means of the in-built heater housed in the tip of the sample insertion probe to yield polyacetylene with the concomitant evolution of 1,2-bis(trifluoromethyl)benzene. The process has been fully detailed by Edwards and Feast[257] from whom the sample of the pre-polymer I was obtained.

(6) Polymethylmethacrylate (PMMA) was cast as a thin film on to aluminium foil substrates from a 2% wt/vol solution in chloroform.

(7) Thin films of Poly n-butyl methacrylate, Poly-sec-butyl methacrylate and Poly-t-butyl methacrylate were cast from 2% wt/vol solutions in chloroform on to aluminium substrates.

The studies also involved spectra obtained from samples of:

(1) Graphite orientated parallel to the basal plane, cleaved to yield a fresh surface. The oriented graphite sample was obtained from the Union Carbide Corporation.

(2) Anthracene ex B.D.H. Ltd., Microanalytical Reagent.

(3) Chrysene ex Phase Separations Ltd.

(4) Pyrene ex Koch Light Ltd.

(5) Perylene ex Ralph W. Emanuel Ltd.

(6) Coronene ex Phase Separations Ltd.

(7) Ovalene ex Ralph W. Emanuel Ltd.

5.2.2 Sample Preparation

Films were mounted on a spectrometer probe tip by means of double sided "Scotch" tape in the usual fashion. The graphite sample was attached to the probe tip by means of 2 brass screws. The polycyclic aromatic compounds were studied as powders pressed onto the tape with a metal spatula and the excess which had not adhered blown off with argon. Cooling was employed in running the polycyclic aromatics to prevent the sublimation of the samples in high vacuum.

5.2.3 Ion Beam Bombardment and Sample Analysis

Details of the ion source used have been given in Chapter Four. Argon (Research Grade, BOC. Ltd) being used: the ion beam being rastered to its fullest extent to average out the inhomogeneous nature of the ion beam profile. Ion energies from 1-5 keV being employed at current densities of the order of 100 nA cm^{-2}, for exposure times of up to 2 hrs. Ion currents were monitored using a Faraday plate earthed through a Keithley 621 Electrometer. After exposure samples were turned to face the X-ray source for the ESCA analysis. The pressure in the sample analysis chamber of the ES300 spectrometer during ion beam bombardment was 4×10^{-8} torr, dropping

to <1 x 10^{-8} torr during ESCA analysis. Spectra were recorded using $Mg_{K\alpha_{1,2}}$ and $Ti_{K\alpha_{1,2}}$ radiation. Spectra were recorded in digital fashion using the DS300 data system, on which data analysis was also performed. Binding energies are quoted to an accuracy of ±0.2 eV, area ratios in general to better than 2% accuracy. In general spectra of the films were taken at a take-off angle of 35°. For the powder samples the take-off angle was optimised on the C_{1s} level. The asymmetry developed by the C_{1s} core-level spectra during ion bombardment represents a problem in estimating the total intensity of the level as the tailing is also part of the total intensity of the level (as is shake-up). However the data analysis package employed enforces an S shaped, Shirley-type background subtraction routine,[241] which may be inappropriate. This is not thought to seriously affect the interpretation of results.

5.3 Results and Discussion

5.3.1 Polyethylene and Graphite

Polyethylene may seem an unlikely candidate for an ESCA investigation of the argon ion modification of polymer surfaces. The High Density Polyethylene, (HDPE) used in this investigation provides only the C_{1s} and valence levels in the ESCA spectra as probes to the modification of the surface. (The ESCA spectra also revealed a very low degree of oxidative functionality to be present on the sample's surface). This low degree of oxidation (<0.5% of the intensity of C_{1s} level) is not reflected in the C_{1s} spectrum of the HDPE which consists of a single symmetric peak of FWHM of 1.6 eV with a

binding energy of 285 eV. This is illustrated, together with the valence region of HDPE, in Figure 5.2. The comparatively well resolved valence region displays two distinct structures superimposed upon a broad inelastic background. The two most prominent features are assignable to electrons photoemitted from orbitals predominantly C_{2s} in character, the leftmost is assigned to the bonding combination of C_{2s} orbitals, at 18.8 eV, the rightmost to the anti-bonding combination at 13.3 eV. The lower energy, low intensity band is assigned to a C-H band (orbitals formed by the combination of C_{2p} and H_{1s} orbitals).[65]

The effects upon these levels of the bombardment of HDPE by 5 keV argon ions at an ion current density of 100 nA cm^{-2} ($\equiv 6.25 \times 10^{11}$ ions cm^{-2} sec^{-1}) after exposure times of 0,5,15,30 and 60 minutes are presented in Figure 5.2. In the valence band, the reaction is marked by the loss of the two distinctive structures present in the C-C region of the untreated polymer. The width of the C-C, C_{2s} region broadens with increasing treatment. In the initial stages of reaction, the valley between the bonding and anti-bonding components of the C_{2s} region of the untreated polymer is filled in by the emergence of at least two more features. The valley between the C_{2s} and C_{2p} (C-H) region is also filled. Even for comparatively simple polymer systems the interpretation of the valence region requires detailed calculations on model systems, if such spectra are to be used for anything other than to fingerprint the polymer. The interpretation of the valence region of a treated polymer surface is thus restricted to comparison with the valence bands of other polymer systems. The valence regions of polystyrene and graphite are presented in

Figure 5.2 (a) C_{1s} core level spectrum of a sample of HDPE bombarded with 5 keV argon ions (100 nA cm^{-2})

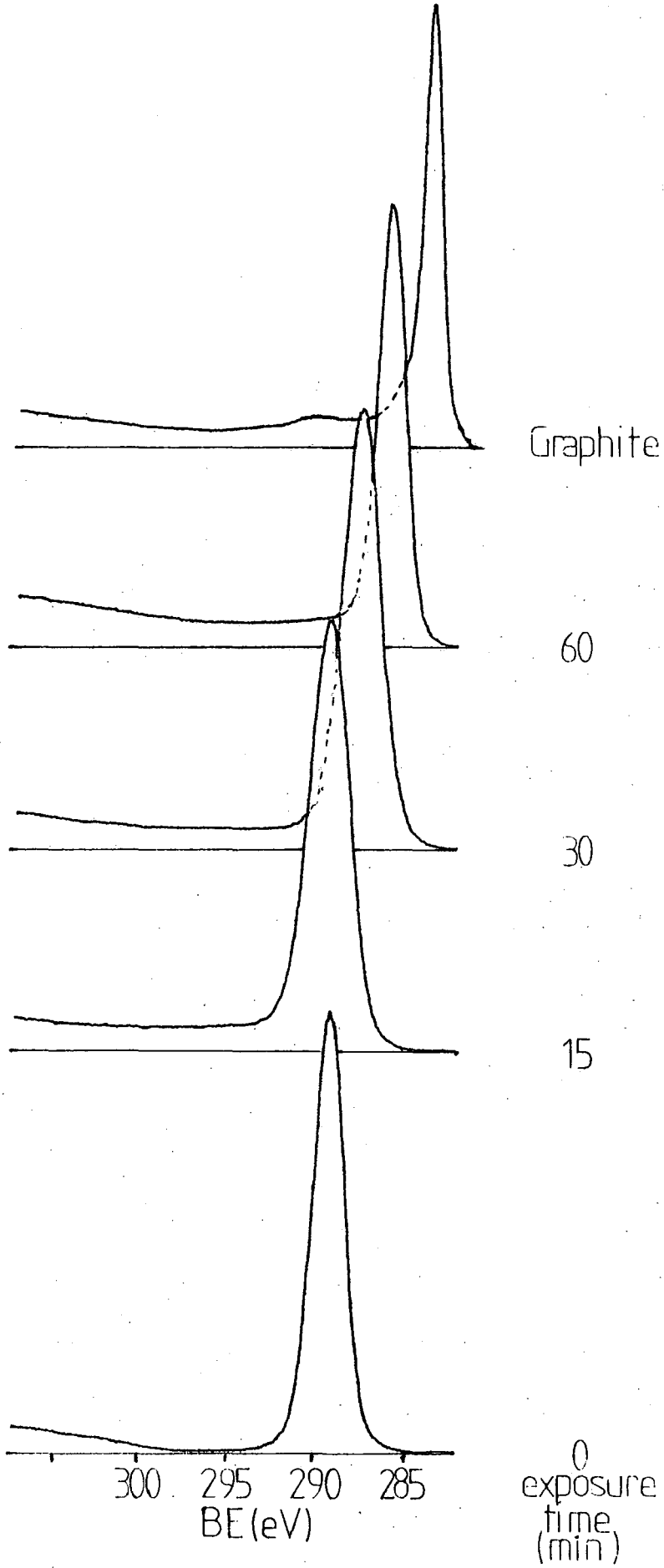

Figure 5.2 (b)

Valence band region of the ESCA spectrum of a sample of HDPE bombarded with 5 keV argon ions (100 nA cm^{-2})

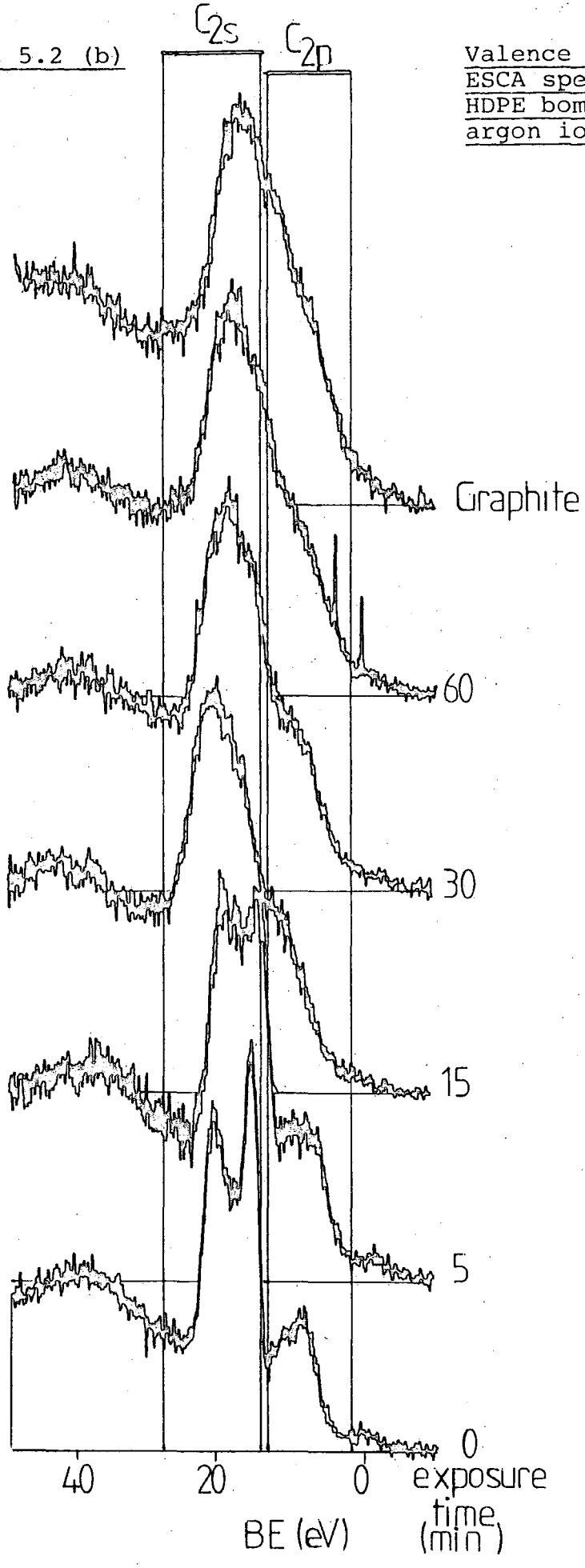

Figure 5.3, the valence band spectra of HDPE, LDPE and polypropylene have already been presented in Figure 1.7 in Chapter One. As the valence region reflects long range interactions in polymers comparisons are dangerous. The introduction of sidechains onto the polyethylene backbone results in drastic broadening of the C_{2s} region of the valence band. The interpretation of such spectra may be extrapolated from the data recorded for the saturated hydrocarbon identified with the monomeric unit associated with that section of a polymer, *e.g.* polypropylene and propane.[65,255] In going from polyethylene to polypropylene one hydrogen atom is replaced by a methyl group, this results in an intense structure located in the middle of the C-C, (C_{2s}) band. Tentatively, the emergence of features between the two distinctive features of the C_{2s} spectrum of the untreated polymer, may be ascribed to cross-linking and branching reactions. After an ion dose of 5×10^{14} ions cm^{-2} the valence band shape closely resembles that of graphite.

Consideration of the C_{1s} core-level spectra for the treated samples reveal a slight decrease in the equilibrium charging shift attained by the sample under ESCA analysis. Though it is difficult to separate slight chemical shift effects from variations in sample charging for such samples. However the use of adventitious hydrocarbon for energy referencing in the ESCA analysis of metal surfaces cleaned by argon ion bombardment has been questioned by Jaegle *et al*[258] who obtained values ranging from 284.1 eV to 283.1 eV for the binding energies of C_{1s} core levels of the adventitious hydrocarbon contamination on the bombarded samples by using the core-levels of the metal substrate for energy referencing. Hence values quoted for

Figure 5.3 Comparison of the valence band regions of Graphite, Polystyrene and Polyvinylnaphthalene

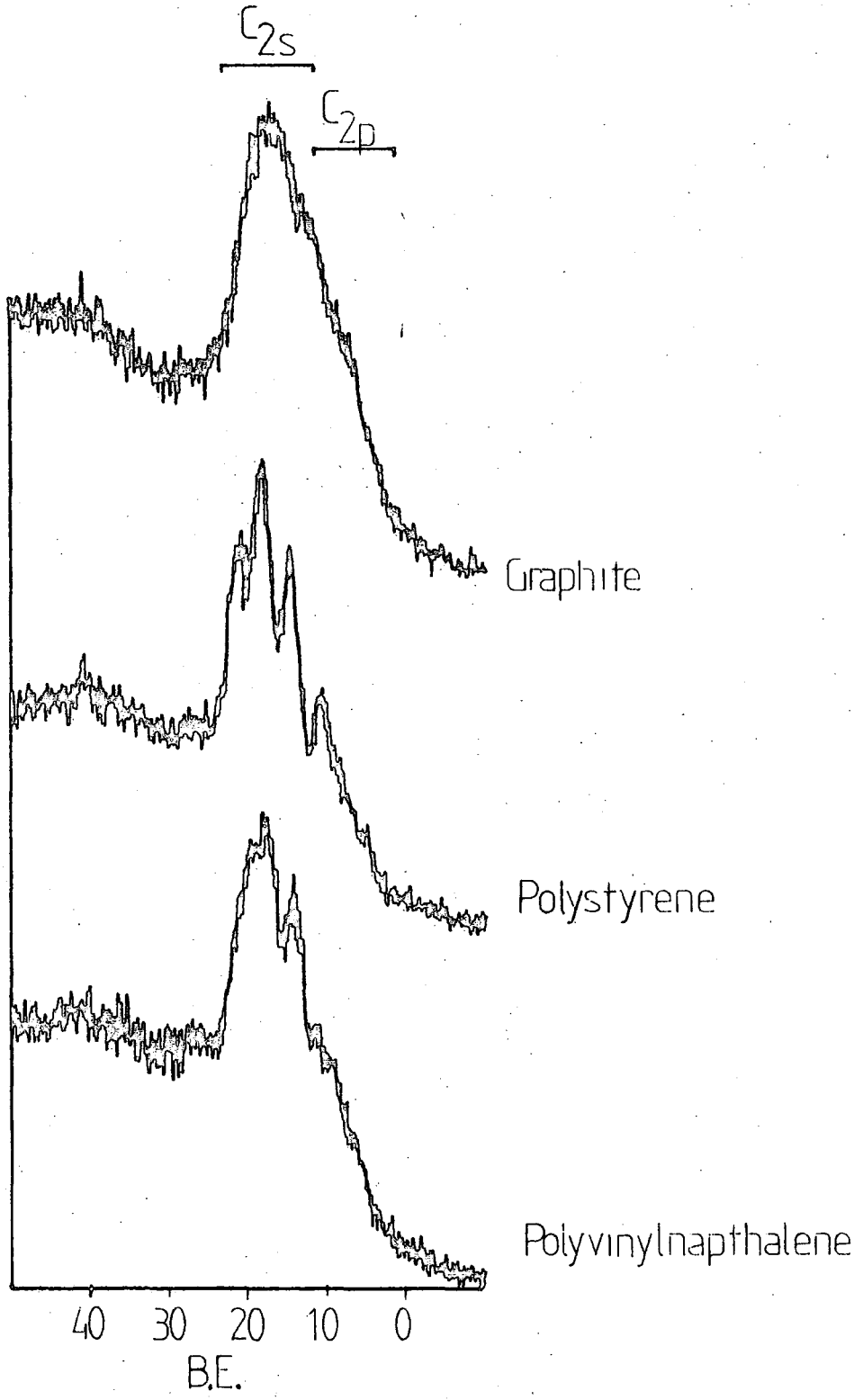

the charging shift δ may be in error. In hydrocarbon systems possible C_{1s} binding energies range from 285 eV for polyethylene, to 283.6 for polyacetylene (polyene).

On bombardment the C_{1s} levels broaden considerably from 1.5 eV FWHM for the untreated polymer to *ca.* 1.9 eV on prolonged treatment after 2 hrs. of bombardment.

Whereas for untreated polyethylene the C_{1s} spectrum consists of a single symmetric peak, the background of inelastically scattered electrons rises linearly from a point 5 eV to the higher binding energy side of the direct photoionisation peak, upon bombardment the peak develops an asymmetric tailing to higher binding energies. The direct photoionisation peak now appears to sit upon a rising background, due to the superposition of the asymmetric tailing of the direct photoionisation peak and the inelastic background. This situation is illustrated in Figure 5.4, in which the C_{1s} envelope of untreated HDPE is compared with that of the polymer after having received an ion dose of 5×10^{14} ions cm^{-2}. Similar asymmetric C_{1s} lineshapes are also observed for plasma polymerised ethylene films.

In a qualitative sense the increasing degree of asymmetry displayed by the C_{1s} core level spectra may be correlated with the increasing density-of-states, DOS, at the Fermi edge of the valence band.[8] In XPS the valence band spectra in the region of the Fermi edge closely resemble the density of occupation of the electronic levels of the material examined, the so-called density-of-states. For an insulator, *e.g.* untreated polyethylene, the DOS for the polymer at the Fermi edge is zero, the Fermi level lying in the gap between the filled

Figure 5.4 The developing asymmetry of the C_{1s} core level of HDPE upon argon ion bombardment
(1) untreated HDPE
(2) after an ion dose of 5 x 10^{14} ions cm^{-2} (Ar^+, 5 keV)

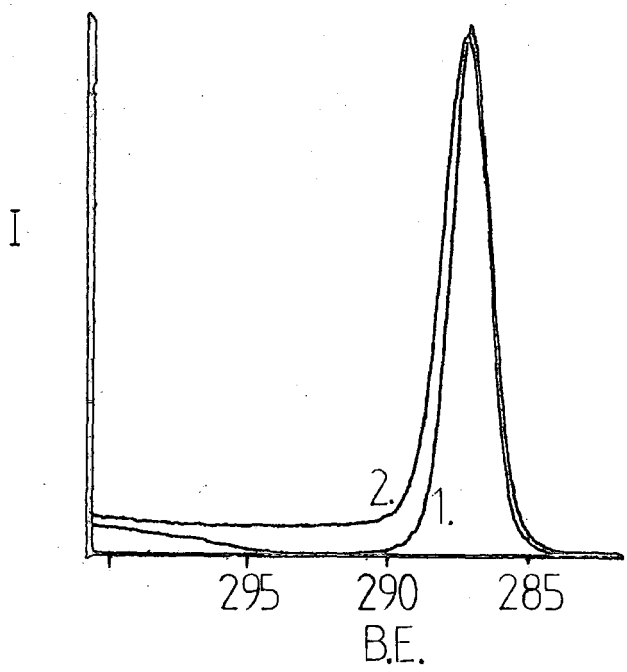

valence levels of the polymer and the higher lying anti-bonding orbitals in the "conduction" band. Graphite and polyacetylene C_{1s} levels also display asymmetric lineshape. The situation is complex, in that the Fermi level is ill-defined for an insulating material. In cases where the density-of-states curve just above the Fermi energy provides a continuous range of allowed one-electron excitations which can occur during core-level emission,[33] in processes analogous to the shake-off and shake-up transitions discussed in Chapter One.

In bulk studies of the radiolysis of polyethylene, the dominant reaction is reported to be crosslinking,[250,259] this indeed forming the basis of a multi-million pound business in speciality polymer products.[260] The γ radiolysis of polyethylene *in vacuo* has been shown by Dole[261] to lead to the formation of polyenes. Crosslinking of a matrix containing polyenes or the dehydrogenation of a cross-linked matrix and inter and intra chain cyclisation processes[262] could be envisaged as possible routes to the formation of the disordered graphite like phase formed on argon ion bombardment. At no time during the bombardment of polyethylene is a discernible shake-up satellite to the C_{1s} direct photoionisation peak observed. The implication being that rather than the random elimination of hydrogen taking place along the polymer chain; once an unsaturated site has been created the unsaturation grows from that point. This could be envisaged in terms of a mechanism for the dehydrogenation by means of which secondary electrons produced by the initial ion impact intermet with these initial sites of unsaturation exciting electronic vibrational transitions of the polymer chain, resulting in the elimination

of hydrogen from the system. Though no facility for detecting gases evolved by the sample during bombardment were present on the instrumentation used, bulk radiolysis studies by Miller *et al*[264] using reactor radiation have shown the bulk of the gas evolved during such treatments to be hydrogen. Most authors have assumed that the mechanism of elimination of hydrogen involves the molecular detachment of a hydrogen molecule from the polymer chain, a view supported by the absence of any activation energy for the process.

The cross-linking of the surface layers on bombardment leads to an increase in the number density of carbon atoms in the surface regions of the polymer, this is reflected in the increase in the integrated absolute intensity of the C_{1s} level with increasing ion dose as shown in Figure 5.5.

Argon incorporation into the sample surface during the bombardment is slight, the intensity of the Ar_{2p} peak is less than 2% of that of the C_{1s} level, corresponding to ∿0.5 atom % Ar being incorporated into the altered layer. This is much less than for a sample of graphite similarly bombarded which incorporates ∿1.2 atom % Ar, upon bombardment the distinctive plasmon satellite structure to the C_{1s} direct photoionisation peak is lost, reflecting the loss of the long range order in the surface on argon ion bombardment. The surface becomes amorphous. Plasmon excitations are closely related to shake-up and shake-off processes. When a core-hole is formed on an atom in graphite, the electron density cloud contracts to stabilise the incipient core-hole, this contraction sets up a collective oscillation of the electron cloud, exciting a so-called plasmon. To generate such a plasmon, the material must possess a delocalised structure, which, in turn, implies

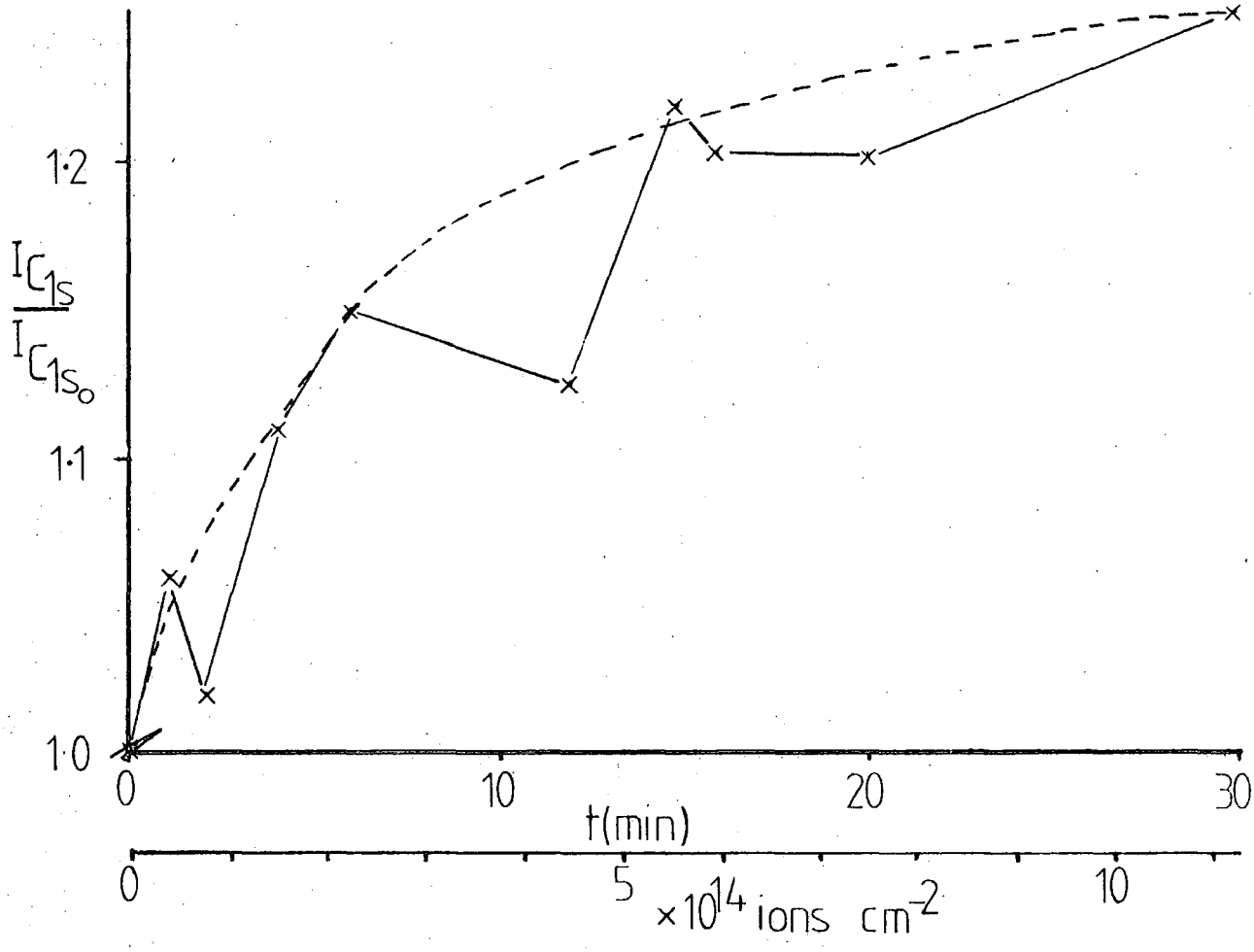

Figure 5.5 Increase in the absolute integrated intensity of the C_{1s} core level upon argon ion bombardment (5 keV, 100 nA cm^{-2})

a degree of order in the structure in the region of the atom on which the core-hole is generated by the photoionisation event. The amorphatisation of the graphite surface on argon ion bombardment results in the destruction of the plasmon satellite to the direct C_{1s} photoionisation peak as shown in Figure 5.6.

Exposure of a sample of HDPE treated for 1 hr. at a current density of 100 nA cm^{-2} to bromine vapour for 5 minutes resulted in a substantial bromine uptake by the sample of ∿8 atom %, *i.e.* the stoichiometry of the surface layer was upon treatment $\sim CBr_{0.08}$. A much higher degree of incorporation than was noted for the argon ion bombarded samples of fluoropolymers examined in Chapter Four. The bromine uptake by the sample also results in the broadening of the C_{1s} level, due to the addition of C-Br functionalities, however the effect is small, the chemical shift introduced by the bromination of the system being essentially indistinguishable from that of the carbon in the cross-linked matrix. The charging of the sample is also modified, increased by the addition of an element having a high photoionisation cross-section.

The exposure of the treated sample to the atmosphere also results in the uptake of oxygen by the sample surface. After several days in the atmosphere a distinct feature due to carbonyl features, BE ∿ 288eV develops. A low degree of oxidation or bromine uptake might be attributable to the reaction of radical sites introduced by the original bombardment with oxygen or bromine. However the diffusion of oxygen into the surface of polyethylene, albeit a highly crosslinked material, is expected to be rapid as would be the reaction of the radicals

Figure 5.6 Loss of plasmon satellites to the C_{1s} direct photoionisation peak of graphite on argon ion bombardment and argon implantation

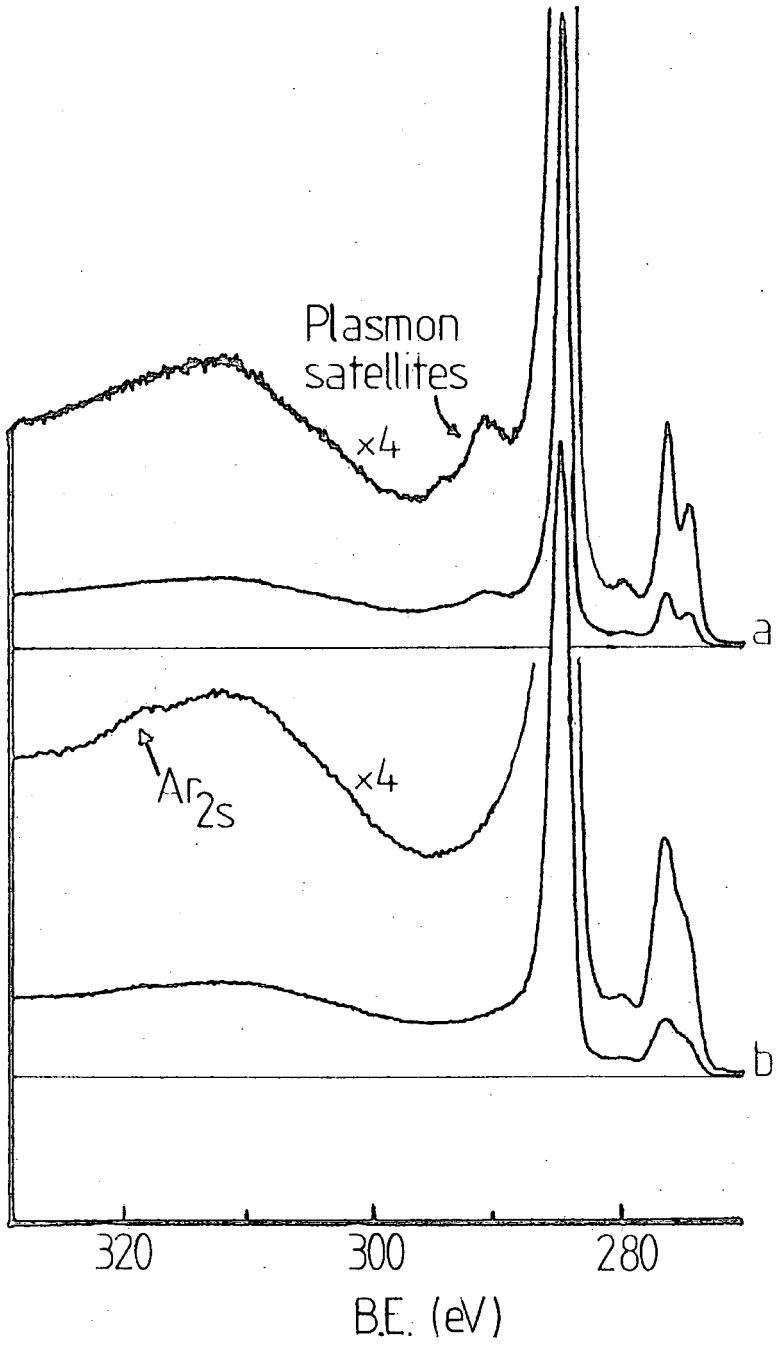

with the oxygen. Therefore it is tentatively suggested that the oxygen uptake is due to the reaction of oxygen with the unsaturated carbon matrix. Were the final altered layer to consist of a disordered graphitic type phase, then in such a phase, to extend the analogy, prismatic edges may be present. Such features are known from the work of Barber *et al*[265] to have sticking coefficients for oxygen much greater than observed for the basal plane. They also noted seven orders of magnitude increase in the sticking coefficient for oxygen on the basal plane after argon ion bombardment. Alternatively were polyene segments to have been introduced into the structure by argon ion bombardment, the oxidation of polyenes on standing in air is well known.[244]

The modification of polyethylene in this fashion is not restricted to bombardment by inert gas ion beams. In an attempt to extend the work of Rabalais and Hu,[146] ion beams derived from CF_4 were used to bombard HDPE. Whilst even on prolonged exposure no fluorine incorporation could be observed in the ESCA spectra, a marked asymmetry to the C_{1s} peak of the type described as resulting from the argon ion bombardment of polyethylene was noted. Using higher doses of low energy, ∿2 keV, electrons Brennan[266] has obtained similar modifications of polyethylene surfaces.

Using electron energy loss spectroscopy, EELS, both to induce damage in polymers and to investigate the nature of the electron beam induced artefacts, Ritsko[176] studied polystyrene polymethylmethacrylate and polyethylene. In polymethylmethacrylate electron radiation induced peaks at 4.2 and 5.1 eV and at 4.7 eV in polystyrene were observed (these are also pro-

duced by UV photolysis of the polymers), these were assigned to unsaturated bond formation in the polymer backbone. In polyethylene electron beam irradiation leads to C-H bond cleavage. Ritsko[176] observed strong absorptions in the EELS spectra at 6.5 eV (due to isolated unsaturated bonds) and absorptions at 5.3, 4.3, 4.0 and 3.6 eV associated with the formation of higher polyenyl groups.

5.3.2 Polyacetylene

Films of amorphous polyacetylene generated under high vacuum conditions using the method of Edwards and Feast[257] were also bombarded. The C_{1s} spectra of untreated polymer and samples of polyacetylene treated for 30 and 60 minutes at an ion current density of 100 nA cm^{-2} of 5 keV argon ions are shown in Figure 5.7. The C_{1s} spectrum of the untreated polymer shows a small feature at 293.5 eV due to the presence of CF_3 groups in the polymer surface due to the incomplete conversion of the precursor polymer I to polyacetylene. (Though various heating rates were employed total conversion was never achieved under the conditions in which it was attempted in these experiments. The assignment of this feature to CF_3 groups is confirmed by monitoring the F_{1s} level, stoichiometries of the film deduced from consideration of the C_{1s} envelope alone coinciding with those deduced from a consideration of the C_{1s}:F_{1s} intensity ratios in the ESCA spectra. The CF_3 component representing between 1-3% of the total area under the C_{1s} envelope, this corresponds to conjugation lengths for the polyene between 13 and 50  units. Though as this estimation involves the subtraction of a small quantity from

Figure 5.7 Effects of argon ion bombardment upon a sample of polyacetylene

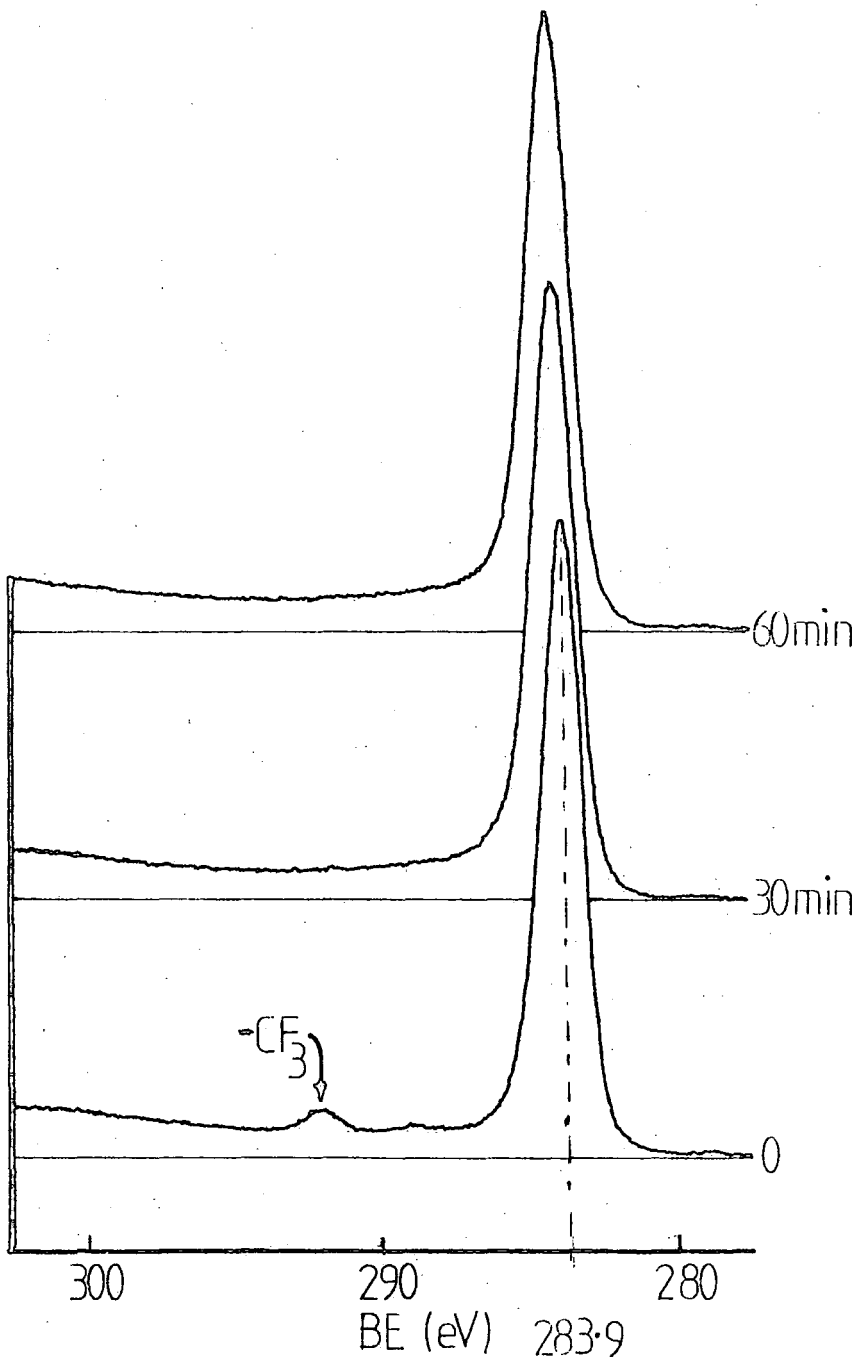

a much greater one, any errors in estimating the small contribution of the CF_3 component, will lead to large errors in the estimation of conjugation length).

Upon argon ion bombardment the features due to CF_3 groups are lost from the C_{1s} spectra. The C_{1s} profile, which takes on an appearance similar to that of ion bombarded graphite, is presented in Figure 5.7. The appearance of the film changes from having a shiny black metallic lustre, taking on a slightly bronze colour.

Upon standing in air the films oxidise, C_{1s} spectra for the oxidised films are shown in Figure 5.8. The exposure leads mainly to the introduction of isolated etheric linkages ($\underline{\overset{+}{C}}$ - $\underline{\overset{*}{O}}$ - C, $BE^{+}C_{1s}$ 286.6 eV, $BE^{*}O_{1s}$, 534.4 eV). The carbon: oxygen stoichiometries of the treated and untreated films after 8 day standing in the atmosphere were found to be $CO_{.37}$, $CO_{.35}$ and $CO_{.26}$ for the untreated film and films treated with doses of 5 keV argon ions of 1.1×10^{15} and 2.2×10^{15} ions cm^{-2} respectively ($\equiv$100 nA cm for 30 min. and 60 min. exposures). The treatment would appear to have little effect in arresting the oxidation of the sample surface. However the increases in the integrated intensities of the C_{1s} core levels of the treated surfaces reveal the extensive crosslinking of the surface on bombardment. However whereas the untreated film had completely bleached during its 8 day exposure to air, the treated films still retained the dark metallic lustre of polyacetylene. Where the treated films have bleached due to oxidation it is at the edges of the films. The effect of argon ion bombardment on polyacetylene films appears to be the formation of a highly crosslinked barrier layer to oxidation.

Figure 5.3 C_{1s} core level spectra of
(a) an untreated sample and
(b) and (c) samples of polyacetylene bombarded with 5 keV argon ions (100 nA cm^{-2}) for 30 min. and 60 min. respectively after 8 days in the atmosphere.

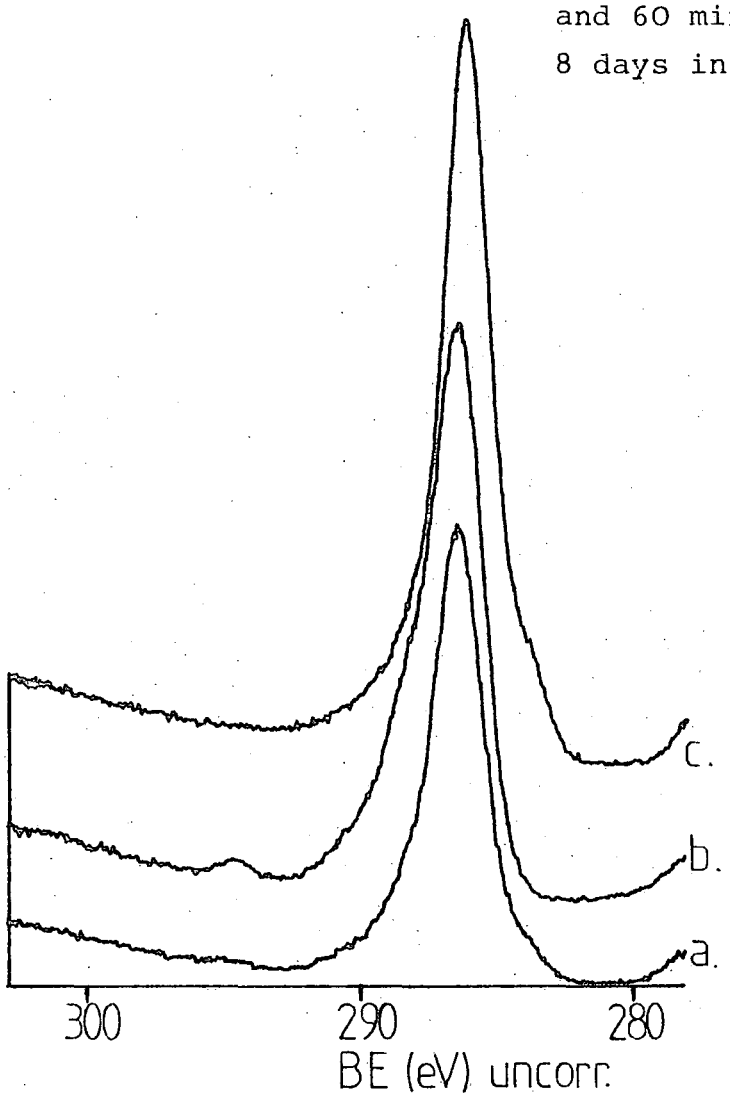

The treatment has already been shown to activate the surface of polyethylene to oxidation, thus it is understandable that the surface of the treated polyacetylene films still oxidises, indeed there is a close similarity in the C_{1s} peak profiles of the oxidised films of treated and untreated material, in each case the dominant feature is the peak due to C-O-C environments. In stark contrast to the range of oxidative functionality introduced into polyethylene surfaces by weathering as reported by Shuttleworth,[205] the oxidation of polyacetylene is for more specific a reaction.

Weber[175] has used ESCA to investigate the ion implantation of 40 keV F^+ ions into polyacetylene, using the F_{1s} spectra to confirm the position and chemical state of the implanted fluorine, however only the F_{1s} spectra were presented, no C_{1s} spectra were reproduced. The quality of the spectra would not allow subtle changes in the C_{1s} spectra to be investigated.

5.3.3 Polystyrene and Polyisoprene

The C_{1s} core-level spectra of untreated polystyrene and polyisoprene both display distinct $\pi \leftarrow \pi^*$ shake-up satellite structures to the direct photoionisation peak as illustrated in Figure 5.9.

The C_{1s} spectrum of polystyrene consists of a single, approximately symmetric, direct photoionisation peak at 285 eV sitting upon a rising background (in contrast to the C_{1s} envelope for polyethylene), and a series of broader shake-up transitions, whose centroid lies at ∿291.9 eV. The shake-up

Figure 5.9 Changes in the C_{1s} core level spectra of
(a) cis-polyisoprene and
(b) polystyrene, on argon ion bombardment.

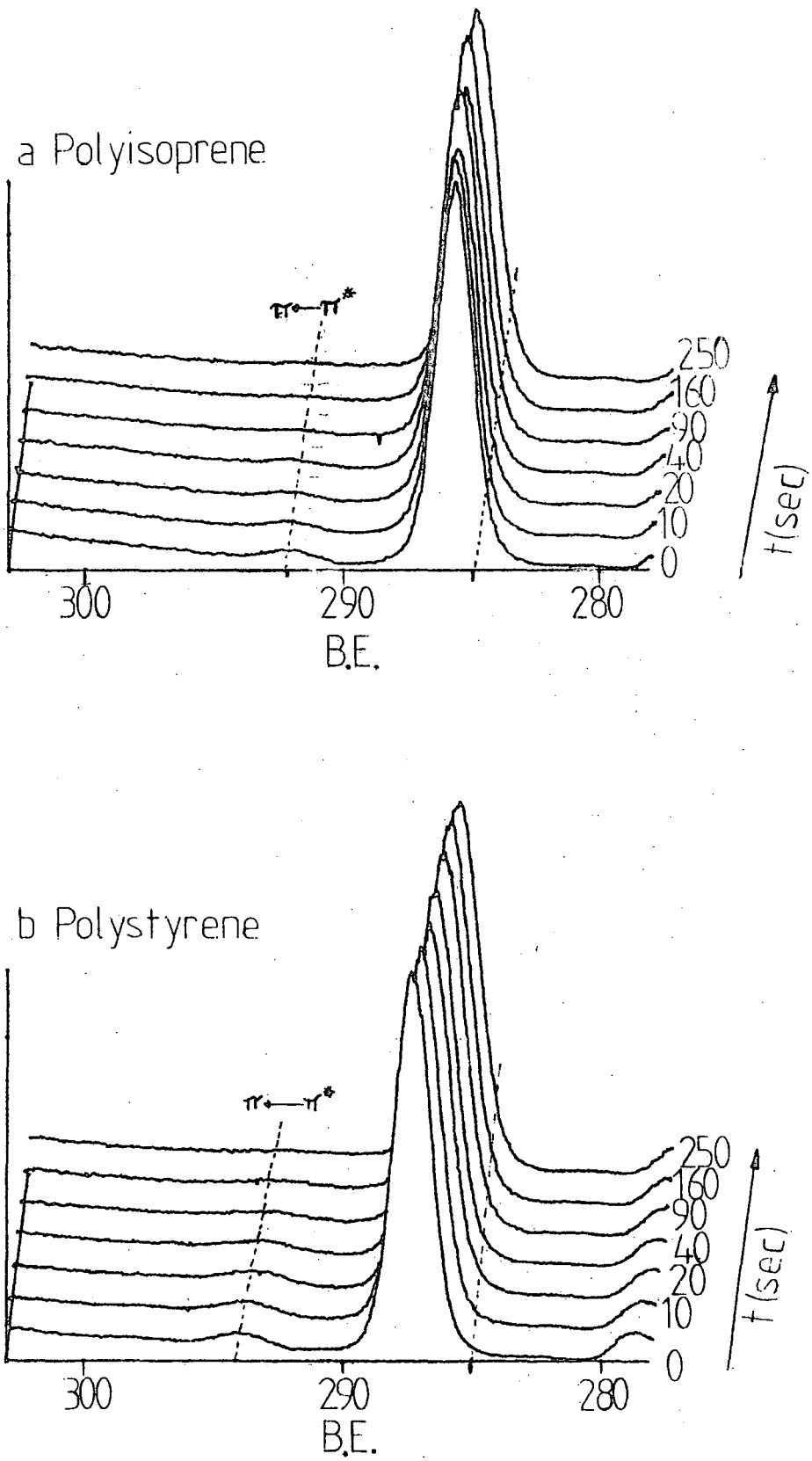

transitions are counted as part of and constitute ∿5.2 % of the total integrated intensity of the C_{1s} envelope.

Similarly the C_{1s} spectrum of polyisoprene consists of a single symmetric direct photoionisation peak at 285 eV and a shake-up satellite at ∿291.5 eV which constitutes ∿2.7% of the intensity of the C_{1s} envelope.

Films of polyisoprene and polystyrene were bombarded with 5 keV argon ions at an ion current density of 100 nA cm^{-2} ($\equiv 6.25 \times 10^{11}$ ions cm^{-2} sec^{-1}) for cumulative exposure times between 0 and 490 seconds. Only a small amount of oxygen was detected in the surface of the films (<<1%) and this was reduced upon treatment. The C_{1s} spectra of the two polymers as a function of treatment time are presented in Figure 5.9. In each case the reaction is accompanied by the rapid loss of intensity and eventual loss of the distinct shake-up satellites, with the concomitant emergence of asymmetry in the C_{1s} level (as evidenced by an apparent increase in the FWHM of the direct photoionisation peak and increase in the background level of the high binding energy side of the direct photoionisation peak relative to that on the low binding energy side.

In polystyrene the shake-up structure broadens slightly with increasing bombardment, the position relative to the present peak of the centroid of the residual shake-up remains constant throughout. In each case the direct photoionisation peak shows an apparent broadening, as also observed for polyethylene upon bombardment, due to the growing asymmetry of the peak rather than lifetime effects or a range of chemical shifts.

Increasing ion dosage also results in a gradual decrease in the apparent charging of the surface during XPS analysis reflecting the modification of the surface layer. Sample charging has already been shown in this work (Chapter Three) and the work of Clark and Dilks[130] to be a very surface sensitive phenomenon. A major factor in deciding the charging of a polymer under X-ray analysis being the sum of the total photoionisation cross-sections of the elements that constitute the polymer. Depletion of the polymer matrix in hydrogen upon bombardment is then expected to have little effect, the total photoionisation cross-section for hydrogen being very low. The change in "charging" reflecting a decrease in the binding energy of the C_{1s} level and changes in charging due to the changes in electronic structure in the surface layers brought about by bombardment.

The loss of shake-up intensity, indicative of the discrete phenyl and olefinic residues in the parent polymers polystyrene and polyisoprene are plotted in Figure 5.10. If the loss of shake-up intensity is a random process, depending upon a given residue interacting with an ion then the decay of shake-up intensity will follow an exponential, first-order rate law type decay. Plots of the natural logarithm of the shake-up intensity *versus* irradiation time (or ion dose) are given in Figure 5.11, for polystyrene and polyisoprene respectively. The increased stability of the phenyl residues of the polystyrene as compared with that of the olefinic residues of polyisoprene is shown by the slower decay of the signal due to shake-up in polystyrene, though the decay of both signals is rapid. (Rate constants $k_{obs\ polystyrene} \sim 1.4 \times 10^{-2}\ sec^{-1}$, $k_{obs\ polyisoprene} \sim 4.7 \times 10^{-2}\ sec^{-1}$ ($\equiv 2.24 \times 10^{-14}\ ion^{-1}\ cm^2$; $7.4 \times 10^{-14}\ ion^{-1}$

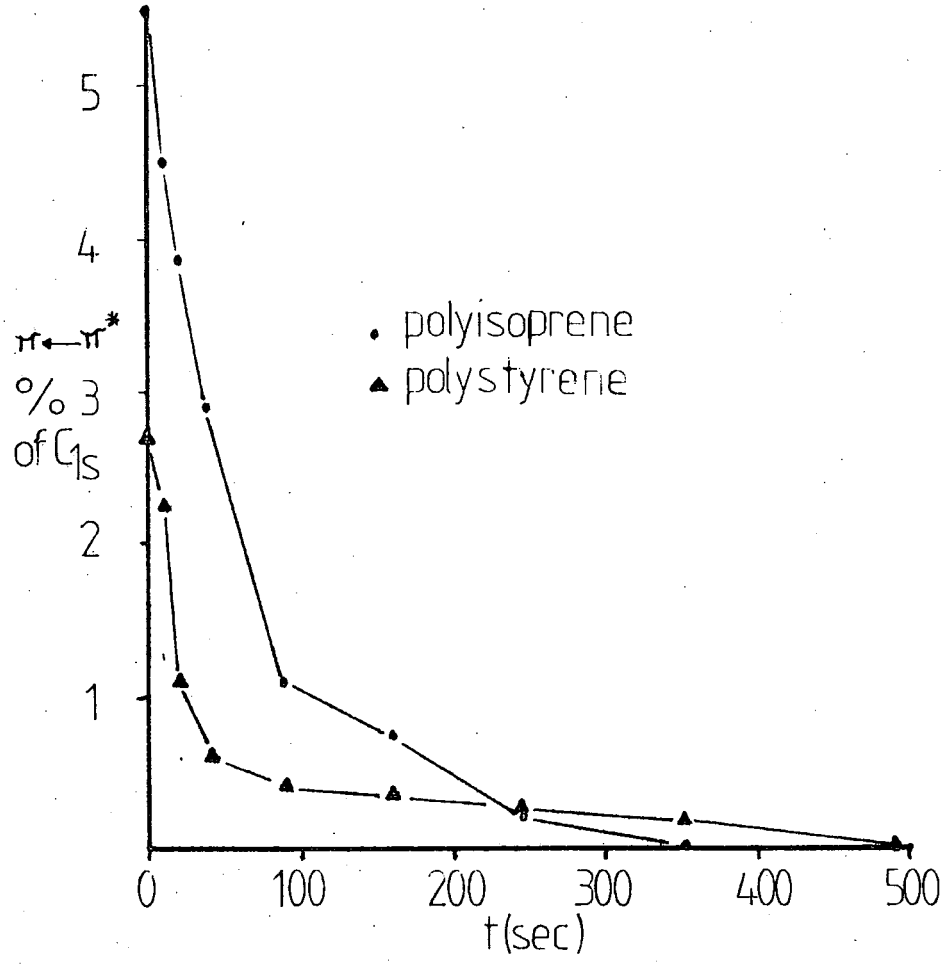

Figure 5.10 Loss of shake-up intensity on argon ion bombardment

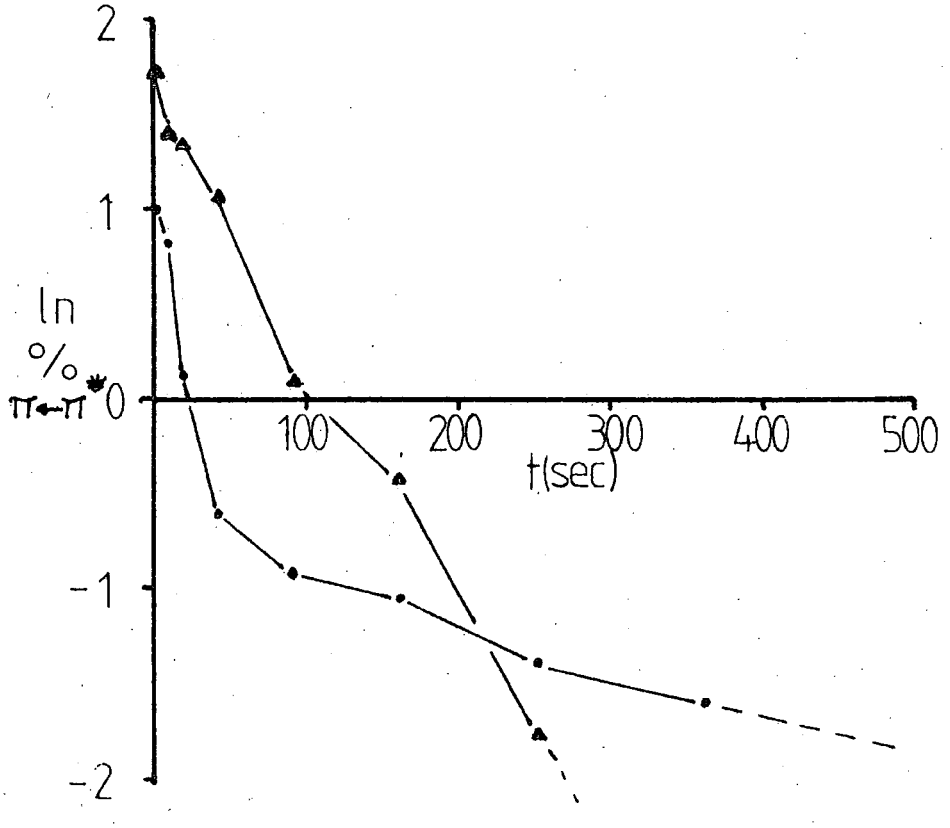

Figure 5.11 ln (shake-up intensity) *versus* treatment time for cis-polyisoprene and polystyrene

cm^2 cross-section for the reaction respectively)). The distinct curvature of the plot for polyisoprene reveals the presence of a rapid and a much slower rate process, though the course of the reaction at extended irradiation times is difficult to plot as the shake-up, not a strong feature to start with, sinks into the background noise. The above analysis depends upon the assumption that the shake-up intensity is indeed due solely to the phenyl and olefinic residues present in the original polymers. This is borne out by the apparent constancy in position and to a large extent the form of the shake-up transition peak during the reaction. Observed in the low dose, high energy radiolysis of polyethylene, olefinic residues are also postulated as intermediates in the argon ion degradation of polyethylene. However even on magnification no shake-up peak was observed in the C_{1s} spectra of bombarded polyethylene, though unsaturation was detected upon bromination. The implication is that once formed olefinic residues are rapidly destroyed, the conjugation extended to a feature producing a broad range of shake-up transitions contributing to a tailing of the direct photoionisation peak. The rapidity with which the shake-up intensity in polyisoprene is lost upon bombardment would bear this out.

Though in a qualitative sense the loss of shake-up intensity of each polymer may be correlated with the increase in the absolute integrated intensity of the C_{1s} envelope there appears however to be no simple relationship between the two. The variations in the absolute integrated intensity of the C_{1s} level after irradiation for a time t ratioed to its value initially *versus* the loss in intensity of the shake-up satellite

are presented for the two polymers in Figure 5.12, both polymers behave in a similar fashion. The rapidity of the loss of shake-up intensity in the case of polyisoprene is not matched by the more gradual rate of increase in the absolute integrated intensity of the C_{1s} signal; this quantity reflecting the number density of carbon atoms in the surface of the polymer. Crude calculations of the effect of producing regions of conjugation in polyisoprene or polyethylene chains based on carbon-carbon bond lengths of 1.54Å, 1.35Å and 1.40Å for C-C, C=C and C⋯C bonds respectively and bond angles appropriate to saturated and unsaturated systems, upon the number density of carbon atoms were made. Neglecting any change in interchain spacing, the effect of the degree of unsaturation within a chain upon the number density was found to be minimal. Thus the increase in the integrated intensity of the C_{1s} level may be identified with a decrease in the interchain spacing in the polymer as might be produced by cross-linking. Additionally the rapid disappearance of shake-up in the case of the bombardment of polyisoprene without the concomitant rapid increase in the absolute intensity of the C_{1s} envelope could be due to the formation of polyene chain segments. Such functionality would also be expected to lead to a broad range of shake-up transitions, giving the peak its distinctive tailing to higher binding energies. The increase in intensity is due to a slower cross-linking process.

For polystyrene this disparity is not so marked, the fate of the phenyl substitutuents on bombardment is not clear. The valence band spectra of treated samples are broad and essentially featureless, similar to those obtained upon prolonged bombardment of polyethylene as shown in Figure 5.2.

Figure 5.12 Correlation of the loss in shake-up intensity with the increase in absolute intensity of the C_{1s} level for -

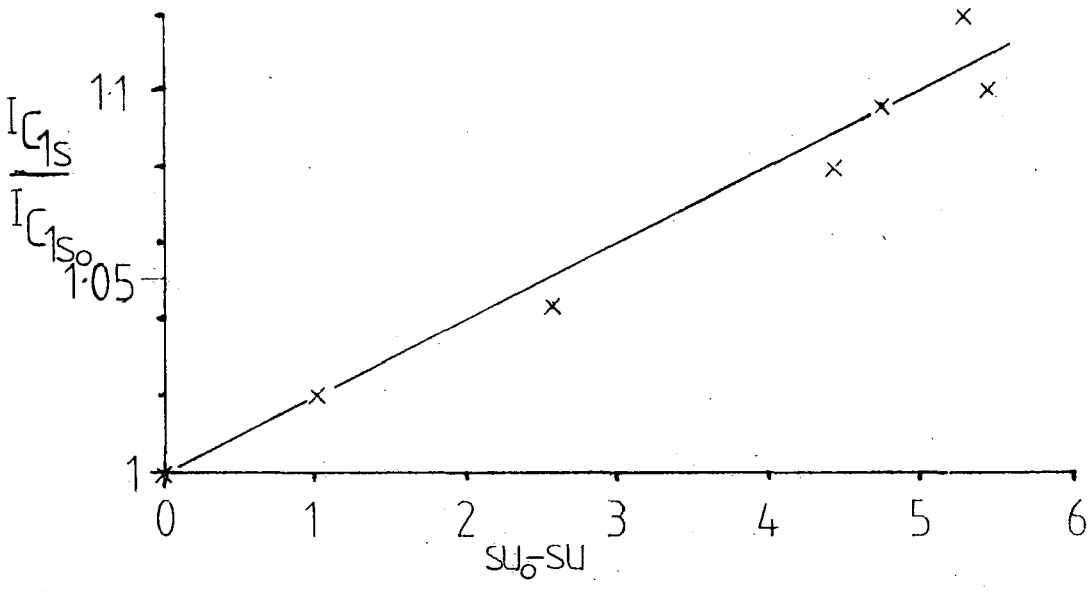

(a) polystyrene

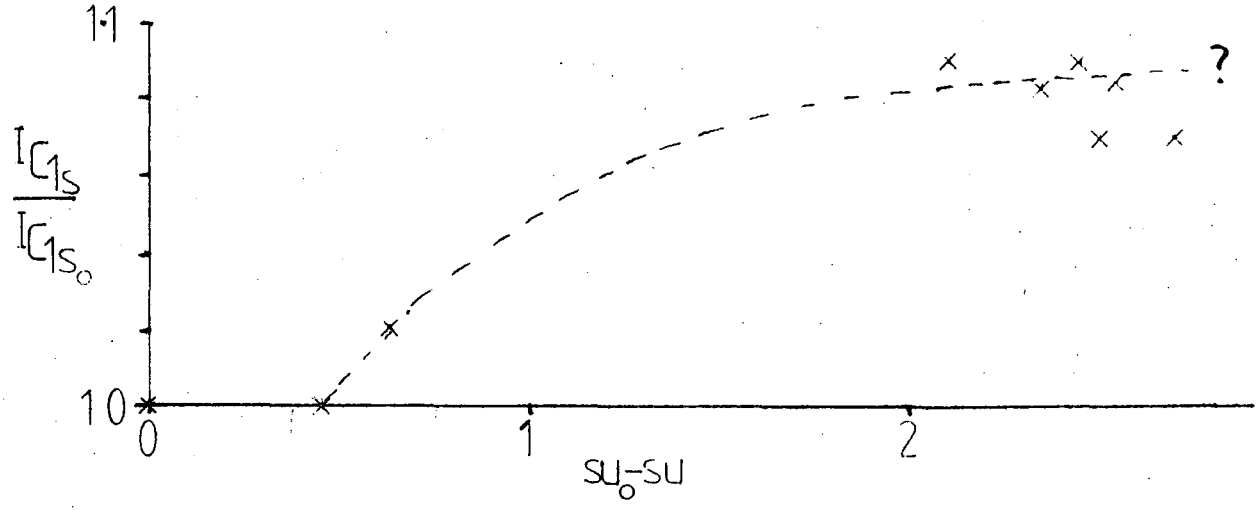

(b) polyisoprene

Previous ESCA studies of the argon ion modification of polystyrene by Ullewig and Evans,[164] Holm and Storp,[162,163] and Briggs[160] concluded that the loss of the distinct shake-up satellite from the pendant phenyl group was indicative of the destruction of the benzene ring. The possibilities that the broadening and increasing asymmetry of the C_{1s} level might represent increasing conjugation, or the formation of graphite like regions, were not considered.

5.3.4 Polymethylmethacrylate and Polybutylmethacrylates

Previous ESCA and SIMS investigations have paid sporadic attention to polyalkylmethacrylates. Gardella and Hercules[170] employed static SIMS to fingerprint a series of polyalkylmethacrylates and investigate the atmospheric hydrolysis of these materials. They found only negligible changes had occurred in the ESCA spectra of the SIMS analysed polymeric surfaces: the analysis conditions employed corresponding to a dose of $\sim 10^{13}$ ions cm^{-2} being accumulated by the surfaces during analysis. Briggs however has shown that after such an ion dose, significant changes occur in the absolute and relative intensities of peaks in the SIMS spectra of polyalkylmethacrylates. The nature of the damage causing this fall off in signal intensity is not known. ESCA studies of the argon ion sputtering of polymers by Williams and Davis[174] centred upon the surface chemistry of the final surface rather than the course of reaction. The final sputtered surface was found to be essentially carbonaceous in nature, the oxygen having been preferentially sputtered from the sample surface. The authors attempted to relate the composition to the depth in the sample *via* sputter rates determined for inorganic

materials such as Si, SiO_2 and Ta_2O_5. Uliewig and Evans[164] found the sputter rate of polymethylmethacrylate, bombarded at the relatively high ion current density of 2-8μA cm^{-2}, to fall off exponentially with time. Ion bombardment induced changes in the surface regions making the surface increasingly more difficult to sputter away until a steady state was reached, the O/C ratio determined by XPS having dropped from 0.43 to 0.03 during the treatment. The SIMS spectrum of PMMA displays a number of features containing fragments derived from the polymer backbone and characteristic peaks due to cleavage of the ester alkyl residue, CH_3^+ and the ester side chain itself $^+O{=}C{-}OCH_3$.

The aim of this present ESCA study has been to follow the changes in the sample surface brought about by argon ion bombardment. Solvent cast films of polymethylmethacrylate and a series of polybutylmethacrylates were exposed to 5 keV argon ions at ion fluxes of 100 nA cm^{-2} for cumulative periods up to 800 seconds.

In each case the bombardment leads to the rapid loss of oxygen from the surface regions of the polymers. The loss is uniform throughout the sampling depth of C_{1s} electrons excited by $Mg_{K\alpha_{1,2}}$ radiation (*i.e.* ∿36Å). The stoichiometries of the surface layer determined from O_{1s}/C_{1s} ratios and by component analysis of the C_{1s} envelope being identical within the limits of experimental error. At prolonged irradiation times, hydrocarbon contamination from repetitive ESCA analysis results in a slight discrepancy between the two stoichiometries. The O_{1s} spectrum, in each case originally a symmetric doublet with components at 532.6 eV due to C=O and 534.3 eV due to C-O, decreases in intensity upon bombardment but retains its

symmetric doublet lineshape, the ester side-chain being lost upon bombardment as a single unit.

The C_{1s} and O_{1s} levels obtained at a take-off angle of 30^{o} for a bombarded sample of PMMA are shown in Figure 5.13. Figure 5.14 displays a plot of the natural logarithm of the fraction of the polymer surface unreacted after a time t *versus* time (in seconds). There is little difference in the rates of reaction of these isomeric poly-butylmethacrylates. Only after extended bombardment is any divergence noted. This emphasises the non specific nature of the reaction. Polymethylmethacrylate however seems to degrade at a slower rate than the poly - butylmethacrylates.

Concomitant with the loss of oxygen containing functionality from the polymer surface there is an increase in the absolute integrated intensity of the C_{1s} level, indicating an increasing number density of carbon atoms in the polymer surface. However attempts to obtain a simple linear correlation between the extent to which the polymer chain had been defunctionalised and the increase in the absolute integrated intensity of the C_{1s} level were not successful. More successful was the following, slightly more complex approach based upon the following assumptions. The ESCA analysis indicates that the ester group is lost as a single unit on irradiation. No evidence regarding chain scission on irradiation is directly obtainable from ESCA. If the carbon atoms present in the alkyl residue of the ester also lost from the system on bombardment (*e.g.* as CH_4 or a butane) then the number density of carbon atoms in the surface will fall. (Though this was not detected in these experiments the

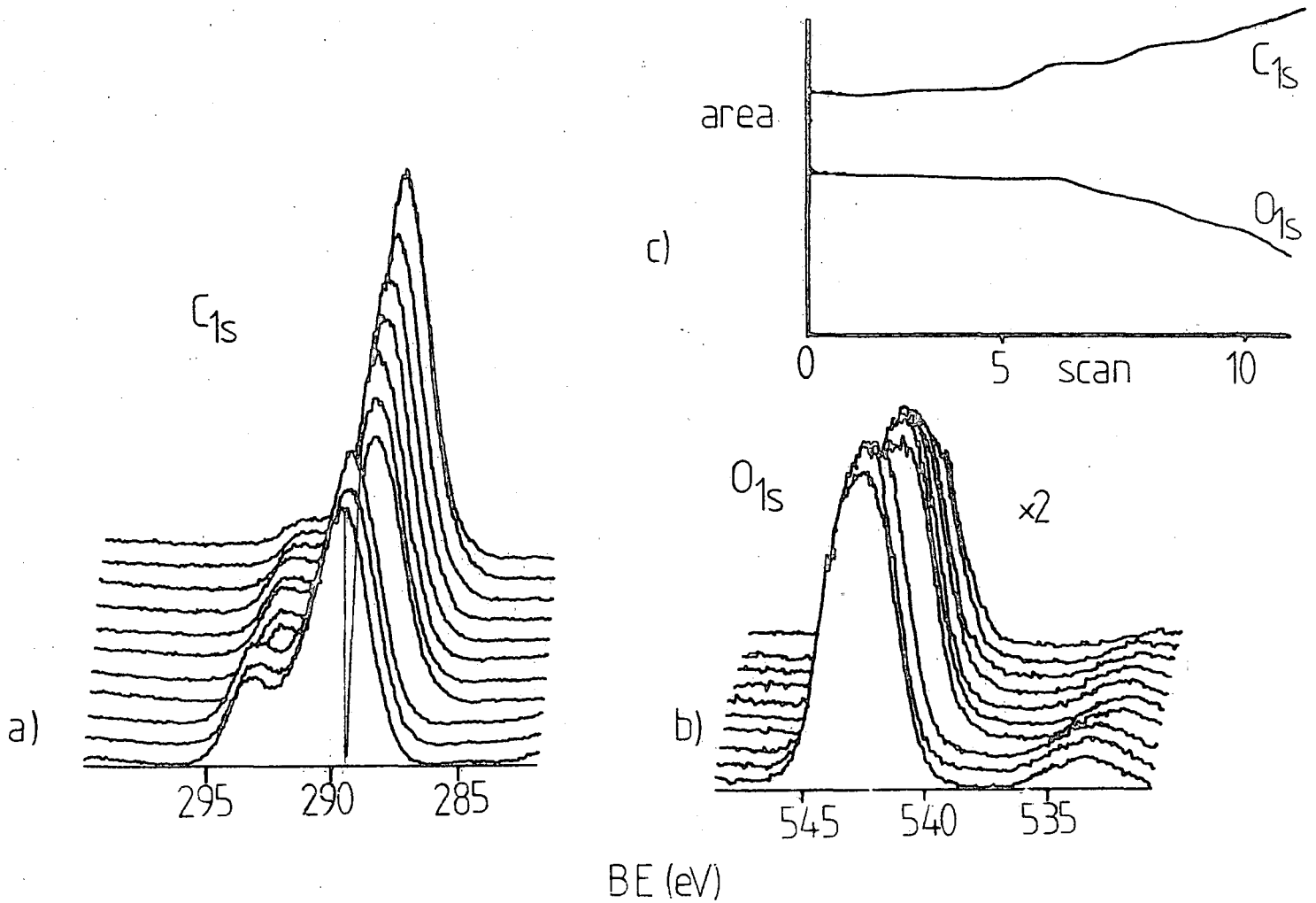

Figure 5.13 Argon ion beam degradation of polymethylmethacrylate (a) C_{1s} and (b) O_{1s} core levels and (c) variation in peak intensities with increasing ion dose

Figure 5.14 Plot of ln Y *versus* irradiation time (5 keV Ar^+, 100 nA cm^{-2}) for polymethylmethacrylate and polybutylmethacrylates.

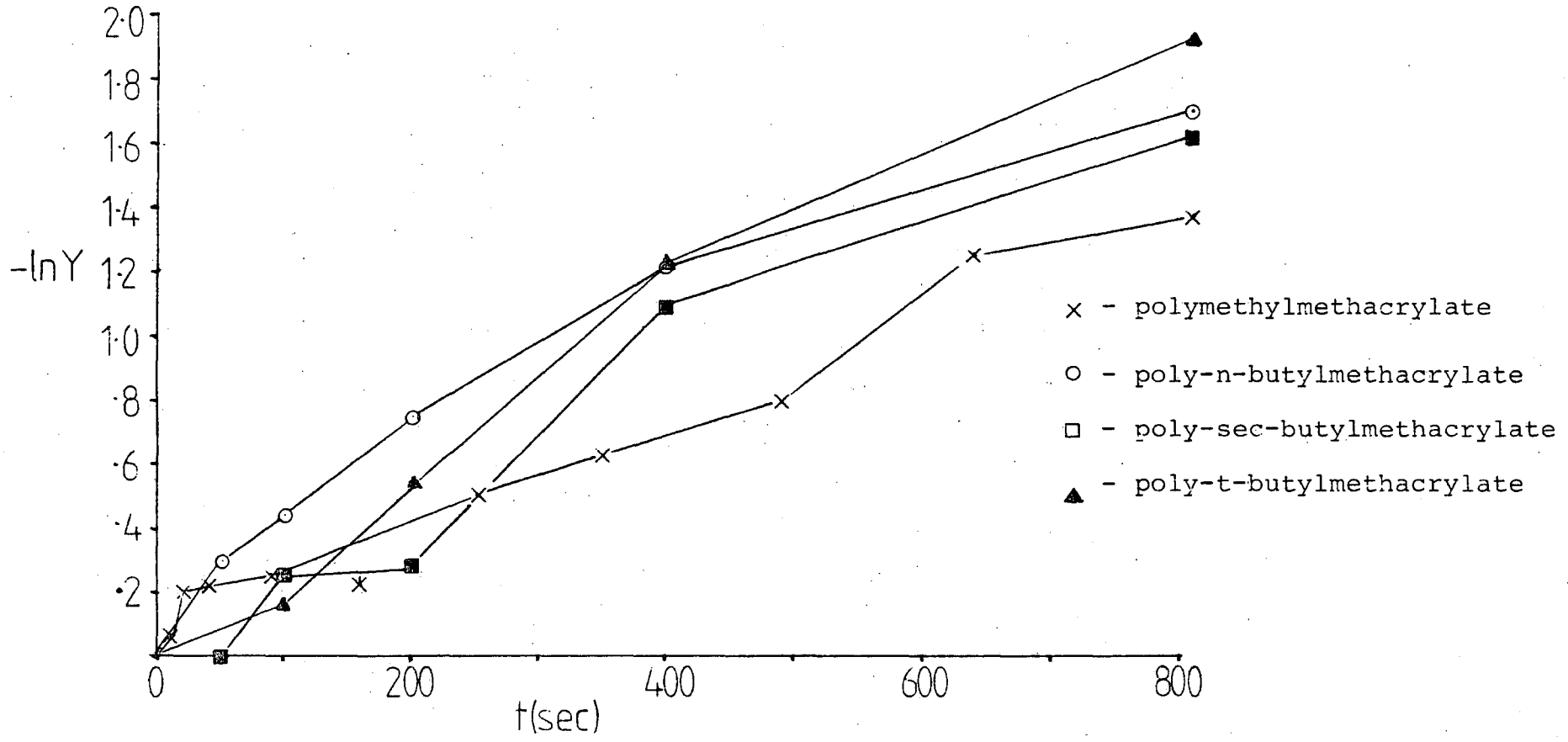

evolution of gas by PMMA on high energy irradiation has been studied by a number of workers,[250,267] notable features of this work being the detection of H_2, CH_4, CO, CO_2 and C_3H_3, however agreement between the various authors as to the relative amounts of each produced was poor, perhaps reflecting the variety of dose rates used, and differing types of radiation and experimental conditions employed, no material balance was established in these experiments. Most of the gaseous fragments may be attributed to the fracture of the ester side groups from the polymer). Thus the increase in the absolute integrated intensity of the C_{1s} level in the ESCA spectra does not directly reflect the effects of crosslinking alone, indeed the effect is greater than that observed as the loss of carbon atoms from the side-chains would serve to reduce the total integrated intensity of the peak were there not to be any reduction in interchain spacing or contraction within the chains themselves.

Consider the following reaction:

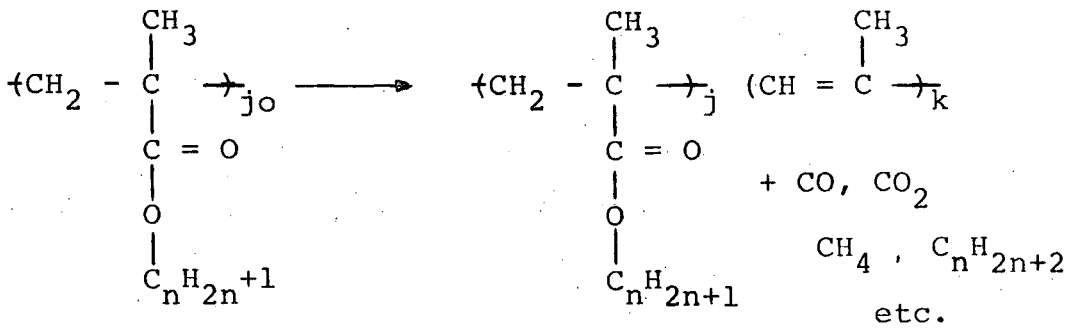

The reaction scheme is speculative, representing the situation if crosslinking were ignored. The main point being to illustrate the effect upon the number density of carbon atoms after the chain has been degraded but excluding the effects of crosslinking.

Let the degree of reaction be y

$$y = \frac{k}{j+k} \qquad (5.1)$$

$$jo = j+k \qquad (5.2)$$

Let jo = 1. j = 1-k.

On reaction the fractional reduction in the number of carbon atoms in the chain is R, where R is given by

$$R = \frac{(4+n)j + 3k}{4 + n} = \frac{4+n - (1 + n)k}{4 + n} \qquad (5.3)$$

Thus to compensate for this the fractional increase in the measured integrated intensity of the C_{1s} level, I/I_o must be divided by this factor R. This corrected factor may then be plotted against the extent of reaction y to yield a reasonably linear correlation between the two (Figure 5.15). The gradient of such a plot reflecting the probability that the elimination of a side chain results in the formation of a cross-link and the volume change on elimination of a side-chain and formation of a cross-link. The correlation however is perhaps fortuitous, the proportionality to the degree of reaction, *i.e.* the number of side chains removed by bombardment being due to two factors cancelling out, the proximity of two activated sites being required for a cross-link to be formed introducing a squared term, the effect of crosslinking being to reduce interchain spacing, *i.e.* contraction in 2 dimensions in an ordered crystalline phase, a cancelling half power. Figure 5.15 also shows that the poly butyl methacrylates, poly-n-butyl, sec-butyl and t-butyl methacrylates all display very similar plots. The difference in the bulk of the various side chains having apparently little effect upon the volume

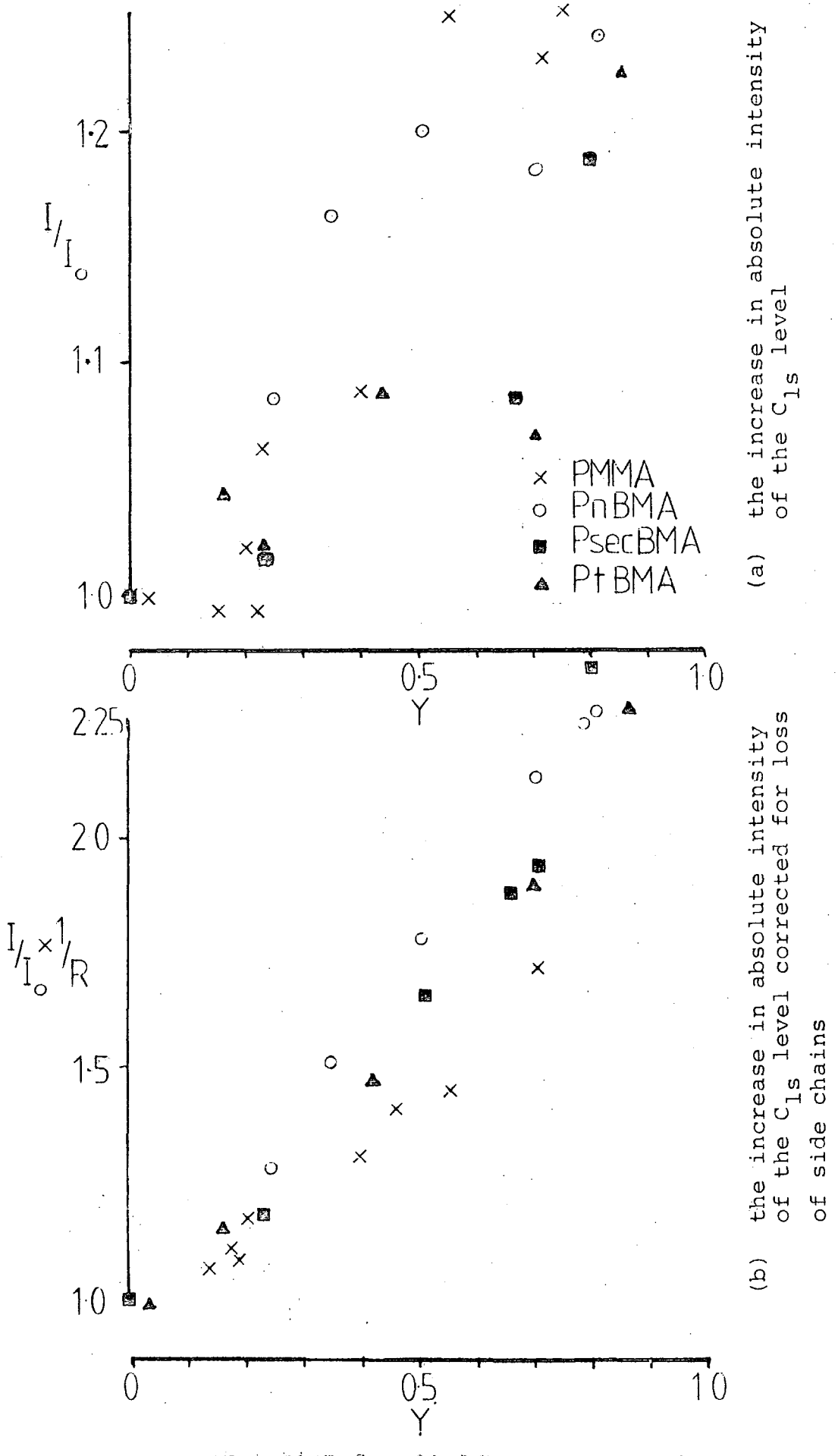

Figure 5:15 Correlation of the extent of reaction with (a)/(b)

change on crosslinking. The corresponding plot for PMMA shows a slightly smaller gradient, either reflecting the smaller volume change on the elimination of a side chain and the formation of a cross-link or a reduced tendency to cross-link upon elimination of a side-chain.

After prolonged bombardment the C_{1s} envelope comes to represent mainly carbonaceous material, the peak having developed a distinct asymmetry as noted for the polymers previously considered (Figure 5.16).

5.3.5 General Features of the Argon Ion Bombardment of Polymers

From consideration of the aforegoing, several common features of the effects of argon ion bombardment of polymers became apparent. Bombardment leads to extensive rearrangement of the surface regions of the polymers. Uniformly there is an increase in the absolute integrated intensity of the C_{1s} level, reflecting an increase in the number density of carbon atoms in the surface regions of the material. The layers formed by the bombardment of polymer films were found by Kaplan *et al*[252] to be graphitic in nature. Indeed the valence regions of the XPS spectra of treated samples have been found to closely resemble that of graphite. However if the surface layer formed is graphitic in nature it must be highly disordered. Although the absolute integrated intensity of the C_{1s} level of the polymers increases upon bombardment, its value never approaches that for a sample of cleaved graphite or a graphite surface disordered by argon ion bombardment. This disorder is also borne out by the inability of bombarded polyethylene surfaces to incorporate as much argon as a

Figure 5.16 Developing asymmetry to C_{1s} level of PMMA on argon ion bombardment -
(a) untreated,
(b) after an ion dose of 5×10^{14} Ar^{+} cm^{-2}

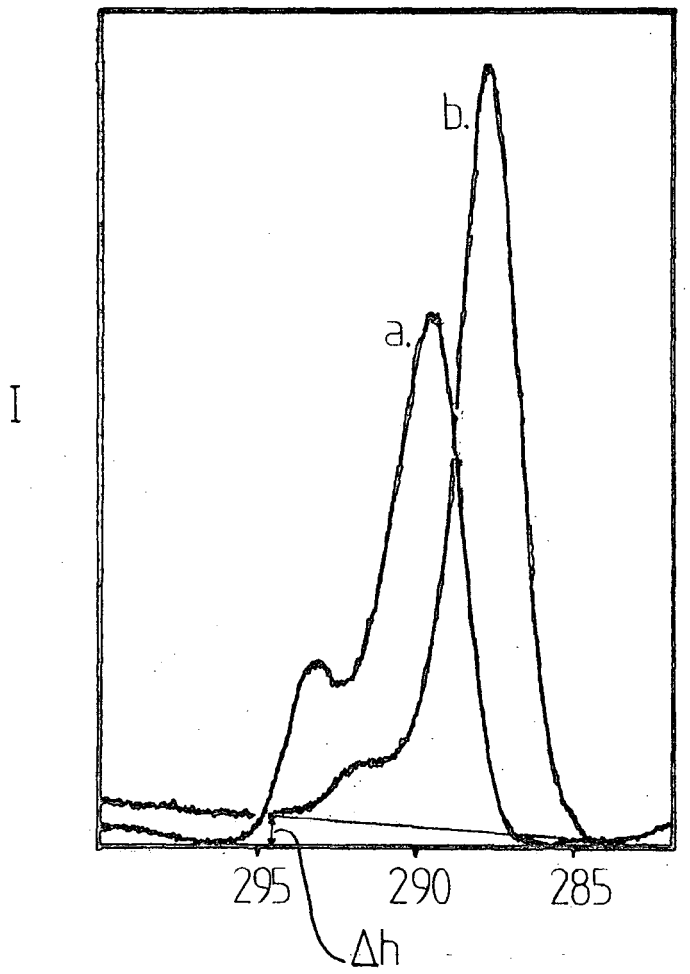

similarly bombarded graphite surface. Dynamic SIMS experiments on polyethylene and polystyrene films using comparable ion fluxes to those employed in the *in situ* ESCA studies, *i.e. ca.* 100 nA cm^{-2}, in addition to changes in the relative intensities of the various components of the spectra, the overall intensity of the spectra also gradually decreases. This latter effect could not be attributed to instabilities in the instrumentation or inadequacies in charge neutralisation as the electrical properties of the surfaces changed with bombardment. On argon ion bombardment, it is thus seen to become progressively more difficult to sputter fragments from the polymer surface as the reaction proceeds. As the material cross-links two effects two effects will serve to reduce the sputter yield. As the surface region becomes more cross-linked, energy transferred to the polymer by collision with an incident ion may be more rapidly dissipated by the lattice rather than leading to the elimination of a fragment. Secondly as the crosslinking reaction proceeds, *i.e.* there are links formed between the chains, the average connectivity of carbon atoms in the surface. The polymer is no longer a single-chain polymer, to remove a fragment from the polymer surface, to cause scission of a fragment, more carbon-carbon bonds must be broken. This argument is analogous to that advanced for the enhancement of the thermal stability of polymers by the use of ladder or double-strand structures as proposed by Tessler and Brown.[268] The idea is illustrated graphically below.

(i) Single Chain $\xrightarrow{Ar^+}$ 2 Bonds Broken to Remove Fragment.

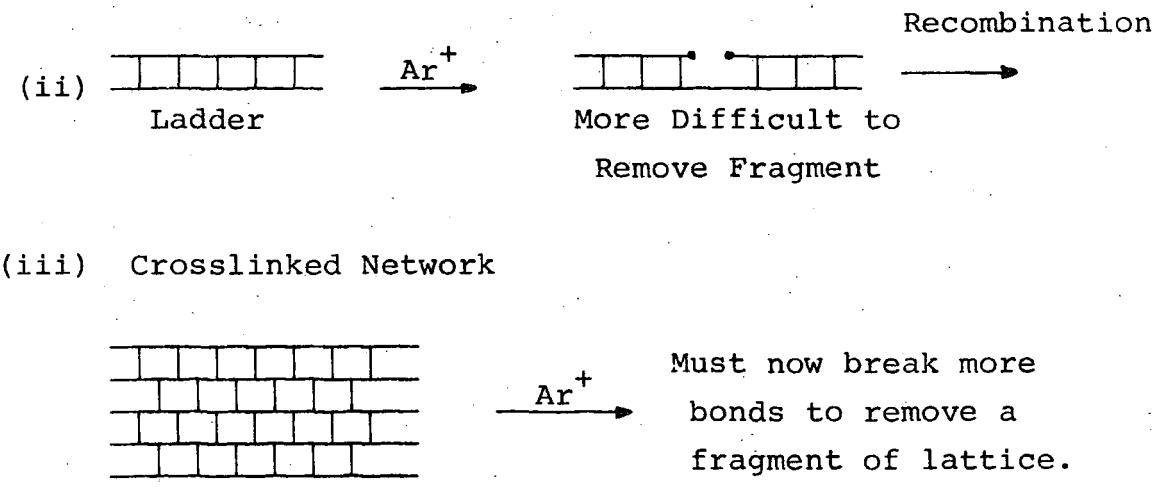

5.4 Conclusions

The argon ion bombardment of polymer surfaces also results in the introduction of unsaturation into the surface (as evidenced by the uptake of bromine by a treated polyethylene sample). On bombardment, subtle changes are also observed in the C_{1s} core-level spectra of the polymers. Whereas the C_{1s} level of untreated polyethylene may be represented as a single symmetric Gaussian peak, on treatment the peak broadens and develops a distinct asymmetric tailing to the higher binding energy side. The observation of such lineshapes in XPS is normally restricted to metals.

The origins of these asymmetric lineshapes can be viewed from essentially two standpoints. The observation of asymmetric lineshapes for metals was made in the earliest stages of development of the ESCA technique, empirically the asymmetry was found to be related to the density of occupied electronic states at the Fermi level of the metal. (This is closely related to the form of the valence band in the XPS spectrum in the region of zero binding energy, the intensity in the XPS

spectrum being approximately proportional to the density of states).[8] The form of the density of states curve in the region of the Fermi level thus provides a continuous range of allowed one-electron excitation energies which may accompany the direct photoionisation event.[33] Thus an asymmetric tailing of the main peak is produced.

Approaching the problem from another direction, shake-up satellites to the C_{1s} level are a familiar feature of the XPS spectra of unsaturated organic compounds. As the conjugation length in a compound increases, the number of allowed shake-up transitions also increases, the shake-up intensity is smeared out over a broad range of such transitions. This is illustrated by Figure 5.17 which shows the C_{1s} core-level for a series of polycyclic aromatic compounds, as the size of the system rises then the shake-up transitions become broader and less distinct, concomitant with this the asymmetry of the direct photoionisation peak is seen to increase. The detailed lineshapes associated with such processes in XPS core-level emission have been discussed by Doniach and Sunjic[269] and are predicted to have the form

$$I(E) = \frac{\cos(\pi\alpha/2 + (1-\alpha)\tan^{-1}(E/\gamma))}{(E^2+\gamma^2)^{(1-\alpha)/2}}$$

where E is the kinetic energy measured from the threshold of the unbroadened one-electron-transition peak

γ = lifetime of the core-hole

α = an asymmetry parameter.

Though the extraction of any useful information concerning the lineshape from experimental data is hampered by the severe broadening effects of the instrumental resolution function.

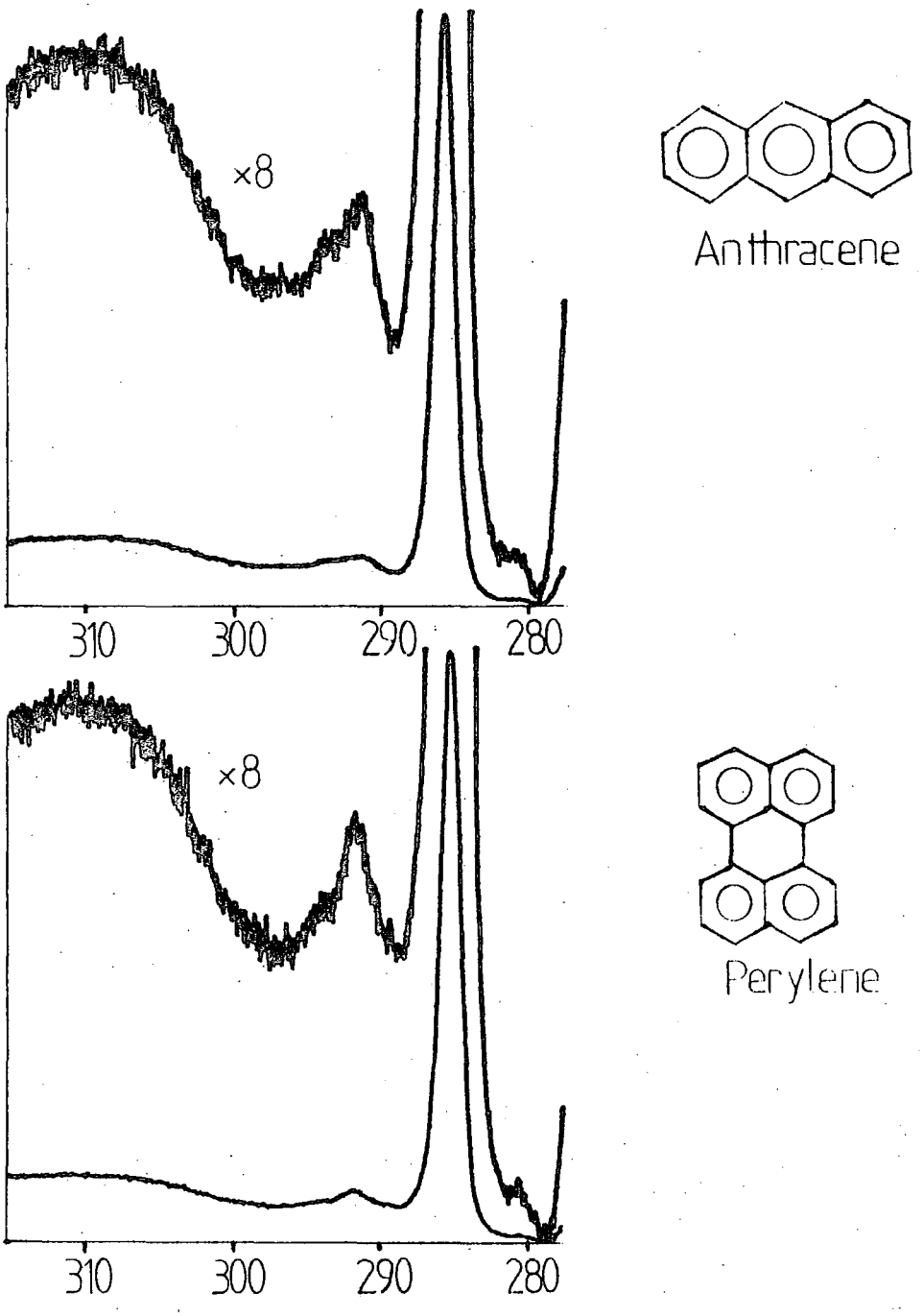

Figure 5.17 C_{1s} core level spectra of a series of polycyclic aromatic compounds and their associated shake-up structures.

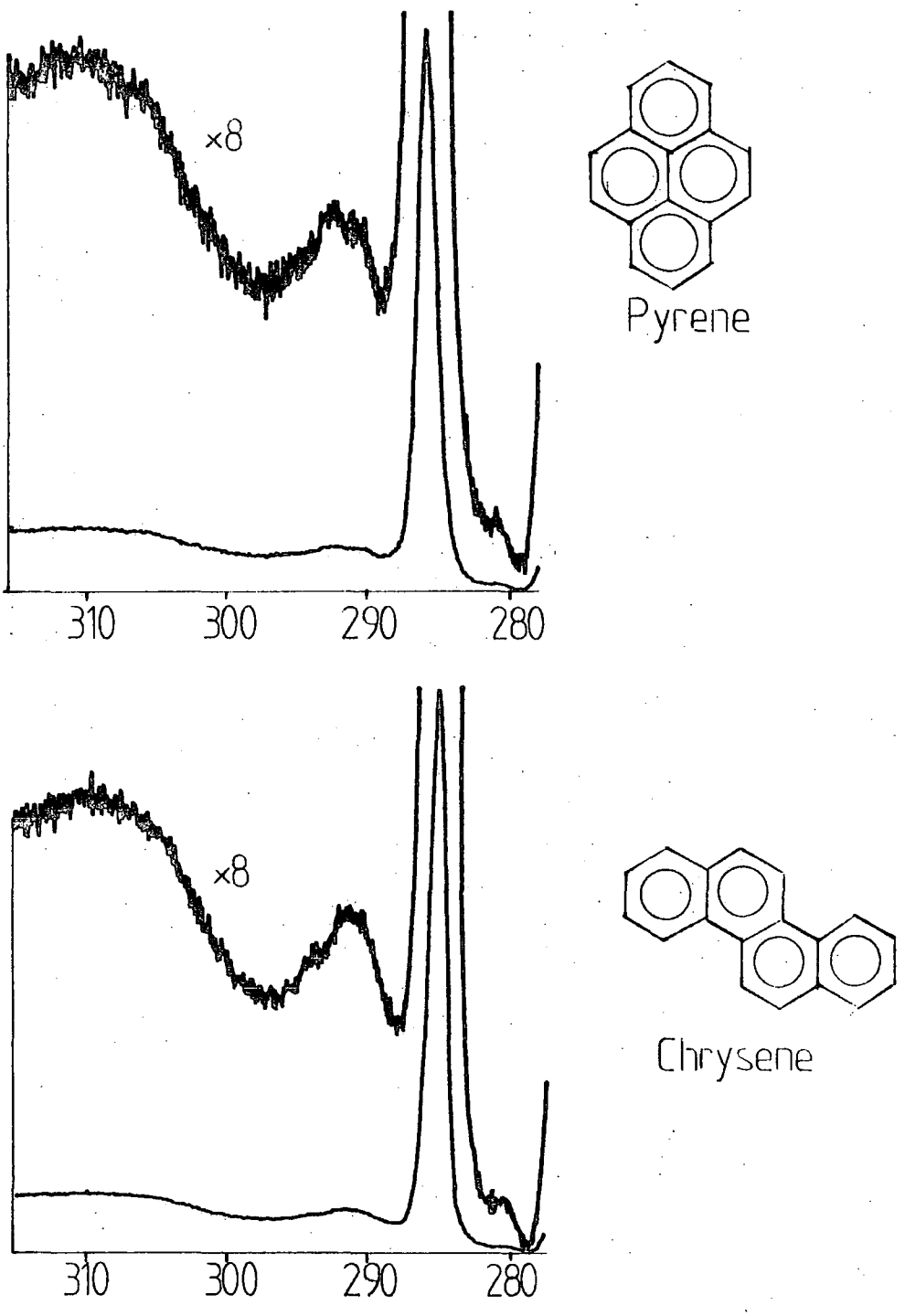

Figure 5.17 (contd.)

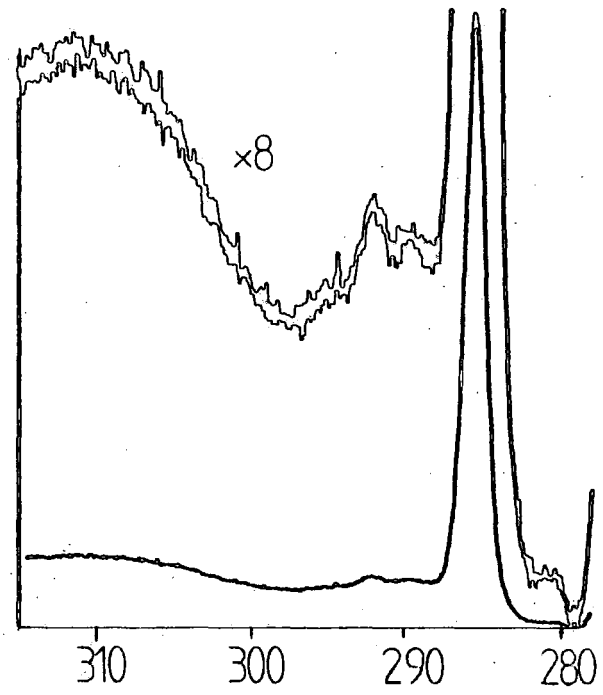

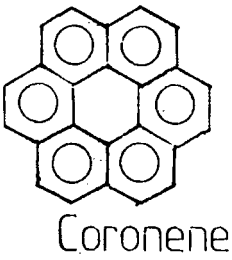
Coronene

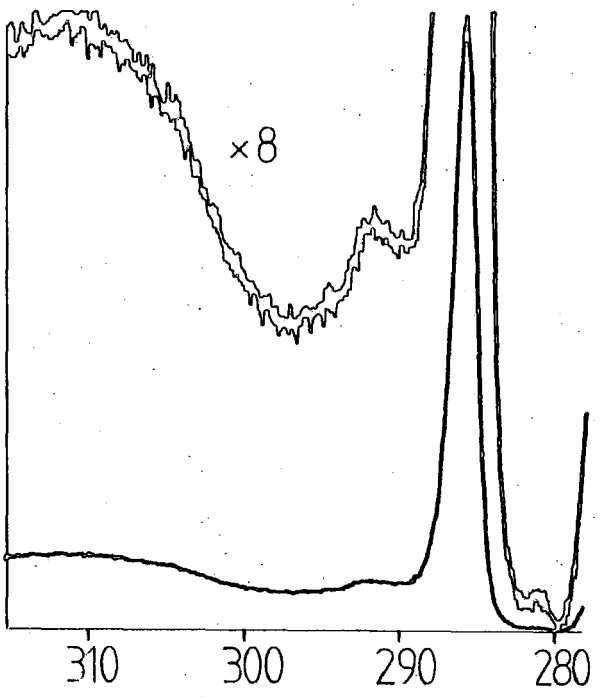

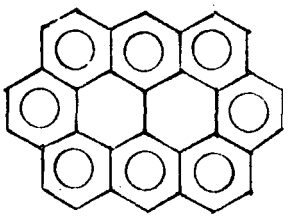
Ovalene

Figure 5.17 (contd.)

Various workers however have used deconvolution procedures to remove this component and derive values for γ and α for the case of metals.

More usefully, the asymmetry of the peak may be deduced from the step in the 'background' level in going from the low to high binding energy side of the peak. Semiquantitatively this step height ratioed to the peak height may be plotted against the carbon to hydrogen ratio for a series of polycyclic aromatic compounds, there is a large degree of correlation between the two, this is illustrated in Figure 5.18. More generally this feature may be used to infer the presence of unsaturation and conjugation in a system. From consideration of the examples given however another feature emerges, even in polycyclic aromatic systems the size of ovalene distinct shake-up satellites are still observable. The argon ion bombardment of polymers however appears to lead to a featureless tailing of the C_{1s} level into the inelastic loss peak as observed for the argon ion bombarded graphite and polyacetylene surfaces. Thus perhaps it is to these that the ion bombarded sample's surfaces owe a resemblance.

In the course of a series of ESCA studies of the modification of polyacrylonitrile and poly(chloroacrylonitrile) by high temperatures, electron impact and UV radiation, Hiraoka and Lee[270] observed asymmetries in core level signals similar to those observed in this study. On the basis of the known thermal degradation pathway of polyacrylonitrile and the ESCA data and IR data, Hiraoka and Lee concluded that a doubly conjugated ladder-type structure was formed which could ultimately cross-link further to yield a graphitic structure.

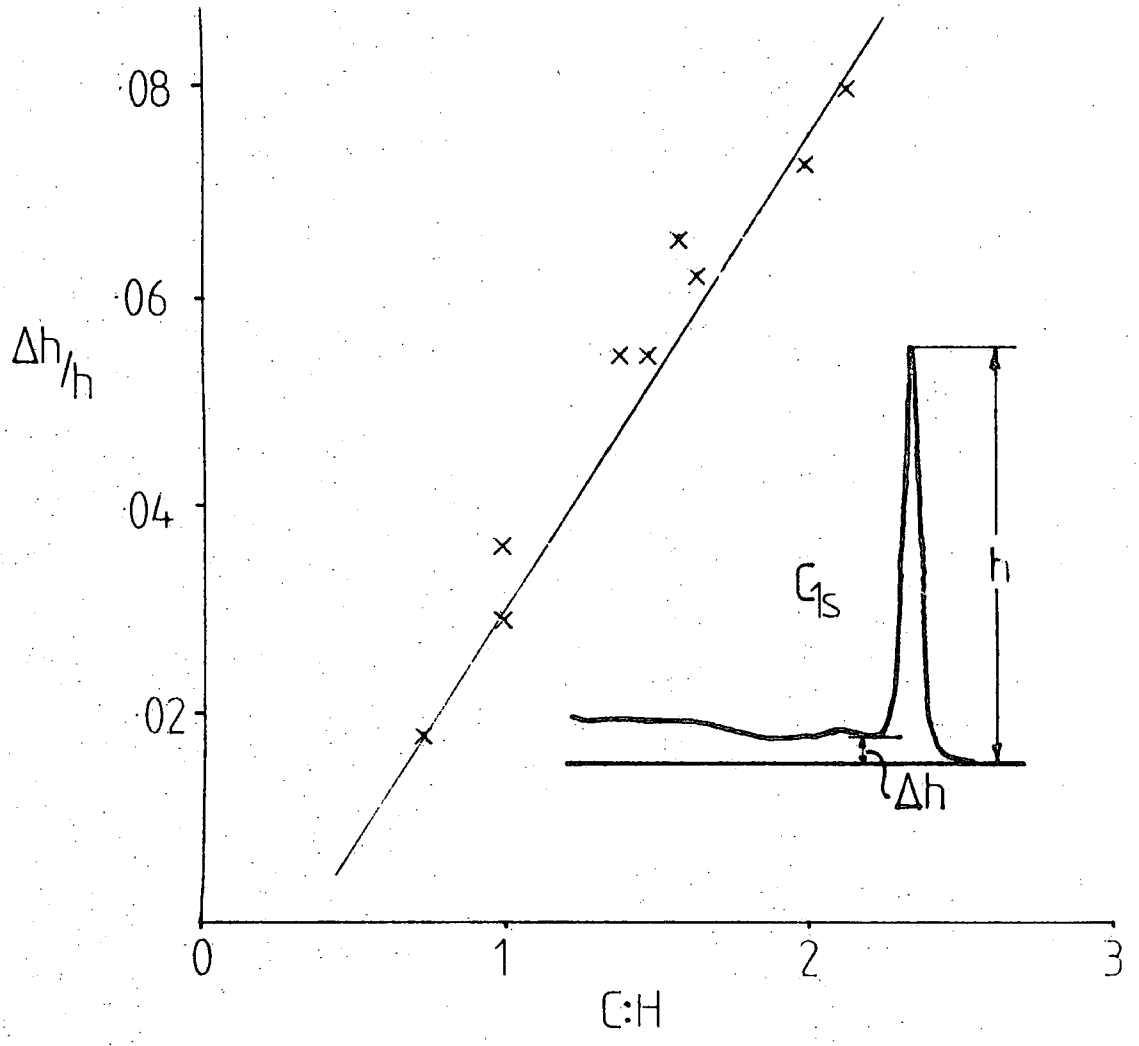

Figure 5.18 Correlation of $^{\Delta h}/_{h}$ with carbon:hydrogen ratio for a series of polycyclic aromatic compounds and unsaturated polymeric system

That this featureless tailing may also be observed for X-ray degraded samples of polyvinylchloride was remarked upon in Chapter Four, in this case the degradative pathway is widely balanced to involve the dehydrochlorination to yield polyene chain segments.

Comparison with the published spectra of solid acenes (which may be taken as a model for the double conjugated ladder type structure proposed by Hiraoka and Lee). On going from benzene to tetracene, Pireaux *et al*[271] found the valence region of the XPS spectra to become progressively broader and the distances of shake-up satellites from the C_{1s} peak to decrease. Pireaux *et al*[271] also commented briefly on the step in the background level about the C_{1s} direct photoionisation peak which is found to increase as the size of the molecule increases. The shake-up also becomes less distinct with increasing molecular size. Pireaux *et al* plotted the first ionisation energy and the enrgies (relative to that of the C_{1s} peak) of the two strongest C_{1s} shake-up satellites position with the sixe of the acene molecule. Extrapolating from their data it would appear that to lead to the apparently featureless asymmetric tailing observed for the argon ion damaged polymers the structures involved would have to exceed at least 6 annelated rings in size if the structures are based up a polyacene type structure as illustrated below.

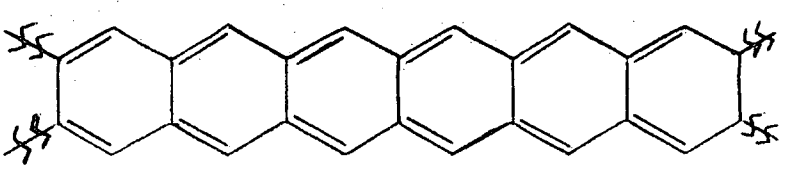

Polyacene

Thus the degradation of polyethylene under argon ion bombardment may be summarised as below (Figure 5.19); the scheme is meant to be representative and not exhaustive.

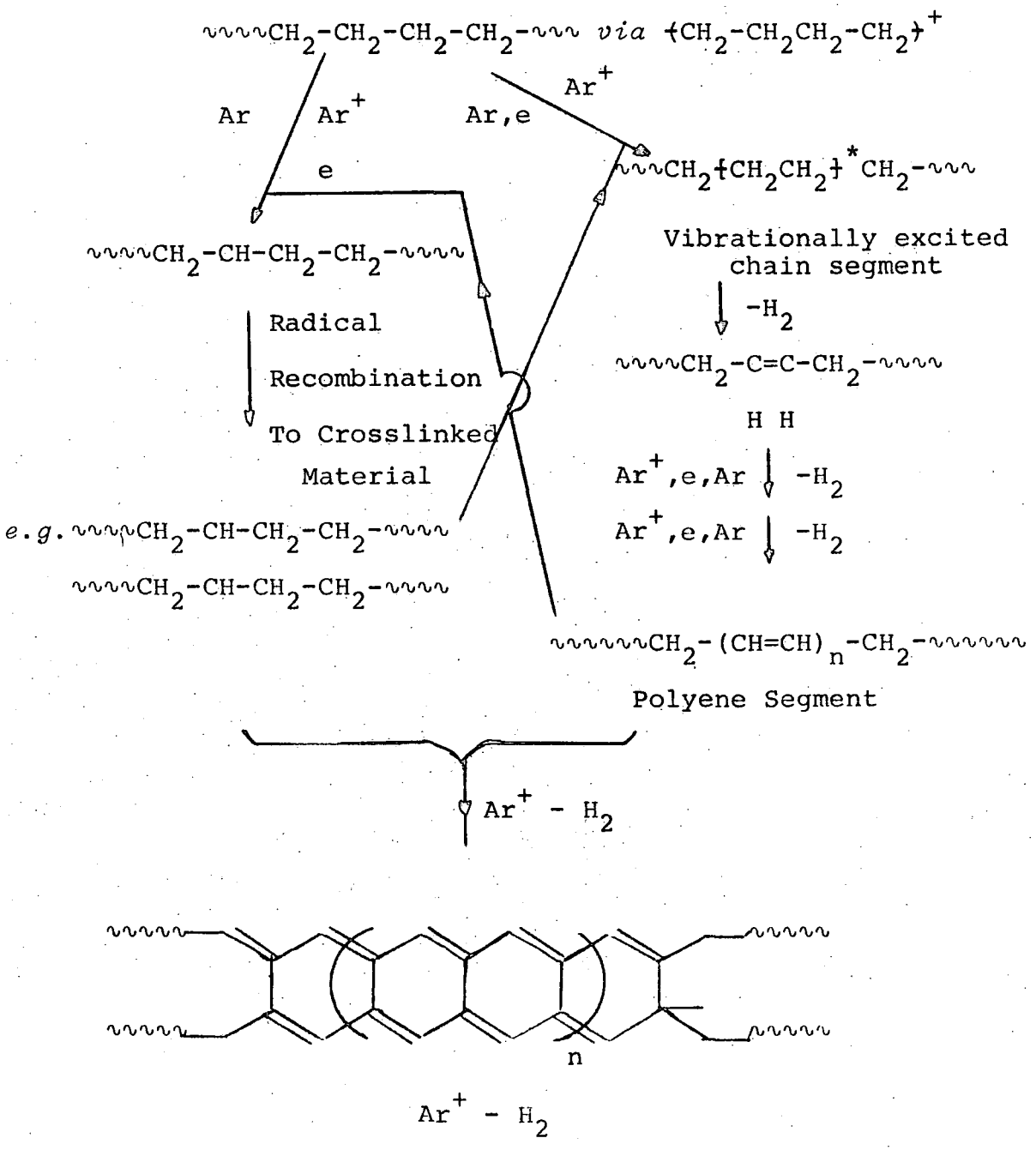

Graphitic Type Material

Figure 5.19

The reaction involves the formation of unsaturation (which is sufficiently highly conjugated so as not to give rise to a distinct shake-up peak, or involves many types of such site,

the net result of which is upon their superposition, a featureless tailing of the C_{1s} level) and the simultaneous cross-linking of the material leading to the increasing absolute intensity of the C_{1s} level.

The argon ion degradation of the other polymers examined in this study may be regarded as a subset or extension of this set of reactions. The ESCA results point to the formation of a common final structure. The common features were set out previously. The high apparent cross-sections of the polymers to argon ion damage may be explained in terms of the reaction being propagated by secondary electrons formed by the initial ion impact. This flux has been found to be quite considerable. Using the electrostatic hemispherical analyser of the ES300 spectrometer in the FRR mode to record the energy distributions of electrons emitted by polymer samples on argon ion bombardment a broad range of electron energies from very low kinetic energies to a few hundred eV. Figure 5.20 shows that the distribution peaks at ∿40eV. The analysis mode used, FRR (see Chapter One) is not recommended for recording low energy electron distributions, having excessive resolution and hence only recording low count rates in this region, this does however serve to protect the electron multiplier. All the polymers considered would undergo electronic excitation or ionisation by this flux. The absorption of electrons by polymers has been studied in detail by Ashley and coworkers.[272] The non-appearance of discrete shake-up features due to isolated double bonds, once formed, since the secondary electrons interact with electron density, the cross-section of such a feature is enhanced, thus the reaction would proceed from this point,

the original isolated double bond is rapidly lost to become part of a growing conjugated system. Japanese workers have examined the correlation between the ionisation energies of polymers and their behaviour as electron beam resits. However the electron energies employed in the exposure of e-beam resists are typically of the order of tens of keV, however the cross-sections for absorption by polymers will be greatest at low energies, *ca.* 10-30 eV, hence the degradation of the resist material is more likely to be associated with the secondary electrons generated by the slowing primary incident electron beam.

Thus the argon ion modification of polymer surfaces has been found to be a relatively rapid method for the controlled defunctionalisation and cross-linking of polymer surfaces. The surfaces so formed are also extensively unsatured and susceptible to atmospheric oxidation, which may detract from the usefulness of such treatments to modify the surface properties (in particular the charging properties) of polymer surfaces. On extended bombardment (*i.e.* ion doses $>\sim 1 \times 10^{15}$ ions cm^{-2}) the polymers tend to what appears from the ESCA data to be a common structure.

Figure 5.20 Secondary electron emission from a sample of HDPE bombarded with 5 keV argon ions (100 nA cm^{-2})

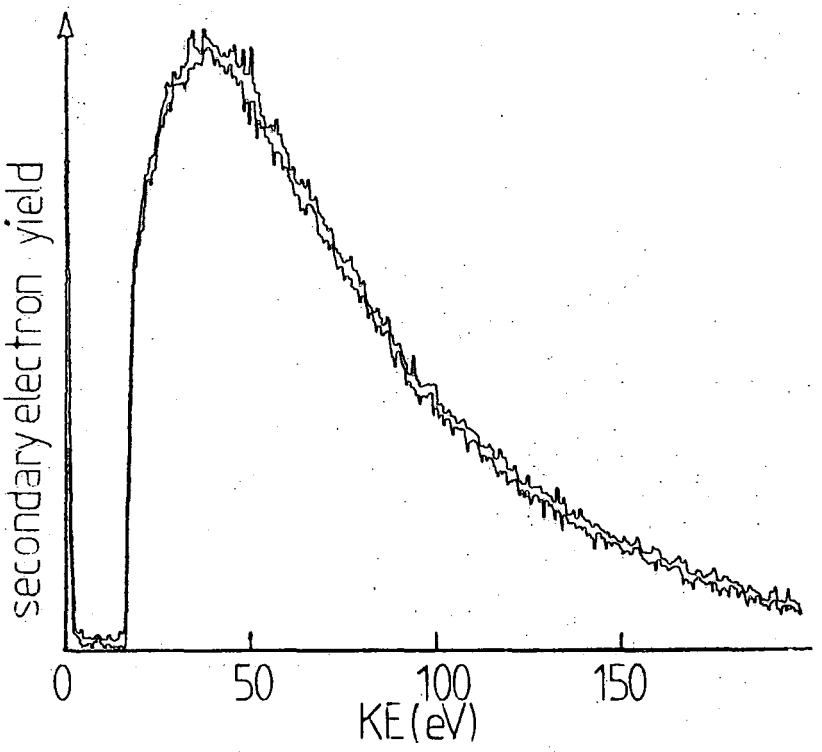

CHAPTER SIX

ION BEAM INDUCED POLYMERISATION IN THE CONDENSED STATE

6.1 Introduction

In electron and ion beam systems, a surface bombarded by the beam is often contaminated by the growth of a thin layer of organic material. This layer is formed by the polymerisation of adsorbed organic contaminants by electron or ion bombardment. Whilst the electron and ion beam deposition of polymers is a much slower process than deposition by plasma polymerisation, they offer a method by means of which deposition may be limited to those parts of a substrate exposed to the beam. These contamination layers formed by electron bombardment have been studied by many workers,[273,279] however only a few workers have examined ion beam induced polymerisation.[280-283] Research in the field has essentially been directed towards the prevention of the formation of these layers, though more recent studies have probed the electrical properties of the films formed. Reflecting the context in which the formation of these films were first observed, electron microscopy, and the nature of the contamination present in such instrumentation, many studies have focussed upon the electron beam polymerisation of silicone and hydrocarbon based diffusion pump oils and greases. These studies have centred upon rates of deposition of the films and their electrical properties, little attention has been paid to the chemical structure of these films. The films are highly crosslinked and intractable, and as such not amenable to many of the solution based methods of polymer characterisation. The field of film deposition by beam induced polymerisation has not produced many publications, the area was last reviewed by Gregor[284-285] in 1966. More recently interest in the field

has waned with the emergence of plasma methods of thin film deposition.

The mechanism of film deposition by electron bombardment of a silicone based diffusion pump oil has been studied in detail by Christy,[278] who developed a phenomenological theory to describe the process. It was assumed that an electron interacts with an adsorbed oil molecule to create an active site which then allows the molecule to crosslink with an adjacent oil molecule. The rate of film growth being related to the partial pressure of monomer and the beam current used. The rate approaching a limiting value as the residence time of a molecule on the surface ions increased by reducing the temperature of the substrate. Relatively high beam currents (cm^{-2}) were employed. Mann[286] observed the dependence of the rate of film growth upon the secondary electron emission from the polymer surface during bombardment. From his investigations he concluded that the low energy secondary electrons possess high cross-sections for activating the adsorbed molecules to polymerisation. Indeed Mayer[279] has shown that films may be formed by exposing contaminated surfaces to electron bombardment with electron energies as low as 6eV.

In forming polymer films, ion beam bombardment has been found by Shimazu and Kawaksta[242,287] to require a much smaller dose than electron bombardment. In ion beam bombardment sputtering acts simultaneously with contamination layer formation, at higher ion energies sputtering processes dominate so no film is formed. Jonkman and Michl[17,288] have observed cluster formation in the SIMS spectra of methane frozen on a copper substrate at 15K, when operating under so-called static SIMS conditions of ion beam current densities of 1-10 nA/cm^2

for beam energies between 500 and 5000eV. (An electron flood-gun was however used for charge neutralisation, the energy of the electrons being kept below 7eV). Thus polymerisation may be possible at very low ion beam current densities. A series of experiments have been undertaken to probe this. Hexafluorobenzene was chosen as a material that does not conventionally polymerise, though the plasma polymerisation of this material has been studied in detail in these laboratories by Clark and Shuttleworth[289] and by AbRahman.[237] A perfluoro system was chosen as such systems display a wide range of chemical shifts and a variety of core-levels for study and hence are particularly amenable to ESCA investigation. Comparisons are drawn with material produced by the plasma polymerisation of hexafluorobenzene and produced by exciting an argon plasma over a film of the condensed starting material.

Previously reported studies of radiation induced polymerisation in the condensed state and in liquid and solution have tended to concentrate on vinyl monomers, where a radical chain polymerisation reaction is envisaged, an account of this type of work up to 1962 was given by Chapiro.[267]

6.2 Experimental

The starting material was condensed onto a cooled gold substrate fixed to the tip of the sample probe. Prior to deposition the substrate was cleaned with an abrasive paste, rinsed in acetone and finally exposed to a discharge excited in hydrogen. The deposition, irradiation and ESCA analysis were all conducted in the sample analysis chamber of the ES300

spectrometer. The substrate was in general cooled to -120°C and allowed to equilibrate for 30 minutes prior to deposition. The starting material (*ca.* 3µl) was then introduced by injection into an evacuated reservoir shaft. The vapour diffusing through the metrosil leak and condensing on the substrate in high vacuum. During deposition the pressure in the source chamber rose, typically to 5×10^{-6} torr. After ∿5 minutes, when the material had deposited to such a thickness that interference colours could be observed at glancing angles in the film forming on the substrate, deposition was halted, the reservoir shaft withdrawn. The pressure in the SAC would then vall to ∿2×10^{-8} torr. The sample was then moved into the ion beam which had been previously aligned and preset to the desired beam current and energy. The ion source has been described previously in Chapter Four. After exposure the probe was allowed to warm up, allowing excess monomer and by-products to evaporate off. The residue was then subjected to ESCA analysis.

The starting material, hexafluorobenzene, was obtained from Bristol Organics and was shown by glc-mass spectroscopic analysis to be analytically pure. The fold substrates were cut from Grade 2 gold sheet, 0.5mm thick obtained from Johnson Matthey Ltd.

The vacuum thermal decomposition behaviour of the materials was investigated by heating the insertion probe tip: temperatures being measured by a Chromel/Alumel thermocouple built into the probe.

Scanning electron micrographs were obtained on a Cambridge Stereoscan scanning electron microscope. No decoration technique was employed, the films being sufficiently thin so as

not to present any problems of charging.

The plasma deposited film derived from hexafluorobenzene was produced by exciting a discharge in the monomer using the inductively coupled RF instrumentation described previously in Chapter Three. The material was deposited onto a gold substrate lying on a glass slide placed in the bottom of a reactor consisting of a horizontal pyrex tube 5cm in diameter, 32cm long sandwiched between 'O' ring sealed glass flanges. The system was pumped by an Edwards ED50, 50 ℓ min^{-1} two stage rotary pump *via* a grease-free, glass vacuum line. The polymer was produced at a nominal monomer pressure of 0.2 torr and a discharge power of 20W for 5 min.

The solid state plasma initiated polymerisation of hexafluorobenzene was performed in the metal flanged reactor described in Chapter Three. The substrate attached to a standard spectrometer insertion probe was cooled to $-130^{o}C$ in a flowing argon atmosphere. A thin film of hexafluorobenzene was then deposited upon the substrate. The flow of hexafluorobenzene was then stopped and the reactor purged with argon at 0.2 torr prior to the striking of a discharge (20W power) over the condensed film; the sample was exposed for 5 minutes. The discharge stopped, the sample was allowed to warm-up, and the excess monomer to evaporate off. The sample was then transferred in air to the ES300 spectrometer for ESCA analysis.

6.3 Results and Discussion

6.3.1 The Ion Beam Induced Polymerisation of Hexafluorobenzene

Previous workers in the field of electron and ion beam induced contamination layer formation in vacuum systems have stressed the importance of adsorbed molecules in the process. Thus the study of these reactions in thin condensed layers of material would appear to be a logical extension. These films, often regarded as a nuisance in vacuum systems, become so usually when the initial polymerisation reaction proceeds beyond the formation of a polymer film to the degradation of the forming film by the ion beam to yield ultimately a conducting, graphitic material. Often it is at this stage that the presence of the films becomes a nuisance as they produce erratic charging effects and degrade to yield conducting pathways on the surfaces of high voltage insulators in electron/ion optical systems. The degradation of the incipient films following pathways similar to those described in the preceding chapters. A fluorocarbon monomer/starting material, hexafluorobenzene was thus chosen for the reasons cited previously.

The argon ion bombardment of condensed films of hexafluorobenzene under high vacuum ($\sim 3 \times 10^{-8}$ torr) conditions and the subsequent boiling off of the excess reagent and volatile by-products lead to the formation of thin films of involatile material.

Films of hexafluorobenzene were produced as described previously. Blank experiments involving the condensation of films of hexafluorobenzene and subsequently allowing

the films to evaporate off again in the spectrometer, with and without ESCA analysis were undertaken. They revealed that no residue was left on a gold substrate by the deposition and evaporation of the monomer from a substrate. The ESCA spectra of the substrate prior to deposition and following the evaporation of the deposited film reveal only a slight increase in hydrocarbon contamination of the cleaned gold surface. The corresponding study which also involved the ESCA analysis of the condensed layer failed to detect any evidence of polymerisation of the hexafluorobenzene under the conditions of ESCA analysis, either as a time-dependent variation in the recorded spectra of the reagent or as a residue left on the substrate surface after the film had been allowed to evaporate away in the spectrometer. Subsequent cooling of the sample in the vacuum system also revealed the absence of any memory effects, the monomer being efficiently removed by the system. Intermittent problems however were experienced due to the presence of water vapour in the vacuum system. Water is a common contaminant in high vacuum systems, as it is difficult to pump and is strongly absorbed by the stainless steel walls of the vacuum chamber. This could be controlled by the use of a titanium sublimation pump attached to the spectrometer and the baking of the spectrometer. However the problem of contamination of the target films by water condensation sporadically led to the abandonment of experimental runs. High background levels of water were evidenced by rapidly growing O_{1s} signals in the ESCA spectra of the substrate surface prior to deposition. Water proved to be a complicating factor, leading in one case to the incorporation of oxygen into the involatile organic residue formed on ion bombardment.

The argon ion bombardment of the condensed films resulted in little visible change in the appearance of the films except for revealing the presence of an inhomogeneity in the ion beam. In addition to producing a beam of ions which may be electrostatically rastered over the surface of the sample, when run at higher argon pressures in the source region of the ion gun (< *ca.* 5 x 10^{-5} torr), collisions between accelerated argon ions and neutral argon atoms may lead to charge exchange. The result is a colliminated beam of energetic argon atoms. The experimental geometry employed results in this collimated beam striking the extreme corner of the sample. This area was too small to subject to ESCA analysis, however adjustment of the area rastered by the ion beam to separate it from the area struck by the neutral component of the beam showed that both beams led to the formation of involatile residues. The thicker films, prepared by the bombardment of a hexafluorobenzene film for 2700 seconds at an ion current density of 20 nA cm^{-2} with 2keV argon ions, displayed a green tint when viewed in white light at glancing angles. A film so produced is discussed below. The bombardment's inhomogeneity led to the production of a slight patterning of the condensed film. The interference colour produced by the portion of the sample exposed to the beam of neutrals (flux density unknown) differing from that of the bulk of the substrates surface. Though whether this inhomogeneity is due to differential thinning of the film by sputtering or local thermal effects or to slight changes in refractive index on reaction, is unclear. The thicknesses of the condensed films were estimated from the interference colours in the films to be of the order of a micron; those of the residue produced somewhat less (the apparent

thickness of the film produced appears to depend upon the ion dose, higher ion doses leading to more material being polymerised, at low doses incomplete coverage was obtained (as revealed by ESCA)). By scraping a sample with a scalpel blade and examining the scratch under an optical microscope, the presence of a thin film of material on the substrate was confirmed.

Scanning electron micrographs were obtained for the films as prepared, the thickness of the films was sufficiently small that no problems of charging in the microscope were encountered, hence gold decoration was not necessary. Additionally the presence of a low Z material on a high Z substrate, gold, revealed the presence of imperfections and pinholes in the film (see Figure 6.1(a)), the high secondary electron flux from the exposed gold substrate showing up as bright patches in the SEM image. The images show the surface of the polymerised film to be mottled and rough, the surface of the film is corrugated at approximately the 1μ level. The film looks fibrous in nature. This film was obtained after the exposure of a condensed film of hexafluorobenzene to a dose of 3.4×10^{14} ions cm^{-2} and gradually allowing the substrate temperature to rise by reducing the cooling so that the excess reagent was allowed to boil off, the film temperature being raised from $-120^{\circ}C$ to $-80^{\circ}C$ over 1 hour. More rapid warming, by simply removing the cooling ($-120^{\circ}C$ - $-80^{\circ}C$ in *ca.* 15 minutes) was found to produce a finely reticulated film. Figure 6.1(b)shows this effect. The detection of pinholes in the film also explains the anomalous nature of some of the ESCA data obtained for this thicker sample. Whilst the film's

Figure 6.1 Effects of heating rate upon polymer film morphology

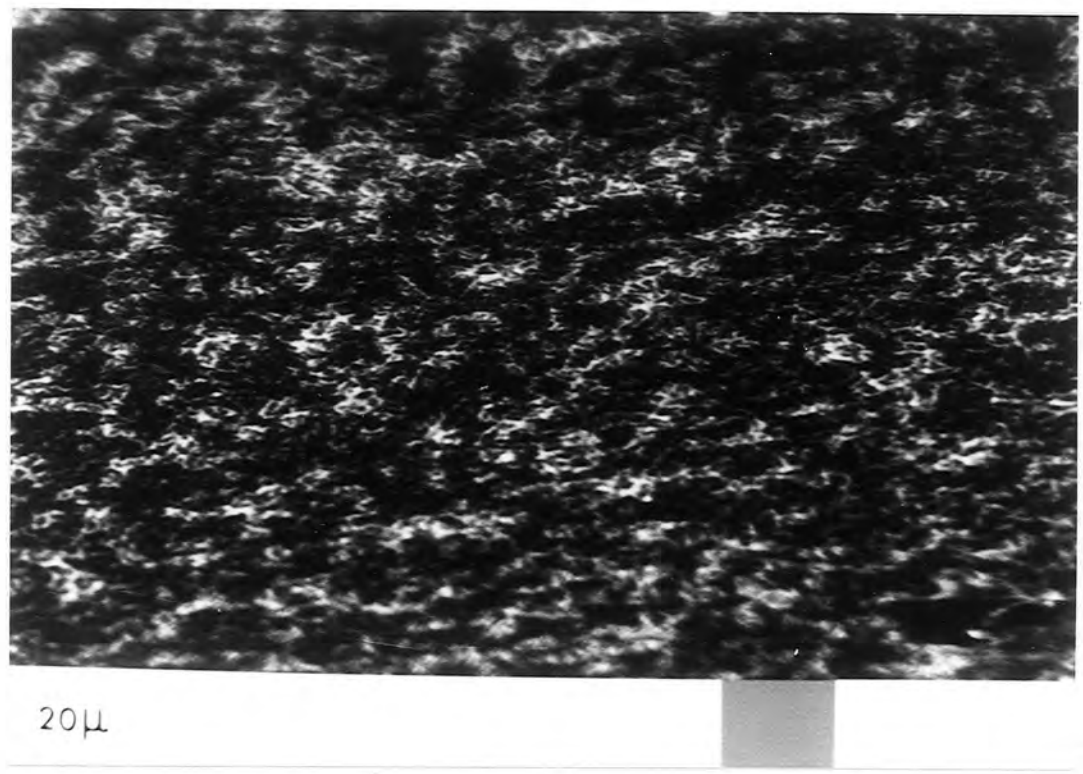

(a) Slow heating

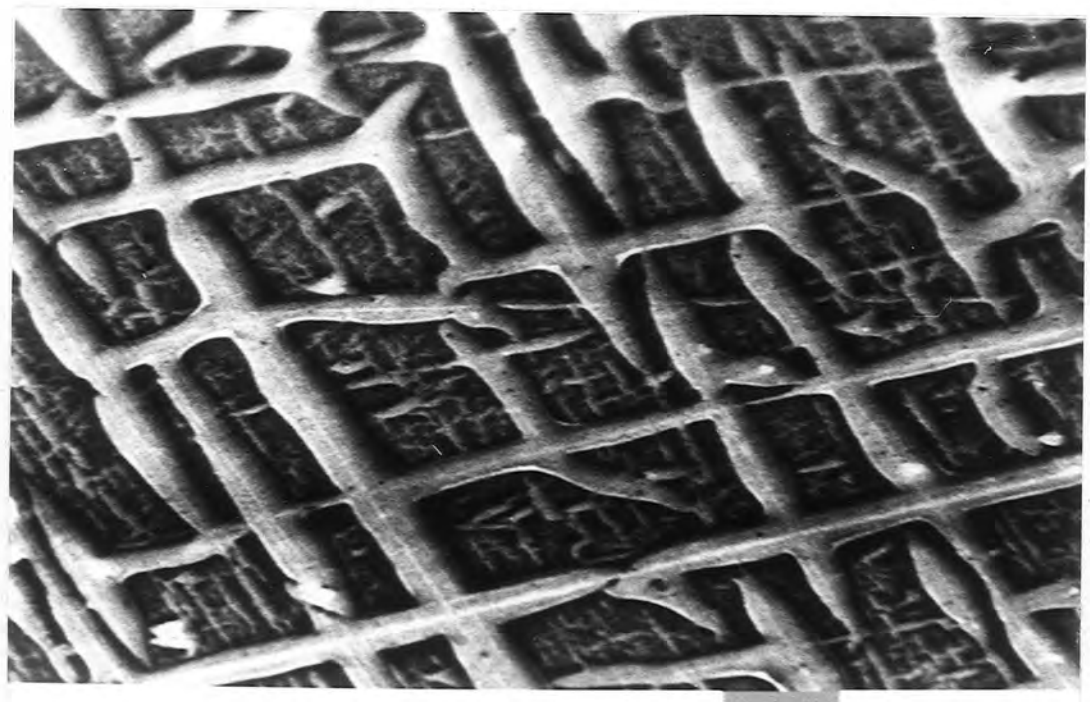

(b) Rapid temperature rise

presence could be detected with the naked eye, the thickness of the film being estimated to be of the order of the wavelength of visible light, the gold substrate was detectable in the ESCA spectra, (the inelastic mean free path of Au_{4f} electrons excited by $Mg_{K\alpha}$ radiation is of the order of 25Å, thus were the film to be complete, to "see" the gold substrate beneath, it would have to be less than 100Å thick. The presence of pinholes also explained the anomalous angular dependence of the C_{1s}:Au_{4f} ratio in the ESCA spectra which pointed to a patched overlayer of material rather than a continuous overlayer of polymeric material on the substrate. The Au_{4f} spectra show no evidence of the reaction of the substrate with any by-products of the reaction, *e.g.* to form gold fluoride.

A specimen was also examined in a transmission electron microscope equipped to perform Reflection High-Energy Electron Diffraction, RHEED. The RHEED experiment involves allowing a beam of high energy electrons (typically 100keV in energy) to impinge at grazing incidence upon a sample surface, the diffraction pattern formed is characteristic of the surface atomic arrangement of the material. In the case of the ion beam polymerised film no diffraction pattern was obtained revealing the amorphous nature of the films. (However it should be remembered that in the use of electrooptical techniques such as SEM, and RHEED to polymeric materials high electron doses are delivered, the data should thus be treated with caution).

The as prepared films were found to be insoluble in the common organic solvents (ether, acetone, chloroform,

carbon tetrachloride and toluene) that were tried to remove the film from the substrates. The films were also unaffected by immersion in the starting material, hexafluorobenzene. The material adhered well to the substrate.

Prior to the removal of the films from the vacuum system they were subjected to ESCA analysis, the thermal stability of the films was also probed by heating the samples under high vacuum and using ESCA to observe the resultant changes in the chemistry of the films.

6.3.2 ESCA Analysis of Ion Beam Polymerised Hexafluorobenzene

The ESCA core-level spectra of the starting material, hexafluorobenzene are shown in Figure 6.2. The C_{1s} spectrum consists of a single direct photoionisation peak at 289.5eV representing carbon atoms in aromatic $\underline{C}F$ environments and a broad series of $\pi \leftarrow \pi^*$ shake-up satellites which represent 10% of the total intensity of the C_{1s} level whose centroid lies at 296.2eV (6.7eV removed from the direct photoionisation peak). The F_{1s} core-level at 690.3eV also displays a shake-up satellite 7.2eV removed from the direct photoionisation peak, though the satellite is less pronounced than in the C_{1s} spectra, constituting only $\sim$6% of the intensity of the F_{1s} level. The F_{2s} level is also presented. Upon bombardment (20 nA cm^{-2}, 45 minutes 2keV Ar^+) the C_{1s} profile of the condensed film is seen to change markedly with the development of distinct shoulders to the high and low binding energy sides of the original $\underline{C}F$ component with the emergence of $\underline{C}F_2$, CF_3 and $\underline{C}$-CF features at 291.8eV, 293.0eV and 287.3eV. The C:F stoichiometry of the

Figure 6.2 C_{1s}, F_{1s} and F_{2s} levels of a condensed film of hexafluorobenzene, prior to and after bombardment (2700s, 2 keV Ar^+, 20 nA) at -120°C and on warming to room temperature after bombardment

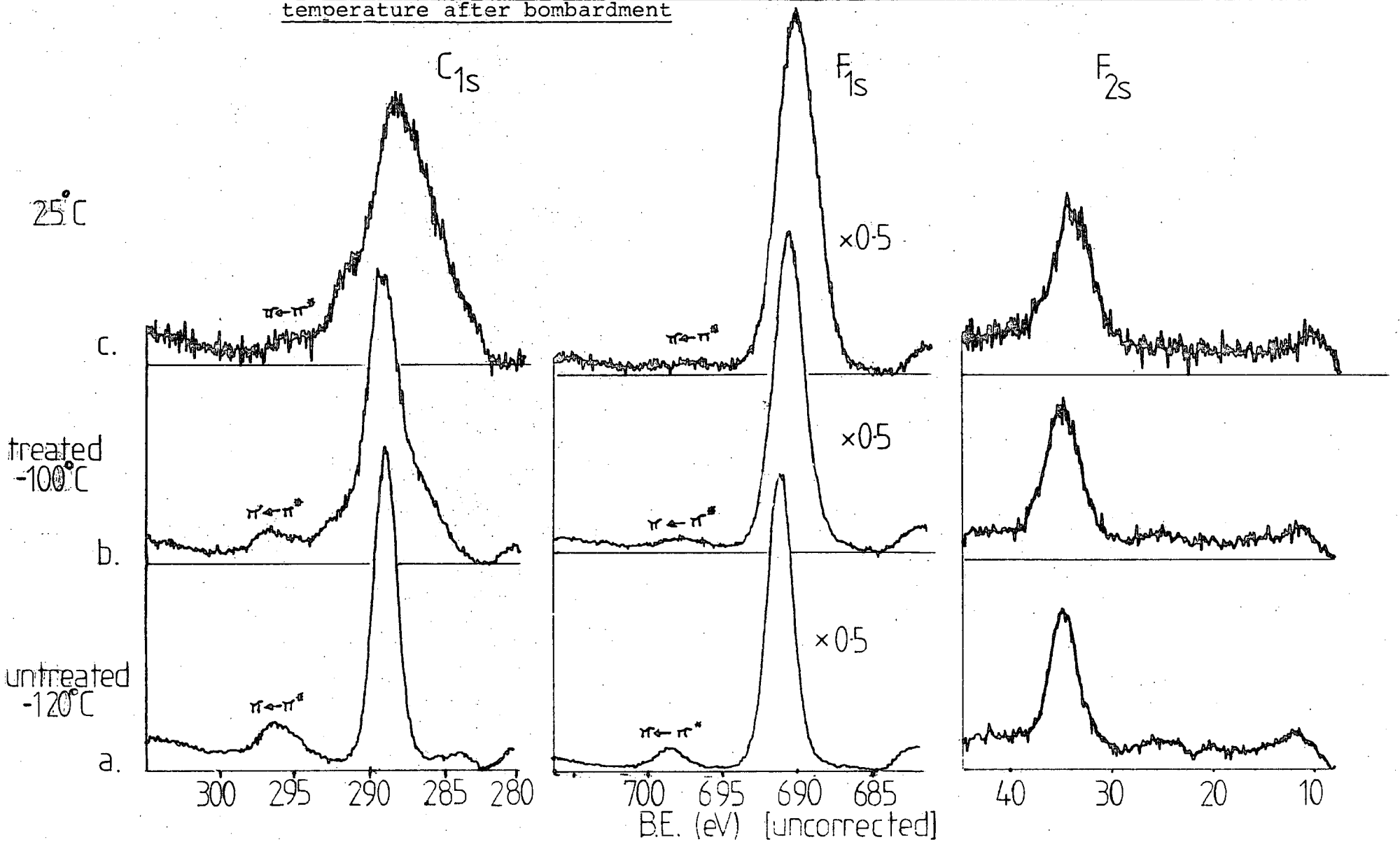

surface regions of the treated condensed film dropped from 1:1 to 1:0.76, fluorine having been lost. (Though the F_{1s}/C_{1s} intensity ratio predicts a somewhat lower fluorine content than component analysis of the C_{1s} envelope, perhaps due to a small degree of contamination on the surface of the film. Surface contamination from extraneous hydrocarbon, etc. builds up rapidly on the cooled sample). The pressure in the source chamber of the spectrometer prior to and after bombardment was 5×10^{-9} torr. On warming the bombarded sample from $-120^{o}C$ to $-100^{o}C$ the pressure rose to 2×10^{-7} torr as the unreacted monomer and more volatile products boiled away. The film was then allowed to warm up slowly to ambient temperature. Having lost the unreacted material and by-products at $\sim-80^{o}C$ the pressure fell to 5×10^{-9} torr. The composition of the film did not change on warming to room temperature, the stoichiometry of the film remaining $CF_{0.82}$ from $-80^{o}C$ to room temperature. The compositions of the film derived from component analysis of the C_{1s} envelope and the C_{1s}/F_{1s} intensity ratios being identical, the F_{1s}/F_{2s} ratios and angular dependent data also confirmed the film to be vertically homogeneous. Another notable feature is the retention, though to a reduced extent of the $\pi \leftarrow \pi^*$ shake-up satellites to the C_{1s} and F_{1s} core levels as shown in Figure 6.2(c). The high binding energy component of the C_{1s} spectrum, due to shake-up from aromatic residues now represents only $\sim$4% of the total C_{1s} intensity, this is approximately in proportion to the $\underline{C}F$ component of the polymer (*cf.* $\underline{C}F$ = 90% $\pi \leftarrow \pi^*$ = 10% for the starting material).

Component analysis of the C_{1s} spectrum of the material formed yield the following features $\underline{C}$, (285eV, $\sim$7%),

$\geq\underline{C}$ - CF, (286.6eV, ∿12%), $\underline{C}$=C (288.0eV ∿24%),

$\geq\underline{C}F$ (290.5, ∿34%), CF_2-(291.9eV ∿12.5%),

$—CF_3$ (293.3eV ∿5%) and π-π*(296eV ∿ 4%).

† *i.e.* a carbon atom in a bridgehead position in a perfluoro environment, the carbon atom may be attached directly only to other carbon atoms or have a single fluorosubstituent. This uncertainty explains the apparent discrepancy between the C:F stoichiometries derived from within the C_{1s} level and from the C_{1s}/F_{1s} ratios. This is illustrated in Table 6.1.

This analysis is consistent with the polymer possessing a highly cross-linked structure. A crude analysis shows that from each carbon atom being attached to 2 other carbon atoms in the monomer, in the polymer this connectivity has risen to an average value of 2·3 (*i.e.* 1 C in 3 is tertiary). The C_{1s} peak profile and the stoichiometries of the ion beam polymerised hexafluorobenzene films resemble very closely the spectra of plasma polymerised hexafluorobenzene obtained from the glow region in an inductively coupled plasma, though the overall fluorine content of the ion beam polymerised film is lower than those given by AbRahman[237] and Shuttleworth[205] from ESCA analysis of plasma polymerised films of hexafluorobenzene. Figure 6.3 compares the C_{1s} spectra of the ion beam (upper) and plasma polymerised (lower) material. The similarity is striking. Though the study of the interactions of ion beams with organic material is of interest in itself, the initial goal was to understand the role of the various components of a plasma in the reactions of a plasma. The above observation reinforces the link between the plasma environment and the local environment around the track of an incident argon ion as it is slowed by the medium.

Figure 6.3 Comparison of the C_{1s} core level spectra of

(1) plasma, and

(2) ion beam polymerised hexafluorobenzene

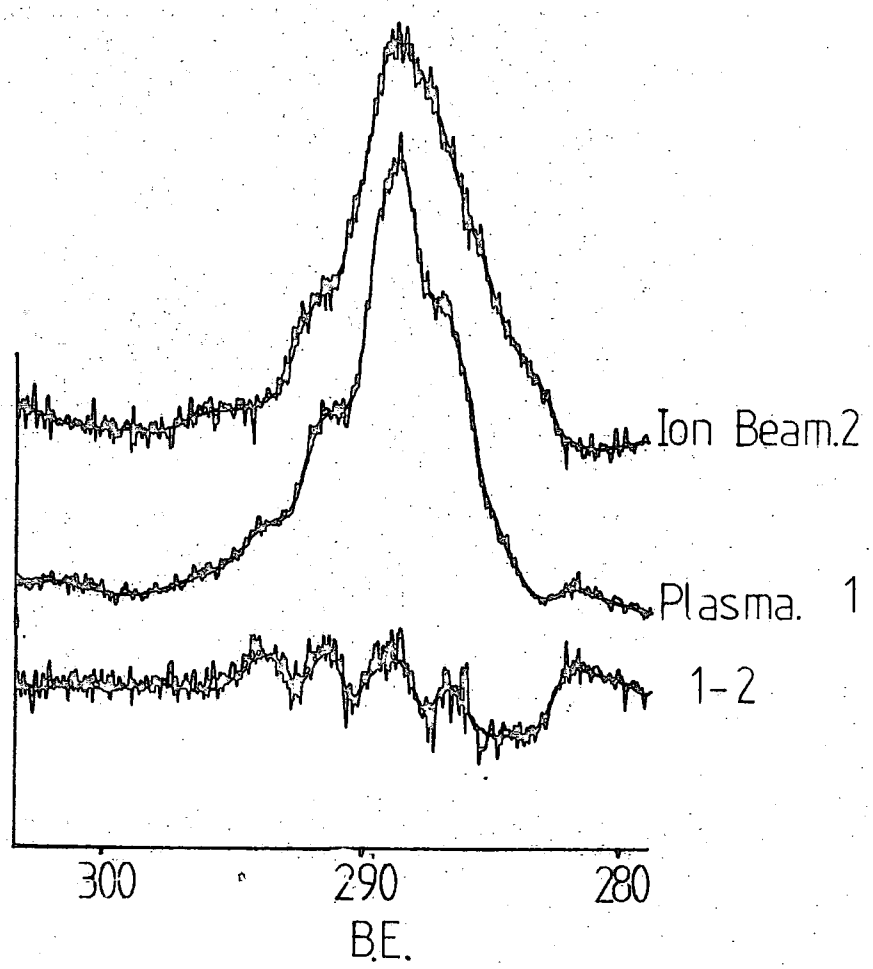

TABLE 6.1 ESCA Analysis of an Ion Beam Polymerised Film of C_6F_6 (2kV, 20 nA, 45 min) and the Thermal Behaviour of the Film Stoichiometries

	$\pi \leftarrow \pi^*$	CF_3	CF_2	CF	C-	C-CF	C	1	2	3
RT	3.4	4.5	10	33	26	13	9	$CF_{0.92}$	$CF_{0.75}$	$CF_{0.82}$
100°C	4.3	4.9	12.5	34.6	24.2	11.7	7	$CF_{0.98}$	$CF_{0.74}$	$CF_{0.83}$
150°C	5.1	5.5	10.7	31.1	27.5	12.9	6.9	$CF_{0.965}$	$CF_{0.69}$	$CF_{0.74}$
200°C	1.9	4.1	11.0	31.0	30.5	13.5	7.4	$CF_{0.95}$	$CF_{0.65}$	$CF_{0.78}$
250°C	2.7	5.2	10.5	29.5	31.0	13.9	6.6	$CF_{0.97}$	$CF_{0.66}$	$CF_{0.68}$

6.3.3 Thermal Stability of the Ion Beam Polymerised Material

Only thin films of the material were formed, insufficient for analysis by Differential Scanning Calorimetry. Shuttleworth performed DSC measurements on polymer films produced by the plasmolysis of hexafluorobenzene. The traces obtained displayed only a single small transition in the range 375-425K, the transition being irreversible. The transition was attributed to the loss of volatile fragments by the matrix or the relief of strain in the crosslinked matrix. (The possibility of the loss of occluded volatiles, *e.g.* unreacted monomer, was not considered). The slow heating of a sample of ion beam polymerised material under high vacuum conditions. The C_{1s} levels of the polymer heated from ambient temperature to 250°C are displayed in Figure 6.4. The detailed component analyses of these levels is presented in Table 6.1 together with stoichiometries for the film based: (a) on the C_{1s} level component analysis alone, assuming the component at ~288eV to be 1 due to -CF- functionalities, 2 due totally to >C=C bridgehead carbons;

Figure 6.4 Variations in the C_{1s} profile of a sample of ion beam polymerised hexafluorobenzene on heating from RT to 250°C

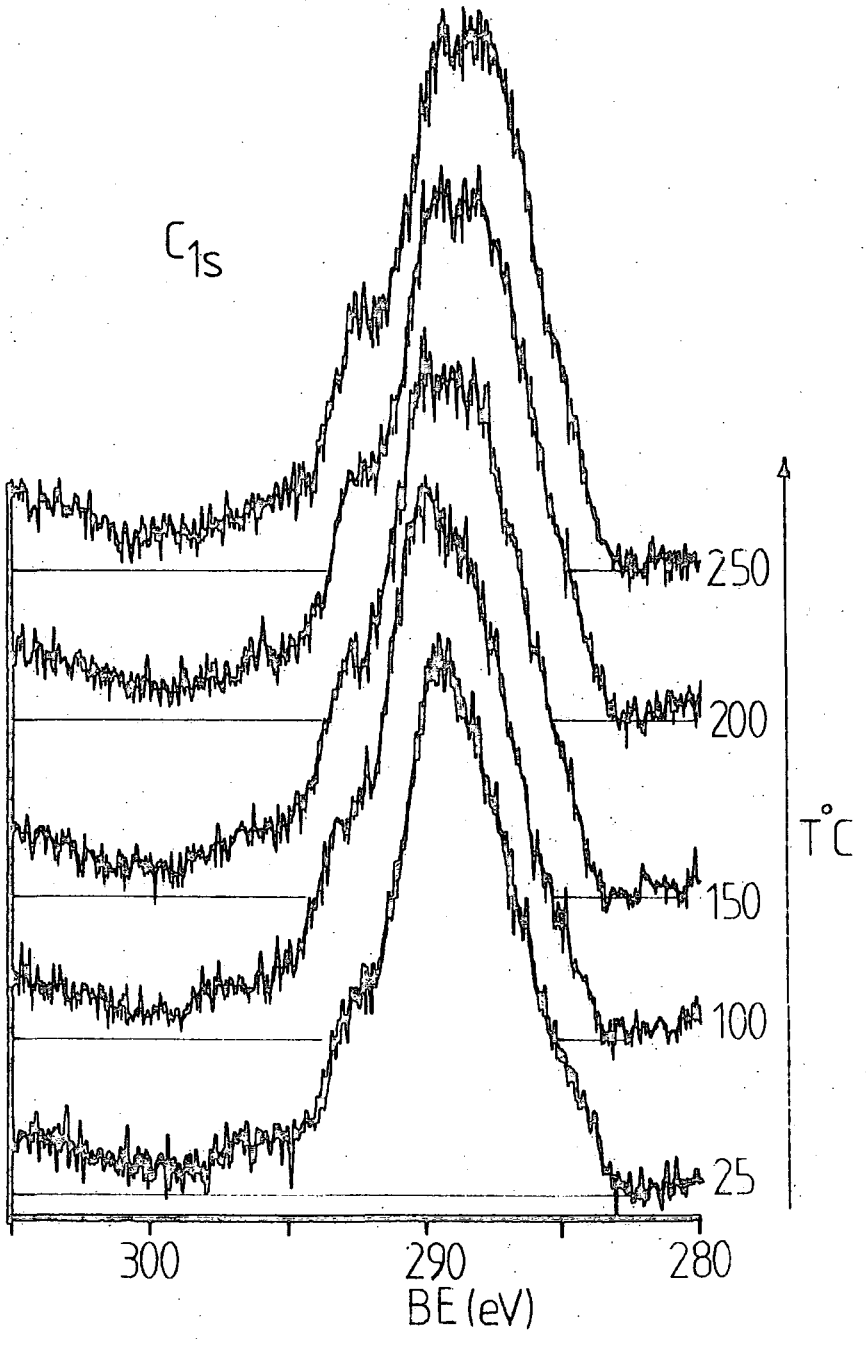

and (b) 3 from the F_{1s}/C_{1s} intensity ratios using experimentally derived sensitivity derived factors. The discrepancy between the stoichiometries derived in the various ways arising from the ambiguity in the assignment of components due to -CF functionalities and bridgehead carbon atoms. The partition between the two however is not clear. Problems may also arise in the partitioning the tailing of the C_{1s} level between CF_3 functionalities and shake-up transitions. The thermolysis results in the slight decrease in the CF component associated with the original environments of these groups in the starting material and the concomitant increase in CF component associated with less highly fluorinated environments, or bridgehead carbon environments. The material appears to defluorinate on heating above 150°C. The changing structure of the film on heating is not however reflected in changes in the integrated intensity of the C_{1s} level, which varies in an erratic fashion.

The film was heated in a stepwise fashion from ambient temperature to 250°C, after each temperature increment the temperature was allowed to equilibrate. Concomitant with each step an initial pressure rise was observed, however the pressure rapidly dropped back again, typically the SAC pressure rose to $\sim 5 \times 10^{-8}$ torr before dropping back to *ca.* 2×10^{-8} torr. This would be consistent with the film tending to an equilibrium structure at each temperature. The changes introduced into the film on heating were not reversed by cooling the film again.

6.3.4 The Influence of Bombardment Conditions upon Film Formation

For a given total ion dose the structure of the deposited films (as determined by means of ESCA) was found to

vary little with the incident ion energy. However increasing ion dose was found to profoundly influence the structure of the film formed. The effect of increasing ion dose being to form polymers with lower fluorine contents, this is marked by the increasing contribution of carbon atoms containing no α fluorine atoms relative to that of CF functionalities in the C_{1s} spectra (Figure 6.5 depicts the effect of increasing ion dose). In contrast to a conventional initiated free radical polymerisation reaction, in a radiation induced polymerisation reaction, the polymerisation is produced by the irradiation, however the polymeric material, once formed is also susceptible to radiation induced damage. The modification of fluoropolymer surfaces by ion beam bombardment has already been considered in Chapter Four. In general this modification takes the form of the defunctionalisation, defluorination of the polymer surface, giving rise to the formation of a carbonaceous material. In the ion beam polymerisation of hexafluorobenzene this occurs concomitant with the polymer formation. This situation is analogous to the Competitive Ablation Polymerisation (CAP) model[290] proposed for plasma polymerisation. The effects of higher power densities in the plasma polymerisation of hexafluorobenzene were investigated by AbRahman[237] (Figure 6.6). The effects of increasing power density upon the structure of the polymer film produced, as expressed by the C_{1s} spectra of the polymer surfaces, closely mirror those of increasing ion dose upon the structure of the final polymer. The increased contribution due to carbonaceous material being due to differing distributions of reactive intermediates produced by the higher power density in the plasma or by the higher incident ablative electron and ion flux on the growing polymer surface.

Figure 6.5 The effect of higher ion doses on the structure of the polymeric material formed from hexafluorobenzene

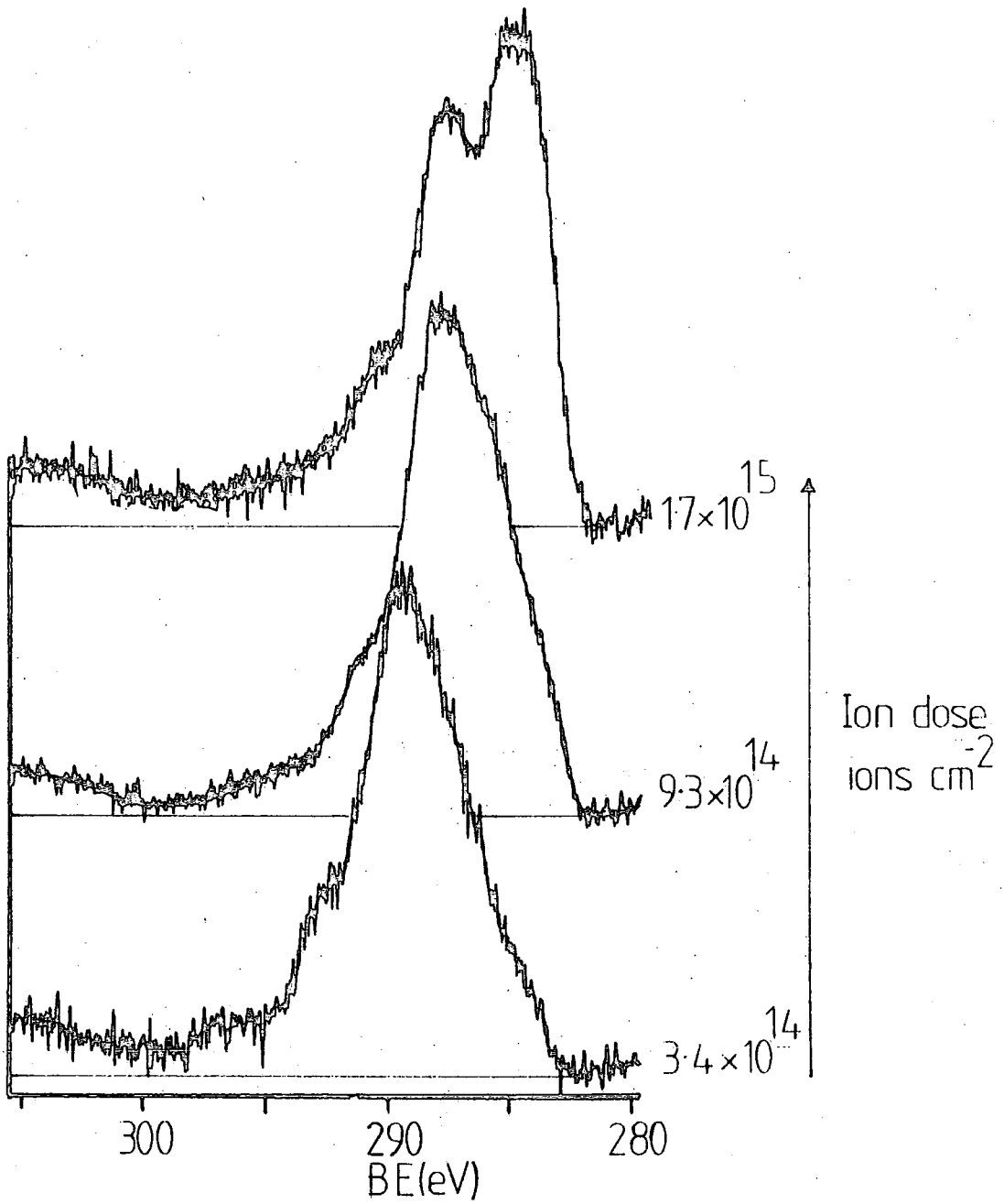

Figure 6.6 C_{1s}, F_{1s} and F_{2s} levels of the plasma polymer prepared at 10,20,30,40 and 50W discharge powers and at a pressure of 200μ. 237

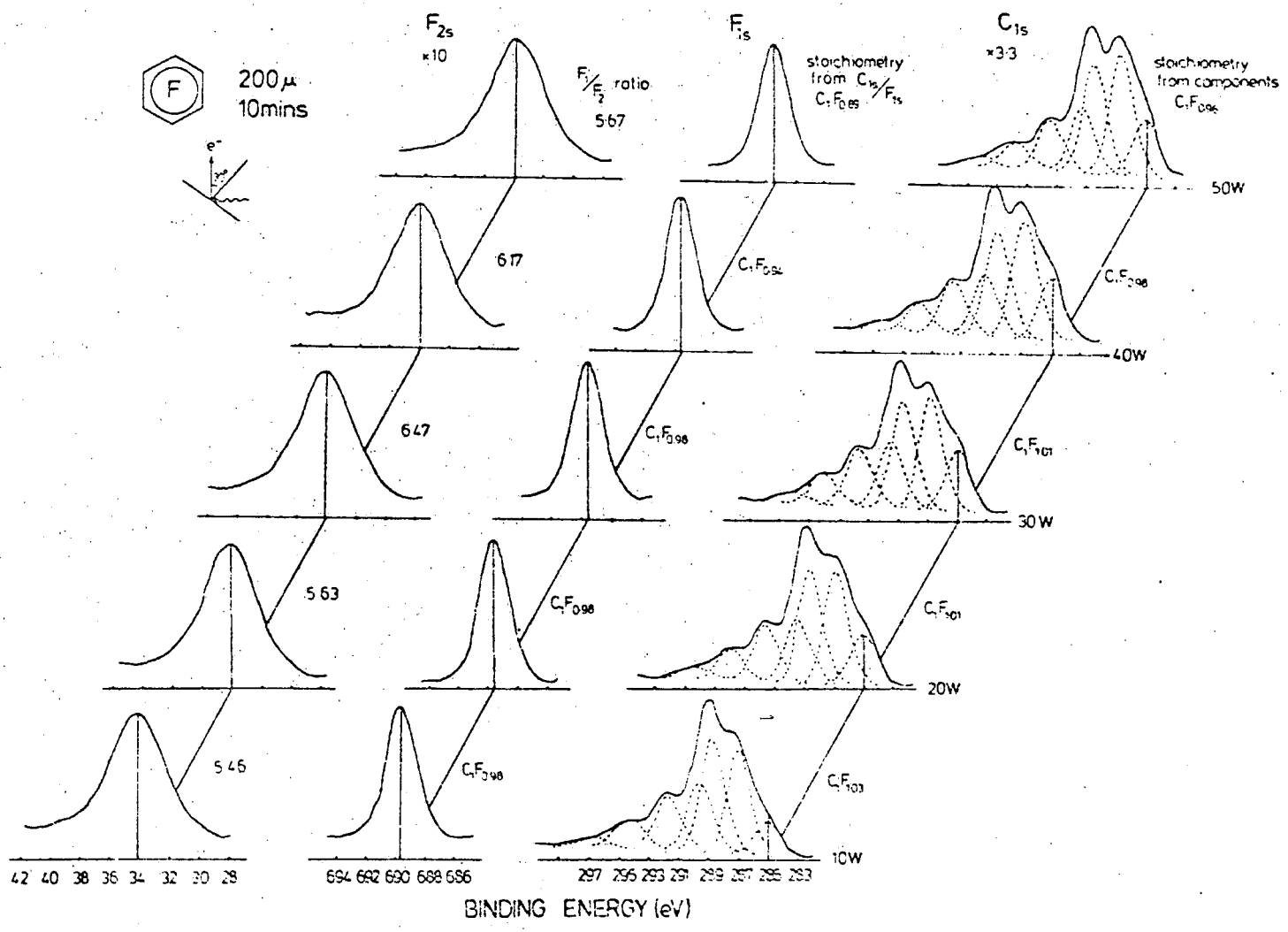

Westwood[291] studied plasma polymerisation in electroded systems and observed that polymer deposition occurred mainly at the cathode. He suggested that the formation of the polymer followed a cationic mechanism. In considering the mechanism of the plasma polymerisation of hexafluorobenzene and other fluoroaromatic species, Clark and AbRahman[126] and AbRahman[237] have placed emphasis on the role of cationic intermediates. Polymeric material was also produced by the simultaneous deposition onto and bombardment of a gold substrate held at -120°C. The material resembling closely that of the material prepared by the bombardment of a predeposited film. The monomer, hexafluorobenzene was only found to deposit on the substrate under the conditions used provided the substrate was held at a temperature lower than -90°C. Attempts to produce polymer material by maintaining the substrate temperature at -80°C (to increase the residence time of the material on the substrate but not lead to film formation) were unsuccessful. This was intended to emulate the conditions under which polymeric materials were deposited in contaminated vacuum systems. The similarity between the products formed by ion beam and plasma polymerisation of hexafluorobenzene would support the involvement of similar species in the solid state, ion beam polymerisation of hexafluorobenzene. Similar materials have also been prepared by electron beam irradiation of condensed films of fluorobenzenes and subjected to ESCA analysis by Brennan.[266] There are considerable similarities between the films prepared by the three approaches suggesting a common mechanistic pathway. One common feature of each approach is the presence of a reasonably large flux of low energy electrons, present either in the plasma environment or produced by a particle (an electron or ion)

colliding with a medium.

ESR studies of the γ radiolysis of hexafluorobenzene in squalene by Anismov *et al*[292] revealed the formation of the anion, $C_6F_6^{\ominus}$, no evidence of $C_6F_6^{\oplus}$ formation was seen in the ESR spectra. Whilst some studies of the secondary emission of electrons on ion and electron by a medium have been undertaken by various workers, the measurement is complicated by secondary electrons with energies less than the work function, (typically 5-6eV for a polymer surface) do not escape from the surface. Hence this flux may be difficult to estimate, however the cross-sections for electron attachment vary rapidly with energy for low energy electrons, they are large in the electron energy range 0-3eV, Christophorou and co-workers[293] have made extensive studies of the formation of the negative ion states of fluorobenzenes. The ionisation energy of hexafluorobenzene is 9.88eV, well within the expected electron energy distribution for the secondary electrons however possessing a much lower cross-section than for electron attachment. However the lifetimes of negative ion states in the gas phase are likely to be in the range 10^{-7} - 10^{-9} sec, and much lower in the condensed state.

Electron impact spectra for the fluorobenzenes have been reported by Kuppermann and co-workers.[294] The threshhold-electron excitation spectrum of hexafluorobenzene has been reported by Brongersma, (see Ref.[293]) displaying a range of states in the range 4-8eV however it is difficult to deduce the cross-sections for the excitations from such experiments. Thus a range of excited states is accessible by secondary electron bombardment. Molecular rearrangements of the benzene ring system arising from excited states have been the subject of

numerous investigations. Thus under ion bombardment, the products of such rearrangements, prismane and benzvalene type structures (Figure 6.7) may well be involved. The energetically most favourable intermediates being that of fulvene and hexadienyne types. Other features observed in the C_{1s} spectra, such as trifluoromethyl substituents, may be envisaged as the rearrangement products of the monomer upon ionisation, fluorine migration being facile.

Through the formation of polymeric material from these proposed intermediates may be envisaged and would account for the features observed in the ESCA spectra, the exact role or contribution of each cannot be assessed at this stage other than on a purely qualitative basis.

Polymeric material was formed after total ion doses of 2.25×10^{14} ions cm^{-2} ($\equiv$ 2.25 ions per 100Å^2). If the density of the polymer is approximated to that of the monomer *i.e.* $\sim$1.6g cm^{-3} and the film thickness to be $\sim 1\mu$ (10^{-6}m) though this is probably an overestimate) then it is possible to estimate the efficiency of the reaction. A single incident ion leading to the incorporation of $\sim$2000 monomer molecules into the polymer. The above is a crude estimate which overestimates the amount of material produced, however, it illustrates the efficiency of the process. However, a chain reaction would seem unlikely considering the monomer employed. Again considering a 10Å x 10Å area of the surface, at the ion current employed, 20 nA, this is equivalent to one ion entering this area every 800s. On this basis the polymerisation in a given area is expected to be due to a single event. Though at lower ion doses, though damage was observed in the ESCA spectra of the

Figure 6.7 Intermediates proposed for the polymerisation of hexafluorobenzene on ion beam bombardment

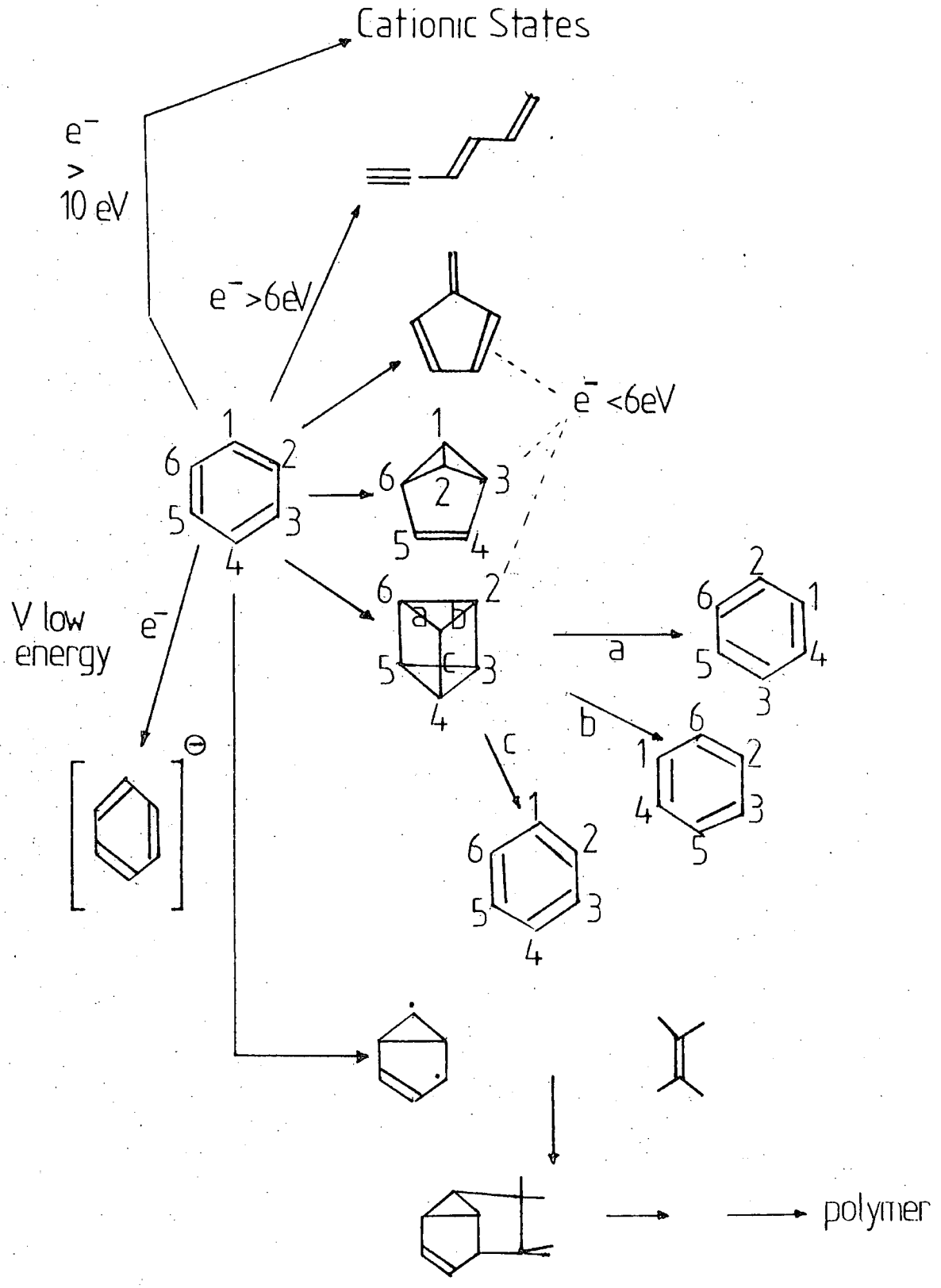

condensed, bombarded films, on warming often no film of polymeric material was formed. The implication is that the reaction proceeds in a stepwise fashion, "oligomerisation" occurring in the region of the spur or track of the incident ion. For polymer formation these spurs must overlap to an extent. ESCA spectra have shown that the polymeric material is formed on bombardment, the components due to the polymer may be observed in the bombarded film held at -120°C. (The spectra may be regarded as a sum of components due to the material formed and the starting material).

Though experimental difficulties precluded a more detailed study of the ion beam polymerisation of organic materials from this limited study and comparison with other studies several points emerge: the similarity of the structure of the materials produced to those by plasma techniques; whereas the original ion was to provide an insight into the mechanism of interaction between ions and organic material, what has emerged is the great apparent similarity between the mechanisms of formation of the materials; it is not however possible to delineate a single common factor responsible for the similarity.

Polymeric material was also formed by condensing hexafluorobenzene on to a cooled gold substrate at -120°C - 130°C and exciting an argon plasma (20W, 0.2 torr, 5 min) above the condensed film. On evaporation of the excess hexafluorobenzen a thin film of material was produced. The ESCA analysis of this material was troubled by the presence of a thick overlayer of hydrocarbon. The spectra merely show that the material produced has fluorine incorporated, no conclusions may be drawn as to the chemical structure of the film. Microscopic examination, both optical and SEM, of the material formed showed it to

be deposited unevenly as an island in the middle of the probe tip surface, within this area the film was highly reticulated.

6.3.5 An ESCA Examination of the Thermal Degradation of Plasma Polymerised Hexafluorobenzene

The thermal degradation of plasma polymerised hexafluorobenzene was investigated using differentiated scanning calorimetry by Shuttleworth. He found the material not to display any reversible transitions, one small transition was observed at 375-425K. The thermal gravimetric analysis of such materials shows a steady weight loss from the material on heating. In this context it was decided to use ESCA to investigate the stability and changes in chemistry in this material on thermolysis. A film of the plasma polymerised hexafluorobenzene was deposited on to a gold substrate (20W, 0.2 torr, 5 min). The sample was then fixed with a screw to a probe tip attached to a standard ES300 insertion probe. The probe tip temperature was increased in 100°C steps from 100 to 500°C. The C_{1s} and F_{1s} spectra of the film taken at a take-off angle of 35° are presented in Figure 6.8. The degradation of the polymer is evident from the increasing contribution of the carbonaceous component of the C_{1s} spectrum with increasing substrate temperatures. Component analyses of the C_{1s} levels on thermolysis are depicted in Figure 6.9. The defluorination of the material due to the thermal degradation of the material is shown in Figure 6.10. (The stoichiometries derived from considering the C_{1s}:F_{1s} intensity ratios and by component analysis of the C_{1s} level are both presented). Concomitant with the degradation, the absolute intensity of the C_{1s} level (Figure 6.11) is found to increase. The changes introduced into the

Figure 6.8 Variation in the C_{1s} profile of a plasma polymerised hexafluorobenzene film on thermolysis

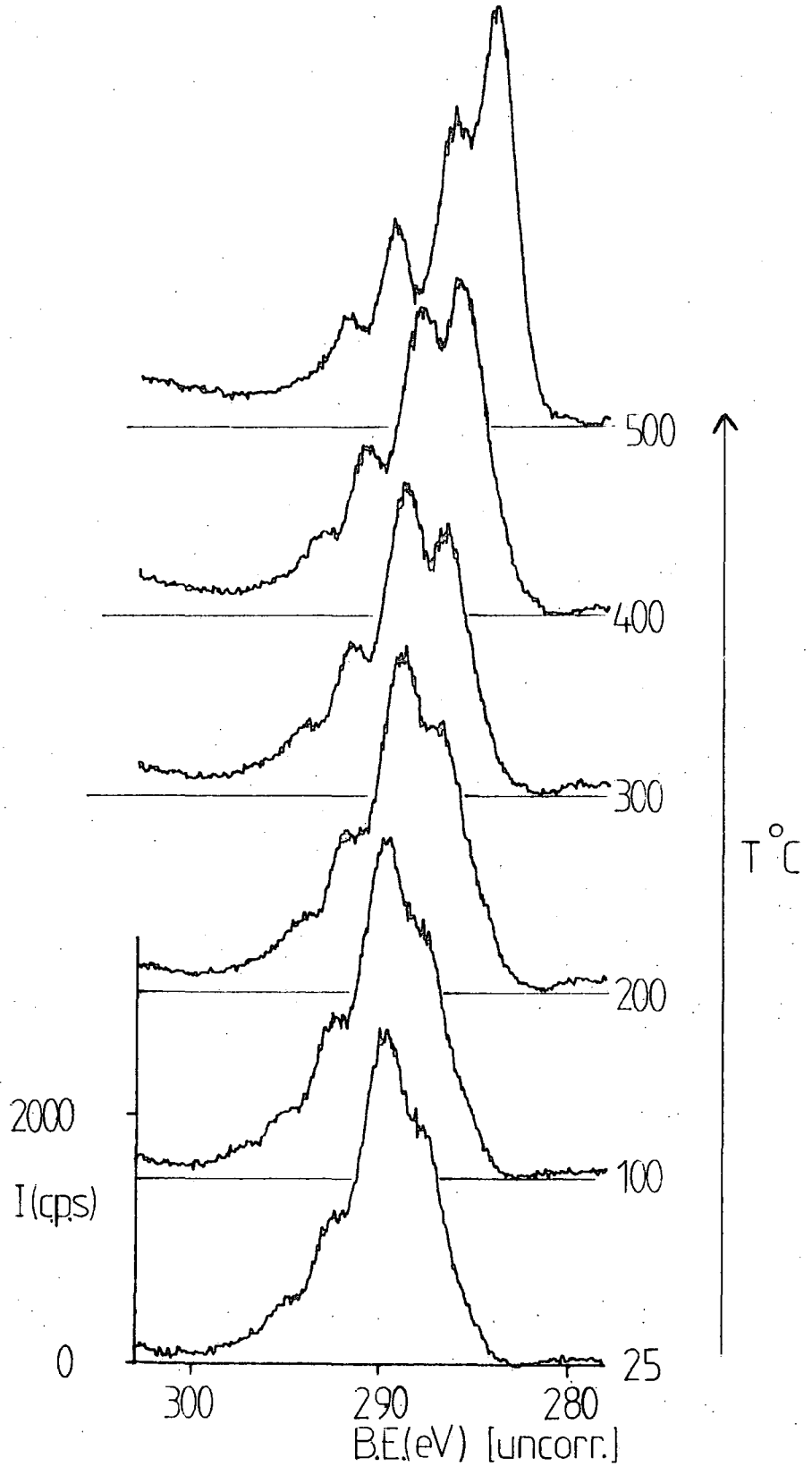

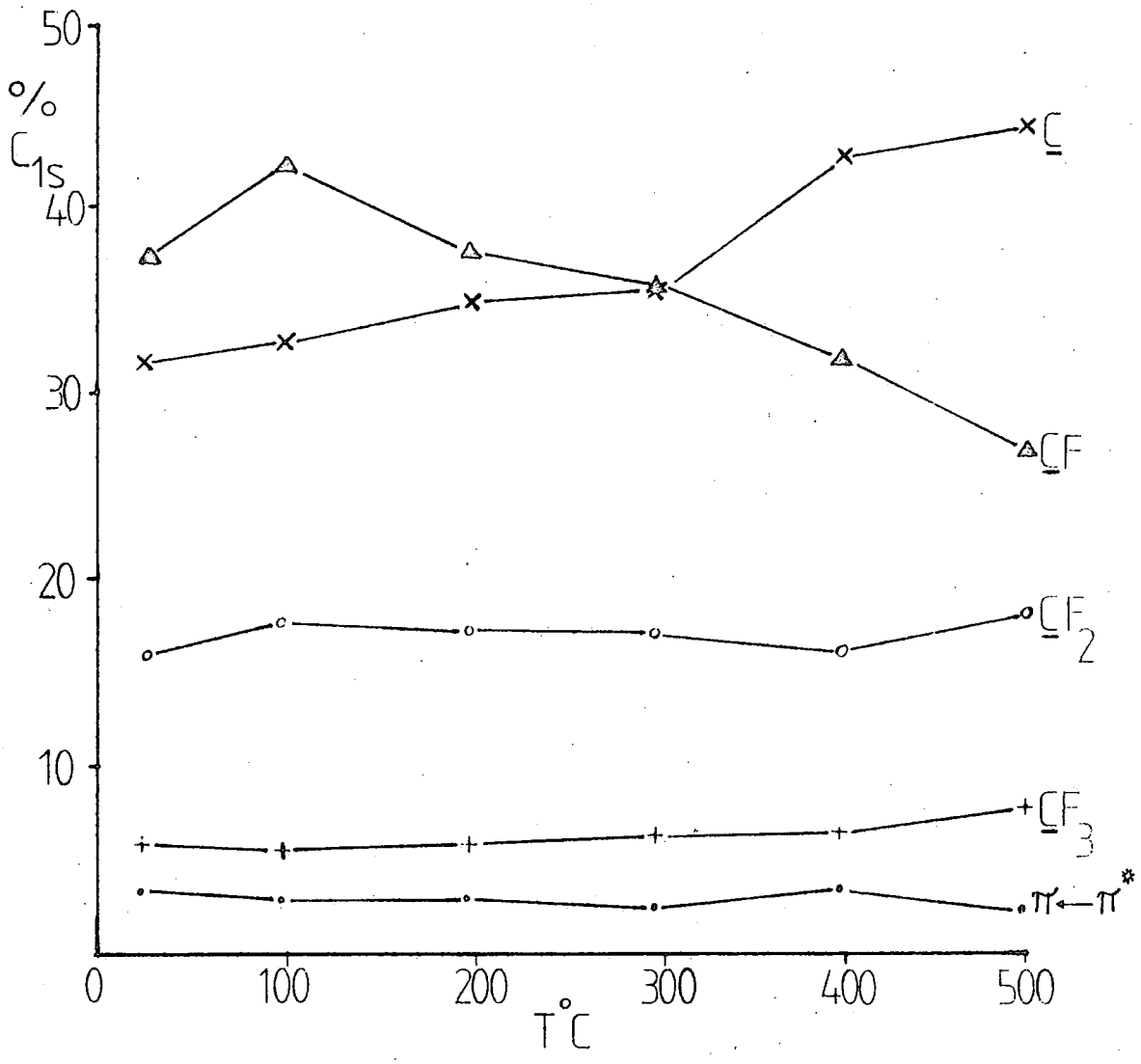

Figure 6.9 Variation in the components of the C_{1s} spectrum of a plasma polymerised hexafluorobenzene film on heating

Figure 6.10 Variation in the C:F stoichiometry of a plasma polymerised film of hexafluorobenzene on thermolysis

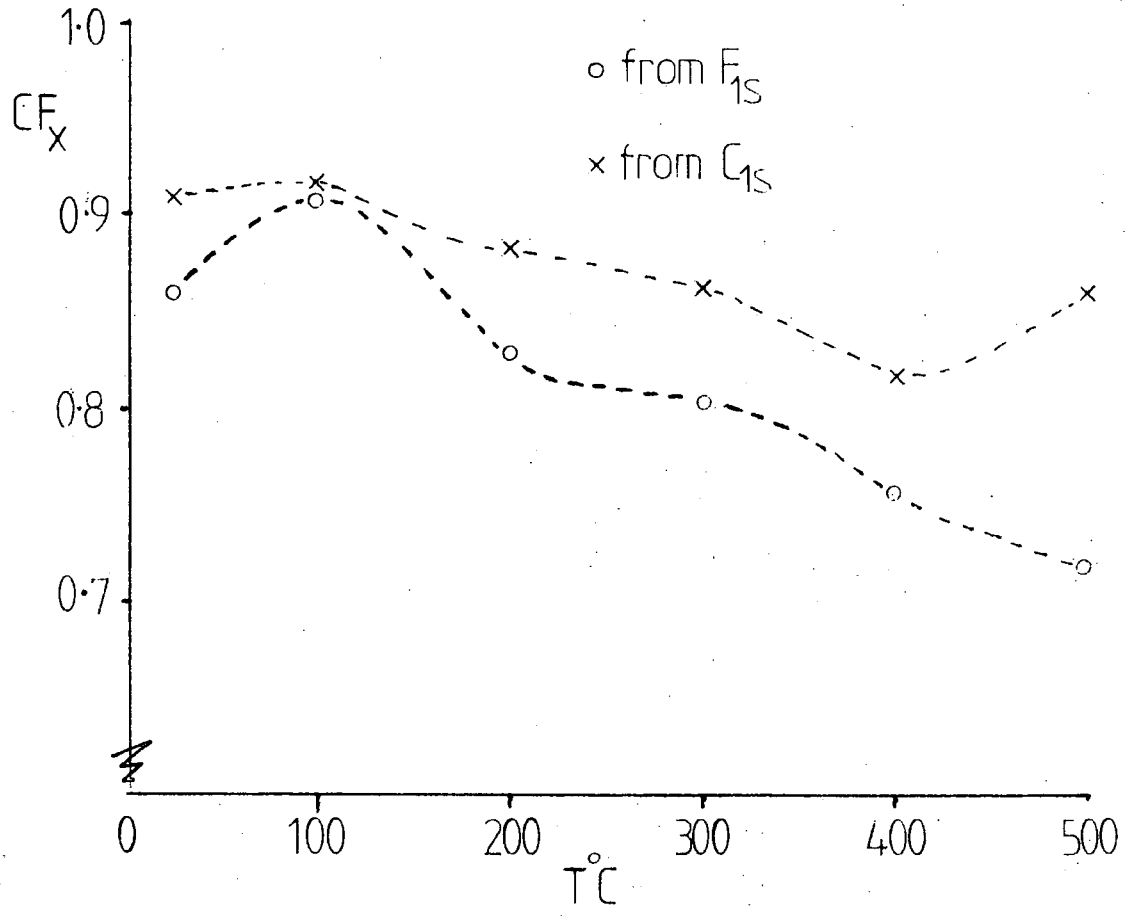

Figure 6.11 Variation in the absolute intensity of the C_{1s} level of a film of plasma polymerised hexafluorobenzene on thermolysis

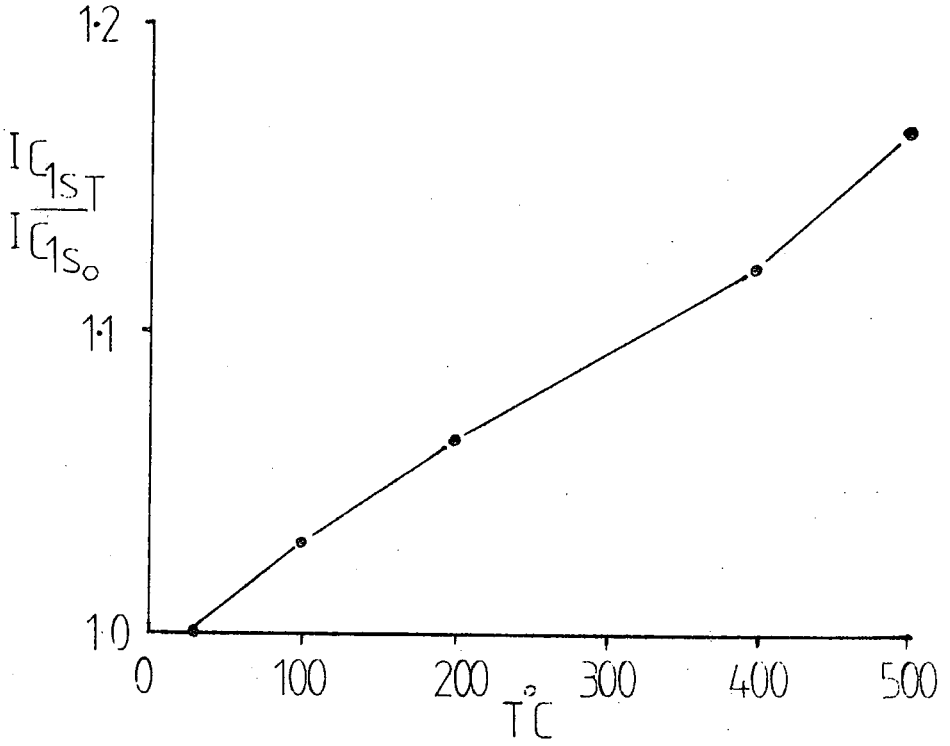

polymer on heating are not reversible by cooling the sample. On removal from the vacuum system the sample was found to have darkened during treatment.

Consideration of Figure 6.9 shows that on thermolysis whilst the material is found to lose fluorine, fluorine is not lost from the CF_2, and CF_3 functionalities present in the polymer as prepared, their contributions to the C_{1s} level remain approximately constant. The major reaction is that of the conversion of CF species into carbon species with no α fluorine, *i.e.* a reaction in which fluorine is eliminated from the polymer matrix. However whether the fluorine is lost as elemental fluorine or as a fluorocarbon fragment is unknown. (A future refinement would be the monitoring of the surface stoichiometry with ESCA with the simultaneous use of a residual gas analyser to monitor the gaseous products of the degradation).

The most obvious feature of the degradation is the drastic simplification of the C_{1s} level upon thermolysis. The elimination of volatile fragments from the matrix leading to a relief of strain in the matrix and cross-linking of the matrix leading to higher absolute intensities of the C_{1s} level. The resolution of the structure of the C_{1s} level as the reaction proceeds is due to the use of links which strain and stress the system and modulate the chemical shift environments of the remaining functionalities. The use of fluorine from the matrix reducing the range of chemical shifts exhibited by the matrix.

6.4 Conclusions

This outline study has shown that films of polymeric material may be produced by the low dose, low ion energy bombard-

ment of hexafluorobenzene. Much of the early work in the field of the ion and electron beam deposition of polymer films dwelt upon the electrical properties of such films. In this study the chemistry of these films has been interrogated, the electrical properties remain to be investigated. The similarity in the chemistry of the plasma and ion beam polymerised films is striking.

The coverage of the materials on a substrate remains difficult to control, a factor which would detract from the use of such materials in *eg*. microelectronic device fabrication.

It would be interesting too, using methods akin to those employed in chemically assisted ion beam etching, where a jet of a reactive gas, *eg*. oxygen is directed at the surface of a sample bombarded by an inert gas ion beam. The use of a jet of monomer and heavy differential pumping might permit the more even deposition of films.

At higher ion beam doses the polymer film formed tends to be more carbonaceous in nature. Such behaviour may be exploited to produce a range of materials from a single starting material, ranging from an insulator to a defunctionalised amorphous carbon matrix, with a corresponding range of electrical properties.

APPENDIX ONE

RESEARCH COLLOQUIA, SEMINARS, LECTURES AND CONFERENCES

The Board of Studies in Chemistry requires that each postgraduate research thesis contains an appendix listing all research colloquia, seminars and lectures by external speakers held in the department as well as all conferences attended by the author, during the period of research.

Lectures held October 1980 - July 1983

Dr. D. Mass (Salford Univ.) - 'Reactions a Go-Go', 16 Oct.1980.
Prof. T.M. Sugden (Cambridge Univ.) - 'Chemistry in Flames', 23 Oct. 1980.
Prof. N. Grassie (Glasgow Univ.) - 'Inflammability Hazards in Commercial Polymers', 30 Oct. 1980.
Prof. A.G. Sykes (Newcastle Univ.) - 'Metallo-proteins: An Inorganic Chemist's Approach', 6 Nov. 1980.
Dr. M. Gerloch (Cambridge Univ.) - 'Magnetochemistry is about Chemistry', 12 Nov. 1980.
Prof. N.N. Greenwood (Leeds Univ.) - 'Metalloborane Chemistry', 13 Nov. 1980.
Dr. T. Gilchrist (Liverpool Univ.) - 'Nitroso-olefins as Synthetic Intermediates', 19 Nov. 1980.
Rev. R. Lancaster - 'Fireworks', 4 Dec. 1980.
Dr. R. Evans (Brisbane Univ., Australia) - 'Some Recent Communications to the Editor of the Australian Journal of Failed Chemistry', 18 Dec. 1980.
Prof. E.A. Dawes (Hull Univ.) - 'Magic and Mystery through the Ages', 22 Jan. 1981.
Mr. H.J.F. Maclean (I.C.I.Ltd.) - 'Managing in the Chemical Industry in the 1980s', 29 Jan. 1981.
Prof. F.G.A. Stone (Bristol Univ.) - 'Chemistry of Carbon to Metal Triple Bonds', 5 Feb. 1981.
Dr. I. Fleming (Cambridge Univ.) - ' Some Uses of Silicon Compounds in Organic Synthesis', 12 Feb. 1981.
Prof. S. Kettle (Univ. of East Anglia) - 'Variations in the Molecular Dance at the Crystal Ball', 18 Feb. 1981.
Dr. K. Bowden (Essex Univ.) - 'The Transmission of Polar Effects of Substituents', 25 Feb. 1981.
Dr. J.F. Stoddart (I.C.I. Ltd.) - 'Stereochemical Principles in the Design and Function of Synthetic Molecular Receptors', 11 Mar. 1981.
Prof. W.P. Jencks (Brandell Univ., Mass.) - 'When is an Intermediate not an Intermediate?', 17 Mar. 1981.
Dr. J.P. Smith (Int. Tin Research Institute) - 'Organotin Compounds - A Versatile Class of Organometallic Compounds', 18 Mar. 1981.
Dr. W.H. Meyer (RCA, Zurich) - 'Properties of Aligned Polyacetyle
9 Apr. 1981.
Prof. M. Gordon (Essex Univ.) - 'Do Scientists have to Count?', 7 May 1981.
Dr. J. Rose (ICI Plastics) - 'New Engineering Plastics', 10 Jun.19
Dr. P. Moreau (Montpelier Univ.) - 'Recent Results in Perfluoro-organometallic Chemistry', 17 Jun. 1981.
Dr. P. Plimmer (Du Pont) - 'From Conception to Commercialization of a Polymer', 21 Sept. 1981.

Prof. E. Kluk (Univ. of Katowice) - ' Some Aspects of the Study of Molecular Dynamics', 14 Oct. 1981.
Dr. P.J. Corrish (Dunlop Ltd.) - 'What would Life be like without Rubber?', 22 Oct. 1981.
Dr. W. Moddeman (Monsanto Ltd.) - 'High Energy Materials, 6 Nov.198
Prof. A.I. Scott (Edinburgh Univ.) - 'An Organic Chemist's View of Life in the n.m.r. tube', 12 Nov. 1981.
Dr. W.O. Ord (Northumbrian Water Authority)- ' The Role of the Scientist in a Regional Water Authority', 26 Nov. 1981.
Dr. R.E. Hester (York Univ.) - 'Spectroscopy with Lasers', 3 Dec.198
Prof. I. Fells (Newcastle Univ.) - 'Balancing the Energy Equation' 28 Jan. 1982.
Dr. D. Pethrick (Strathclyde Univ.) - 'Conformational Dynamics of Small and Large Molecules', 10 Feb. 1982.
Dr. D.W. Turner (Oxford Univ.) - 'Photoelectrons in a Strong Magnetic Field', 17 Feb. 1982.
Prof. R.K. Harris (Univ. of East Anglia) - 'N.m.r. in the 1980s', 18 Feb. 1982.
Prof. R.O.C. Norman FRS (York Univ.) - 'Turning Points and Challenges for the Organic Chemist', 25 Feb. 1982.
Dr. P. Banfield (I.C.I. Organics) - 'Computer Aided Synthesis Design: A View from Industry', 3 Mar. 1982.
Dr. R. Whyman (I.C.I. Ltd.) - 'Making Metal Clusters Work", 4 Mar. 1982.
Prof. D.J. Burton (IOwa Univ.) - 'Some Aspects of the Chemistry of Phosphonium Salts and Phosphates', 28 Jun. 1982.
Prof. Neidlein (Heidelberg Univ.) - ' New Aspects and Results of Bridged Annulene Chemistry', 13 Sep. 1982.
Dr. W.K. Ford (Xerox, New York) - 'The Dependence of the Electron Structure of Polymers on their Molecular Architecture', 27 Sep. 1982.
Prof. H. Suhr (Univ. of Tübingen) - 'Preparative Chemistry in Non-Equilibrium Plasmas', 14 Oct. 1982.
Mr. F. Shenton (County Analyst, Durham) - 'There is Death in the Pot', 14 Oct. 1982.
Dr. C.E. Housecroft (Notre Dame Univ.) - 'Bonding Capabilities of Butterfly-shaped Fe_4 Units', 27 Oct. 1982.
Prof. M.F. Lappert, FRS (Sussex Univ.) - 'Approaches to Assymetri Synthesis and Catalysis using Electron-rich Olefins and Some of their Metal Complexes', 28 Oct. 1982, and 'The Chemistry of some Unusual Subvalent Compounds of Group IV and V Elements', 28 Oct. 1982.
Dr. D.H. Williams (Cambridge Univ.) - 'Studies on the Structures and Modes of Action of Antibiotics', 4 Nov. 1982.
Dr. J. Cramp (I.C.I.Ltd.) - 'Lasers in Industry', 11 Nov. 1982.
Dr. G. Bertrand (Paul Sabatier Univ., Toulouse) - 'Curtius Re-arrangement in Organometallic Series: A Route for New Hybridized Species', 15 Nov. 1982.
Prof. F.R. Hartley (R.M.C.S., Shrivenham) - 'Supported Metal Complex Hydroformylation Catalysts', 24 Nov. 1982.
Dr. D.R. Richards, (P.E.R.M.E.) - 'Terminally Functional Polymers their Synthesis and Uses', 25 Nov. 1982.
Dr. G. Wooley (Trent Poly.) - 'Bonds in Transition Metal Cluster Compounds', 8 Dec. 1982.
Dr. D.C. Sherrington (Strathclyde Univ.) - 'Polymer Supported Phase Transfer Catalysts', 12 Jan. 1983.
Prof. D.W.A. Sharp (Glasgow Univ.) - 'Some Redox Reactions in Fluorine Chemistry', 27 Jan. 1983.
Dr. P. Moore (Warwick Univ.) - 'Mechanistic Studies in Solution by Stopped Flow F.T. n.m.r. and High Pressure N.m.r. Line Broadening', 9 Feb. 1983.

Sir G. Allen FRS (Unilever Ltd.) - 'U.K. Research Ltd',10 Feb.1983
Prof. A.G. MacDiarmid (Pennsylvania Univ.) - 'Metallic Covalent Polymers: $(SN)_x$ and $(CH)_x$ and their Derivatives',17 Feb.1983
Dr. D. Bloor (Queen Mary College) - 'The Solid State Chemistry of Diacetylene Monomers and Polymers', 2 Mar. 1983.
Prof. A.C.T. North (Leeds Univ.) - 'The Use of a Computer Display System in Studying Molecular Structures and Interactions', 3 Mar. 1983.
Prof. D.C. Bradley, FRS (Queen Mary College) - 'Recent Development in Organo-Imido Transition Metal Chemistry', 8 Mar. 1983.
Prof. H.G. Viehe (Univ. of Louvain, Belgium) - 'Oxidations on Sulphur', 11 Mar. 1983 and 'Fluorine Substitution in Radical and Biradical Addition Reactions', 11 Mar. 1983.
Dr. I. Gosney (Edinburgh Univ.) - 'New Extrusion Reactions: Organic Synthesis in a Hot Tube', 16 Mar. 1983.
Prof. J. Passmore (Univ. of New Brunswick) - 'Novel Selenium - Iodine Cations', 21 Apr. 1983.
Prof. P.H. Plesch (Keele Univ.) - 'Binary Ionisation Equilibria between two ions and two Molecules. What Ostwald never thought of', 4 May 1983.
Prof. K. Berger (Munich Univ.) - 'New Reaction Pathways to Partially Fluorinated Heterocyclic Compounds', 10 May 1983.
Dr. N. Isaacs (Reading Univ.) - 'The Applications of High Pressure to the Theory and Practice of Organic Chemistry',11 May 1983.
Dr. T.D. Marder (U.C.L.A.) - 'The Chemistry of Metal-Carbon and Metal-Metal Multiple Bonds', 13 May 1983.
Dr. J.M. Vernon (York Univ.) - 'New Heterocyclic Chemistry involving Lead Tetra-Acetate', 25 May 1983.
Dr. A. Pietrykowski (Warsaw Univ.) - 'Synthesis Structure and Properties of Aluminoxanes', 15 Jun. 1983.

Conferences Attended

(a) Advances in Polymer Characterisation, an International Symposium', Durham, July 1981.
(b) S.E.R.C. Graduate Summer School, Sheffield, July 1982.
(c) Ion Implantation, a one-day Symposium. Institute of Physics, London, September 1982.
(d) 33rd Annual Meeting of Nobel Prizewinners (11th in Chemistry) 26 June - 1 July 1983, Lindau, West Germany.
(e) S.E.R.C. Summer School on Surface Physics, York, July 17-27, 1983.
(f) Two Graduate Symposia at Durham University, April 1982 and 1983.

APPENDIX II - Listing of computer program written for an Apple II Europlus computer to calculate effect of reaction gradients on ESCA data as described in Chapter Three.

```
 10  TEXT
 20  DEF  FN A(X) =  INT ( 10000 * X) / 10000
 30  HOME
 40  VTAB (5)
 50  REM  WAVE  IN ANGSTROM
 60 LC = 15
 70 LF = 9
 80 LV = 20
 90  INPUT "M/M0=0.1 AFTER WHAT DEPTH (ANGSTROMS)?";X0
100 K1 =  LOG (10) / X0
110  INPUT "MONOLAYER THICKNESS (ANGSTROMS)?";M0
120  PRINT
130  INPUT "NO MONOLAYERS TO BE CONSIDERED?";NM
140  IF NM > 200 THEN 130
150  DIM MP(200)
160  FOR N = 1 TO NM
170 X1 = N * M0:X2 = (N - 1) * M0
180 MP(N) = ( EXP ( - K1 * X2) -  EXP ( - K1 * X1)) / K1
190  NEXT
200 M0 = MP(1)
210  FOR N = 1 TO NM
220 MP(N) = MP(N) / M0
230  NEXT
240  REM  WORK IN ARBITRARY UNITS OF KT
250  REM  REACTION PROCEEDS AS 1ST ORDER PROCESS IN EACH MONOLAYER
260  DIM PR(7,NM)
270  PRINT : INPUT "TO,TIM=TO*2↑M,M=0-7,  ?";TO
280  PRINT : INPUT "LEAST SQ FIT RATE ON HOW MANY PTS?";I
284 HC = 0
285  PRINT : INPUT "HARDCOPY Y/N  ?";A$
286  IF A$ = "Y" THEN HC = 1
290  FOR N = 1 TO NM
300  FOR M = 0 TO 7
310 KT = TO * (2 ↑ M)
320 PR(M,N) = 1.0 -  EXP ( - KT * MP(N))
330  NEXT
340  NEXT
350  REM  SET UP WEIGHTING  OF MONOLAYER CONTRIB TO SIGNAL
360  DIM WZ(NM,2),WZ(NM,2)
370 C3 =  SQR (3) / 2
380 C7 =  COS ((70 *  ATN (1) / 45))
390  FOR N = 1 TO NM
400 X1 = N * M0:X2 = (N - 1) * M0
410 L = LF * C3
420  GOSUB 690
430 WZ(N,0) = A
440 L = LC * C3
450  GOSUB 690
460 WZ(N,1) = A
470 L = LV * C3
480  GOSUB 690
490 WZ(N,2) = A
500 L = LF * C7
510  GOSUB 690
520 WZ(N,0) = A
530 L = LC * C7
540  GOSUB 690
550 WZ(N,1) = A
560 L = LV * C7
```

```
570  GOSUB 690
580 W7(M,2) = A
590  NEXT
600  REM  NORMALISE TO CNTRIB 1ST MONO=1
610  FOR M = NM TO 1 STEP  - 1
620  FOR N = 0 TO 2
630 W3(M,N) = W3(M,N) / W3(1,N)
640 W7(M,N) = W7(M,N) / W7(1,N)
650  NEXT
660  NEXT
670  GOTO 710
680  REM  SUBROUT FOR DEPTH DEP
690 A = L * ( EXP ( - X1 / L) -  EXP ( - X2 / L))
700  RETURN
710  REM  CALCULATE PROFILE Y VS T
720 MI = 0:MX = 0
730  FOR M = 1 TO NM
740  FOR N = 0 TO 5
750  IF PR(N,M) > MX THEN MX = PR(N,M)
760  IF PR(N,M) < MI THEN MI = PR(N,M)
770  NEXT
780  NEXT
790  HGR2
800  HCOLOR= 1
810  HPLOT 5,0 TO 5,150
820  HPLOT 5,150 TO 205,150
830  FOR M = 1 TO NM
840  HPLOT 5,150
850 LI = 5
860 TM = TO * (2 ↑ LI)
870  FOR N = 0 TO LI
880 YY = 150 * PR(N,M) / MX:YY = 150 - YY
890 XX = (TO * (2 ↑ N)) / TM:XX = XX * 200 + 5
900  HPLOT  TO XX,YY
910  NEXT
920  NEXT
930  REM  NEXT PRODUCE PLOTS RATES
940  DIM RA(7,3)
950  DIM RB(7,3)
960  FOR N = 0 TO 7
970  FOR M = 1 TO NM
980 RA(N,0) = RA(N,0) + ((1 - PR(N,M)) * W3(M,0))
990 RB(N,0) = RB(N,0) + ((1 - PR(N,M)) * W7(M,0))
1000 RA(N,1) = RA(N,1) + (PR(N,M) * W3(M,1))
1010 RB(N,1) = RB(N,1) + (PR(N,M) * W7(M,1))
1020 RA(N,2) = RA(N,2) + ((1 - PR(N,M)) * W3(M,1))
1030 RB(N,2) = RB(N,2) + ((1 - PR(N,M)) * W7(M,1))
1040 RA(N,3) = RA(N,3) + ((1 - PR(N,M)) * W3(M,2))
1050 RB(N,3) = RB(N,3) + ((1 - PR(N,M)) * W7(M,2))
1060  NEXT
1070  NEXT
1080  DIM NS(2),NZ(2)
1090  FOR P = 0 TO 2
1100  FOR N = 1 TO NM
1110 NS(P) = NS(P) + W3(N,P)
1120 NZ(P) = NZ(P) + W7(N,P)
1130  NEXT : NEXT
1140  FOR N = 0 TO 7
1150 RA(N,0) = RA(N,0) / N3(0)
1160 RB(N,0) = RB(N,0) / NZ(0)
1170 RA(N,1) = RA(N,1) / N3(1)
1180 RB(N,1) = RB(N,1) / NZ(1)
```

```
1190 RA(N,2) = RA(N,2) / W3(1)
1200 RB(N,2) = RB(N,2) / W7(1)
1210 RA(N,3) = RA(N,3) / W3(2)
1220 RB(N,3) = RB(N,3) / W7(2)
1230  NEXT
1240  DIM LA(7,3)
1250  DIM LB(7,3)
1260  FOR N = 0 TO 7
1270  FOR M = 0 TO 3
1280  IF RA(N,M) = 0 THEN LA(N,M) =  - 99: GOTO 1300
1290 LA(N,M) =  LOG (RA(N,M))
1300  IF RB(N,M) = 0 THEN LB(N,M) =  - 99: GOTO 1320
1310 LB(N,M) =  LOG (RB(N,M))
1320  NEXT : NEXT
1330  HGR2
1340  HCOLOR= 1
1350  HPLOT 5,0 TO 5,150
1360  HPLOT 5,150 TO 205,150
1370 MI = 0:MX = 0
1380  FOR N = 0 TO 5
1390  FOR M = 0 TO 3
1400  IF LA(N,M) <  >  - 99 AND LA(N,M) > MX THEN MX = LA(N,M)
1410  IF LA(N,M) <  >  - 99 AND LA(N,M) < MI THEN MI = LA(N,M)
1420  NEXT : NEXT
1430 RA = MX - MI
1440  FOR N = 0 TO LI
1450 Y1 = (LA(N,1) - MI) / RA:Y1 = Y1 * 150:Y1 = 150 - Y1
1460 XX = ((TO * 2 + N) / TM) * 200 + 5
1470  IF N = 0 THEN  HPLOT XX,Y1
1480  HPLOT  TO XX,Y1
1490  NEXT
1500  HCOLOR= 2
1510  FOR N = 0 TO LI
1520 Y2 = (LA(N,2) - MI) / RA:Y2 = Y2 * 150:Y2 = 150 - Y2
1530 XX = ((TO * 2 + N) / TM) * 200 + 5
1540  IF N = 0 THEN  HPLOT XX,Y2
1550  HPLOT  TO XX,Y2
1560  NEXT
1570  REM **********************
1580  REM  MATRIX DUMPER
1590  TEXT
1600 D$ =  CHR$ (4)
1605  IF HC = 1 THEN  PRINT D$;"PR#1"
1607  PRINT : PRINT
1610  PRINT "EXPONENTIAL DECAY OF ACTIVE SPECIES WITH DEPTH.H CONCENTRATION DROPS TO 10% OF D=0 VALUE IN ";XO;"A
1620  PRINT "DEPTH OF MONOLAYER CONSIDERED =";HO;"ANGSTROM ."
1630  PRINT NM;" MONOLAYERS CONSIDERED."
1640  PRINT "HYDROGEN ATOM CONC VS MONOLAYER."
1650  PRINT "----------------------------"
1660  FOR N = 1 TO NM
1670  PRINT  INT (N),HP(N)
1680  NEXT
1690  PRINT
1700  PRINT
1710  PRINT "WEIGHTING FACTOR/MONOLAYER/LEVEL."
1720  PRINT "-------------------------------,"
1730  PRINT "DOUBLE TAKE-OFF"
1740  FOR N = 1 TO NM
1750  PRINT  INT (N);"  "; FN A(W3(N,0));"  "; FN A(W3(N,1));"  "; FN A(W3(N,2))
1760  NEXT
1770  PRINT : PRINT
1780  PRINT "70 DEG TAKE-OFF"
1790  FOR N = 1 TO NM
1800  PRINT  INT (N);"  "; FN A(W7(N,0));"  "; FN A(W7(N,1));"  "; FN A(W7(N,2))
```

```
1810  NEXT
1820  REM  PRINT OUT DEPTH PROFILE
1830  REM  Y VS MONOLAYER VS KT
1840  PRINT "-----------------------------------"
1850  PRINT
1860  PRINT "Y VS MONOLAYER VS TIME(KT),"
1870  FOR N = 1 TO NM
1880  PRINT  INT (N);
1890  FOR TI = 1 TO 5
1900  PRINT "   "; FN A(PR(TI,N));
1910  NEXT
1920  PRINT
1930  NEXT
1940  PRINT : PRINT
1950  PRINT "F1S DATA 30  70"
1960  FOR N = 0 TO 7
1970  PRINT TO * (2 ↑ N),RA(N,0),RB(N,0)
1980  HTAB (15)
1990  PRINT "     "LA(N,0),LB(N,0)
2000  NEXT
2010  PRINT "       ============"
2020  PRINT : PRINT
2030  PRINT "CH COMPONENT DATA"
2040  FOR N = 0 TO 7
2050  PRINT TO * (2 ↑ N),RA(N,1),RB(N,1)
2060  HTAB (15)
2070  PRINT "     "LA(N,1),LB(N,1)
2080  NEXT
2090  PRINT "       ============"
2100  PRINT : PRINT
2110  PRINT "CF2 COMPONENT DATA"
2120  FOR N = 0 TO 7
2130  PRINT TO * (2 ↑ N),RA(N,2),RB(N,2)
2140  HTAB (15)
2150  PRINT "     "LA(N,2),LB(N,2)
2160  NEXT
2170  PRINT "       ============"
2180  PRINT : PRINT
2190  PRINT "F2S DATA"
2200  FOR N = 0 TO 7
2210  PRINT TO * (2 ↑ N),RA(N,3),RB(N,3)
2220  HTAB (15)
2230  PRINT "     "LA(N,3),LB(N,3)
2240  NEXT
2250  PRINT "-----------------------------------"
2260  PRINT : PRINT
2270  PRINT "F1S/F2S 30  70."
2280  FOR N = 0 TO 7
2290  PRINT TO * (2 ↑ N),RA(N,0) / RA(N,3),RB(N,0) / RB(N,3)
2300  NEXT
2310  REM  LEAST SQ FIT
2320  PRINT : PRINT : PRINT "=========================": PRINT
2330  PRINT "CORE";"  ";"RATE30","RATE70"
2340  PRINT "-------------------------------------"
```

```
2350  FOR CC = 0 TO 3
2360  GX = 0:GY = 0:PY = 0:GC = 0:GD = 0:X = 0:M3 = 0:M7 = 0
2370  GS = 0
2380  I = 5
2390  FOR N = 0 TO I - 1
2400  X = T0 * (2 ↑ N)
2410  GX = GX + X
2420  GS = GS + X ↑ 2
2430  GC = GC + X * LA(N,CC)
2440  GD = GD + X * LB(N,CC)
2450  GY = GY + LA(N,CC)
2460  PY = PY + LB(N,CC)
2470  NEXT
2480  M3 = ((I * GC) - GX * GY) / ((I * GS) - (GX ↑ 2))
2490  M7 = ((I * GD) - GX * PY) / ((I * GS) - (GX ↑ 2))
2500  PRINT CC;" ";M3,M7
2510  NEXT
2520  PRINT : PRINT : PRINT
2525  TEXT
2526  PRINT D$;"PR#0"
2530  STOP
2540  END
```

REFERENCES

1. D.T. Clark, Physica Scripta, 16, 307, 1977.

2. A. Einstein, Ann.Phys., 17, 132 (1905).

3. (a) H. Robinson and W.F. Rawlinson, Philos.Mag., 28, 277 (1914).
   (b) H. Robinson, Proc.Roy.Soc., A104, 455 (1923).
   Ic) H. Robinson, Philos.Mag., 50, 241 (1925).

4. M. de Broglie, Compt.Rend. 172, 274,527,806 (1921).

5. J.A. Van der Akker and E.C. Watson, Phys.Rev., 37, 1631 (1931).

6. K. Siegbahn and K. Edvarson, Nucl.Phys., 1, 137 (1956).

7. K. Siegbahn, "Alpha, Beta and Gamma Ray Spectroscopy", Chapter 3, Ed. K. Siegbahn, North Holland Publishing Co., Amsterdam (1965).

8. K. Siegbahn, C. Nordling, A. Fahlman, R. Nordberg, K. Hamrin, J. Hedman, G. Johannson, T. Bergmark, S.E. Karlsson, I. Lindgren and B. Lindberg, "ESCA: Atomic, Molecular, and Solid State Structure Studied by Means of Electron Spectroscopy", Almquist and Wiksells, Uppsala (1967).

9. (a) R.G. Steinhardt and E.J. Serfass, Anal.Chem., 25, 697 (195
   (b) R.G. Steinhardt, F.A.D. Granados and G.I. Post, Anal.Chem., 27, 1046 (1955).

10. K. Siegbahn, C. Nordling, G. Johansson, J. Hedman, P.F.Hedman K. Hamrin, U. Gelius, T. Bergmark, L.D. Werme, R. Manne and Y. Baer, "ESCA Applied to Free Molecules", North Holland Publishing Co. (1969).

11. K. Siegbahn (1982): Les Prix Nobel, Stockholm, Norstedt and Söner; Rev.Mod.Phys., 54, 709; Science, 217, 111.

12. J.G. Jenkin, R.C.G. Leckey, J. Liesegang, J. Electron Spectrosc.Rel.Phenom., 12, 1 (1977); 14, 477 (1978).

13. T.A. Carlson (Ed.): X-Ray Photoelectron Spectroscopy, Benchmark Papers in Phys.Chem. and Chem.Phys., vol.2, 1978, Publ.Dowden, Hutchinson and Ross.

14. T.H. Rhodin and J.W. Gadzuk, 'Electron Spectroscopy and Surface Chemical Bonding', in "The Nature of the Surface Chemical Bond", Eds., T.N. Rhodin and G. Erth, 112, North Holland Publishing Co., Amsterdam (1979).

15. A.D. Baker and C.R. Brundle, 'An Introduction to Electron Spectroscopy', in 'Electron Spectroscopy, Theory, Techniques and Applications', Vol.1, Eds., C.R. Brundle and A.D. Baker, Academic Press, London (1977).

16. L.S. Cederbaum, and W. Domcke, J.Electron Spectrosc.Rel. Phenom, 13, 161 (1978).

17. D.T. Clark, 'Structure and Bonding in Polymers as Revealed by ESCA', in "Electronic Structure of Polymers and Molecular Crystals", Eds. J. Lallik and J.M. Andre, Plenum Press, New York (1975).

18. J.F. Mc Gilp, and I.G. Main, J.Electron Spectrosc.Rel. Phenom, 6, 397 (1975).

19. S. Evans, 'Energy Calibration in Photoelectron Spectroscopy'. in Handbook of X-Ray and Ultraviolet Photoelectron Spectroscopy', Ed. D. Briggs, Heyden, London (1977).

20. A. Rosen and I. Lindgren, Phys.Rev., 176, 114 (1968).

21. P.S. Bagus, Phys.Rev., 139A, 619 (1975).

22. D.A. Shirley in "Advances in Chemical Physics", 23, 85, Ed. I. Prigogine and S.A. Rice, Wiley, New York (1973).

23. U. Gelius and K. Siegbahn, Farad.Disc.Chem.Soc., 54, 257 (1972).

24. L.C. Snyder, J.Chem.Phys., 55, 95 (1971).

25. D.B. Adams and D.T. Clark, Theor.Chim.Acta, 31, 171 (1973).

26. M.F. Guest, I.H. Hillier, V.R. Saunders and M.H. Wood, Proc.Roy.Soc., A333, 201 (1975).

27. W.R. Salaneck, Phys.Rev.Lett., 40, 60,(1978).

28. T.A. Koopmans, Physika, 1, 104 (1933).

29. D.T. Clark, I. Scanlan and J. Müller, Theoret.Chim.Acta. Berl., 35, 341 (1974).

30. B.J. Cromarty, Ph.D. Thesis, University of Durham, 1978.

31. R. Manne and T. Åberg, Chem.Phys.Lett., 7, 282 (1970).

32. M.A. Brisk and A.D. Baker, J.Electron.Spectrosc.Rel.Phenom., 7, 197 (1977).

33. C.S. Fadley, p.116 in 'Electron Spectroscopy, Theory, Techniques and Applications', Vol.2, Eds., C.R. Brundle and A.D. Baker, Academic Press, London, (1978).

34. D.T. Clark and A. Dilks, J.Polym.Sci., Polym.Ehcm.Edn., 15, 15 (1977).

35. P. Auger, J.Phys.Radium, 6, 205 (1925).

36. P. Auger, Compt.Rend., 65, 180 (1925).

37. J.J. Lander, Phys.Rev., 91, 1382 (1953).

38. T.A. Carlson, 'Photoelectron and Auger Spectroscopy', Plenum Press, New York (1975).

39. D. Coster and R. de L. Kronig, Physica, 2, 13 (1935).

40. E.H.S. Burhop, 'The Auger Effect and Other Radiationless Transitions', Cambridge University Press (1952).

41. J.E. Houston, R. R. Rye, J.A. Kelber and G.C. Nelson, Surf.Sci., 116, 148 (1982).

42. J.P. Coad, M. Gettings and J.G. Riviere, Faraday Discuss. Chem.Soc., 60, 269 (1975).

43. C.D. Wagner, Discuss. Faraday Soc., 60, 291 (1975).

44. C. C. Chang, Surf.Sci., 25, 53 (1971).

45. C.D. Wagner, 'Identification of Chemical States by XPS' in 'Photon, Electron and Ion Probes of Polymer Structure and Properties', ACS. Symposium Series 162, A.C.S. (1981).

46. C.D. Wagner, L.H. Gale and R.H. Raymond, Anal.Chem., 51, 466 (1979).

47. S. Hagstrom, C. Nordling and K. Siegbahn, Phys.Lett., 9, 235 (1964).

48. C. Nordling, S. Hagstrom and K. Siegbahn, Z.Physik, 178, 433 (1964).

49. H.R. Thomas, Ph.D. Thesis, University of Durham,(1977).

50. C.D. Wagner, W.M. Riggs, L.E. Davis, J.F. Moulder and G.E. Muilenburg (Editor), 'Handbook of X-Ray Photoelectron Spectroscopy', Perkin Elmer Corporation, Physical Electronic Division, (1979).

51. C.J. Powell, N.E. Erickson and T.E. Madey, J.Electron Spectrosc.Rel.Phenom, 17, 361 (1979).

52. W.L. Jolly and D.H. Hendrickson, J.Am.Chem.Soc., 3, 193 (1970

53. J.N. Murrell and B.J. Ralston, J.Chem.Soc.Faraday Trans.11, 68, 1393 (1972).

54. M.E. Schwartz, Chem.Phys.Lett., 6, 631 (1970).

55. D.A. Shirley, Chem.Phys.Lett., 15, 325 (1972).

56. C.S. Fadley, 'Basic Concepts of X-Ray Photoelectron Spectroscopy', in 'Electron Spectroscopy, Theory, Techniques and Applications', Vol.2, 1, Eds., C.R. Brundle and A.D. Baker, Academic Press (1978).

57. W.R. Salaneck, Solid State Commun., 27, 685 (1978).

58. J.H. van Vleck, Phys.Rev.Lett., 45, 405 (1934).

59. C.S. Fadley, D.A. Shirley, A.J. Freeman, P.S. Bagus and J.V. Mallow, Phys.Rev. Lett., 23, 1397 (1969).

60. G.M. Bancroft, I. Adams, H. Lampe and T.K. Sham, Chem. Phys.Lett., 32, 173 (1975).

61. R.P. Gupta and S.K. Sen, Phys.Rev.Lett., 28, 1311 (1972).

62. T. Novakov, ref. 26 of C.S. Fadley in 'Electron Spectroscopy' Ed. D.A. Shirley, North Holland Publishing Co. (1972).

63. T. Novakov and J.M. Hollander, Bull.Amer.Phys.Soc., 14, 524 (1969).

64. T. Novakov and J.M. Hollander, Phys.Rev.Lett., 21,1133 (1968).

65. J.J. Pireaux, J. Riga, R. Caudano and J.J. Verbist,'Photon, Electron, and Ion Probes of Polymer Structure and Properties', (A.C.S. symposium series 162), ACS (1982).

66. D.T. Clark and J. Peeling, J.Polym.Sci.,Polym.Chem., 17, 1317 (1979).

67. D.A. Huchital and R.T. McKeon, Appl.Phys.Lett.,20, 158 (1972).

68. D.T. Clark, 'ESCA Applied to Polymers' in "Advances in Polymer Science', Springer-Verlag, 24, 125 (1977).

69. D.T. Clark, A. Dilks, and H.R. Thomas, J.Polym.Sci., Polym.Chem., Ed. 16, 1461 (1978).

70. D.T. Clark, A. Dilks, H.R. Thomas and D. Shuttleworth, J.Polym.Chem.,Ed., 17, 627 (1979).

71. D. Betteridge, J.C. Carver and D.M. Hercules, J.Electron Spectrosc.Rel.Phenom., 2, 327 (1973).

72. C.R. Ginnard and W.M. Riggs, Anal.Chem., 46, 1306 (1974).

73. *c.f.* R.S. Swingle II and W.M. Riggs, CRC Crit.Rev.Anal. Chem., 5, 267 (1975).

74. S. Kohiki, T. Ohmura and K. Kusao, J.Electron Spectrosc. Rel.Phenom., 28, 229 (1983).

75. D.T. Clark and A. Dilks, 'Characteristion of Metal and Polymer Surfaces, Vol.2, ed. L.H. Lee, Academic Press, New York, (1977).

76. D.T. Clark and H.R. Thomas, J.Polym.Sci.Polym.Chem.Ed., 16, 791 (1978).

77. D.T. Clark and A. Dilks, J.Polym.Sci.Polym.Chem.Ed., 16, 911 (1978).

78. D.T. Clark and A. Dilks, J.Electron.Spectrosc.Rel.Phenom., 11, 225 (1977).

79. R.O. Ansell, T. Dickinson, A.F. Povey and P.M.A. Sherwood, J.Electroanal.Chem., 98, 79 (1979).

80. G.K. Wertheim and P.H. Citrin, "Photoionisation in Solids I", Topics in Applied Physics, 26, 197 (1978).

81. W.L. Dunn and T.S. Dunn, S.I.A. Surface and Interface Analysis, 4(3), 77 (1982).

82. C.S. Fadley, Ph.D. Thesis, University of California (1970).

83. A. Proctor and P.M.A. Sherwood, SIA Surface and Interface Analysis 2 (5), 191 (1980).

84. A.F. Carley and R.W. Joyner, J.Electron Spectrosc.and Rel. Phenom., 16, 1 (1979).

85. H. Ebel and W. Gurker, Phys.Lett., 50A, 449 (1975).

86. G.K. Wertheim, J.Electron Spectrosc.Rel.Phenom,6, 239 (1975).

87. (a) J.H. Schofield, Lawrence Livermore Laboratory Report, U.G.R.L., 51326, Jan (1973).

(b) J.H. Schofield, J.Electron Spectrosc.Rel.Phenom, 8, 129 (1976).

88. J. Cooper and R.N. Zare, J.Chem.Phys., 48, 942 (1968).

89. F.O. Ellison, J.Chem.Phys., 61, 507 (1974).

90. D.R. Penn., J.Electron.Spectrosc.Rel.Phenom., 9, 29 (1976).

91. D.T. Clark and H.R. Thomas, J.Polym.Sci.,Polym.Phys.Edn., 15, 2843 (1977 and references therein.

92. D.T. Clark and D. Shuttleworth, J.Polym.Sci.,Polym.Chem. Edn., 16, 1093 (1977).

93. D.T. Clark, W.J. Brennan and M.M. Abu-Shbak, J.Electron Spectrosc.Rel.Phenom., 28, 11 (1982) and references therein.

94. B.L. Henke, Adv.X-Ray Analysis, 13, 1 (1969).

95. C.D. Wagner, Farad.Disc.Chem. Soc., 60, 306 (1975).

96. G. Johansson, J. Hedman, A. Berndtsson, M. Klarson and R. Nilsson, J.Electron Spectrosc.Rel.Phenom.,2, 295 (1973).

97. S. Pignataro and G. Distofano, Z.Naturforsch, A309 815 (1975)

98. T. Ohta, T. Fukitawa and H. Furoda, Chem.Phys.Lett., 32, 369 (1975).

99. L. Yin, I. Adler, T. Tsang, L.J. Matienzo and S.O. Grim, Chem.Phys.Lett., 24, 81 (1974).

100. T. Robert and G. Offergeld, Chem.Phys.Lett., 29, 606 (1974).

101. D.T. Clark, A. Dilks, J. Peeling and H.R. Thomas, Faraday Disc., 60, 183 (1975).

102. (a) D.T. Clark and D.B. Adams, J.Electron Spectrosc.Rel. Phenom., 7, 401 (1975).

(b) D.T. Clark, D.B. Adams, A.Dilks, J. Peeling and H.R. Thomas, J.Electron Spectrosc.Rel.Phenom., 8, 51 (1976).

103. D.T. Clark and A. Dilks, J.Polym.Sci., Polym.Chem.Ed., 14, 533 (1977).

104. A.H.K. Fowler, unpublished results.

105. H.P. Chang and J.H. Thomas III, J. Electron Spectrosc.Rel. Phenom., 26, 203 (1982).

106. D.R. Wheeler and S.V. Pepper, J.Vac.Sci.Technol. 20(2), 226 (1982).

107. H. Siegbahn in Encyclopaedia of Physics, Vol.XXXI, Corpuscles and Radiation in Matter I, ed. W. Mellhorn, Springer-Verlag, Berlin, (1982).

108. K. Yates, A. Barrie and F.J. Street, J.Phys., E6, 130, (1973)

109. E.M. Purcell, Phys.Rev., 54, 818 (1938).

110. D.W. Turner, G. Beamson and H.Q. Porter, Nature, 290, 556 (1981).

111. R.M. Eisberg, "Fundamentals of Modern Physics", Chp.14, J. Wiley and Sons, New York (1981).

112. J.C. Helmer and W.H. Weichert, Appl.Phys.Lett.,13, 268 (1968).

113. K. Siegbahn, J. Electron Spectrosc.Rel.Phenom., 5, 3, (1974).

114. U. Gelius, E. Basilier, S. Svensson, T. Bergmark and K. Siegbahn, J.Electron Spectrosc.Rel.Phenom, 2, 405, (1974).

115. M.P. Seah, Surf.Interface Anal., 2, 222 (1980).

116. L. Tonks and I. Langmuir, Phys.Rev., 33, 195 (1929).

117. A.T. Bell, "Fundamentals of Plasma Chemistry", in "Techniques and Applications of Plasma Chemistry", eds., J.R. Hollah and A.T. Bell, J. Wiley and Sons, New York (1974).

118. E.D. Johnson and L. Malter, Phys.Rev., 80, 58 (1950).

119. J.D. Swift and M.J.R. Schwar, 'Electrical Probes for Plasma Diagnostics', Iliffe Books Ltd., London (1970) and references therein.

120. M. Hudin 'Plasma Treatment of Solid Materials' in 'Techniques and Applications of Plasma Chemistry', eds., J.R. Hollahan and A.T. Bell, J. Wiley and Sons, New York (197

121. A.N. Mearns, Thin Solid Films, 3, 201 (1969).

122. V.M. Kolotyrkin, A.B. Gil'man and A.K. Tsapuk, Russ.Chem. Phys., 36, 579 (1967).

123. 'Plasma Chemistry of Polymers', Ed. M. Shein; Dekker, New York (1976).

124. R.M. Fredericks and J. Asmussen,Jr., J.Appl.Phys., 42, 3647 (1971).

125. H. Helm, T.D. Märk and W. Lindinger, Pure and Appl.Chem., 52, 1739 (1980).

126. D.T. Clark and M.Z. AbRahman, J.Polym.Sci.Polym.Chem.Ed., 19, 2689 (1981).

127. F.K. McTaggart, 'Plasma Chemistry in Electrical Discharges', Elsevier Publishing Co., Amsterdam (1967).

128. J.R. Hollahan and A.T. Bell, eds., 'Techniques and Applications of Plasma Chemistry", J. Wiley and Sons, New York (1974).

129. A. Dilks, Ph.D. Thesis, University of Durham (1977).

130. D.T. Clark and A. Dilks, J.Polym.Sci., Polym.Chem., Ed., 15, 2321 (1977).

131. H.F. Winters, Topics in Current Chemistry, 94, 77 (1980).

132. H.D. Hagstrum, J.Vac.Sci.Technol. 12, 7 (1975).

133. H. Suhr, Applications of Non-equilibrium Plasmas to Organic Chemistry in ref. 128 and references therein.

134. A.G. Loudon, A. Maccoll and S.K. Wong, J.Chem.Soc.B, 1733 (1970).

135. K. Otazai, S. Nagai, T.Yamamoto and S. Fukushima, Bull. Chem.Soc.Jpn., 27, 476 (1954).

136. H. Yasuda, ' Formation of Polymeric Materials by a Non-polymerisation Process: Glow Discharge Polymerisation' in 'Contemporary Topics in Polymer Science', Ed. M.Shen, 103, Plenum Publishing Corp. (1979).

137. C.I. Simonesçu and F. Dénes, Cellulose Chem.Technol. 14, 285 (1980).

138. A.E. Pavlath and K.S. Lee, J.Macromol.Sci.Chem.A, 10, 579 (1976).

139. M.M.Millard and A.E. Pavlath, J.Macromol.Sci.Chem.A., 10, 619 (1976).

140. H.F. Winter in Proc. of 'Workshop on Plasma Chemistry and Arc Technology" Minneapolis, Minnesota, August 1980.

141. D.W. Dwight, Ion Beam Surface Modification W82-15196, NASA Cl. 165062, NASA Grt.No. NSG 3204, March 1982.

142. J.W. Rabalais in 'Photon, Electron and Icn Probes of Polymer Structure and Properties', ed. D.W. Dwight, T.J.Fabish and H.R. Thomas, ACS Symposium Series 162, Publ.Amer. Chem.Soc., (1981).

143. Y. Kikuchi and S. Tsuda, Denki Kagaku, 29, 389 (1961).

144. Y. Osada, A.T. Bell and H. Shen, Am.Chem.Soc.Div.Polym. Prepr., 19(2), 482, (1978).

145. H. Yasmuda, J.Pol.Sci.Macromolecular Reviews, 16 199 (1981) and refs. therein.

146. H. K. Hu, J.W. Rabalais and J.A. Schultz, J.Phys.Chem., 86, 3364 (1982).

147. J.H. Lindhard, M. Scharff, H.E. Schiøtt, Kgl.Danske.Vid.Selsk Matt-Fys.Medd, 33, 14 (1963), described in Ref. 148.

148. P.D. Townsend, J.C. Kelly and N.E.W. Hartley, 'Ion Implantation, Sputtering and their Applications', Academic Press, New York (1976).

149. D.E. Aspnes and A.A.Studna, Surf.Sci., 96, 224 (1980).

150. R.J. MacDonald and D. Haneman, J.Appl.Phys., 37, 1609 (1966).

151. J.A. Taylor, G.M. Lancaster and J.W. Rabalais, Appl.Surf. Sci., 1, 503 (1978).

152. A. Benninghoven, Surf.Sci., 53, 596 (1975).

153. D. Briggs and A.B. Wooton, Surf.Interface Anal (SIA), 4, 109 (1982).

154. G.K. Wehner, Adv.Electron.Phys. 7, 239 (1955).

155. G. Carter and G.S. Colligon, 'Ion Bombardment of Solids', Elsevier, New York (1968).

156. L. Maissel in 'Handbook of Thin Film Technology, ed. L.I. Maissel and R. Glang, McGraw-Hill, New York, (1970), p.401.

157. P. Joyes, J.Phys.Paris, 29, 774 (1968); 30, 243 (1969); P.Joyes, Radiation Effects, 19, 235 (1973).

158. Z. Zrovbek, Surf.Sci., 44, (1974), 47.

159. C.A. Anderson and J.R. Hinthorne, Anal.Chem., 45, 1421 (1973).

160. D. Briggs, S.I.A. Surf.Interface Anal. 4, 151 (1982).

161. D. Briggs, S.I.A.,Surf.Interface Anal., 5, 115 (1983).

162. R. Holm and S. Storp, J.Electron Spectrosc.Rel.Phenom., 16, 183 (1979).

163. R. Holm and S. Storp. Appl.Phys. 12, 101 (1977).

164. D.M. Ullevig and J.F. Evans, Anal.Chem., 52, 1467 (1980).

165. J.E. Campana, J.J. De Corpo and R.J. Colton, Appl.Surf.Sci., 8, 337 (1981).

166. J.S. Sovey, J.Vac.Sci.Technol., 16(2), 813 (1979).

167. D.T. Clark and W.J. Feast, J.Macromol.Sci., Revs.Macromol. Chem., C12 (2), 191 (1975).

168. P. Cadman and G.M. Gossedge, J.Mater.Sci., 14, 2672 (1979).

169. G.R. Sparrow and H.E. Mishmash in Quantitative Surface Analysis of Materials, W.S. McIntyre (Ed.), ASTM STP643 (1978), 164.

170. J.A. Gardella and D.M. Hercules, Anal.Chem., 52, (1980) 226.

171. J.W. Rabalais in 'Photon, Electron and Ion Probes of Polymer Structure and Properties', ed. D.W. Dwight, T.J. Fabish and H.R. Thomas, ACS Symposium Series 162, Publ.Amer.Chem.Soc., (1981).

172. D. Briggs, A. Brown, J.A. Van den Berg, J.C. Vickermann, Springer Ser.Chem.Phys., 1983, 25, (Ion.Form.Org. Solids), 162.

173. J.E. Campana, N.M. Ross, S.C. Rose, J.R. Wyatt and R.J.Cotton Springer.Ser.Chem.Phys., 1983, 25, (Ion Form.Org.Solids), 144.

174. D.E. Williams and L.E. Davis, in 'Characterisation of Metal and Polymer Surfaces, vol.2, Ed., L.H. Lee, Academic Press, New York, (1977).

175. D.C. Weber, P. Brandt, C. Carosella and L.G. Banks, J.C.S. Chem.Commun., 522 (1981).

176. J.J. Ritsko, Ann.Rep.Conf. on Elect.Ins. and Dielectric Plen., Nat.Acad.Sciences, Washington, D.C.,(1978), p.109

177. C. Mayoux, A. Antoniou, Bu AI, and R. Lacoste, Eur.Polym.J., 9, 1069 (1973).

178. R. Dahm in Chapter 10 of Surface Analysis and Pretreatment of Plastics and Metals, ed. D. Brewis, Appl.Sci.Publ. Ltd., (1982).

179. G. Koo, Fluoropolymers, ed. L.A. Wall, Wiley Interscience, New York (1972).

180. H.F. Mark and W.G. Gaylord (Eds.), Encyclopaedia of Polymer Science and Technology, Vol.13, Wiley, New York, (1970).

181. W.A. Zisman in Contact Angle, Wettability and Adhesion, ACS Adv.Chem.Ser., 43, 9 (1964).

182. M.W. Pascoe, Tribology, 184 (1973).

183. M.O.W. Richards and M.W. Pascoe in 'Advances in Polymer Friction and Wear', Vol.5A, ed. L.H. Lee, Plenum Press New York (1974), p.123.

184. G. Rappaport, U.S. Patent 2,809,130 (1957).

185. Minnesota Mining and Manufacturing Co., Brit.Patent, 765,284 (1957).

186. D.M. Brewis, R.H. Dahm and M.B. Konieczko, Macrol.Chem., 43, 191 (1975).

187. J. Jansta, F.P. Dousek and J. Riha, J.Electroanal.Chem., 38, 445 (1972).

188. J. Jansta, F.P. Dousek and J. Riha, J.Appl.Polym.Sci., 19, 3201 (1975).

189. R.J. Purvis and W.R. Beck, U.S. Patent 2,780,063 (1957).

190. D.L. Ryan, Brit.Patent, 890,466 (1962).

191. F.W. Ryan, G.M. Sessler, J.E. West and H. Schonhorn, J.Appl.Polym.Sci., 17, 3199 (1973).

192. G.M. Gossedge, Ph.D. Thesis, University College of Wales (197

193. R.F. Roberts, F.W. Tyan, H. Schonhorn, G.M. Sessler and J.E. Wert, J.Appl.Polym.Sci., 20, 255 (1976).

194. S.L. Vogel and H. Schonhorn, J.Appl.Polym.Sci., 23, 2493 (197

195. H. Schonhorn and R.H. Harven, J.Appl.Polym.Sci., 11, 1461 (1967)

196. H. Brecht, F. Mayer and H. Binder, Makromol.Chem., 33, 89 (1973).

197. D.W. Dwight and W.M. Riggs, J.Electron.Spectrosc.Rel.Phenom., 5, 447 (1974).

198. D. Briggs and J.D. Gribbin in ref. 178.

199. R.H. Hansen and H. Schonhorn, Polymer Lett. 4, 203 (1966).

200. H. Schonhorn, F.W. Ryan and R.H. Hansen, J.Adhesion, 2, 93 (1970).

201. H. Yasuda, H.C. Marsh, S. Brandt and C.H. Reilley, J.Polym. Sci.,Polym.Chem.Ed., 15, 991 (1977).

202. H. Yasuda and H.C. Marsh, Chicago Meeting A.C.S. Chicago, U.S.A., 25th Annual Polymer Preprints (Aug.1975), 16(2), 142 (1975).

203. T. Hirotsu and S. Ohnishi, J. Adhesion, 11, 57 (1980).

204. G.C.S. Collins, A.C. Lowe and D. Nicholas, Euro Polymer J., 9, 1173 (1973).

205. D. Shuttleworth, Ph.D. Thesis, University of Durham,(1978).

206. J.R. Hollahan, B.B. Stafford, R.D. Falls and S.T. Payne, J.Polym.Sci., 13, 807 (1969).

207. G. Smolinsky and M.J. Vasile, Eur.Polymer J., 15, 87 (1979).

208. R.B. Ingalls and L.A. Wall, J.Chem.Phys., 35, 370 (1961); 41, 1112 (1964).

209. A.M. Dubinskaya and L. Duskina, Vysokomol.soyed. A14(7), 1467 (1972).

210. A.Dilks, Electron Spectroscopy, Theory, Techniques and Applications,Vol.4 ed. C.R. Brundle and A.D. Baker, Academic Press, NewYork (1981)

211. R.W. Paynter, Surf.Interface.Anal. 3(4), 186 (1981).

212. M. Pijolat and G. Hollinger, Surf.Sci., 105 114 (1981).

213. H.C. Heller, S. Schlick and T. Cole. J.Phys.Chem., 71, 97 (1967).

214. R. Klein and M.D. Scheer, J.Phys.Chem., 62, 1011 (1958).

215. R.B. Ingalls and L.A. Wall, J.Chem.Phys., 34, 370 (1961).

216. R.B. Ingalls and J.R. Hardy, Can.J.Chem., 38, 1734 (1960).

217. A.M. Dubinskaya, Vysokomol.Soyed, B14(10), 783 (1972).

218. A.M. Dubinskaya, Kinet.Katal., 19, 1171 (1978).

219. A.M. Dubinskaya, Kinet.Katal., 17, 1459 (1976).

220. W. Jost, Diffusion In Solids, Liquids and Gases, Academic Press, New York (1952).

221. J. Crank, The Mathematics of Diffusion, O.U.P., (1956).

222. D.A. Frank - Kamenetskii, 'Diffusion and Heat Exchange in Chemical Kinetics', Trans.H.Thorn., Princeton Univ. Press, Princeton, N.J., (1955), pp.96-103.

223. H.N. Friedlander and V. Menikheim, 'Molecular Behaviour and The Development of Polymeric Materials', Chapman and Hall, London (1974), p.272.

224. T.W. Gallaher, T.C. De Vore, R.O. Carter III, and C. Anderson, Applied Spectroscopy, 34, 408 (1980).

225. W.I. Parsamyan, V.V. Azatyan and A.B. Walbandyan, Am.Khim. Zh., 20, 950 (1967); Am.Chem.Abs., 69:76218x (1968).

226. For a review see W. Jones, S.D. MacKnight and L. Teny, Chemical Reviews, 73(5), 407 (1973).

227. P.M. Scott and K.R. Jennings, J.Phys.Chem., 73, 1521 (1969).

228. H.C. Berg and D. Kleppner, Rev.Sci.Intst., 33, 248 (1962).

229. J.W. Coburn and H.F. Winters, J.Vac.Sci.Technol., 16 391 (1979

230. Y Y Tu, T.J. Chuang and H.F. Winters, Phys.Rev.B, 23, 823 (198

231. C.J. Mogab and H.J. Levinstein, J.Vac.Sci.Technol.,17,721 (198

232. H.W. Lehmann and R. Widmer, J.Vac.Sci.Technol.,17, 1177 (198

233. J.C.Knights and R.A.Lujan, J.Appl.Phys., 49, 1291 (1978).

234. M.H. Brodsky, Thin Solid Films, 50, 57 (1978).

235. J. Bauer, L. Biste and D. Bolze, Phys.Stat.Sol.,(a), 39, 173 (1977).

236. E. Kay, J. Coburn and A. Dilks in Topics in Current Chemistry, 94, 1, (1980), Springer-Verlag, Berlin.

237. M.Z. AbRahman, Ph.D. Thesis, University of Durham, (1981).

238. R.W. Kirk in 'Techniques and Applications of Plasma Chemistry', eds. J.R.Hollahan and A.T. Bell, Wiley Interscience, New York (1974).

239. F.A. Bovey, p.149, 'The Effects of Ionising Radiation on Natural and Synthetic High Polymers', Interscience, New York (1958).

240. R.E. Floria, p.317, 'Fluoropolymers, High Polymers, XXV, ed. L.A. Wall, Wiley, New York (1972).

241. A. Barrie and F.J. Street, J.Electron Spectrosc.Relat.Phenom. 7, 1 (1975).

242. K. Shimvzu, H. Kawakatsu, K. Kanaya, J.Phys.D.,8, 1453 (1975)

243. D. Briggs, J.Mater.Sci., 12, 429 (1977).

244. H.W. Gibson and J.M. Pochan, Macromolecules, 15, 242 (1982).

245. Z. Mayer, J.Macromol.Sci.Rev.Macrmol.Chem., 10, 263 (1973).

246. G. Palona and M. Carenja, J.Appl.Polym.Sci., 14, 1737 (1970).

247. H.P. Chang and J.H.Thomas,III, J.Electron Spectrosc.Relat. Phenom., 26, 203 (1982).

248. E. Mathias and G.H. Miller, J.Phys.Chem., 71, 2671 (1967).

249. J.W. Ryan, Modern Plastics, 31(2), 152 (1953).

250. A. Charlesby, Atomic Radiation and Polymers, Pergamon, New York (1960).

251. J.S. Abel, H. Mazurek, D.R. Day, E.W. Maby, S.D.Senturia, G. Dresselhaus and M.S. Dresselhaus, Materials Research Society Symposium Proceedings, ed. S.T. Picraux and W.J. Chogke, (North Holland, New York, 1978) vol.7, p.173.

252. T. Ventatesan, S.R. Forrest, M.L. Kaplan, C.A. Murray, P.H. Schmidt, and B.J. Wilkens, J.Appl.Phys., 54(6), 3150 (1983).

253. T. Ventatesan, S.R. Forrest, M.L. Kaplan, P.H. Schmidt and A.J. Lovinger, Appl.Phys.Lett., 41, 708 (1982).

254. T.D. Thomas, J.Chem.Phys., 52, 1373 (1970).

255. An ESCA gas phase study of relaxation energies and valence bond formation on the linear alkane series.
J.J. Pireaux, S. Svensson, E. Basilier, P-Å Malmquist, U. Gelius, R. Caudano and K. Siegbahn, University of Uppsala Institute of Physics, UUIP, 920, March, 1976.

256. D.T. Clark and A. Dilks, J.Polym.Sci.,Polym.Chem.Ed. 14, 533 (1976).

257. J.H. Edwards and W.J. Feast, Polymer, 21, 595 (1980).

258. A. Jaegle, A. Kalt, G. Wanse and J.C. Peruchetti, Analusis, 9(5), 252-7 (1981).

259. L. Mandelkern in 'The Radiation Chemistry of Macromolecules Vol.1, ed. M. Dole, Academic Press, New York (1972).

260. Raychem Ltd., Technical Literature.

261. M.B. Fallgatter and M. Dole, J.Phys.Chem., 68, 1988 (1964).

262. M. Dole, D.C. Milner and T.F. Williams, J.Am.Chem.Soc., 79, 4809 (1957).

263. M. Dole, D.C. Milner and T.F. Williams, J.Am.Chem.Soc., 80, 1580 (1958).

264. A.A. Miller, E.J. Lawton and J.S. Balwitt, J.Phys.Chem., 60, 599 (1956).

265. M. Barber, E.L. Evans and J.M. Thomas, Chem.Phys.Lett., 18, 423 (1973).

266. W.J. Brennan, Ph.D. Thesis, to be submitted.

267. A. Chapiro, 'Radiation Chemistry of Polymeric Systems, High Polymers, Vol.XV, Wiley Interscience, New York (1962)

268. see C. Arnold in J.Polymer Sci.D, Macromolecular Reviews, 14, 265 (1979).

269. S. Doniach and M. Sunjic, J.Phys. C3, 285 (1970).

270. H. Hiraoka and W. Lee, IBM Research Report RJ2155(29568)12/19/77.

271. J.J. Riga, J.J. Pireaux, R. Caudano and J.J. Verbist, Physica Scripta, 16, 346 (1977).

272. L.R. Painter, E.T. Arakawa, M.W. Williams and J.C. Ashley, Radiation Research, 83, 1 (1980).

273. J.H.L. Watson, J.Appl.Phys., 18, 153 (1947).

274. V.E. Cosslett, J.Appl.Phys., 18, 844 (1947).

275. J. Hillier, J,Appl.Phys., 19, 226, (1948).

276. H. König and G. Helwig, Z.Phys., 129, 491 (1951).

277. A.E. Ennos, Br.J.Appl.Phys., 4, 101 (1953).

278. R.W. Christy, J.Appl.Phys., 31, 1680 (1960).

279. L. Mayer, J.Appl.Phys., 34, 2088 (1963).

280. R. Speidel, Z.Phys., 154, 238 (1959).

281. G. Möllenstedt and R. Speidel, Z.Angew.Phys., 13, 231 (1961).

282. K. Kanaya, H. Kawakatsu, S. Matsui, H. Yamazaki, I. Okazaki and K. Tanaka, Optik, 21, 399 (1966).

283. C.R. Fritzsche, J.Appl.Phys., 53(12), 9053 (1982).

284. L.V. Gregor "Gas Phase Deposition of Insulating Films" in Physics of Thin Films edited by G. Hass and R.E. Thun, (Academic Press, New York, 1966), Vol.3, p.131.

285. L.V. Gregor, IBM J.Res.Dev., p.140 (1968).

286. H.T. Mann, Electrochemical Technology, 1, 287 (1963).

287. K. Shimiza and H. Kawakatsu, Proc.Int.Symp.Contamin.Control 4th Inst.Environ.Sci., (1978), 321-4.

288. H.T. Jonkman and J. Michl in Secondary Ion Mass Spectroscopy SIMS II. Proceedings of 2nd International Conference on Secondary Ion Mass Spectroscopy, Stamford University (1979

289. D.T. Clark and D. Shuttleworth, J.Polym.Sci.,Polym.Chem.Ed., 18, 27 (1980).

290. H. Yasuda and T. Hsu, Surf.Sci., 76, 232 (1978).

291. A.R. Westwood, Eur.Polym.J., 7, 363 (1971); 7, 377 (1971).

292. O.A. Anisimov, V.M. Grigoryants and Yu.N.Molin,Chem. Phys.Lett., 74, 15 (1980).

293. L.G. Christophorou, M. Grant and D.L. McCorkle, Adv.Chem. Phys.XXXVI, p.413, Wiley Interscience, New York, (1977). ed. I. Prigogine and S.A. Rice.

294. R.P. Frueholz, W. M. Flicker, O.A. Mosher and A.J. Kuppermann J.Chem.Phys., 70, 3057 (1979).